Nutraceutical approaches to promote healthy aging: the yeast *Saccharomyces cerevisiae* for the discovery of anti-aging interventions

Tesi di: Giulia Stamerra

Numero di Matricola: 736177

SUMMARY

ABSTRACT

Since the second half of past century in many developed Countries, life expectancy has gradually increased, reaching, and in some extreme cases exceeding, the threshold of 85 years.

However, the increase of life expectancy is not associated with a corresponding increment of healthy conditions for the older population. Nowadays, a huge part of population over 65 years suffers a multitude of diseases, most of them highly disabling, like cardiovascular diseases, tumour or neurodegenerative disorders.

This aspect has increased the interest on age-related issues, emphasizing the importance of reducing the gap between longevity and health during aging. For this purpose, efforts of many research lines have focused on studying which are the main factors that affect aging, in order to develop approaches that mitigate the detrimental effects of aging on health. Many aging-related pathways are evolutionarily conserved from some single-celled organisms to complex multicellular ones. Such knowledge has allowed us the use of simple model organisms to study this complex biological phenomenon. In this work we used the single-celled eukaryote *Saccharomyces cerevisiae*, which undergoes both replicative and chronological aging, two complementary models of aging, which respectively resemble the aging process of mitotically active and post-mitotic mammalian cells. In this context, replicative lifespan (RLS) is defined as the number of buds generated by a single mother cell in the presence of nutrients before death. On the contrary, chronological lifespan (CLS) is the mean and maximum period of time of surviving cells in stationary phase. It is determined, starting three days from the diauxic shift, by the capability of quiescent cells to resume growth once returning to rich fresh medium. Considering that there is a strong connection between cellular aging, nutrients and metabolism, we investigated the possible effects of some nutraceutical compounds, in order to identify molecules for anti-aging interventions, as well as add useful information to understand the aging process. To this end, during the first and second year of my PhD project, I studied the effects of resveratrol (RSV) on CLS. RSV is a polyphenolic compound counted among the Sirtuin Activator Compounds (STACs), which has been proposed to confer health benefits on different age-related diseases. Sirtuins are a family of NAD^+-dependent deacetylases, the founding member of which is Sir2 of *S. cerevisiae,* whose activity is involved in both RLS and

CLS. Unexpectedly, we found that RSV supplementation increased oxidative stress in concert with a strong reduction of the anti-aging gluconeogenesis pathway. The deacetylase activity of Sir2 on its gluconeogenic target Pck1 was enhanced, resulting in its inactivation and indicating that RSV really acts as STAC. As a consequence, this brought about detrimental effects on the survival metabolism resulting in a short-lived phenotype. Next, we focused on the study of quercetin (QUER), a nutraceutical compound with health-promoting properties on different pathologies, including cardiovascular disorders, cancer and dyslipidaemia. Nevertheless, QUER cellular targets are still being explored. We found that QUER displays anti-aging properties favouring CLS extension. All data point to an inhibition of the deacetylase activity of Sir2 following QUER supplementation, resulting in increased levels of acetylation and activity of Pck1. This determines a metabolic remodelling in favour of the pro-longevity gluconeogenesis pathway, increasing trehalose storage and ensuring healthy aging improvement.

Another aspect analysed in this thesis concerns the homeostasis of the cofactor nicotinamide adenine dinucleotide (NAD^+) during chronological aging, since, together with its biosynthetic precursors, it is emerging as a potential nutraceutical compound and its levels critically affect the activity of Sir2. In this regard the expression of the specific mitochondrial NAD^+ carriers, namely Ndt1 and Ndt2, has been altered, with opposite effects on both metabolism and CLS. The lack of both carriers decreases NAD^+ levels and increases CLS, whereas *NDT*1 overexpression increases NAD^+ content and negatively affects CLS. All results have shown that Sir2 deacetylase activity significantly affects chronological longevity, thus identifying it as a crucial target in the aging process. In mammals, SIRT1, functional ortholog of yeast Sir2, also plays an important role in the orchestration of metabolism and cell survival, underlining the real possibility of transposing the knowledge acquired from yeast to complex organisms, including humans. Moreover, the results obtained for RSV and QUER highlight that the administration of a nutraceutical compound to a more complex organism with organs/tissues having different metabolic profiles could result in an unexpected physiological response due to its interaction with specific target(s). The ability to both develop personalized foods and deliver them to the target of interest represents the next aim in the development of nutraceutical interventions.

Chapter 1

INTRODUCTION
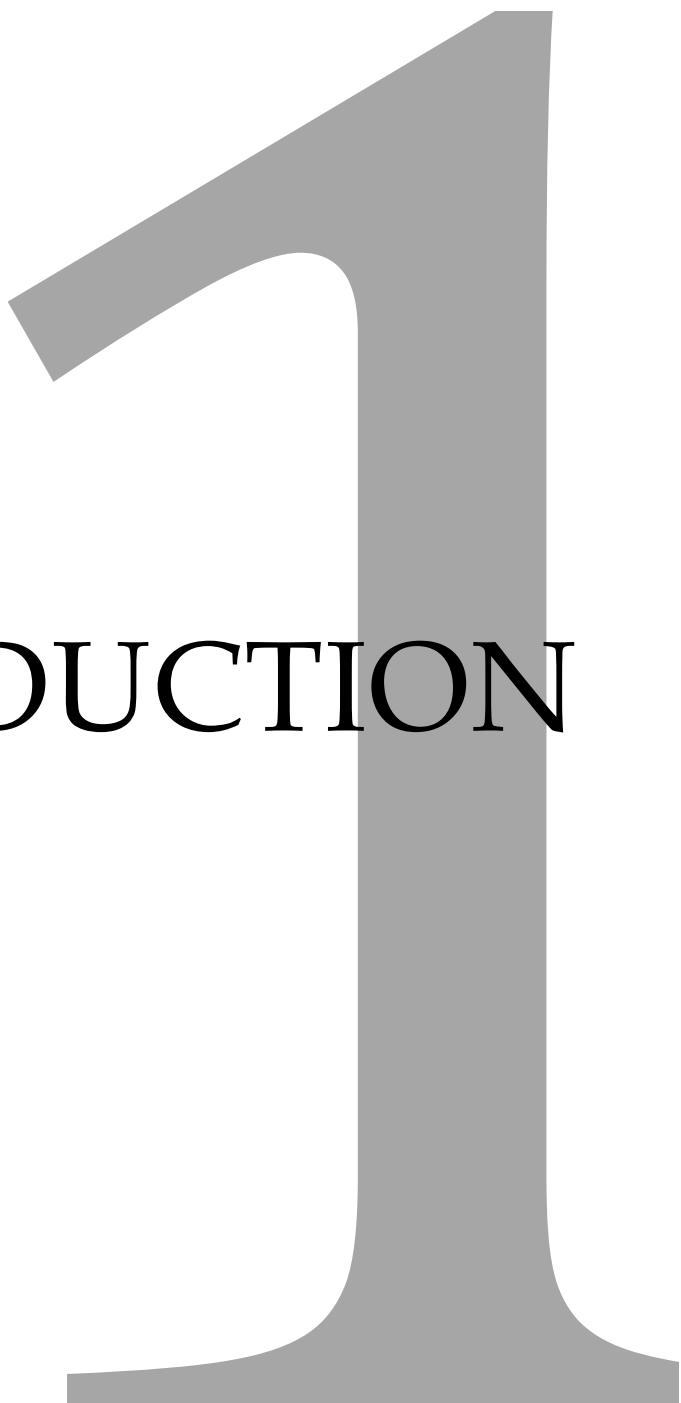
1.1 AGING

Aging is defined a physiological and gradual process of cell organism becoming older. This process leads to a time-dependent functional and structural decline, which ultimately results in loss of cellular homeostasis and death. It is a complex and multifactorial process characterized by an age-specific decrease in the reproductive rate and an increase in mortality, which are determined by a drastically decline or loss of fitness (1). Since the second half of the last century, as a result of an improvement of socio-economic conditions in many countries, life expectancy has gradually increased, beyond 80 years old in many European countries (2). However, this increase is associated with an increase in disease incidence, making age as a major risk factor for many pathologies (3). Indeed, the analysis on the spread of diseases such as arthritis, diabetes, cardiovascular diseases, cancer and pulmonary disorders, underlines that they affect a large percentage of the population aged over 65 (Fig.1).

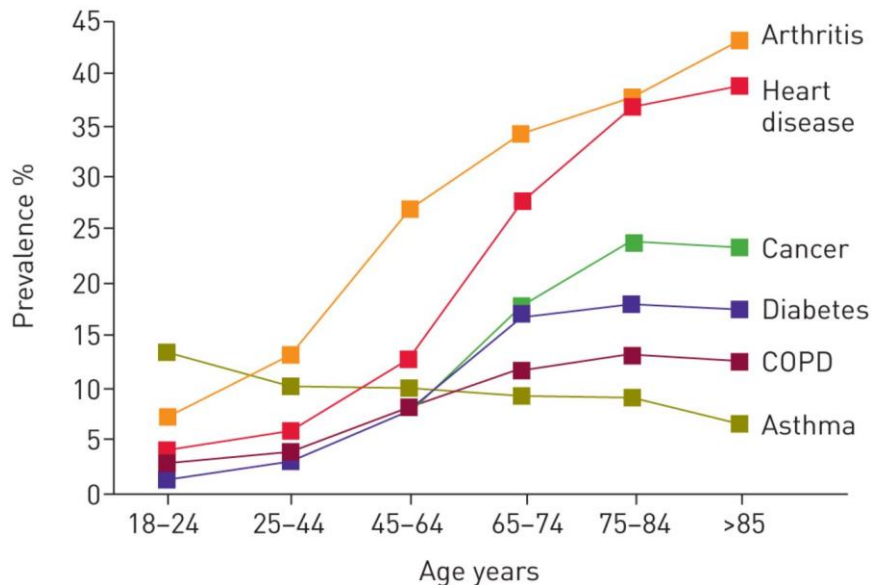Fig.1 **Prevalence of diseases as a function of age.** COPD: chronic obstructive pulmonary disease.

The financial burden of caring for an old population is substantial. According to a financial evaluation of the Center for Disease Control and Prevention, the costs for health-care, long-term care and hospice for people with dementia and neurodegenerative disorders is expected to increase $ 183 billion in 2011 to $ 1.1

trillion in 2050 (4). This aspect has increased the interest on age-related issues, emphasizing the importance of reducing the gap between longevity and health during aging. For this end, efforts of many research lines have focused on studying which are the main factors that affect aging, in order to develop approaches that mitigate the effects of aging on health. Among the main hallmarks of the aging process, one can mention genomic instability, epigenetic alterations, loss of proteostasis, deregulation of metabolism and mitochondrial dysfunctions (5, 6). For an exhaustive argumentation, a summary overview of these processes will be described, although not all of them are discussed in this thesis. Genomic instability means progressive accumulation of DNA damage over time; the stability of genome is continually threatened by exogenous/environmental agents, including chemicals and physical ones, and endogenous agents like errors of DNA polymerase during replication as well as reactive oxygen species (ROS) (7). Normally, the cell detects damage through specific pathways defined DNA damage checkpoint and, depending of the kind of lesion, activates appropriate damage repair systems. During aging the homeostasis of detection and repair systems decreases, making the cell more prone to accumulate DNA damages and this can result in tumour developing (8). Epigenetic represents the reversible heritable mechanisms occurring without any alteration of the DNA sequence and it is involved in the modulation of gene expression (9). In response to the aging process, epigenetic alterations occur, including changes in histone posttranslational modifications, loss of histone proteins and/or the addition of histone variants, affecting also genome stability (10). Proteostasis represents another critical factor involved in longevity regulation (11). It is estimated that about 30% of the newly synthesised proteins are improperly folded and directed towards their degradation. Under normal conditions, cells can use the protein quality control system, which principally includes chaperon proteins, to maintain a state of protein homeostasis. Many diseases that are typical of old age, such as Parkinson's and Alzheimer's diseases, are strongly associated with alterations of proteostasis, which results in proteins aggregation, cellular stress and death. Among the major contributors to aging and age-related pathologies, metabolism plays a pivotal role (12). In addition, it depends on nutrient intake, making it properly conditioned by the diet. Mitochondrial metabolism is one of the main factors involved in longevity regulation and mitochondrial dysfunctions have been classified as an aging hallmark. During aging, alterations of both mitochondrial oxidative metabolism and biosynthetic one occur, making the cell

more susceptible to oxidative stress and alteration of biosynthetic intermediates (6). All the processes described above concern functional alterations occurring in single cell, emphasizing that the aging process depends on a cellular decline that subsequently has consequences on organs, tissues and finally on organism. Many aging-related pathways are evolutionarily conserved from some single-celled organisms to complex multicellular ones (13). This knowledge has allowed us the use of model organisms, more accessible from the experimental point of view, to study this complex biological phenomenon. Indeed, the survival curves of several divergent organisms, ranging from the single-celled yeast to human, are very similar to each other (14) (Fig.2).
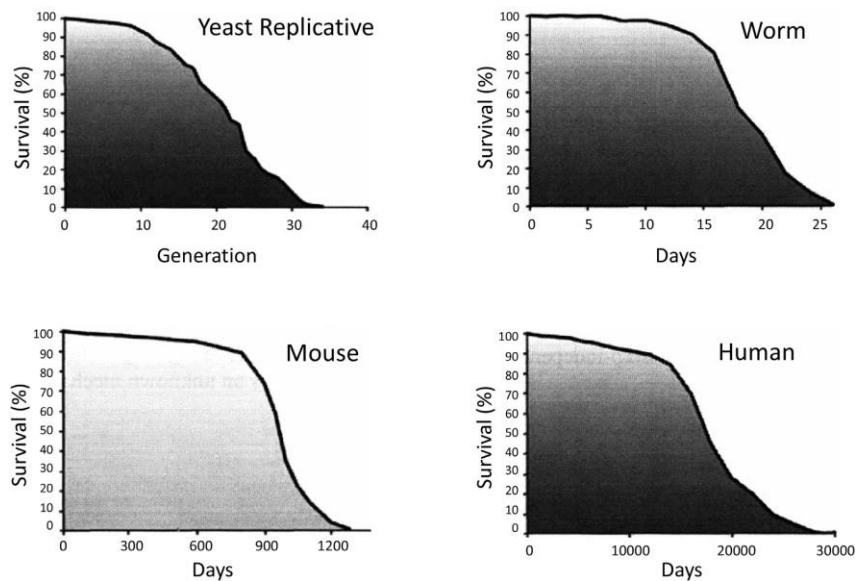

Fig.2 **Survival curves of divergent organisms.** The similarity in the survival curves of different organisms suggests a common regulation of the aging process and the possibility of using simple and experimentally more accessible model organisms to study it. Reproduced from (14).

1.1.1 THE YEAST *Saccharomyces cerevisiae* AS A MODEL FOR AGING RESEARCH

In the context of aging research, useful information has been provided by the unicellular yeast *Saccharomyces cerevisiae*, which has now become a useful model system for the study of molecular mechanisms underlying human longevity (15). It is commonly known as baker's yeast or brewer's yeast and the name *cerevisiae* derives from the old name of beer (16). *S. cerevisiae* is a single-celled eukaryote and, under optimal conditions, divides every 90 minutes through a process of budding in which the generated daughter cells are smaller than mothers. Unbudded yeast cells have a diameter of approximately 5 µm. *S. cerevisiae* can be present in haploid (mating type a or α) or diploid state. Under optimal nutrient conditions, two yeast strains with opposite mating type can form the diploid strain. Conversely, under nutrient-poor conditions, diploid strain can be induced to undergo meiosis and sporulation, forming four haploid spores, two for each mating type. Concerning the metabolism of *S. cerevisiae*, it is defined as facultative anaerobic organism; the capability to grow with a fermentative or respiratory metabolism is a condition that makes this yeast indispensable in the production of bread. It may display either a fully respiratory or a fermentative metabolism or even a mixed respiratory-fermentative metabolism, depending on the growth conditions (for example the type and/or the concentration of a given carbon source and the presence/absence of oxygen).

The first speculations on the possibility of using yeast to investigate complex biologic phenomena started in 1988 (17). A few years later, *S. cerevisiae* became the first eukaryote whose genome was completely sequenced, highlighting the presence of several genes conserved with mammals (18). From this discovery, the interest to use it as a model system arose, also considered that it offers a number of experimental advantages compared with mammalian cells, which are listed below: (i) it has simple nutritional requirements and a relatively fast cell division (ii) it exists in either haploid or diploid states (iii) as facultative aerobe, it can survive in the absence of functional mitochondria, thereby enabling the study of human mitochondrial myopathies (iv) it allows the construction of humanized yeast models, which can reproduce the detrimental effects of some neurodegenerative disorders, like Parkinson's and Alzheimer's, permitting the study of human genes

that lack a corresponding yeast counterpart (v) depending on the carbon source, yeast activates different metabolic pathways, whose dysfunction is responsible for metabolic diseases, such as diabetes and dyslipidaemias (vi) yeast offers the possibility of exploring natural or synthetic compounds, with potential positive effects on human health (19–23). Yeast contributed to our understanding of biochemical pathways, which drive the biogenesis of organelles and membranes, cell growth and division, the response to various endogenous and environmental stresses, as far as the comprehension of more complex dynamics, like cancer, mitochondrial disorders and apoptosis-associated diseases (24). Since yeast undergoes both replicative and chronological aging, it is widely utilized as a model in aging research (25). They represent two complementary models of aging.

Yeast replicative aging simulates the aging process of dividing cells of multicellular eukaryotes, like fibroblasts and leukocytes (25). When growth conditions are optimal and nutrients are available, yeast cells grow in a balanced way and, once they reach a critical size, divide asymmetrically, generating daughter cells smaller than the mother. This phase is defined as exponential growth phase. In this context, replicative lifespan (RLS) is defined as the number of buds generated by a single mother cell in the presence of nutrients before death (26, 27) (Fig.3). In other terms, the RLS defines the replicative potential of a mother cell in the presence of nutrients. Generally, after 25-35 divisions, replicative aged mother cells start to die. RLS analysis is usually performed by separation of daughter cells from mother ones by using a dissection microscope fitted with a micromanipulator. Besides the difference in size, the mother cell is clearly distinguishable by the bud-scars left after separation of the daughters. However more innovative and advanced systems have been developed, among which systems that allow selective killing of daughter cells (25).

When nutrients become limiting, yeast enters a phase of quiescence (stationary phase), in which cell growth and division stop and cells acquire physiological and metabolic features allowing their survival. The length of time that a yeast population survives in this phase is defined as chronological lifespan (CLS) (28).
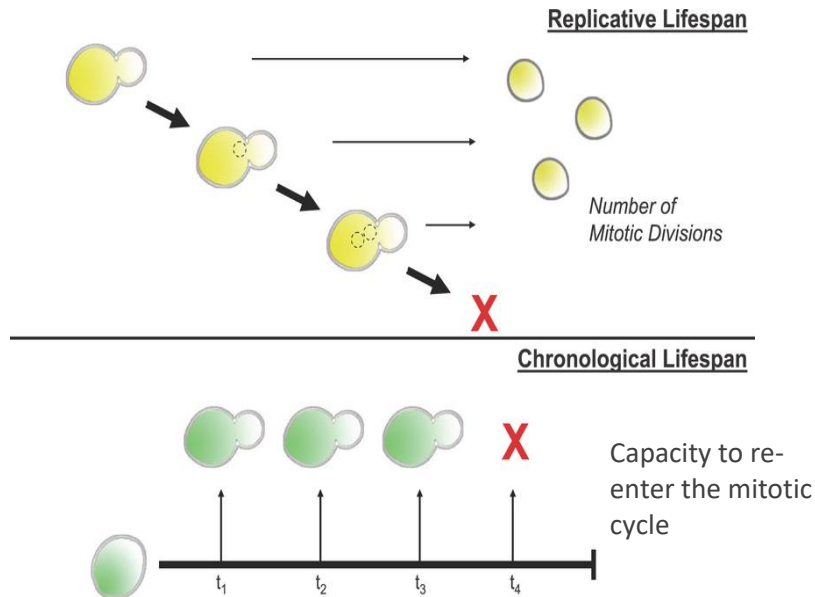
Fig.3 **Schematic representation of yeast replicative and chronological aging.** In the upper part, yeast replicative lifespan is measured by the number of daughter cells generated by the mother in the presence of nutrients before death. At the bottom part, yeast chronological lifespan is measured by the capability of quiescent cells in stationary phase to resume growth upon return to rich fresh medium.

In a standard CLS experiment, yeast cells grow in batch in synthetic complete medium containing 2% glucose (SDC), a four-fold excess of the supplements required for auxotrophies, yeast nitrogen base, ammonium sulphate (nitrogen source), sodium phosphate, vitamins, metals and salts. In these conditions, yeast growth is sustained by a prevalent fermentative metabolism (28). When glucose is depleted, the diauxic shift occurs, resulting in a shift from a respiro-fermentative-based metabolism to a strictly respiratory-based one, in which the C2 compounds previously produced, namely ethanol and acetate, are utilized during the post-diauxic phase. This shift determines a metabolic reprogram, including the activation of stress response genes, gluconeogenesis, glyoxylate and tricarboxylic acid (TCA) cycle, whose outcome influences the length of survival during the stationary phase. Finally, when nutrients are completely exhausted, cells stop dividing and enter a quiescent phase in which they continue to be metabolically active, albeit to a lesser extent. In this context, the measurement of CLS is determined, starting three days from the diauxic shift, by the capability of quiescent cells to resume growth and form a colony once returning to rich fresh medium (28)

(Fig.3). The mean survival of wild-type strains depends on their genetic background and ranges from 6-7 days (DBY746/SP1) to 15-20 days (S288C/BY4700). The growth curve of *S. cerevisiae* in batch cultivation is shown in Fig.4.
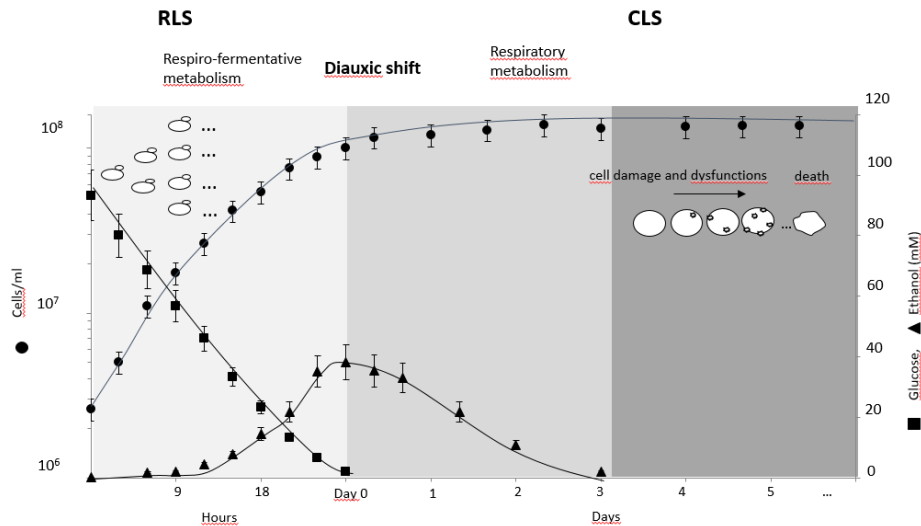
Fig.4 **Growth curve of yeast cells and metabolites production/consumption.** Yeast cells were grown in batches at 30°C in minimal medium (Difco Yeast Nitrogen Base without amino acids, 6.7 g/L), supplemented with 2% w/v glucose. Auxotrophies were compensated with a four-fold excess of supplements. At designated time-points glucose and ethanol concentrations in the growth medium were determined.

Among the physiological and metabolic features of the cells in stationary phase we can remember the following:

- absence of mitotic division, thus cells result unbudded and in G0 phase;
- decrease of metabolism despite cells remain responsive to exogenous and endogenous stimuli. This characteristic allows them to re-enter the mitotic cycle once the environmental and nutritional conditions become favourable again;
- alteration/remodelling of cell wall structure which results in a thickening;
- mitochondria are more rounded and increased in number compared with those in exponential phase, indicating that processes of mitochondrial fission is promoted;
- more resistance to a variety of stresses, such as heat and osmotic ones;
- the intracellular concentrations of both glycogen and trehalose increase;

12

- lipid vesicles become increasingly abundant in the cytoplasm, and triacylglycerol synthesis increases;

- autophagy is activated. It is a highly conserved metabolic process that consists of the *de novo* synthesis of cytosolic vesicles, called autophagosomes, which during their biogenesis sequester damaged organelles and proteins. Once the maturation process has been completed, vesicles fuse with the vacuole of yeast cells and release their content. The cytosolic material previously stored is degraded thanks to the action of specific hydrolases. Finally, degradation products derived from this catabolic process can be transported again to the cytoplasm and recycled by the cell. This pathway is activated by environmental and endogenous stress, including the change in nutrient availability, thus representing an important signal transduction pathway in preserving cellular homeostasis (29, 30).

1.1.2 CARBON METABOLISM IN *S. cerevisiae*

Metabolism consists of biochemical reactions required for nutrient utilization in order to produce energy and intermediates for biomass synthesis, catabolism and anabolism reactions respectively. A crucial component of metabolism is the carbon metabolism, namely all the reactions allowing nutrients utilization, particularly glucose, which represents the hexose monosaccharide preferentially metabolized by yeast. The hexose monosaccharide sugars, including glucose, enter the cell thanks to many transporters, called hexose transporters (HXT) that allow a facilitated diffusion. The transporters mediating this import are at least twenty encoded by the genes *HXT1-HXT17*, *GAL2*, *SNF3*, *RGT2* (31). The last three have peculiar features that distinguish them from the others, even though maintaining a similar amino acid sequence: Gal2 is specific for galactose import, while Snf3 and Rgt2 act as glucose sensors and are activated at high and low glucose concentrations, respectively (32). The transporters show a highly conserved structure within helix transmembrane domain, while a major variability is observed in the N- and C-terminal domains, which are exposed on the cytoplasmic side (31). The expression of these transporters is strictly dependent on glucose concentration. For example, Hxt1 is expressed at high glucose levels and it shows a low affinity for the molecule, while Hxt2 has a low K_M and maximises glucose import in case of

nutrient deficiency (33). Once glucose is imported within the cell, it is phosphorylated and oxidized through the glycolysis (from the Greek word glykis=sweet) pathway, which leads to the synthesis of pyruvate, NADH and two ATP molecules.

Glycolysis pathway is a sequence of ten enzyme-catalysed reactions. The first five steps are regarded as the preparatory (or investment) phase, since they involve the consumption of two molecules of ATP for two phosphorylation reactions. The second half of glycolysis is known as the pay-off phase, which allows the production of two molecules of pyruvate, four molecules of ATP and two of NADH, with a net yield of two ATP molecules.

The pyruvate obtained from glycolysis can follow three major fates: (i) decarboxylation to acetaldehyde which generates acetyl-CoA by the pyruvate dehydrogenase (PDH) bypass; (ii) anaplerotic carboxylation to oxaloacetate and (iii) the direct oxidative decarboxylation to acetyl-CoA by the pyruvate dehydrogenase (PDH) complex, which is located in the mitochondrial matrix.

(i) In the cytosol, pyruvate can be converted to acetyl-CoA by the so-called PDH-bypass pathway that requires the activity of three different enzymes: (a) pyruvate decarboxylase, which converts pyruvate to acetaldehyde; (b) acetaldehyde dehydrogenase (Ald), converting acetaldehyde to acetate; and (c) acetyl-CoA synthetase (Acs), which activates acetate to cytosolic acetyl-CoA that can then be transported unidirectionally into the mitochondrion via the carnitine acetyltransferase system. Cytosolic acetyl-CoA is crucial for biomass synthesis: deletion mutants in this metabolic branch are unable to grow on glucose, while they grow if acetate, which allows the production of acetyl-CoA, is added to the medium (34).

(ii) Carboxylation of pyruvate to give oxaloacetate is an important anaplerotic pathway that allows the replenishment of the TCA cycle. Also in this case, this pathway is essential for cells growing with a fermentative regime: strains carrying deletions in genes encoding Pyc1 and Pyc2, the two isoforms of pyruvate carboxylase, can not grow in a exclusively fermentative regime and with glucose as sole carbon source (35). This is due to the need to maintain an active TCA cycle, albeit to a lesser extent, in order to produce cytosolic oxaloacetate. Indeed, the TCA cycle is fundamental for the production of intermediates for amino acids biosynthesis and oxaloacetate is the aspartate ketoacid (35). However, *pyc1Δ* and *pyc2Δ*, can grow on non-fermentable carbon sources, such as ethanol, because the

glyoxylate shunt is active and allows oxaloacetate generation, bypassing the carbonylation of pyruvate. These two first metabolic fates of pyruvate, fermentation and carbonylation, are highly regulated by glucose levels and represent the main branches that pyruvate follows when the concentration of glucose is elevated, regardless of the presence of oxygen.

(iii) Pyruvate is able to cross the outer mitochondrial membrane, while the passage through the porin across the inner mitochondrial membrane requires the mitochondrial pyruvate carrier (MPC), which represents a link between cytosolic pyruvate metabolism and the TCA cycle (36, 37). Once in the mitochondrial matrix, pyruvate is oxidized to acetyl-CoA thanks to the PDH complex. Both MPC and PDH are enzymatic complexes: MPC is a heteromeric complex consisting of three proteins encoded by *MPC1*, *MPC2*, *MPC3* genes (36). The expression of *MPC1* is not affected by the kind of metabolism taking place in the cell while the other two, *MPC2* and *MPC3*, are specific for fermentative and respiratory metabolism, respectively (38). PDH is a mitochondrial enzyme composed of three major subunits E1, E2, E3, in turn formed by several subunits. The enzyme is the main link between glycolysis and TCA cycle and is subject to a strict regulation. For example *LPD1* transcription, gene encoding an E3 subunit, is repressed by glucose presence (39).

Then acetyl-CoA produced by the PDH complex, fuels the TCA cycle: the main metabolic function of this pathway is the generation of reducing power in the form of NADH for the mitochondrial electron transport chain, through the oxidative decarboxylation of acetyl-CoA. Moreover, as previously said, it also has an important anabolic function by supplying the cell with intermediate metabolites necessary for the biosynthesis of amino acids. The NADH generated from the TCA cycle, as well as that produced from glycolysis and from pyruvate oxidation to acetyl-CoA, is conveyed towards the mitochondrial transport chain, which allows the regeneration of NAD^+, with oxygen as the final electron acceptor and the subsequently generation of H_2O. The mitochondrial electron transport chain is described in detail in (6). In Fig.5 a scheme of the metabolic pathways described above is represented.
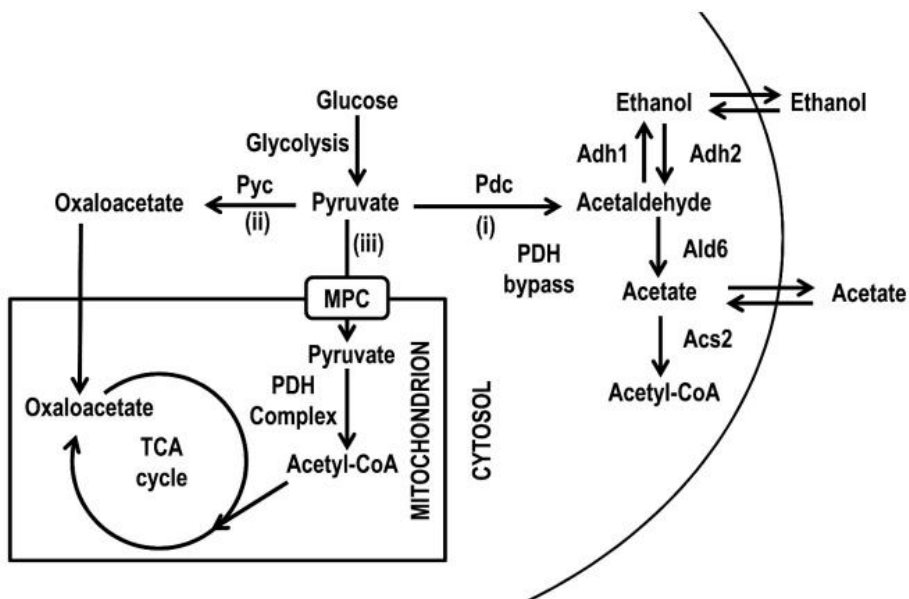
Fig.5 **Key reactions involved in pyruvate metabolism in** *S. cerevisiae***.** Reproduced from (37)

1.1.3 GLUCONEOGENESIS AND GLYOXYLATE CYCLE

As mentioned previously, the ability of yeast cells to shift their metabolism and adapt it to conditions of nutrient scarcity, determines the length of the stationary phase and thus the chronological longevity. Indeed, when glucose is depleted cells consume the earlier produced ethanol and acetate through gluconeogenesis and concurrently they boost respiration (40). The gluconeogenesis pathway retraces glycolysis in anabolic direction, allowing the synthesis of glucose-6-phosphate from some non-carbohydrate carbon substrates, such as glycerol and pyruvate. Glucose is essential not only as energy source, but also as anabolic metabolite. Indeed, the synthesis of nucleotides requires the formation of ribose-5-phosphate obtained from glucose-6-phosphate. However this pathway also involves independent steps from glycolysis: from pyruvate to phosphoenolpyruvate two reactions are required. The former is due to the carbonylation of pyruvate to oxaloacetate by the enzyme pyruvate carboxylase. The latter requires the enzyme phosphoenolpyruvate carboxykinase (Pck1) which converts oxaloacetate into phosphoenolpyruvate. Up to fructose-1,6-bisphosphate, the gluconeogenesis proceeds in anti-parallel sense compared to glycolysis. At this point, the reaction that gives the fructose-6-

phosphate is catalysed by the enzyme fructose-6-biphosphatase (Fbp1). Both Pck1 and Fbp1 are strictly regulated by glucose levels: their expression is activated only when glucose concentrations reach at least 0.005%. Moreover, Pck1 is the enzyme catalysing the rate limiting step of gluconeogenesis and whose activity is influenced by its (de)acetylation state (41, 42). The acetylation/deacetylation of metabolic enzymes plays a crucial role in cell adaptation to changing energy status and it is regulated by the amount of a key metabolic intermediate, acetyl-CoA, that links metabolism with signalling, chromatin structure, and transcription (41). In yeast Sir2, a NAD⁺-dependent protein deacetylase and founding member of Sirtuin family, is the enzyme responsible for the deacetylation and subsequently inactivation of Pck1. Pck1 provides the first and clear evidence of a metabolic enzyme whose (de)acetylation state regulates the gluconeogenic flux. In addition, its acetylation is necessary and sufficient for CLS extension under water starvation, a condition known for increasing lifespan and healthspan in yeast, worms, fruit flies and mammals (41, 43). In addition, the gluconeogenesis pathway is crucial during chronological aging because it allows the production of glycogen and trehalose starting from glucose-6-phosphate. This latter, a glucose dysaccharide, on the one hand allows energy storage and on the other acts as a molecular chaperon allowing the proper folding of proteins damaged principally by oxidative stress (44). As energy reserve, trehalose is preferred to glycogen since cleavage of one glycosidic trehalose bond rapidly provides two glucose molecules, whereas cleavage of a single glycosidic bond in a glycogen molecule provides only one glucose molecule. Concerning the stress protectant role of this sugar, it is due to its intrinsic property to substitute for water molecules and to stabilize membrane structure. In this way it excludes water molecules, protecting cells from desiccation and proteins from denaturation (45). Whereas glycogen accumulation occurs before glucose depletion and peaks at the diauxic shift, trehalose is accumulated in the post-diauxic phase (46). Glycogen reserves are partially utilized to fuel the metabolic adaptations to respiratory-based growth on fermentation products and for trehalose synthesis.

In yeast the reaction from pyruvate to acetaldehyde is irreversible, differently from mammals in which the oxidation of lactic acid to pyruvate can occur and it is catalyzed by the enzyme lactate dehydrogenase. Moreover, when the gluconeogenesis pathway is activated, the availability of pyruvate is reduced, since glucose is depleted. For this reason, a metabolic bypass that allows to obtain substrates for gluconeogenesis is necessary. This bypass is the glyoxylate cycle

which shares some enzymes with the TCA cycle, displaying a fundamental role for anaplerosis of biosynthetic intermediates. Compared to the TCA cycle, glyoxylate cycle lacks decarboxylation reactions. As a result, the compounds with two carbon atoms, which enter the cycle as acetyl-CoA, can be converted to compounds with four or more carbon atoms, such as malate and citrate. As previously said, this pathway shares some enzymes with the TCA cycle, while others are unique enzymes, such as isocitrate lyase (Icl1). In a standard CLS experiment, *ICL1* deletion determines a short-lived phenotype and impairment in acetate metabolism, confirming a critical role of this pathway for chronological survival (42). The glyoxylate cycle is both cytosolic and peroxisomal: the cytosolic enzymes are required during a fermentative metabolism, while the peroxisomal components are required to use the acetyl-CoA units generated from the β-oxidation of fatty acids. The production of acetyl-CoA is necessary to supply this metabolic flux because, as said above, acetaldehyde is not directly convertible into ethanol. Mitochondrial and cytosolic acetyl-CoA are not interconvertible, but ethanol can diffuse through cell membranes, being in both cytosol and mitochondria and converted to acetyl-CoA. In this context, the glyoxylate cycle is fundamental since it allows the anabolism of cytosolic acetyl-CoA to give glucose-6-phosphate. By employing two molecules of acetyl-CoA, succinate is generated. This molecule is transported into mitochondria through the antiport of succinate-fumarate mitochondrial shuttle, Sfc1. Then fumarate is converted to malate by the enzyme fumarase (Fum1), present both in cytosol and mitochondria, therefore converted to oxaloacetate that represents the substrate for gluconeogenesis.

Chronologically aged cells, on the one hand, modulate carbon metabolism by increasing the glyoxylate/gluconeogenesis fluxes and, on the other, modulate/increase mitochondrial respiration. Mitochondria are considered essential organelles, since they provide energy in the form of ATP, as well as the biosynthesis of some amino acids and nucleotides. Their functionality is strictly related to the aging process and aging-associated diseases, because ROS (generally in the form of anion superoxide) are principally generated by electron leakage from the mitochondrial respiratory transport chain, contributing to the chronological aging phenotype. Indeed, an imbalance between the anion superoxide production and the cellular antioxidant capacity, seriously affects yeast CLS (47). However, the influence of these organelles on the aging process also depends on other functions,

like the mitochondrial carbon metabolism and the NAD$^+$/NADH homeostasis as reviewed in (6).

Long-term survival in the stationary phase also includes the possibility of storing and subsequently using lipid reserves. In yeast, lipids, mainly triglycerides, are stored in the lipid droplets. Lipids are mobilized and subjected to β-oxidation in peroxisomes. In aging studies, the proper function of these oxidative cell organelles results to be crucial since peroxisomal deficiency and the inability to perform β-oxidation negatively affects CLS (48).

Thereby, it is evident that metabolism plays a crucial role in regulating the aging process. Considering that there is a strong connection between cellular aging, nutrients and metabolism, we investigated the possible effects of some nutraceutical compounds, in order to identify molecules for pro-longevity interventions, as well as to add useful information in the comprehension of the aging process. In particular, we focused on the study of nutraceutical interventions known to promote healthy aging and to counteract some metabolic disorders, with the aim of identifying metabolic targets that may be useful for the development of anti-aging supplements.

1.2 NUTRACEUTICAL – DEFINITION

Dr Stephen De Felice coined the term "Nutraceutical" from "Nutrition" and "Pharmaceutical" in 1989. The term nutraceutical is being generally used in common language, in commercial messages and marketing but has no regulatory definition. According to De Felice, nutraceutical can be defined as "a food (or part of a food) that provides medical or health benefits, including the prevention and/or treatment of a disease". In nutraceutical definition are also included dietary supplements and medical foods. On the contrary, functional foods represent a different class. Functional foods have no a unique definition but are different from nutraceuticals since they are categorized as food that can possess an additional function/property upon the addition of one or more ingredients. For example, a work highlighted the benefits on health of improving the nutritional quality of eggs by enhancing levels of anti-oxidants, like vitamin E, carotenoids and selenium, and n-3 fatty acids such as docosahexaenoic acid (49). Thus, functional food provides the organism with the required amount of vitamins, fatty acids, proteins,

carbohydrates, etc, needed for its healthy survival. When food is prepared using "scientific intelligence", by adding compounds which are known for possessing anti-oxidant and pro-longevity properties, is called functional food. When functional food allows the prevention and/or treatment of diseases, it is defined a nutraceutical. In contrast, dietary supplements may not be represented as a conventional foodstuff. They are compound that contain vitamins, amino acids and/or fatty acids, which are ingested in pill, capsule, tablet or liquid form (50). Medical foods are prescribed for the treatment of specific diseases and intended for use under medical supervision (4). Regarding the chemical structure, nutraceuticals can be classified as isoprenoid derivatives (terpenoids, terpens and carotenoids), phenolic compounds (isoflavones, flavanones and flavonoids), carbohydrate derivatives (ascorbic acid or vitamin D), fatty acids and more complex lipids (n-3 polyunsatured fatty acids, sphingolipids and lecithins), amino acids derivatives (capsaicinoids, indoles, folate and choline) and minerals (calcium and potassium) (4). Dietary carotenoids are obtained from different fruits and vegetables, such as carrots and spinaches. Carotenoids confer health benefits and are abundant in the macula of the eye, which is responsible for central vision. Macular degeneration is a common disease in the elderly and is among the main visual disorders in this population. Indeed, the treatment of patients affected by this problem with lutein and zeaxanthin (members of the carotenoid family) has been demonstrated to improve the retinal function (51). Other studies have highlighted a role for lycopene (another important member of the carotenoid family, which is responsible for the red colour of tomatoes) in lung cancer prevention thanks to its anti-oxidants activity (52). Indeed, lycopene is unstable and highly reactive towards oxygen and free radicals.

Polyphenols are naturally occurring compounds found in different fruits, vegetables and beverages. These molecules represent secondary metabolites of plants and are generally involved in defence against oxidative stress. Epidemiological studies have shown an inverse correlation between risk of neurogenerative disorders and intake of food rich in polyphenols due to the anti-oxidant properties of these molecules (4). The major source of dietary polyphenols are cereals, legumes (corn, nuts and beans), fruits (apple, grape and cherry) vegetables and beverages (fruit juices, green tea and red wine) (53). For example, a glass of red wine or a cup of green tea contains about 100 mg polyphenols.

Vitamin D, the so-called sunshine vitamin, is another important member of the nutraceutical compounds. Its importance depends on its function in bone metabolism and in prevention of osteoporosis, especially when used in combination with calcium (54). However, other studies have shown its efficacy also in reducing the risk of diabetes and cancer (55).

Nutraceutical fatty acids are becoming of significant interest thanks to their capability to act as biochemical modulators of skeletal biology (56). Indeed, dietary fat sources, which exert health properties on skeletal tissue belong to omega-6 and omega-3 families of essential fatty acids. This is probably due to alteration of prostanoid formation and cell-to-cell communication. Omega-3 fatty acids are found in fish oil and some plants. Among their beneficial properties, are known to have anti-inflammatory effects and to reduce the total content of blood triglycerides (4).

Nutraceutical amino acids consist mainly of glutamic acid, aspartic acid, tryptophan, valine and arginine, which confer health benefits on cancer prevention, immune function, depression, muscle metabolism and thyroid function, respectively (57). Table 1 summarises the main nutraceutical compounds, the foods in which they are found and the benefits they have for health.

Table 1. **Main nutraceutical compounds and health-benefits.**

Nutraceutical compounds	Foods	Biological activities
Lutein and Zeaxanthin	Carrots and spinaches	Retinal function improvement
Lycopene	Tomatoes	Lung cancer prevention
Polyphenols	Cereals, legumes, fruits, vegetables	Anti-oxidant properties, inflammation and cognitive improvement
Vitamin D	Salmons and sardines	Osteoporosis prevention and diabetes reduction
Omega-3 and Omega-6	Fish oil	Skeletal muscle improvement
Nutraceutical amino acids	Red seaweed	Cancer prevention, muscle metabolism and thyroid improvement

1.2.1 THE ROLE OF NUTRACEUTICALS IN ANTI-AGING RESEARCH

In recent years, significant progresses in understanding the aging process have been obtained. From a genetic point of view, it is very complex to reduce the harmful effects of aging on health. For this reason, efforts of many research lines are focused on the discovery of dietary supplements that prevent and/or delay the progression of cardiovascular pathologies, neurodegenerative diseases or cancer. Although there is no a commonly accepted theory for the cause of aging, some evidence has suggested that oxidative stress could play a pivotal role in both aging and age-associated diseases (58). In 1956, Harman proposed the free radical theory of aging. From the point of view of chemical structure, a free radical is a highly reactive molecule with at least one unpaired electron. Since molecules attempt to achieve a stable state, free radicals can react with nucleic acids, lipids of membranes and proteins, causing damages and increasing the risk of contracting cancer and diseases. According to this theory, aging results from accumulation of non-repaired lesions. In this attempt, many studies focused on the discovery of anti-oxidant compounds (59, 60). For example, Villeponteau and co-workers wished to identify an anti-aging nutritional supplement in form of oral formulation that maximally reduced oxidative stress. They tested the YouthGuard nutritional compound (containing anti-oxidants, minerals, vitamins and omega-3 fatty acids) and discovered its beneficial effects on atherosclerosis plaques and clogged arteries (59). Other studies suggest that supplements of vitamin E, vitamin C or both can contribute to decrease the risk of chronic diseases like Alzheimer's and Parkinson's diseases, senile macular degeneration, cataracts and ischemic heart disease (61). A meta-analysis on the link between vitamin E and mortality has been conducted in 2005 (62). The study was conducted on more than 135000 subjects and led to the discovery of the existence of a dose–response relationship between vitamin E supplementation and mortality in randomized, controlled trials. Another study revealing the importance of the dosage of a given nutraceutical compound was carried out in 2001 by Cornelli and collaborators (63). They showed that a low dose of a combination of antioxidants decreased oxidative stress in healthy volunteers, while higher doses of the same compound had a pro-oxidative effect.

Recent published works have shown that nutraceutical compounds could be useful, in combination with conventional drugs, in the treatment of different age-associated pathologies. The following represent some examples:

Alzheimer's and Parkinson' diseases and nutraceuticals: Alzheimer's disease is considered the most common form of dementia. Frequently, it is diagnosed in subjects over 65 years of age (64). There were about 27 million of people with this disease in 2006 and is estimated that it will reach 75 million in 2030 and 131.5 million in 2050 (64). As previously mentioned, different research lines suggest that oxidative stress might have a crucial role in many neurodegenerative disorders, including Alzheimer's disease. Nutraceutical anti-oxidants like curcumin, lycopene, β-carotene may exert beneficial effects by specifically counteracting free radicals and delay Alzheimer's disease development (65). Parkinson's disease is a degenerative disorder of the central nervous system that mainly affects the motor system, resulting in shaking, rigidity and slowness of movement. The symptoms in advanced stages also include thinking and behavioural problems. This is brought about by the destruction of dopamine-generating cells in the substantia nigra, due to unknown causes. Vitamin E and glutathione supplementations have shown promising results in preliminary studies, principally inhibiting oxidative stress, inflammation and apoptosis, as well as ensuring mitochondrial homeostasis (66).

Aging brain and nutraceuticals: human brain aging is associated with different neurobiological changes. For proper brain function, it is important to maintain a balance between support/structural cells, such as glia cells, and functional cells, like neurons. However, with age in the nervous system of mammals structural and neurobiochemical changes occur, such as thinning of the cortex, senile plaques formation, neurofibrillary tangles and cerebral β-amyloid angiopathy (67). Several research lines and clinical studies suggest that herbal supplements and phytochemicals can mitigate the decline in cognitive functions associate with brain aging and pathologies like dementia. Dietary interventions delay this pathological progression thanks to their anti-oxidative, anti-inflammatory and anti-amyloidogenic properties. Constant and moderate consumption of plant foods rich in flavonoids (red wine, tea and berries) determine cognitive improvements. Different preclinical and epidemiological studies suggest the potential of polyphenols to reverse neurodegenerative pathology and the loss of memory, learning and neurocognitive performance (68). Three main processes may account for flavonoid effects: (i) some polyphenols can modulate, directly or indirectly, the

activity of protein and lipid kinases, such as the phosphatidylinositol 3-kinase and mitogen-activated protein kinases, resulting in gene expression of pro-survival proteins and leading to the inhibition of apoptosis caused by neurotoxic species. (ii) Flavonoids promote angiogenesis, favouring the peripheral and cerebral vascular blood flow. (iii) Polyphenolic compounds can react with pro-inflammatory compounds generated during brain aging and/or neurodegenerative disorders and mitigate their detrimental effects, such as oxidative stress (69). However, the potential of many polyphenols to exert their function specifically in the brain depend on their (in)ability to penetrate the blood-brain barrier (BBB). For example, lipophilic compounds can penetrate the BBB, while the flow of hydrophilic compounds through the barrier depends on their interaction with specific transporters (70). The efficacy of isoflavones on memory and cognition depends on their ability to mimic the action of estrogens in the brain and to modulate the synthesis of acetylcholine and neurotrophic factors. Curcumin, the main constituent of the spice turmeric (*Curcuma longa*), improves cognitive function in healthy elderly subjects thanks to its ability to scavenge oxidative and inflammatory stress and to reduce amyloid plaque burden (69). Higher consumption of tea/green tea, rich in epigallocatechin-3-gallate, is associated with a reduced prevalence of cognitive impairments, decreasing the incidence of dementia and Alzheimer's and Parkinson's diseases. This is probably due to its ability to chelate metal ion, principally iron, to promote anti-inflammatory response and to facilitate cholinergic transmission.

Cardiovascular diseases and nutraceuticals: cardiovascular disorders rank among the most common health-related and economic issues worldwide. The foods consumed daily are crucial contributors to cardiovascular risk, including hypertension, cerebrovascular diseases, hearth failure and diabetes (71). Nutraceutical compounds in the form of vitamins, minerals and omega-3 polyunsatured fatty acids are recommended for both prevention and treatment of arterial pathologies (64). Spirulina, a blue-green microalga, rich in vitamins, minerals and carotenoids, has been shown to exert an antihypertensive effect. Indeed, its oral supplementation resulted in systolic and diastolic blood pressure reduction (72). Flavonoids play a major role in in prevention and curing of cardiovascular pathologies, by inhibiting the angiotensin-converting enzyme and the cyclooxygenase enzymes (64). In addition, flavonoid intake is inversely correlated with mortality caused by coronary hearth diseases. For example, omega-

3 fatty acids specifically present in fish affect plasma lipids and hearth diseases, like arrhythmias (73).

Cancer and nutraceuticals: nutraceuticals, mostly phytochemicals derived from dietary or medicinal plants, have been suggested to have chemopreventive activities by modulating the process of apoptosis. Apoptosis is a self-defense mechanism to remove dysfunctional cells such as the precursors of metastatic cancer cells. Indeed, defect in apoptosis mechanism is considered as an important cause of carcinogenesis. A dysregulation of proliferation alone is not sufficient for cancer formation; an inhibition of apoptotic pathway is needed. Cancer cells acquire resistance to apoptosis by overexpressing antiapoptotic proteins (Bcl2, IAPs, and FLIP) and/or by downregulating proapoptotic proteins (Bax, Apaf-1, caspase-8) (74). A wide range of phytochemicals with hormonal activity, the so called phyto-estrogens, are recognized to have preventive effects against prostate and breast cancers (75). Some dietary supplements can interact with drug cancer therapies and modulate/amplify their action mechanism. Probably, the most-well documented nutraceutical-drug interaction is the potential for St John's Wort, a herbal supplement which can be bought at the food store, to induce cytochrome P4503A4, a major cytochrome involved in the activation of many cancer drugs (76). Regarding the treatment of the late-stage cancers, nutraceutical interventions seem to have promising effects. For example, green tea polyphenols inhibit neovascularization and angiogenesis, influencing the development and the possible metastasis of existing cancers.

Diabetes, obesity and nutraceuticals: metabolic syndromes represent typical diseases of the elderly, which increase the propensity to cardiovascular diseases and type II diabetes. Occurrence of both metabolic syndromes and diabetes and the associated vascular diseases share different pathogenic features like inflammation and persistent platelet activation. Some nutraceutical compounds have been shown to prevent or delay diabetes complications (like neural dysfunctions) through protection against oxidative stress. For example, vitamin C, a chain-breaking antioxidant that scavenges ROS directly, reduces sorbitol levels and lipid peroxidation in animals with diabetes (77). Also vitamin D deficiency is often associated with obesity and type II diabetes, probably due to its deposition in the lipid stores where it becomes less bioavailable. Two randomized controlled trials that used combination of calcium and vitamin D treatment found that it may reduce the risk of type 2 diabetes (78). Also flavonoids have beneficial effects against type

II diabetes. Isoflavones are phytoestrogens with structural and functional similarities to human estrogens. The consumption of soy isoflavones has been associated to lower incidence and mortality rate of type II diabetes and osteoporosis (64).

Obesity represents a global public health problem with more than 300 million people involved. It is a risk factor for disorders like hypertension, thrombosis, hyperlipidaemia and diabetes. Nutraceutical approaches are currently being investigated on a large-scale as useful and potential treatment for obesity. Herbal stimulants, such as caffeine, chitosan and green tea, have anti-obese properties and facilitate body weight loss (79). Different studies have demonstrated the effects of nutraceutical from fruits or plants in reducing oxidative stress and promoting healthy aging in invertebrate models, including yeast (80). In this thesis we have evaluated the possible effects of two polyphenols and nutraceutical compounds, namely resveratrol and quercetin, on yeast chronological aging.

1.2.2 RESVERATROL

Resveratrol (3,5,4'-trihydroxystilbene) (RSV) is a nonflavonoid polyphenol and nutraceutical compound on which a number of research lines are focusing due to its pharmacological potential. Its chemical structure consists of two phenolic rings bonded together by a double bond, which is responsible for the isometric cis- and trans- forms of RSV(Fig.6).

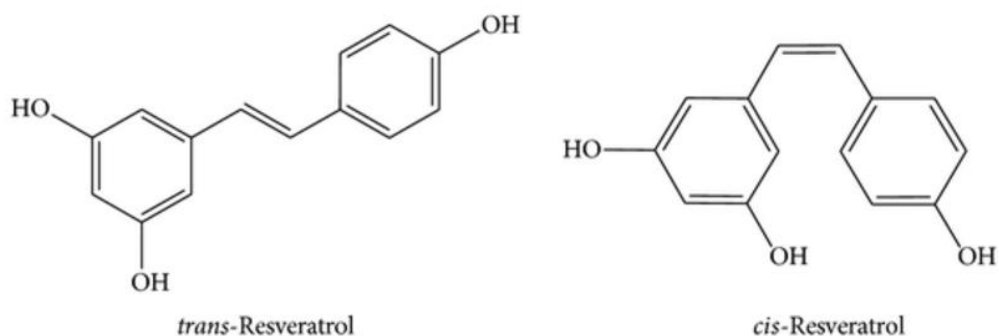Fig.6 **Chemical structure of trans- and cis-resveratrol.**

The trans-isomer is the most stable from the steric point of view. The chemical structure of RSV determines a low water solubility (<0.05mg/mL), which affects its

absorption. To increase its solubility, ethanol (50 mg/mL) or organic solvents, like dimethyl sulfoxide (16 mg/mL), may be used. Since RSV shows lipophilic features, it is highly absorbed in the intestine, through passive diffusion or with transporters like integrins.

Once in the bloodstream, RSV can be found in the form of glucuronide, sulfate or free. This latter can bind albumin and lipoproteins, like LDL, and promote mobilization and lipid metabolism (81). RSV is a phytoalexin, with antifungal and antibacterial properties, found in many plants including grapes, peanuts, and berries. RSV was first isolated in *Veratrum grandiflorum*, or white hellebore plant, in 1940 (82). Grapevine and the products derived therefrom, such as grapes and red wine, are sources of RSV (83).

In particular, RSV intake with red wine has been proposed to explain the "French Paradox", a term coined in 1980 that describes the apparently paradoxical epidemiological studies that in France revealed low rates of coronary heart diseases despite a diet rich in saturated fats (84). This apparent paradox has been ascribed to beneficial properties of RSV linked to French dietary habits of constant and moderate consumption of red wine, in which the concentrations of RSV are about 0.1–14.3 mg/L. As a natural compound, RSV utilization as a nutraceutical and therapeutic compound for several diseases has been widely researched in preclinical studies. For example, RSV modulates the nuclear factor κB signaling pathway, which regulates inflammation, immune response to infection and cellular response to endogenous and environmental stimuli.

In addition, it has been shown to significantly inhibit the IGF-1R/Akt/Wnt pathways and activate p53, therefore influencing tumour development and metastasis (82). One of the biological activities that has been ascribed to RSV involves its antioxidant properties. Because of their high reactivity, free radicals have the potential to be extremely detrimental and harmful on human health. Radical chain reactions consist of three distinct phases: initiation, which frequently is a homolytic cleavage event, propagation, in which the reactive free radical generated can react with stable molecules to form new free radicals, and so on. Finally, the termination step occurs when two free radical species react with each other to form a stable, non-radical adduct.

Given the hazardous nature of free radicals, antioxidant molecules are often added to foods to prevent the radical chain reactions. They act by inhibiting the initiation and/or propagation step, leading to the termination of the reaction and reducing

the oxidation process. In particular, RSV is both a free radical scavenger and an antioxidant molecule thanks to its ability to induce the activities of several antioxidant enzymes (85, 86).

The capability of polyphenols to counteract oxidative stress depends both on the redox properties of their phenolic hydroxy groups and the potential for electron delocalization across their molecular structure. For RSV, three different mechanisms have been proposed in order to explain its antioxidant properties: (i) stabilization of the unstable semi-reduced form of ubiquinone (the major site for ROS production along the electron transfer chain into mitochondria) (ii) scavenging of anion superoxide (iii) inhibition of lipid peroxidation caused by Fenton reaction products (85). However, some studies suggested a pro-oxidant effect of RSV depending on cell type, RSV concentration and the amount of oxidative stress to counterbalance (85, 86). These results could explain the anticancer and apoptotic inducing properties of RSV, besides the cytotoxicity of a diet excessively rich in polyphenols.

Some results provide interesting insights into the effect of this compound on the lifespan of mammalian cells and model organism like yeast, highlighting its potential in the comprehension of the aging process and age-related pathologies (47, 87). In this context, a molecular screen for the detection of compounds able to activate the sirtuin SIRT1, led to the discovery that RSV activates SIRT1 *in vitro*, feature that allows to define RSV as a sirtuin activator compound (STAC) (23). Sirtuins comprise an evolutionarily conserved family of NAD$^+$-dependent histone and protein deacetylases with several biological functions, many of which are linked to the aging process (88). The founding member of this family, Sir2, was initially characterized in yeast as a factor involved in transcriptional silencing at mating type loci and telomeres (89). Later was discovered the involvement of Sir2 in the regulation of the aging process and this topic will be explored in the following paragraphs.

RSV and similar polyphenols (flavones and stilbenes) were reported to activate SIRT1 *in vitro* with a direct allosteric activation, which lowered the peptide substrate K_M (23). However, other studies have also hypothesized that RSV could bind the fluorophore on the peptide during the molecular screen rather than directly activate SIRT1 (90). However, considering that RSV has effects on SIRT1 also *in vivo* studies, the idea that this Sirtuin is effectively activated by RSV, directly or indirectly, is supported (91).

Also the deacetylase activity of Sir2 further increases in the presence of RSV, both *in vitro* and *in vivo* (23, 86). Particularly, we demonstrated an increase in deacetylation activity of Sir2 specifically on its gluconeogenic target, Pck1 (86). The allosteric activation mechanism proposed for RSV includes the binding of this molecule to the N terminal domain of SIRT1, resulting in a lowering of the K_M for its substrates (92). This regulatory domain is also present in Sir2. Indeed, the interaction between Sir2 and Sir4 requires this domain and enhances the Sir2-mediated deacetylation of histone H4K16. RSV, by binding this domain, could increase the affinity for Pck1 (86).

1.2.3 QUERCETIN

Quercetin (3,3',4',5,7-pentahydroxyflavanone) (QUER) is one of the important flavonoids (the term is derived from the Latin word "flavus," meaning yellow) present in different plants and fruits such as onions, apples, tea and capers, and it is known for its anti-inflammatory, antihypertensive and antioxidant properties (93) (Fig.7).
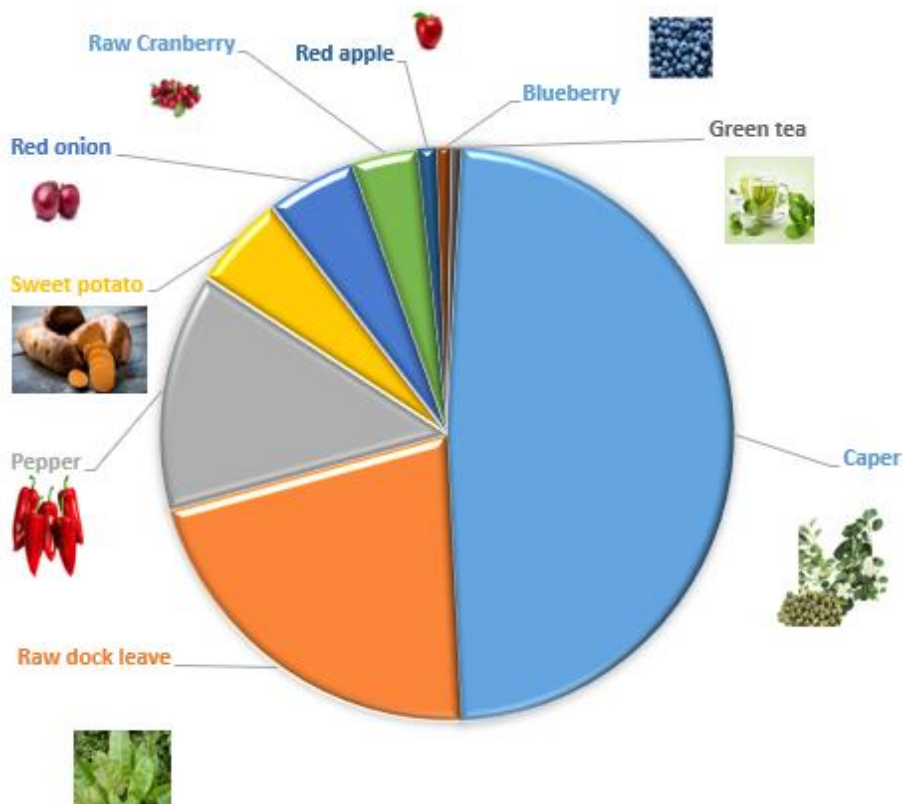
Food and Beverage Source	Quercetin content (mg/100g)
Caper	180.2
Raw dock leave	19.94
Pepper	50.6
Sweet potato	20.55
Red onion	19.94
Raw cranberry	14.01
Red apple	4.45
Blueberry	3.12
Green tea	2.7

Fig.7 **Foods and beverages rich in quercetin.** Information provided by (Muhammad et al., 2018).

Its molecular structure comprises a skeleton of diphenylpropane, namely two benzene rings linked together by a pyranic ring (heterocyclic ring). More precisely, QUER is a flavanol because it presents a hydroxyl group in position 3 of the ring C, which can also be glycosylated (Fig.8). The most common QUER glycoside is the quercetin-3-O-β-glucoside. The biosynthesis of QUER is a defensive response of some plants to environmental stress. Flavonoids often function as protection from ultraviolet sunlight and lipid peroxidation (94).

QUER is poorly soluble in hot water (0.06 mg/mL) and insoluble in cold water, quite soluble in alcohol like ethanol (2 mg/mL), lipids and organic solvents like dimethyl sulfoxide (30 mg/mL). Concerning QUER availability, namely the amount that is absorbed and available for physiologic activity or storage when it is orally administered, depends on its molecular structure (95). In particular, differently from its form in several supplements, most of the QUER in foods is linked to a sugar molecule, as previously said. Differences in QUER-conjugated glycosides affect its bioavailability.

For example, in onions the most common form of QUER is QUER-3-glucoside (isoquercetin) and is absorption is about 52%. On the contrary, the absorption of a standard QUER supplement is 24% (95). Generally, QUER glucoside, compared with QUER aglycone, has major availability. This is probably due to two factors: (i) QUER glucoside is more water soluble than QUER aglycone and (ii) the glycosylated form is absorbed with high efficiency thanks to the sodium-dependent glucose transporter 1.
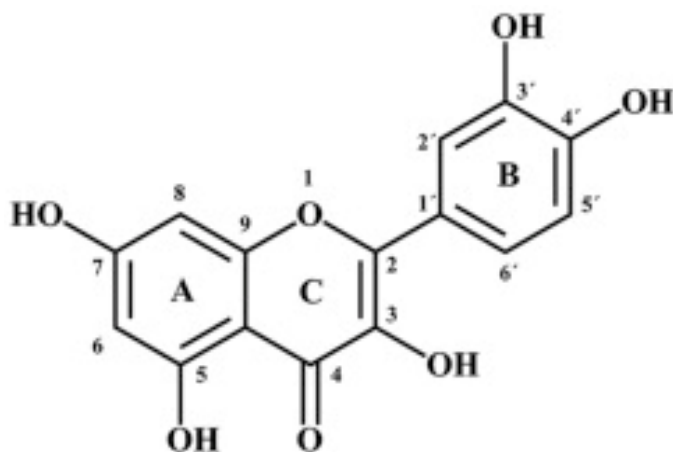

Fig.8 Chemical structure of quercetin.

As antioxidant flavonoid QUER reduces the negative effects of free radicals through the quick transfer of hydrogen atoms to the radicals. Thus, QUER counteracts oxidative stress, which contributes to diseases like atherosclerosis, diabetes and ischemic hearts. QUER has been studied extensively in several models, such as the nematode *Caenorhabditis elegans*, mammalian cell cultures, mice and humans (93). Many beneficial effects of QUER were reported for *S. cerevisiae* (96–98). For instance, a short-term pre-treatment with QUER increased oxidative stress resistance of H_2O_2-treated cells and increased CLS (97). The antioxidant protection of QUER was also ascribed to the capability to chelate transition metals, such as iron and copper, that determine the conversion of H_2O_2 to the reactive hydroxyl radicals.

However, another study highlighted that QUER increases yeast RLS under stress exposure through the activation of specific signal transduction pathways (96). Indeed, transcription regulators Yap1 and Msn2/4 play a crucial role in ensuring an adaptative response to oxidative stress in yeast. The pre-treatment with QUER

determined an efficient response to oxidative stress Msn2/4-dependent, indicating that QUER increased stress resistance both preventing protein oxidation by providing its hydrogen atoms and mediating a transcriptional response (96). A microarray analysis revealed changing in gene expression following QUER treatment of yeast cells (98).

Particularly, QUER induced several genes related to carbohydrate metabolism that are under catabolite repression and whose expression increases in response to glucose depletion, as after the diauxic shift. Among the up-regulated genes, there are *GSY2* necessary for glycogen synthesis, *GPH1* and *GDB1* encoding glycogen phosphorylase and debranching enzyme, respectively, and *TPS1* for trehalose biosynthesis. In addition, QUER supplementation increased the expression of genes encoding proteins of the cell wall integrity pathway, like *SLT2*. By Western analysis with anti-phospho-p44/42 antibody that recognizes the active phosphorylated form of Slt2, it has been shown that QUER effectively activates this pathway (98). Both *in vitro* and *in vivo* studies have shown that QUER activates SIRT1, directly or indirectly (23, 99). However, given the peculiar molecular structure of polyphenols, including quercetin, the stimulation of SIRT1 activity is influenced by their stability and metabolism (100). Indeed, the metabolism of QUER in human cells leads to the formation of SIRT1-inhibitory metabolites, including quercetin-3-O-glucuronide.

This result underlines that different metabolites of the same substance can have opposite effects on the specific activity of a molecular target, with different repercussions on organ/tissue/ organism.

1.3 PATHWAYS THAT LINK METABOLISM, NUTRIENT AVAILABILITY AND LONGEVITY IN YEAST

Given that different nutritional sources and/or their absence have a strong impact on the type of metabolism adopted by yeast cells and their longevity, the main metabolic regulators involved in the response to nutritional stimuli will be listed below.

1.3.1 Ras/PKA PATHWAY

This pathway is known as the most important glucose-sensing signalling pathway in *S. cerevisiae*. About 90% of the genes involved in the diauxic shift are regulated by this pathway (101). The protein kinase A (PKA) is a heterotetramer consisting of two negative regulatory subunits encoded by the *BCY1* gene and two catalytic subunits encoded by *TPK1*, *TPK2* and *TPK3* genes with share high sequence homology (102). These three genes are considered partially redundant given that is necessary and sufficient that only one of them is functional to have a vital phenotype, while deleting all three genes leads to a lethal phenotype. However, some authors have proposed the possibility of a modulation of specific and independent molecular targets by the proteins encoded by these genes, highlighting the need for further investigations (103). The regulation of PKA is determined by the presence of adenosine cyclic monophosphate (cAMP).

When the regulatory subunits Bcy1 binds the cAMP loses affinity for the catalytic subunits and separates from them. In this way, the inhibitory action of the regulatory subunits on the PKA activity is not performed, resulting in kinase activation. This highlights that the level of cAMP is crucial for the activation of PKA: it depends on cAMP production thanks to the adenylate cyclase encoded by *CYR1* and its utilization thanks to the low and high-affinity phosphodiesterase activities, encoded by *PDE1* and *PDE2*, respectively. PKA is able to regulate through an inhibitory phosphorylation the activities of both Pde1 and Pde2: an *in vitro* assay has shown that PKA phosphorylates these phosphodiesterases (104).

Although a direct *in vivo* phosphorylation has not been demonstrated, is hypotized that PKA inhibits the activities of these phosphodiesterases at high glucose levels. On the other hand, Cyr1 activity is stimulated by Ras1 and Ras2 GTPases, and Gpa2, α-subunit of the heterotrimetric G protein. Ras1 and Ras2 have similar functions, but their expressions differ. Ras1 mRNA expression collapses when cells are growing in media containing non-fermentable carbon sources, such as glycerol or pyruvate (105). These G proteins are activated when bind the guanyl-nucleotide factor GTP and in turn phosphorylate and activate Cyr1, promoting cAMP production.

A genetic study have shown that a double deletion in *RAS2* and *CYR1* causes lethality, which is suppressed upon *PDE3* deletion, confirming the involvement of

these proteins in the modulation of cAMP levels (106). Once active, PKA acts on different molecular targets: it activates a signalling cascade that allows the transcription of genes for the synthesis of ribosomal proteins, inhibits the transcription factors Adr1 and Msn4, required for the transcription of genes necessary for the diauxic shift, and the kinase Rim15 (107).

1.3.2 Snf1

Sucrose non-fermenting 1 (Snf1) protein kinase, a yeast homologue of mammalian AMP-activated protein kinase, is fundamental for the growth on sugars other than glucose, such as maltose or galactose, and non-fermentable carbon sources like ethanol and glycerol, playing a fundamental role in the shift from fermentative to oxidative metabolism in response to glucose deprivation.

Moreover, Snf1 kinase has a crucial role in the cellular response to several forms of stress, such as salt stress and heat shock. The Snf1/AMPK protein kinases are conserved throughout all eukaryotes and share an αβγ heterotrimeric structure (108). The catalytic α-subunit comprises the kinase domain and the regulatory domain. The former displays 1 sub-domains and contains the activation loop (also called T-loop). The latter domain in both yeast and mammals contains an auto-inhibitory sequence (AIS), which was shown to inhibit the kinase activity. The function of the γ subunit (Snf 4 in yeast) is to regulate the activity of the α-catalytic subunit (109). The β-subunit acts as a scaffold keeping the α and the γ subunits together. Phosphorylation of a conserved threonine within the T-loop of the catalytic subunit is fundamental for Snf1/AMPK activity. At high glucose concentrations, Snf1 assumes a molecular conformation that causes the auto-inhibition of the protein. When glucose is depleted Snf4 binds Snf1, allowing an initial activation of the protein. The complete activation is achieved thanks to the phosphorylation of threonine 210 by several kinase activities. Snf1 is also regulated at the level of subcellular localization. However, the molecular details and how glucose influences its activities still remain unclear. Once in active form, Snf1 affects many glucose-repressed genes by inhibiting the transcriptional repressor Mig1. Indeed, Snf1 phosphorylates Mig1 and promotes its nuclear export (110). Snf1 is also required for the transcription of genes by Cat8 and Sip4 necessary for

derepression of a variety of genes under non-fermentative growth conditions and after the diauxic shift, like *FBP1*, *PCK1* e *ICL1* (111).

1.3.3 TORC1/Sch9, CALORIE RESTRICTION AND HORMESIS

The TORC1/Sch9 pathway is not directly activated by glucose although it has effects on its metabolism. This pathway is the main responsive signalling system for the amino acids and, depending on their availability, it is activated. The acronym TOR means Target of Rapamycin, a molecule that inhibits the complex. TORC1 comprises the regulatory subunits Lst8, Kog1 and Tco89, and the kinase subunit Tor1 (112).

The EGO complex, composed of Ego1, Ego3, Gtr1 and Gtr2, mediates TORC1 activation by amino acids (113). Gtr1 and Gtr2 are Ras-family GTPases and orthologues of the metazoan Rag GTPases, while the Ego1 and Ego3 are the likely functional homologue of the mammalian Ragulator complex. To activate the system the mediators Gtr1/2 must be in the state Gtr1^{GTP}-Gtr2^{GDP}. This system is in turn regulated by the Seh1-Associated Complex (SEAC) consisting of 8 proteins divided into two sub-complexes: the former is the SEAC Inhibiting TORC1 (SEACIT) complex, while the latter is the SEAC activating TORC1 (SEACAT) complex.

SEACIT acts as a GTPase activating protein (GAP), allowing the hydrolysis of GTP in GDP on Gtr1, which results in the pathways inhibition following amino acids deprivation (114). When amino acids are present, SEACAT inhibits SEACIT, allowing the switch from the inactive form Gtr1^{GDP} to the active one Gtr2^{GTP}. The main target of TORC1 is Sch9, a kinase belonging to the AGC family proteins. AGC is an acronym deriving from protein kinase <u>A</u>, protein kinase <u>G</u> and protein kinase <u>C</u>. Sch9 is the main effector of TORC1 and is regulated by numerous phosphorylations at the C-terminal necessary for its activation (115). In addition to being one of the major regulators of gene expression of ribosomal proteins, the TORC1 pathway orchestrates the proper entry into the stationary phase. In this context, it regulates the activity of the kinase Rim15, which integrates the signals coming from different nutrient-sensing pathways. Indeed, also PKA phosphorylates and inhibits Rim15 activity (116).

This means that both TORC1/Sch9 and PKA signalling pathways converge on the protein kinase Rim15 to control entry into G0. Indeed, a work demonstrated that Sch9 interacts with Rim15 *in vivo* and phosphorylates it (117). Rim15 activity is strongly related to its phosphorylation state: when the PKA or TORC1/Sch9 pathways are activated, Rim15 is in the phosphorylated inactive form and is localized in the cytoplasm. Following nutrient depletion the upstream pathways are repressed, leading to an active dephosphorylated form of Rim15 that can perform its functions in the nucleus. Indeed, once activated, the kinase leads to the phosphorylation of Msn2 and Msn4 that function as a dimer, and Gis1. Msn2/4 are a direct target of Rim15, at least in *in vitro* studies (118). Gis1, on the other hand, is indirectly activated by Rim15, which phosphorylates the dimer Igo1/2. In this phosphorylated and active form, Igo1/2 inhibits the Cdc55-protein phosphatase 2A (PP2A^{Cdc55}), favouring the maintenance of an active phosphorylated form of Gis1 (119).

The two transcription factors Gis1 and Msn2,4 have zinc finger domains through which interact with specific DNA sequences. The former is more specific for the post diauxic shift element (PDSE) sequences, while the latter binds preferentially stress responsive element (STRE) sequences. Among the genes induced following the activation of these transcription factors there are the environmental stress response (ESR) genes that control different cellular processes, ranging from metabolism to cell cycle regulation and stress response and adaptation. Another important effector under the control of Sch9 is the transcription factor Hap4. Hap4, besides controlling the sphingolipid metabolism, is part of a complex of proteins that also comprises Hap2, Hap3, and Hap5, which acts primarily as a transcriptional activator of genes regulating the complexes involved in the electron transport chain (113, 120). This aspect implies that Sch9 activity is strictly related to the mitochondria functionality and respiration performance. For example, strains with an altered and defective TORC1/Sch9 signalling have a higher density of mitochondrial respiratory-chain enzymes, increase coupled respiration and enhance ROS production during the exponential phase, resulting in an adaptive signal that extends CLS (121).

The idea that ROS can act as signal molecules and induce an adaptive response to oxidative stress resulting in beneficial effects on the aging process, is supported by the concept of hormesis, in this case we refer specifically to mitohormesis. King Mithridates VI used to assume small amounts of poisons to protect himself from

recurrent attempts at attacks on his life through poisoning. He was confident that he could immunize himself by the constant intake of small doses of poison. The concept of hormesis is very similar: small doses of toxic stimulus, in this case of oxidative stress, can have beneficial effects and provide adaptation, allowing an efficiently response against wider doses of toxic stimuli of a similar nature.

By using genetic and pharmacological yeast models of respiratory deficiency, it has been demonstrated that a reduced TORC1/Sch9 signalling reconfigures mitochondrial respiration towards a state that increases both mitochondrial membrane potential and ROS production during exponential growth, which results in an adaptive ROS signal that increases CLS (122).

A similar adaptive response is observed when imposing a calorie restriction (CR) regime or extreme CR, both conditions that extend longevity in many model organisms (123). In yeast, CR is obtained by reducing the content of glucose from standard 2% until 0.5%, even if other concentrations have been used (124). A severe form of CR is achieved by transferring post-diauxic cells from their expired medium to water (42, 125). Also in this case, the adaptive response to the stress condition given by the reduced glucose content in a condition of CR is mediated by the TORC1/Sch9 pathway, since CR fails to further increase the RLS of cell lacking *SCH9* or *TOR1*, demonstrating that these deletion mutants are genetic mimics of CR (126). A scheme of Ras/PKA and TORC1/Sh9 is shown in Fig.9.
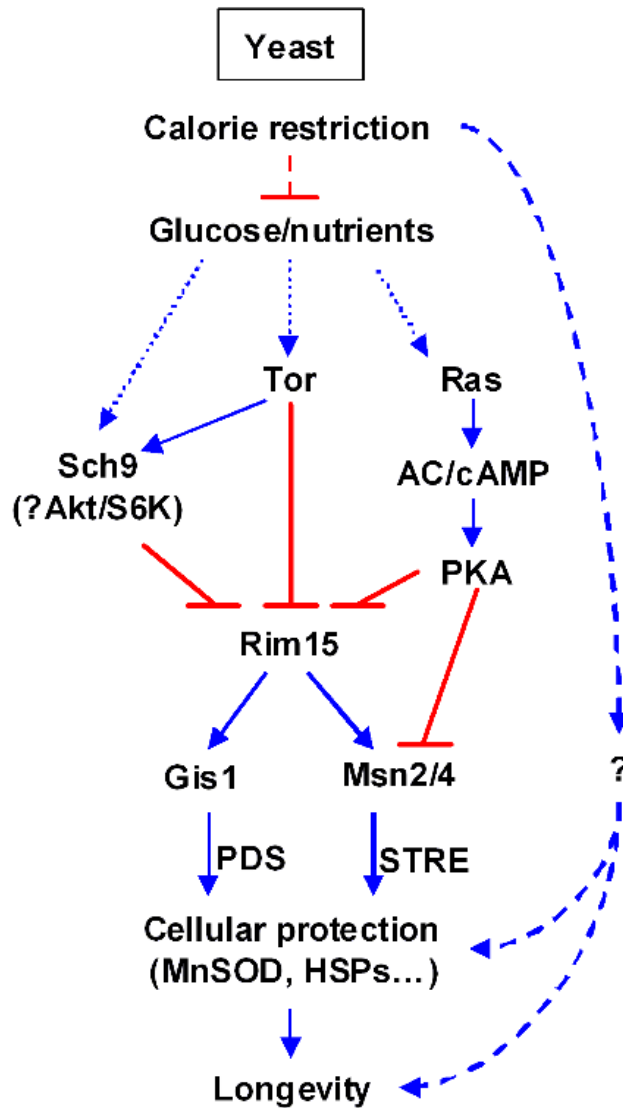
Fig.10. Schematic representation of Ras/PKA and TORC1/Sch9 pathways in yeast. In yeast, nutrient-sensing pathways controlled by Ras/PKA and TORC1/Sch9 converge on the protein kinase Rim15. In turn, the stress response transcription factors Msn2, Msn4, and Gis1 allow the transcription of genes for stress response, which leads to RLS extension. Adapted by (Wei et al., 2008).

1.3.4 SIRTUINS

Sirtuins are a family of NAD$^+$-dependent protein deacetylases. The silent information regulator 2 (Sir2) of *S. cerevisiae* is the founding member of this family and regulates silencing at the mating-type loci, telomeres, and ribosomal DNA (rDNA) loci (127). In mammals seven Sirtuins are present, termed SIRT1-7, which share the sequence homology of catalytic domain with yeast Sir2. The *SIR* genes were first identified in the context of a screening of haploid mutants unable to sexually conjugate with cells of the opposite mating type (128). As mentioned in the section 1.2, the mating of yeast only occurs between two haploid strains, which can be either the a or α mating type, leading to a diploid strain *MAT*a/*MAT*α in which the co-expression of both a and α genes determines the silencing of the system. Mating type is determined by a single *locus*, *MAT,* localized on chromosome III in *S. cerevisiae*, which in turn governs the sexual behaviour of both haploid and diploid cells.

Experimental evidence revealed that through a genetic recombination, haploid yeast can switch mating type, suggesting the presence of at least one other mating-related gene, which normally was maintained silent. Further studies confirmed this hypothesis, showing the presence, in addition to the *locus MAT*, of two *loci* both localized on chromosome III: one was defined homotallic mating-type right arm (HMR) and the other homotallic mating-type left arm (HML), respectively at the right and left of the centromere. The genes that are responsible for the silencing of these two loci are *SIR2*, *SIR3*, *SIR4* and, to a lesser extent, *SIR1*. A similar silencing mechanism was later demonstrated at telomeres and rDNA loci. *SIR2*, *SIR3* and *SIR4* are all required for silencing at both mating type loci and telomeres but only *SIR2* is required for silencing at rDNA (129, 130).

Silencing causes a more compact, inaccessible regional chromatin structure, as demonstrated in (131). In particular, the silencing of these three regions occurs in different ways: at *HMR* and *HML loci*, Sir2 forms a complex with Sir1/3/4 that binds the DNA sequences thanks to a scaffold formed by Rap1 and Abf1 proteins. Sir2 locally deacetylates an adjacent nucleosome on histone 3 (H3) and histone 4 (H4) tails, promoting the spread of the SIR complex across the silenced domains. For telomeric silencing, Sir2 forms a heterodimer with Sir4 that binds the repeated regions of telomeres through the DNA-binding proteins Rap1 and Ku70:Ku80.

Following the deacetylation of lysine 16 on H4 by Sir2, Sir3 binds with high affinity this deacetylated residue and mediates the binding of other Sir2/4 complexes

allowing the spread across the sub-telomeric regions. These interactions mediated by the DNA-binding proteins ensure that the action of the SIR complex is site-specific. The silencing of rDNA sequences requires the regulator of nucleolar silencing and telophase (RENT) complex in which Sir2 forms a complex with Net1 and Cdc14. The main function of this complex is to stabilize these regions in order to avoid their excision through homologous recombination that could determine the production of the pro-aging extra chromosomal rDNA circles (ERCs). In fact, the first evidence of a strict connection between silencing, Sir2 activity and longevity, was seen in yeast in a context of RLS (132). Sir2 activity is required for RLS since this latter is dependent on the stability of the rDNA repeats.

Regardless of the silenced *locus*, Sir2 is the protein of the complex that effectively mediates the deacetylation of the histone residue. The reaction involves the consumption of a molecule of NAD^+, which is used as acceptor of the acetyl group, with the formation of ADP-Ribose-O-acetyl (O-AADPR) and nicotinamide (NAM). The scheme of the reaction is shown in Fig. 11. Sir2 deacetylase activity is influenced by both these reaction products. The former promotes the link of Sir2 with Sir3, favouring the formation of SIR complex on DNA in *in vitro* studies (133). The latter inhibits Sir2 activity, both *in vitro* and *in vivo* (47, 134). For more details on NAD^+ homeostasis that affects Sir2 activity see (6) in Chapter 4. Since this Sir2-mediated reaction depends on the availability of NAD^+, a strict connection between Sir2 activity and metabolism is widely accepted.
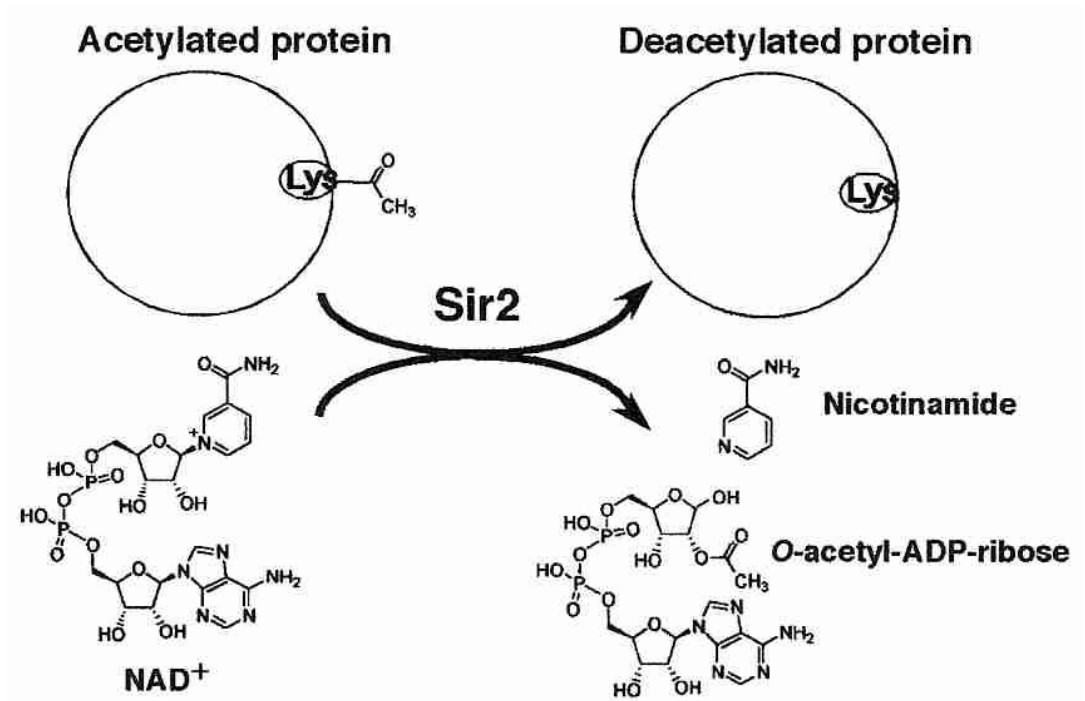
Fig.11 **Sir2 deacetylation reaction.** Sir2 catalyses an NAD+-dependent deacetylation of histone tails or other non-histone acetylated proteins; the reaction transfers the acetyl group from acetylated lysine residues to the ADP -ribose moiety of NAD+, generating deacetylated targets, NAM and O-AcADPR.

This is supported by the knowledge that Sir2 can also deacetylate cytosolic substrates and that different metabolic enzymes are subject to (de)acetylation also in mammals too. For example, SIRT1, the mammalian orthologue of Sir2, positively modulates the activity of acetyl-CoA synthetase (AceCS1) through its deacetylation (Hallows et al., 2006). In *S. cerevisiae*, Sir2 regulates the activity of Pck1, which is inactivated by the Sir2-dependent deacetylation, explaining why Sir2 plays an antagonist role in the extension of CLS, also in extreme CR condition, such as that obtained by resuspending chronological aging cells in water (41). Indeed, both the survival in exhausted medium and in water require a metabolic rearrangement that involves both oxidative metabolism and gluconeogenesis.

SIR2 inactivation is sufficient to determine a faster/efficient ethanol depletion and to further increase CLS in extreme CR condition (40, 125).

Moreover, with the lack of Sir2, the increase in the acetylated active form of Pck1 occurs with the resulting development of a metabolic scenario in which the

glyoxylate/gluconeogenic fluxes are enhanced, while respiration is reduced (47). This means that following *SIR2* inactivation, ethanol utilization is conveyed towards the aforementioned pathways and its anabolic utilization favours the storage of reserves, namely glycogen and trehalose, and subsequently increases CLS. This underlines that ethanol metabolic fate and utilization as carbon/energy source and not just its mere presence, affects chronological longevity (40).

The first evidence that Pck1 activity was influenced by its acetylation state originated in 2009 (41). By using a microarray approach, the authors identified different cytosolic substrates of the essential nucleosome acetyltransferase of H4 (NuA4) complex. Among these, they discovered the acetylation at two residues of Pck1 (Lys 19 and 514) by the Esa1 acetyltransferase. In particular, the acetylation at Lys 514 was crucial for its enzymatic activity, probably causing a conformational change in the C-terminal binding domain in favour of the substrate, and for CLS extension of chronologically aging cells in water. Indeed, the substitution of K514 with arginine (K514R) but not with glutamic acid (K514Q), which mimics constitutive acetylation, determined the absence of enzymatic activity *in vitro*. The substitution of K19 with arginine (K19R), on the other hand, did not cause significant changes in the enzymatic activity of Pck1. Similar results have been obtained *in vivo* studies: the mutant expressing the variant K514R, which therefore can not be acetylated, displayed the same features of *PCK1* inactivation. It didn't grow on non-fermentable carbon sources, such as ethanol and glycerol, and significantly reduced CLS in both exhausted medium and water.

Gluconeogenesis is a pathway that maintains blood glucose levels within a proper range during fasting in mammals. Mammalian PCK1 is regulated both transcriptionally and enzymatically; although it shares minimal primary structural identity with yeast Pck1, also mammalian PCK1 is subjected to acetylation by TIP60, orthologue of yeast Esa1. However, the function of acetylation is unclear: acetylation in cultured mammalian cells induces degradation (135). A later work revealed an unexpected capability of the hyperacetylated form of mammalian PCK1 to promote anaplerotic reactions under high glucose levels, and thus synthetize oxaloacetate from phosphoenolpyruvate and replenishing the TCA cycle (136). So, the state of hyperacetylation did not lead to PCK1 degradation. At lower glucose concentrations, SIRT1 restored the gluconeogenic activity of PCK1. In addition, the authors discovered that phosphorylation controlled, on the one hand, PCK1 stability, by increasing the levels of ubiquitination and thus degradation, and on the

other the efficiency by which SIRT1 deacetylated PCK1. Also yeast Pck1 is phosphorylated but its function is still unknown (137). Further investigations about how these post-translational modifications control gluconeogenic metabolism are necessary.

1.4 SCOPE OF THE THESIS

The average age of the population in industrialized countries is gradually increasing. However, this increase does not correlate with a similar improvement in the quality of life and typical diseases of the elderly such as diabetes, metabolic disorders, neurodegenerative and cardiovascular diseases are becoming more frequent with consequent negative impact on social and economic aspects. In particular, many efforts are currently focused on the identification and development of interventions based on dietary supplementations (nutraceutical interventions) that can represent a safe strategy to achieve the improvement of healthy aging. In the field of aging and aging-related pathologies, the yeast *S. cerevisiae* represents a useful experimental system.

Chapter 1 gives a general overview of the aging process, yeast as a model to study it and the main nutraceutical interventions investigated until now. The purpose of this chapter is to describe the main nutraceutical compounds and their effects on health, aging and related diseases. Many of these compounds are known to possess beneficial effects. However, the specific mechanism that allows them to elicit these outcomes on health is still unknown. In this regard, the yeast *S. cerevisiae* is recognized as a model organism since its pathways regulating metabolism and longevity are conserved with mammals.

Chapter 2 and Chapter 3 are focused on the effects of resveratrol and quercetin on yeast metabolism and chronological aging. These chapters highlight that resveratrol and quercetin, both recognized for their beneficial and antioxidant properties, elicit opposite effects on yeast metabolism and consequently on aging. This because the two compounds oppositely affect the deacetylase activity of Sir2, an NAD^+-dependent protein deacetylase regulating both metabolism and aging/longevity. Sir2 activity is known to regulate anabolism towards gluconeogenesis and catabolism towards an efficient mitochondrial respiration. In this context, a reduced or impaired Sir2 activity correlates on the one hand with an improvement in the

gluconeogenic flux and trehalose accumulation and, on the other, with an enhanced respiratory performance.

In Chapter 4 the role of mitochondrial metabolism during aging in yeast is investigated. This chapter also intends to describe analogies and differences with mammalian cells.

Chapter 5 is focused on the implications of an altered expression on mitochondrial NAD+ carriers on metabolism and chronological aging. The study of homeostasis of NAD+ represents a topic strictly related to aging, since (i) alterations of its levels are found in many metabolic pathologies common to the elderly population, although it is unclear in which cellular compartments this unbalance could have the main impact on the aging process and (ii) NAD+ levels affect Sir2 enzymatic activity. Moreover, NAD+ precursors appear promising as nutraceuticals to restore healthy longevity.

All the results highlighted the importance of a proper metabolic adaptation required for chronological survival and Sir2 represents a crucial component in this scenario since its activity strongly influences both the oxidative and the anabolic metabolism.

Chapter 6 is a paper concerning skin infections caused by *Candida albicans* spreading, a ubiquitous commensal of the mammalian microbiome which can cause infections under particular conditions. This chapter is unrelated to the topic of the thesis but given the important results obtained, we considered opportune to enclose it. In addition, *C. albicans* infections in the elderly population and immunocompromised subjects represent the cause of substantial morbidity and mortality rates.

1.5 REFERENCES

1. Flatt, T. (2012) A new definition of aging? *Front. Genet.* **3**, 1–2

2. Mackenbach, J. P. (2013) Political conditions and life expectancy in Europe, 1900-2008. *Soc. Sci. Med.* **82**, 134–146

3. Niccoli, T., and Partridge, L. (2012) Ageing as a risk factor for disease. *Curr. Biol.* **22**, R741–R752

4. Gupta, C., and Prakash, D. (2015) Nutraceuticals for geriatrics. *J. Tradit. Complement. Med.* **5**, 5–14

5. López-Otín, C., Blasco, M. A., Partridge, L., Serrano, M., and Kroemer, G. (2013) The hallmarks of aging. *Cell.* **153**, 1194–1217

6. Baccolo, G., Stamerra, G., Damiano Pellegrino, C., Orlandi, I., and Vai, M. (2018) Mitochondrial Metabolism and Aging in Yeast. in *International Review of Cell and Molecular Biology*, pp. 1–33, Elsevier Ltd, **340**, 1–33

7. Friedberg, E. C., McDaniel, L. D., and Schultz, R. A. (2004) The role of endogenous and exogenous DNA damage and mutagenesis. *Curr. Opin. Genet. Dev.* **14**, 5–10

8. Sperka, T., Wang, J., and Rudolph, K. L. (2012) DNA damage checkpoints in stem cells, ageing and cancer. *Nat. Rev. Mol. Cell Biol.* **13**, 579—590

9. Dupont, C., Armant, D. R., and Brenner, C. A. (2009) Epigenetics: definition, mechanisms and clinical perspective. *Semin. Reprod. Med.* **27**, 351—357

10. Pal, S., and Tyler, J. K. (2016) Epigenetics and aging. *Sci. Adv.* **45**, 253–254

11. Kaushik, S., and Cuervo, A. M. (2015) Proteostasis and aging. *Nat. Med.* **21**, 1406–1415

12. Barzilai, N., Huffman, D. M., Muzumdar, R. H., and Bartke, A. (2012) The Critical Role of Metabolic Pathways in Aging. *Diabetes.* **61**, 1315 LP-1322

13. Tissenbaum, H. A., and Guarente, L. (2002) Model organisms as a guide to mammalian aging. *Dev. Cell.* **2**, 9–19

14. Zainabadi, K. (2018) A brief history of modern aging research. *Exp. Gerontol.* **104**, 35–42

15. Bilinski, T., Bylak, A., and Zadrag-Tecza, R. (2017) The budding yeast *Saccharomyces cerevisiae* as a model organism: possible implications for gerontological studies. *Biogerontology.* **18**, 631–640

16. Mortimer, R. K. (2000) Evolution and variation of the yeast (*Saccharomyces*) genome. *Genome Res.* **10**, 403–409

17. Botstein, D., and Fink, G. R. (1988) Yeast: an experimental organism for modern biology. *Science.* **240**, 1439—1443

18. Goffeau, A., Barrell, B. G., Bussey, H., Davis, R. W., Dujon, B., Feldmann, H., Galibert, F., Hoheisel, J. D., Jacq, C., Johnston, M., Louis, E. J., Mewes, H. W., Murakami, Y., Philippsen,

P., Tettelin, H., and Oliver, S. G. (1996) Life with 6000 Genes conveniently among the different interna- Old Questions and New Answers The genome . At the beginning of the se- of its more complex relatives in the eukary- cerevisiae has been completely sequenced *Schizosaccharomyces pombe* indicate. *Science.* **274**, 546–567

19. Smith, M. G., and Snyder, M. (2006) Yeast as a model for human disease. *Curr. Protoc. Hum. Genet.* **Chapter 15**, 1–8

20. Meunier, B., Fisher, N., Ransac, S., Mazat, J. P., and Brasseur, G. (2013) Respiratory complex III dysfunction in humans and the use of yeast as a model organism to study mitochondrial myopathy and associated diseases. *Biochim. Biophys. Acta - Bioenerg.* **1827**, 1346–1361

21. Camacho-Pereira, J., Tarragó, M. G., Chini, C. C. S., Nin, V., Escande, C., Warner, G. M., Puranik, A. S., Schoon, R. A., Reid, J. M., Galina, A., and Chini, E. N. (2016) CD38 Dictates Age-Related NAD Decline and Mitochondrial Dysfunction through an SIRT3-Dependent Mechanism. *Cell Metab.* **23**, 1127–1139

22. Kurat, C. F., Natter, K., Petschnigg, J., Wolinski, H., Scheuringer, K., Scholz, H., Zimmermann, R., Leber, R., Zechner, R., and Kohlwein, S. D. (2006) Obese yeast: Triglyceride lipolysis is functionally conserved from mammals to yeast. *J. Biol. Chem.* **281**, 491–500

23. Howitz, K. T., Bitterman, K. J., Cohen, H. Y., Lamming, D. W., Lavu, S., Wood, J. G., Zipkin, R. E., Chung, P., Kisielewski, A., Zhang, L. L., Scherer, B., and Sinclair, D. A. (2003) Small molecule activators of sirtuins extend *Saccharomyces cerevisiae* lifespan. *Nature.* **425**, 191–196

24. Mohammadi, S., Saberidokht, B., Subramaniam, S., and Grama, A. (2015) Scope and limitations of yeast as a model organism for studying human tissue-specific pathways. *BMC Syst. Biol.* 10.1186/s12918-015-0253-0

25. Longo, V. D., Shadel, G. S., Kaeberlein, M., and Kennedy, B. (2012) Replicative and Chronological Aging in *Saccharomyces cerevisiae*. *Cell Metab.* **16**, 18–31

26. MORTIMER, R. K., and JOHNSTON, J. R. (1959) Life span of individual yeast cells. *Nature.* **183**, 1751–1752

27. K.A. Steinkraus, M. Kaeberlein, B. K. K. (2009) NIH Public Access. *Annu. Rev Cell   Dev Biol.* **24**, 29–54

28. Fabrizio, P., and Longo, V. D. (2003) The chronological life span of *Saccharomyces cerevisiae*. *Aging Cell.* **2**, 73–81

29. Werner-Washburne, M., Braun, E., Johnston, G. C., and Singer, R. A. (1993) Stationary phase in the yeast *Saccharomyces cerevisiae*. *Microbiol. Rev.* **57**, 383–401

30. Martinez-lopez, N., Athonvarangkul, D., Singh, R., and Building, F. (2015) Longevity Genes. **847**, 73–87

31. Busti, S., Coccetti, P., Alberghina, L., and Vanoni, M. (2010) Glucose signaling-mediated coordination of cell growth and cell cycle in *Saccharomyces cerevisiae*. *Sensors.* **10**, 6195–6240

32. Ozcan, S., and Johnston, M. (1995) Three different regulatory mechanisms enable yeast hexose transporter (HXT) genes to be induced by different levels of glucose. *Mol. Cell. Biol.* **15**, 1564–1572

33. Diderich, J. A., Schepper, M., Van Hoek, P., Luttik, M. A. H., Van Dijken, J. P., Pronk, J. T., Klaassen, P., Boelens, H. F. M., De Mattos, M. J. T., Van Dam, K., and Kruckeberg, A. L. (1999) Glucose uptake kinetics and transcription of HXT genes in chemostat cultures of *Saccharomyces cerevisiae*. *J. Biol. Chem.* **274**, 15350–15359

34. Flikweert, M. T., Kuyper, M., van Maris, a J., Kötter, P., van Dijken, J. P., and Pronk, J. T. (1999) Steady-state and transient-state analysis of growth and metabolite production in a *Saccharomyces cerevisiae* strain with reduced pyruvate-decarboxylase activity. *Biotechnol. Bioeng.* **66**, 42–50

35. Jitrapakdee, S., Adina-Zada, A., Besant, P. G., Surinya, K. H., Cleland, W. W., Wallace, J. C., and Attwood, P. V. (2007) Differential regulation of the yeast isozymes of pyruvate carboxylase and the locus of action of acetyl CoA. *Int. J. Biochem. Cell Biol.* **39**, 1211–1223

36. Herzig, S., Raemy, E., Montessuit, S., Veuthey, J.-L., Zamboni, N., Westermann, B., Kunji, E. R. S., and Martinou, J.-C. (2012) Identification and Functional Expression of the Mitochondrial Pyruvate Carrier. *Science.* **337**, 93–96

37. Orlandi, I., Coppola, D., and Vai, M. (2014) Rewiring yeast acetate metabolism through MPC1 loss of function leads to mitochondrial damage and decreases chronological lifespan. *Microb. Cell.* **1**, 393–405

38. Bender, T., Pena, G., and Martinou, J. J.-C. (2015) Regulation of mitochondrial pyruvate uptake by alternative pyruvate carrier complexes. *EMBO J.* **34**, 1–14

39. Bowman, S. B., Zaman, Z., Collinson, L. P., Brown, A. J., and Dawes, I. W. (1992) Positive regulation of the LPD1 gene of *Saccharomyces cerevisiae* by the HAP2/HAP3/HAP4 activation system. *Mol Gen Genet.* **231**, 296–303

40. Orlandi, I., Ronzulli, R., Casatta, N., and Vai, M. (2013) Ethanol and acetate acting as carbon/energy sources negatively affect yeast chronological aging. *Oxid. Med. Cell. Longev.* 10.1155/2013/802870

41. Lin, Y. yi, Lu, J. ying, Zhang, J., Walter, W., Dang, W., Wan, J., Tao, S. C., Qian, J., Zhao, Y., Boeke, J. D., Berger, S. L., and Zhu, H. (2009) Protein Acetylation Microarray Reveals that NuA4 Controls Key Metabolic Target Regulating Gluconeogenesis. *Cell.* **136**, 1073–1084

42. Casatta, N., Porro, A., Orlandi, I., Brambilla, L., and Vai, M. (2013) Lack of Sir2 increases acetate consumption and decreases extracellular pro-aging factors. *Biochim. Biophys. Acta - Mol. Cell Res.* 10.1016/j.bbamcr.2012.11.008

43. Guarente, L., and Picard, F. (2005) Calorie restriction - The SIR2 connection. *Cell.* **120**, 473–482

44. Wiemken, A. (1990) Trehalose in yeast, stress protectant rather than reserve carbohydrate. *Antonie Van Leeuwenhoek.* **58**, 209−217

45. Benaroudj, N., Lee, D. H., and Goldberg, A. L. (2001) Trehalose Accumulation during

Cellular Stress Protects Cells and Cellular Proteins from Damage by Oxygen Radicals. *J. Biol. Chem.* **276**, 24261–24267

46. Lillie, S. H., and Pringle, J. R. (1980) Reserve carbohydrate metabolism in *Saccharomyces cerevisiae*: responses to nutrient limitation. *J. Bacteriol.* **143**, 1384–1394

47. Orlandi, I., Pellegrino Coppola, D., Strippoli, M., Ronzulli, R., and Vai, M. (2017) Nicotinamide supplementation phenocopies SIR2 inactivation by modulating carbon metabolism and respiration during yeast chronological aging. *Mech. Ageing Dev.* **161**, 277–287

48. Lefevre, S. D., van Roermund, C. W., Wanders, R. J. A., Veenhuis, M., and Van der Klei, I. J. (2013) The significance of peroxisome function in chronological aging of *Saccharomyces cerevisiae*. *Aging Cell*. **12**, 784–793

49. Surai, P. F., and Sparks, N. H. C. (2001) Designer eggs: from improvement of egg composition to functional food. *Trends Food Sci. Technol.* **12**, 7—16

50. Kalra, E. K. (2003) Nutraceutical-definition and introduction. *AAPS PharmSci*. **5**, 27–28

51. Ma, L., Dou, H.-L., Huang, Y.-M., Lu, X.-R., Xu, X.-R., Qian, F., Zou, Z.-Y., Pang, H.-L., Dong, P.-C., Xiao, X., Wang, X., Sun, T.-T., and Lin, X.-M. (2012) Improvement of retinal function in early age-related macular degeneration after lutein and zeaxanthin supplementation: a randomized, double-masked, placebo-controlled trial. *Am. J. Ophthalmol.* **154**, 625—634.e1

52. Palozza, P., Simone, R. E., Catalano, A., and Mele, M. C. (2011) Tomato lycopene and lung cancer prevention: From experimental to human studies. *Cancers (Basel)*. **3**, 2333–2357

53. Katalinic, V., Milos, M., Kulisic, T., and Jukic, M. (2006) Screening of 70 medicinal plant extracts for antioxidant capacity and total phenols. *Food Chem.* **94**, 550—557

54. Sunyecz, J. A. (2008) The use of calcium and vitamin D in the management of osteoporosis. *Ther. Clin. Risk Manag.* **4**, 827–836

55. Martin, T., and Campbell, R. K. (2011) Vitamin D and Diabetes. *Diabetes Spectr.* **24**, 113–118

56. Watkins, B. A., Li, Y., and Seifert, M. F. (2001) Nutraceutical fatty acids as biochemical and molecular modulators of skeletal biology. *J. Am. Coll. Nutr.* **20**, 410S—420S

57. Sharma, V., Singh, L., Verma, N., and Kalra, G. (2016) "The Nutraceutical Amino Acids"-Nature's Fortification for Robust Health. *Br. J. Pharm. Res.* **11**, 1–20

58. Harman, D. (1956) Aging: A Theory Based on Free Radical and Radiation Chemistry. *J. Gerontol.* **11**, 298–300

59. Villeponteau, B., Cockrell, R., and Feng, J. (2000) Nutraceutical interventions may delay aging and the age-related diseases. *Exp. Gerontol.* **35**, 1405–1417

60. Chondrogianni, N., Kapeta, S., Chinou, I., Vassilatou, K., Papassideri, I., and Gonos, E. S. (2010) Anti-ageing and rejuvenating effects of quercetin. *Exp. Gerontol.* **45**, 763—771

61. Vranesić-Bender, D. (2010) The role of nutraceuticals in anti-aging medicine. *Acta Clin.*

Croat. **49**, 537–544

62. Miller, E. R., Pastor-barriuso, R., Dalal, D., Riemersma, R. A., Appel, L. ., and Guallar, E. (2005) Review Meta-Analysis : High-Dosage Vitamin E Supplementation May Increase. *Ann. Intern. Med.* **142**, 37–46

63. Cornelli, U., Terranova, R., Luca, S., Cornelli, M., and Alberti, A. (2001) Bioavailability and antioxidant activity of some food supplements in men and women using the D-Roms test as a marker of oxidative stress. *J. Nutr.* **131**, 3208 — 3211

64. Nasri, H., Baradaran, A., Shirzad, H., and Rafieian-Kopaei, M. (2015) New concepts in neutraceuticals as alternative for pharmaceuticals. *Int. J. Prev. Med.* **5**, 1487–1499

65. Mecocci, P., Tinarelli, C., Schulz, R. J., and Polidori, M. C. (2014) Nutraceuticals in cognitive impairment and Alzheimer's disease. *Front. Pharmacol.* **5**, 1–11

66. Hang, L., Basil, A. H., and Lim, K. L. (2016) Nutraceuticals in Parkinson's Disease. *NeuroMolecular Med.* **18**, 306–321

67. Firlag, M., Kamaszewski, M., Gaca, K., and Bałasińska, B. (2013) Age-related changes in the central nervous system in selected domestic mammals and primates. *Postepy Hig. Med. Dosw.* **67**, 269–275

68. Nurk, E., Refsum, H., Drevon, C. A., Tell, G. S., Nygaard, H. A., Engedal, K., and Smith, A. D. (2009) Intake of flavonoid-rich wine, tea, and chocolate by elderly men and women is associated with better cognitive test performance. *J. Nutr.* **139**, 120 — 127

69. De Domenico, S., and Giudetti, A. M. (2017) Nutraceutical intervention in ageing brain. *J. Gerontol. Geriatr.* **65**, 79–92

70. Lin, J. H., and Yamazaki, M. (2003) Role of P-glycoprotein in pharmacokinetics: clinical implications. *Clin. Pharmacokinet.* **42**, 59 — 98

71. Sosnowska, B., Penson, P., and Banach, M. (2017) The role of nutraceuticals in the prevention of cardiovascular disease. *Cardiovasc. Diagn. Ther.* **67**, S21–S31

72. Torres-Duran, P. V., Ferreira-Hermosillo, A., and Juarez-Oropeza, M. A. (2007) Antihyperlipemic and antihypertensive effects of Spirulina maxima in an open sample of mexican population: A preliminary report. *Lipids Health Dis.* **6**, 1–8

73. Sidhu, K. S. (2003) Health benefits and potential risks related to consumption of fish or fish oil. *Regul. Toxicol. Pharmacol.* **38**, 336–344

74. Wong, R. S. (2011) Apoptosis in cancer: from pathogenesis to treatment. *J. Exp. Clin. Cancer Res.* **30**, 87

75. Thomasset, S. C., Berry, D. P., Garcea, G., Marczylo, T., Steward, W. P., and Gescher, A. J. (2007) Dietary polyphenolic phytochemicals - Promising cancer chemopreventive agents in humans? A review of their clinical properties. *Int. J. Cancer*. **120**, 451–458

76. Borrelli, F., and Izzo, A. A. (2009) Herb–Drug Interactions with St John's Wort (Hypericum perforatum): an Update on Clinical Observations. *AAPS J.* **11**, 710–727

77. Davì, G., Santilli, F., and Patrono, C. (2010) Nutraceuticals in diabetes and metabolic

syndrome. *Cardiovasc. Ther.* **28**, 216–226

78. Danescu, L. G., Levy, S., and Levy, J. (2009) Vitamin D and diabetes mellitus. *Endocrine.* **35**, 11–17

79. Liu, Y., Sun, M., Yao, H., Liu, Y., and Gao, R. (2017) Herbal Medicine for the Treatment of Obesity: An Overview of Scientific Evidence from 2007 to 2017. *Evidence-based Complement. Altern. Med.* 10.1155/2017/8943059

80. Dong, Y., Guha, S., Sun, X., Cao, M., Wang, X., and Zou, S. (2012) Nutraceutical interventions for promoting healthy aging in invertebrate models. *Oxid. Med. Cell. Longev.* 10.1155/2012/718491

81. Gambini, J., Inglés, M., Olaso, G., Lopez-Grueso, R., Bonet-Costa, V., Gimeno-Mallench, L., Mas-Bargues, C., Abdelaziz, K. M., Gomez-Cabrera, M. C., Vina, J., and Borras, C. (2015) Properties of Resveratrol: In Vitro and In Vivo Studies about Metabolism, Bioavailability, and Biological Effects in Animal Models and Humans. *Oxid Med Cell Longev*. **2015**, 837042

82. Berman, A. Y., Motechin, R. A., Wiesenfeld, M. Y., and Holz, M. K. (2017) The therapeutic potential of resveratrol: a review of clinical trials. *npj Precis. Oncol.* **1**, 35

83. Bavaresco, L., Fregoni, C., Cantù, E., and Trevisan, M. (1999) Stilbene compounds: from the grapevine to wine. *Drugs Exp. Clin. Res.* **25**, 57—63

84. Catalgol, B., Batirel, S., Taga, Y., and Ozer, N. K. (2012) Resveratrol: French paradox revisited. *Front. Pharmacol.* **3**, 1–18

85. de la Lastra, C. A., and Villegas, I. (2007) Resveratrol as an antioxidant and pro-oxidant agent: mechanisms and clinical implications. *Biochem. Soc. Trans.* **35**, 1156–1160

86. Orlandi, I., Stamerra, G., Strippoli, M., and Vai, M. (2017) During yeast chronological aging resveratrol supplementation results in a short-lived phenotype Sir2-dependent. *Redox Biol.* **12**, 745–754

87. Pallauf, K., Rimbach, G., Rupp, P. M., Chin, D., and Wolf, I. M. A. (2016) Resveratrol and Lifespan in Model Organisms. *Curr. Med. Chem.* **23**, 4639—4680

88. Bhullar, K. S., and Hubbard, B. P. (2015) Lifespan and healthspan extension by resveratrol. *Biochim. Biophys. Acta - Mol. Basis Dis.* **1852**, 1209–1218

89. Shore, D., Squire, M., and Nasmyth, K. a (1984) Characterization of two genes required for the position-effect control of yeast mating-type genes. *EMBO J.* **3**, 2817–2823

90. Borra, M. T., Smith, B. C., and Denu, J. M. (2005) Mechanism of human SIRT1 activation by resveratrol. *J. Biol. Chem.* **280**, 17187–17195

91. Chung, J. H. (2012) Using PDE inhibitors to harness the benefits of calorie restriction: Lessons from resveratrol. *Aging (Albany. NY).* **4**, 144–145

92. Sinclair, D. A., and Guarente, L. (2014) Small Molecule Allosteric Activator of Sirtuins. *Annu Rev Pharmacol Toxicol*. **54**, 363–380

93. Anand David, A. V., Arulmoli, R., and Parasuraman, S. (2016) Overviews of Biological Importance of Quercetin: A Bioactive Flavonoid. *Pharmacogn. Rev.* **10**, 84—89

94. Mariani, C., Braca, A., Vitalini, S., De Tommasi, N., Visioli, F., and Fico, G. (2008) Flavonoid characterization and in vitro antioxidant activity of Aconitum anthora L. (Ranunculaceae). *Phytochemistry*. **69**, 1220–1226

95. Kaşıkcı, M., and Bağdatlıoğlu, N. (2016) Bioavailability of Quercetin. *Curr. Res. Nutr. Food Sci. J.* **4**, 146–151

96. Bayliak, M. M., Burdylyuk, N. I., and Lushchak, V. I. (2016) Quercetin increases stress resistance in the yeast *Saccharomyces cerevisiae* not only as an antioxidant. *Ann. Microbiol.* **66**, 569–576

97. Belinha, I., Amorim, M. A., Rodrigues, P., De Freitas, V., Moradas-Ferreira, P., Mateus, N., and Costa, V. (2007) Quercetin increases oxidative stress resistance and longevity in *Saccharomyces cerevisiae*. *J. Agric. Food Chem.* **55**, 2446–2451

98. Vilaça, R., Mendes, V., Mendes, M. V., Carreto, L., Amorim, M. A., de Freitas, V., Moradas-Ferreira, P., Mateus, N., and Costa, V. (2012) Quercetin Protects *Saccharomyces cerevisiae* against Oxidative Stress by Inducing Trehalose Biosynthesis and the Cell Wall Integrity Pathway. *PLoS One*. **7**, 1–11

99. Chung, S., Yao, H., Caito, S., Hwang, J.-W., Arunachalam, G., and Rahman, I. (2010) Regulation of SIRT1 in cellular functions: role of polyphenols. *Arch. Biochem. Biophys.* **501**, 79−90

100. de Boer, V. C. J., de Goffau, M. C., Arts, I. C. W., Hollman, P. C. H., and Keijer, J. (2006) SIRT1 stimulation by polyphenols is affected by their stability and metabolism. *Mech. Ageing Dev.* **127**, 618–627

101. Zaman, S., Lippman, S. I., Schneper, L., Slonim, N., and Broach, J. R. (2009) Glucose regulates transcription in yeast through a network of signaling pathways. *Mol. Syst. Biol.* **5**, 1–14

102. Santangelo, G. M. (2006) Glucose Signaling in *Saccharomyces cerevisiae*. *Microbiol. Mol. Biol. Rev.* **70**, 253–282

103. Ptacek, J., Devgan, G., Michaud, G., Zhu, H., Zhu, X., Fasolo, J., Guo, H., Jona, G., Breitkreutz, A., Sopko, R., McCartney, R. R., Schmidt, M. C., Rachidi, N., Lee, S.-J., Mah, A. S., Meng, L., Stark, M. J. R., Stern, D. F., De Virgilio, C., Tyers, M., Andrews, B., Gerstein, M., Schweitzer, B., Predki, P. F., and Snyder, M. (2005) Global analysis of protein phosphorylation in yeast. *Nature*. **438**, 679–684

104. Ma, P., Wera, S., Van Dijck, P., and Thevelein, J. M. (1999) The PDE1-encoded Low-Affinity Phosphodiesterase in the Yeast *Saccharomyces cerevisiae* Has a Specific Function in Controlling Agonist-induced cAMP Signaling. *Mol. Biol. Cell*. **10**, 91–104

105. Tamanoi, F. (2011) Ras signaling in yeast. *Genes and Cancer*. **2**, 210–215

106. Xue, Y., Batlle, M., and Hirsch, J. P. (1998) GPR1 encodes a putative G protein-coupled receptor that associates with the Gpa2p G(α) subunit and functions in a Ras-independent pathway. *EMBO J.* **17**, 1996–2007

107. Gorner, W., Durchschlag, E., Martinez-Pastor, M. T., Estruch, F., Ammerer, G.,

Hamilton, B., Ruis, H., and Schuller, C. (1998) Nuclear localization of the C2H2 zinc finger protein Msn2p is regulated by stress and protein kinase A activity. *Genes Dev.* **12**, 586–597

108. Crozet, P., Margalha, L., Confraria, A., Rodrigues, A., Martinho, C., Adamo, M., Elias, C. A., and Baena-GonzÃ¡lez, E. (2014) Mechanisms of regulation of SNF1/AMPK/SnRK1 protein kinases. *Front. Plant Sci.* **5**, 1–17

109. Carling, D., Thornton, C., Woods, A., and Sanders, M. J. (2012) AMP-activated protein kinase: new regulation, new roles? *Biochem. J.* **445**, 11–27

110. Hedbacker, K. (2008) SNF1/AMPK pathways in yeast. *Front. Biosci.* **13**, 2408

111. Hedges, D., Proft, M., and Entian, K. D. (1995) CAT8, a new zinc cluster-encoding gene necessary for derepression of gluconeogenic enzymes in the yeast *Saccharomyces cerevisiae*. *Mol. Cell. Biol.* **15**, 1915–1922

112. Loewith, R., Jacinto, E., Wullschleger, S., Lorberg, A., Crespo, J. L., Bonenfant, D., Oppliger, W., Jenoe, P., and Hall, M. N. (2002) Two TOR complexes, only one of which is rapamycin sensitive, have distinct roles in cell growth control. *Mol. Cell*. **10**, 457–468

113. Swinnen, E., Ghillebert, R., Wilms, T., and Winderickx, J. (2014) Molecular mechanisms linking the evolutionary conserved TORC1-Sch9 nutrient signalling branch to lifespan regulation in *Saccharomyces cerevisiae*. *FEMS Yeast Res.* **14**, 17–32

114. Panchaud, N., Péli-Gulli, M. P., and De Virgilio, C. (2013) SEACing the GAP that nEGOCiates TORC1 activation: Evolutionary conservation of Rag GTPase regulation. *Cell Cycle*. **12**, 2948–2952

115. Urban, J., Soulard, A., Huber, A., Lippman, S., Mukhopadhyay, D., Deloche, O., Wanke, V., Anrather, D., Ammerer, G., Riezman, H., Broach, J. R., De Virgilio, C., Hall, M. N., and Loewith, R. (2007) Sch9 Is a Major Target of TORC1 in *Saccharomyces cerevisiae*. *Mol. Cell*. **26**, 663–674

116. Pedruzzi, I., Dubouloz, F., Cameroni, E., Wanke, V., Roosen, J., Winderickx, J., and De Virgilio, C. (2003) TOR and PKA Signaling Pathways Converge on the Protein Kinase Rim15 to Control Entry into G0. *Mol. Cell*. **12**, 1607–1613

117. Wanke, V., Cameroni, E., Uotila, A., Piccolis, M., Urban, J., Loewith, R., and De Virgilio, C. (2008) Caffeine extends yeast lifespan by targeting TORC1. *Mol. Microbiol.* **69**, 277–285

118. Lee, P., Kim, M. S., Paik, S. M., Choi, S. H., Cho, B. R., and Hahn, J. S. (2013) Rim15-dependent activation of Hsf1 and Msn2/4 transcription factors by direct phosphorylation in *Saccharomyces cerevisiae*. *FEBS Lett.* **587**, 3648–3655

119. Bontron, S., Jaquenoud, M., Vaga, S., Talarek, N., Bodenmiller, B., Aebersold, R., and De Virgilio, C. (2013) Yeast Endosulfines Control Entry into Quiescence and Chronological Life Span by Inhibiting Protein Phosphatase 2A. *Cell Rep.* **3**, 16–22

120. Lavoie, H., and Whiteway, M. (2008) Increased respiration in the sch9?? mutant is required for increasing chronological life span but not replicative life span. *Eukaryot. Cell*. **7**, 1127–1135

121. Pan, Y., Schroeder, E. A., Ocampo, A., Barrientos, A., and Shadel, G. S. (2011) Regulation

of yeast chronological life span by TORC1 via adaptive mitochondrial ROS signaling. *Cell Metab.* **13**, 668—678

122. Ocampo, A., Liu, J., Schroeder, E. A., Shadel, G. S., and Barrientos, A. (2012) Mitochondrial respiratory thresholds regulate yeast chronological life span and its extension by caloric restriction. *Cell Metab.* **16**, 55–67

123. Taormina, G., and Mirisola, M. G. (2014) Calorie restriction in mammals and simple model organisms. *Biomed Res. Int.* 10.1155/2014/308690

124. Lin, S.-J., Kaeberlein, M., Andalis, A. A., Sturtz, L. A., Defossez, P.-A., Culotta, V. C., Fink, G. R., and Guarente, L. (2002) Calorie restriction extends *Saccharomyces cerevisiae* lifespan by increasing respiration. *Nature*. **418**, 344–348

125. Fabrizio, P., Gattazzo, C., Battistella, L., Wei, M., Cheng, C., McGrew, K., and Longo, V. D. (2005) Sir2 blocks extreme life-span extension. *Cell*. **123**, 655–667

126. Kaeberlein, M., Powers, R. W., Steffen, K. K., Westman, E. A., Hu, D., Dang, N., Kerr, E. O., Kirkland, K. T., Fields, S., and Kennedy, B. K. (2005) Cell biology: Regulation of yeast replicative life span by TOR and Sch9 response to nutrients. *Science*. **310**, 1193–1196

127. Blander, G., and Guarente, L. (2004) The Sir2 family of protein deacetylases. *Curr. Opin. Chem. Biol.* **9**, 417–432

128. Mackay, V., and Manney, T. R. (1974) Mutations affecting sexual conjugation and related processes in *Saccharomyces cerevisiae*. II. Genetic analysis of nonmating mutants. *Genetics*. **76**, 273–288

129. Rine, J., and Herskowitz, I. (1987) Four genes responsible for a position effect on expression from HML and HMR in *Saccharomyces cerevisiae*. *Genetics*. **116**, 9–22

130. Smith, J. S., and Boeke, J. D. (1997) An unusual form of transcriptional silencing in yeast ribosomal DNA. *Genes Dev.* **11**, 241–254

131. Loo, S., and Rine, J. (1994) Silencers and domains of generalized repression. *Science.* **264**, 1768–1771

132. Kaeberlein, M., McVey, M., and Guarente, L. (1999) The SIR2/3/4 complex and SIR2 alone promote longevity in *Saccharomyces cerevisiae* by two different mechanisms. *Genes Dev.* **13**, 2570–2580

133. Martino, F., Kueng, S., Robinson, P., Tsai-Pflugfelder, M., van Leeuwen, F., Ziegler, M., Cubizolles, F., Cockell, M. M., Rhodes, D., and Gasser, S. M. (2009) Reconstitution of Yeast Silent Chromatin: Multiple Contact Sites and O-AADPR Binding Load SIR Complexes onto Nucleosomes In Vitro. *Mol. Cell*. **33**, 323–334

134. Bitterman, K. J., Anderson, R. M., Cohen, H. Y., Latorre-Esteves, M., and Sinclair, D. A. (2002) Inhibition of Silencing and Accelerated Aging by Nicotinamide, a Putative Negative Regulator of Yeast Sir2 and Human SIRT1. *J. Biol. Chem.* . **277**, 45099–45107

135. Jiang, W., Wang, S., Xiao, M., Lin, Y., Zhou, L., Lei, Q., Xiong, Y., Guan, K.-L., and Zhao, S. (2011) Acetylation Regulates Gluconeogenesis by Promoting PEPCK1 Degradation via Recruiting the UBR5 Ubiquitin Ligase. *Mol. Cell*. **43**, 33–44

136. Latorre-Muro, P., Baeza, J., Armstrong, E. A., Hurtado-Guerrero, R., Corzana, F., Wu, L. E., Sinclair, D. A., López-Buesa, P., Carrodeguas, J. A., and Denu, J. M. (2018) Dynamic Acetylation of Phosphoenolpyruvate Carboxykinase Toggles Enzyme Activity between Gluconeogenic and Anaplerotic Reactions. *Mol. Cell*. **71**, 718–732

137. Oliveira, A. P., and Sauer, U. (2012) The importance of post-translational modifications in regulating *Saccharomyces cerevisiae* metabolism. *FEMS Yeast Res.* **12**, 104–117

Chapter

During yeast chronological aging resveratrol supplementation results in a short-lived phenotype Sir2-dependent

Ivan Orlandi, Giulia Stamerra, Maurizio Strippoli and Marina Vai.

Research Paper

During yeast chronological aging resveratrol supplementation results in a short-lived phenotype Sir2-dependent

Ivan Orlandi, Giulia Stamerra, Maurizio Strippoli, Marina Vai*

SYSBIO Centre for Systems Biology Milano, Dipartimento di Biotecnologie e Bioscienze, Università di Milano-Bicocca, Piazza della Scienza 2, 20126 Milano, Italy

A B S T R A C T

Resveratrol (RSV) is a naturally occurring polyphenolic compound endowed with interesting biological properties/functions amongst which are its activity as an antioxidant and as Sirtuin activating compound towards SIRT1 in mammals. Sirtuins comprise a family of NAD^+-dependent protein deacetylases that are involved in many physiological and pathological processes including aging and age-related diseases. These enzymes are conserved across species and SIRT1 is the closest mammalian orthologue of Sir2 of *Saccharomyces cerevisiae*. In the field of aging researches, it is well known that Sir2 is a positive regulator of replicative lifespan and, in this context, the RSV effects have been already examined. Here, we analyzed RSV effects during chronological aging, in which Sir2 acts as a negative regulator of chronological lifespan (CLS). Chronological aging refers to quiescent cells in stationary phase; these cells display a survival-based metabolism characterized by an increase in oxidative stress. We found that RSV supplementation at the onset of chronological aging, namely at the diauxic shift, increases oxidative stress and significantly reduces CLS. CLS reduction is dependent on Sir2 presence both in expired medium and in extreme Calorie Restriction. In addition, all data point to an enhancement of Sir2 activity, in particular Sir2-mediated deacetylation of the key gluconeogenic enzyme phosphoenolpyruvate carboxykinase (Pck1). This leads to a reduction in the amount of the acetylated active form of Pck1, whose enzymatic activity is essential for gluconeogenesis and CLS extension.

1. Introduction

Resveratrol (3,5,4′-trihydroxystilbene) (RSV) is a natural non-flavonoid, polyphenolic product belonging to the stilbenoid family, which is synthesized by a rather restricted and heterogeneous group of plant species. Grapevine (*Vitaceae*) is among these, and the products derived therefrom such as grapes and red wine are sources of RSV in human diet [1,2]. In particular RSV intake with red wine has been proposed to explain the "French Paradox", a term coined on the basis of epidemiological studies that in France revealed low rates of coronary heart diseases despite a diet rich in saturated fats [3]. This apparent paradox has been ascribed to protective/beneficial effects of RSV linked to French dietary habits of moderate consumption of red wine [3,4]. Very numerous *in vitro* and *in vivo* studies dealing with the different aspects of the various health-promoting effects of RSV have been reported, including its antioxidative, anti-inflammatory, neuroprotective, anticancer and cardioprotective properties [5–8]. Nevertheless, the exact molecular mechanisms underlying the RSV action and its direct cellular targets are still being explored [9,10]. In this context, after a high-throughput screen in which RSV was identified as a natural

SIRT1 activating compound (STAC) [11], a series of reports provided evidence that SIRT1 is required for most of RSV metabolic actions either *via* a direct activation of SIRT1 by RSV or an indirect one [9,12–14]. The mammalian SIRT1 is a member of a family of evolutionarily conserved NAD^+-dependent deacetylases, namely Sirtuins, In mammals, there are seven Sirtuin isoforms (SIRT1-SIRT7) endowed with multifaceted functionality comprising transcriptional regulation and chromatin structure maintenance in the nucleus as well as activation/inactivation of metabolic enzymes in the cytoplasm and mitochondria in response to nutritional and environmental stimuli [15–18]. SIRT1 is the most well-studied member of the mammalian Sirtuins and its deacetylase activity plays a crucial role in metabolic responses to nutritional availability in different tissues and in physiological processes known to be affected during aging. Consequently, the modulation of SIRT1 activity can represent a potential therapeutic approach for treating age-related or metabolic diseases in order to improve the quality of life and extend health span [12,17,19–21].

SIRT1 is the closest mammalian orthologue of the Sirtuin founding member, namely Sir2 of *Saccharomyces cerevisiae* [22]. In yeast, Sir2 is a key modulator of both replicative and chronological aging [23,24]. In

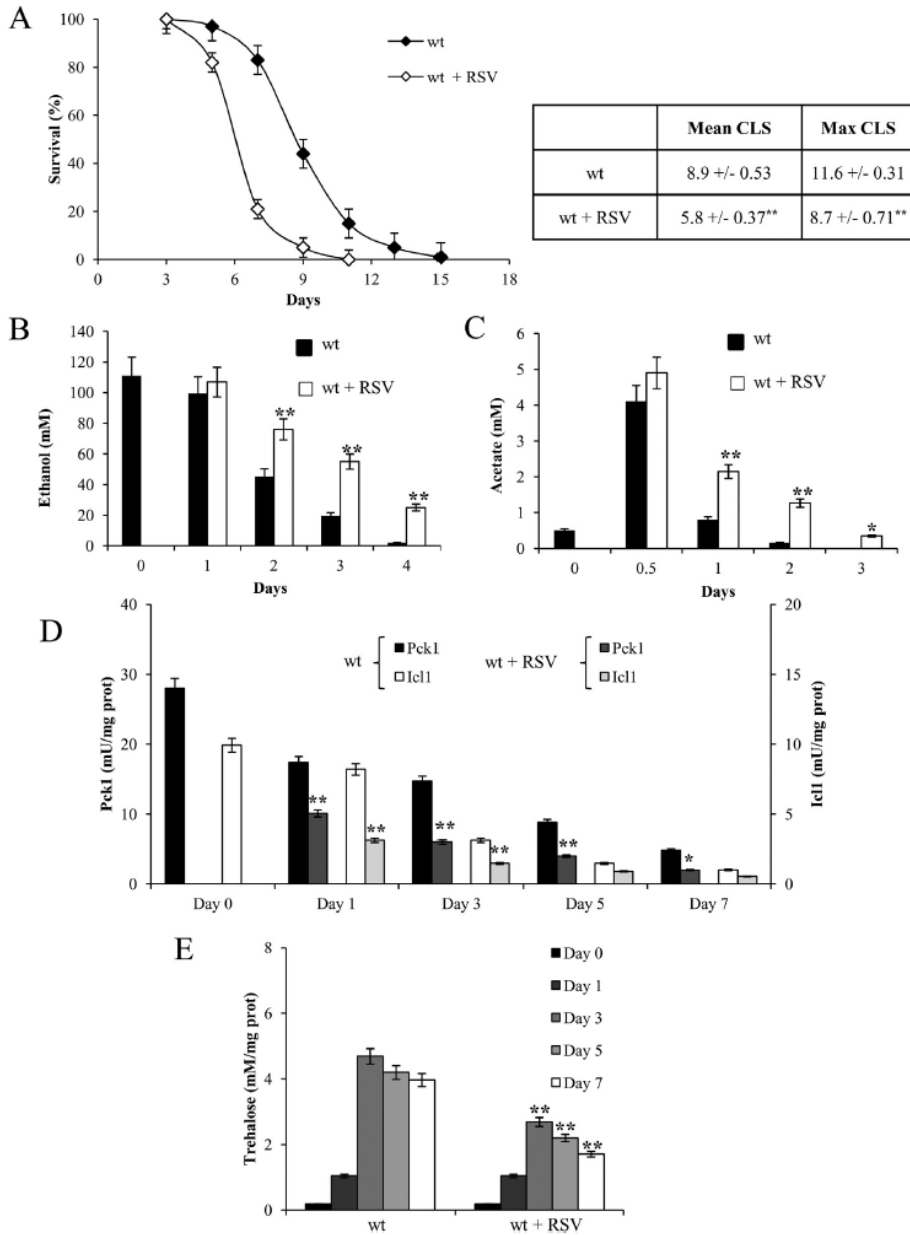|	Mean CLS	Max CLS
wt	8.9 +/- 0.53	11.6 +/- 0.31
wt + RSV	5.8 +/- 0.37**	8.7 +/- 0.71**

Fig. 1. RSV supplementation at the diauxic shift determines a short-lived phenotype. Wild type (wt) cells were grown in minimal medium/2% glucose and the required supplements in excess (see Materials and methods). At the diauxic shift (Day 0), resveratrol (RSV, 100 μM) was added to the expired media and (A) survival over time of treated and untreated cultures was assessed by colony-forming capacity on YEPD plates. 72 h after the diauxic shift (Day 3) was considered the first age-point, corresponding to 100% survival. Data referring to the time points where chronological aging cultures showed 50% (Mean CLS) and 10% (Maximum CLS) of survival are reported in the Table. In parallel, for the same cultures the concentrations of extracellular ethanol (B) and acetate (C) together with Icl1 and Pck1 enzymatic activities (D) and intracellular trehalose content (E) were measured. All data refer to mean values of three independent experiments with three technical replicates each. Standard deviations (SD) are indicated. Statistical significance as assessed by one-way ANOVA test is indicated (*P ≤ 0.05 and **P ≤ 0.01).

Table 1
RSV supplementation at the diauxic shift affects respiration.

	J_R				J_{TET}			
	Day 0	Day 1	Day 3	Day 5	Day 0	Day 1	Day 3	Day 5
wt	9.51 ± 0.24	14.11 ± 0.31	7.22 ± 0.29	4.31 ± 0.12	1.64 ± 0.24	3.68 ± 0.19	3.93 ± 0.24	4.18 ± 0.29
wt + 100 µM RSV		17.49** ± 0.18	9.45** ± 0.22	8.35** ± 0.26		6.81* ± 0.24	7.95** ± 0.21	8.27** ± 0.26
sir2Δ	7.89** ± 0.26	10.52** ± 0.13	5.72** ± 0.19	3.34** ± 0.14	1.09** ± 0.24	1.23** ± 0.21	1.49** ± 0.17	1.68** ± 0.19
sir2Δ + 100 µM RSV		10.44** ± 0.21	5.59** ± 0.15	3.27** ± 0.21		1.28** ± 0.25	1.55** ± 0.16	1.72** ± 0.23

	J_{MAX}				netR			
	Day 0	Day 1	Day 3	Day 5	Day 0	Day 1	Day 3	Day 5
wt	19.11 ± 0.34	26.41 ± 0.13	25.36 ± 0.16	12.01 ± 0.20	7.38 ± 0.28	10.41 ± 0.32	3.21 ± 0.27	0.28 ± 0.29
wt + 100 µM RSV		26.62 ± 0.25	25.22 ± 0.23	12.18 ± 0.18		9.18* ± 0.22	1.65** ± 0.17	0.08** ± 0.09
sir2Δ	18.89 ± 0.22	26.19 ± 0.19	24.98 ± 0.27	11.35 ± 0.18	6.83 ± 0.16	9.87** ± 0.32	4.40** ± 0.27	1.45** ± 0.24
sir2Δ + 100 µM RSV		26.33 ± 0.16	26.11 ± 0.25	11.21 ± 0.22		9.92** ± 0.23	4.35** ± 0.16	1.38** ± 0.21

Oxygen uptake rates (J) are expressed as pmol/10^6 cells/s. Basal respiration rate (J_R), non-phosphorylating respiration rate (J_{TET}), uncoupled respiration rate (J_{MAX}) and net respiration (netR = J_R - J_{TET}). Substrates and inhibitors used in the measurements of the respiratory parameters are detailed in the text. Day 0, diauxic shift. Data refer to mean values determined in three independent experiments with three technical replicates each. SD is indicated. Values obtained for untreated wt cells were used as reference for comparisons with the corresponding ones determined for RSV-treated and sir2Δ cells. (*P ≤ 0.05 and **P ≤ 0.01, one-way ANOVA test).

the former, which is a useful model of cellular aging for mitotically active mammalian cells [25], Sir2 activity promotes replicative lifespan (RLS) [26,27]. Furthermore, a quantitative trait locus (QTL) analysis investigating the role of natural genetic variation associated with RLS identified SIR2 as the QTL with the largest effect on RLS [28]. RLS measures the reproductive potential of individual yeast cells determined by counting how many daughter cells (buds) are generated by an asymmetrically dividing mother cell in the presence of nutrients prior to senescence [29]. Treatment with RSV and also with some of its synthetic derivatives has been reported to extend RLS and require SIR2 [11,30,31], although in this regard Sir2 activation by RSV has been questioned and is a topic of some controversy [32].

Yeast chronological aging is a complementary model to the replicative one: it allows us to simulate cellular aging of nondividing, albeit metabolic active, mammalian cells such as those of the brain and heart [23,33]. The chronological lifespan (CLS) refers to the mean and maximum length of time a non-dividing culture survives in stationary phase. It is estimated, starting 72 h after the diauxic shift, by measuring the percentage of cells able to resume growth upon return to fresh rich medium [34]. Unlike RLS, Sir2 activity does not promote CLS [35–37]. In addition, lack of Sir2 along with CLS-extending mutations/deletions that reduce nutrient-responsive pathways such as Sch9 and Ras ones, further increases the CLS [36]. The same CLS-extending effect is observed in combination with a severe form of Calorie Restriction (CR) obtained by incubation of post-diauxic cells in water [35–37].

In chronological aging cells, lack of Sir2 affects, on the one hand, carbon metabolism by increasing anabolic pathways such as gluconeogenesis and, on the other, respiratory activity by reducing non-phosphorylating respiration. The former leads to an increase of protective factors such as trehalose and the latter to a low content of the harmful superoxide anion ($O_2^{•-}$) [35,37]. These features together with an increased resistance to heat shock and oxidative stress [36] contribute to the establishment of an efficient protective quiescent state that favors a better long-term survival.

Herein, we investigated the effects of RSV supplementation at the onset of chronological aging. The results indicate that RSV displays pro-aging properties promoting CLS restriction. In particular, RSV interferes with the metabolic reprogramming that is required to trigger the metabolic adaptations to nutrient scarcity determining a decrease in trehalose stores and an increase in oxidative stress. Our findings also implicate an enhancement of Sir2 enzymatic activity in eliciting the RSV effects.

2. Materials and methods

2.1. Yeast strains, growth conditions and CLS determination

All yeast strains used in this work were generated by PCR-based methods and are listed in Table S1. For each strain generated, prototrophic derivatives of W303-1A were constructed by integration of the corresponding wt allele of the auxotrophic mutation at the original genomic locus. The accurancy of gene replacements and correct deletions/integrations was verified by PCR with flanking and internal primers. Cells were grown in batches at 30 °C in minimal medium (Difco Yeast Nitrogen Base without amino acids, 6.7 g/L) with 2% w/v glucose and supplements added in excess [38]. Cell growth was monitored by counting cell number using a Coulter Counter-Particle Count and Size Analyser [39] and, in parallel, the extracellular concentration of glucose and ethanol were measured in medium samples collected at different time points in order to define the growth profile (exponential phase, diauxic shift (Day 0), post-diauxic phase and stationary phase) of the cultures [38]. Duplication time (Td) was obtained by linear regression of the cell number increase over time on a semi-logarithmic plot. CLS was measured according to [36] by counting colony-forming units (CFU) starting with 72 h (Day 3, first age-point) after Day 0. The number of CFU on Day 3 was considered the initial survival (100%). Treatments were performed at Day 0 by adding resveratrol (RSV, dissolved in DMSO, Sigma-Aldrich) at the final concentrations of 100 µM. Survival experiments in water (pH adjusted to 3.2) were performed as described [40]. Every 48 h, 100 µM RSV, 5 mM nicotinamide (NAM, Sigma-Aldrich) or both were added to the culture after washing. Viability was assessed by CFU.

2.2. Metabolite measurements and enzymatic assays

At designated time points, aliquots of the yeast cultures were centrifuged, and both pellets (washed twice) and supernatants were collected and frozen at −80 °C until used. Glucose, ethanol and acetic acid concentrations in the growth medium were determined using enzymatic assays (K-HKGLU, K-ETOH, and K-ACET kits from Megazyme). Extraction and determination of intracellular trehalose as in [41]. The released glucose was quantified using the K-HKGLU kit. Immediately after preparation of cell-free extracts [38], phosphoenolpyruvate carboxykinase (Pck1) and isocitrate lyase (Icl1) activities were assayed according to [42]. Catalase and superoxide dismutase activities were determined in cell-free extracts prepared as in [43]. The
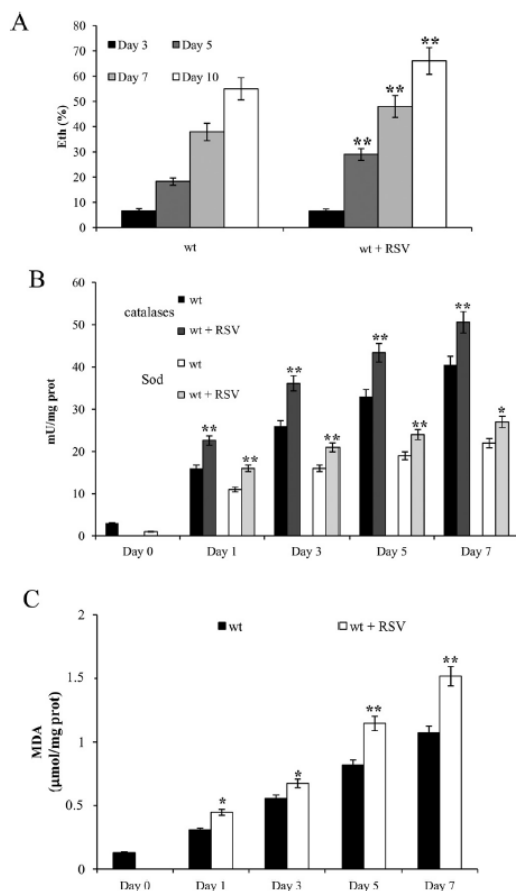
58

Fig. 2. RSV supplementation at the diauxic shift triggers oxidative stress. Cultures of Fig. 1 were analyzed for the presence of intracellular superoxide by the conversion of non-fluorescent dihydroethidium into fluorescent ethidium (Eth). (A) Summary graphs of the percentage of fluorescent/superoxide positive cells (% Eth) are reported. About 1000 cells for each sample (three technical replicates) in three independent experiments were examined. At the indicated time points, catalases/Sod enzymatic activities (B) and the levels of intracellular malondialdehyde (MDA) (C) were measured. All the measurements were normalized to the protein content. Day 0, diauxic shift. SD is indicated. Statistical significance as in Fig. 1 (*P ≤ 0.05 and **P ≤ 0.01).

former was measured spectrophotometrically at 240 nm by following the disappearance of H_2O_2 [44] and the latter at 550 nm by following the rate of ferricytochrome c reduction [45]. Total protein concentration was estimated using the BCA™ Protein Assay Kit (Pierce).

2.3. Estimation of oxygen consumption rates, superoxide levels and lipid peroxidation

The basal oxygen consumption of intact cells was measured at 30 °C using a "Clark-type" oxygen electrode (Oxygraph System, Hansatech Instruments, Nortfolk, UK) as previously reported [40]. The addition of 37.5 mM triethyltin bromide (TET, Sigma-Aldrich) and 10 μM of the uncoupler carbonyl cyanide 3-chlorophenylhydrazone (CCCP, Sigma-Aldrich) to the oxygraph chamber accounted for the non-phosphorylating respiration and the maximal/uncoupled respiratory capacity,

respectively [37]. The addition of 2 M antimycin A (Sigma-Aldrich) accounted for non-mitochondrial oxygen consumption. Respiratory rates for the basal oxygen consumption (J_R), the maximal/uncoupled oxygen consumption (J_{MAX}) and the non-phosphorylating oxygen consumption (J_{TET}) were determined from the slope of a plot of O_2 concentration against time, divided by the cellular concentration.

Staining with dihydroethidium (DHE, Sigma-Aldrich) was performed according to [46] to analyze superoxide anion ($O_2^{\cdot -}$). Cells were counterstained with propidium iodide to discriminate between live and dead cells. A Nikon Eclipse E600 fluorescence microscope equipped with a Leica DC 350F ccd camera was used. Digital images were acquired using FW4000 software (Leica).

Lipid peroxidation was determined by quantifying malondialdehyde (MDA) using the BIOXYTECH® LPO-586™ Colorimetric Assay Kit (OxisResearch). The assay is based on the reaction of the chromogenic N-methyl-2-phenylindole with MDA forming a stable chromophore with maximum absorbance at 586 nm.

2.4. Immunoprecipitation and Western analysis

Total protein extracts preparation, immunoprecipitation and Western analysis were performed as described [35]. Acetylation levels of histones were analyzed on extracts prepared by mild alkaline treatment [47] and SDS-PAGE was performed on 12% polyacrylamide slab gels. Gels were blotted onto Hybond-P PVDF membranes (Amersham). Correct loading/transfer was confirmed by staining filters with Ponceau S Red (Sigma-Aldrich). The primary antibodies used were: anti-HA (12CA5, Roche), anti-acetylated-lysine (Ac-K-103, Cell Signaling), anti-3-phosphoglycerate kinase (Pgk1) (22C5, Invitrogen), anti-H4 (ab16483, Abcam) and anti-H4K16ac (ab1762, Abcam). Secondary antibodies were purchased from Amersham. Binding was visualized with the ECL Western Blotting Detection Reagent (Amersham). After ECL detection, films were scanned on a Bio-Rad GS-800 calibrated imaging densitometer and quantified with Scion Image software.

2.5. Statistical analysis of data

All values are presented as the mean of three independent experiments ± Standard Deviation (SD). Three technical replicates were analyzed in each independent experiment. Statistical significance was assessed by one-way ANOVA test. The level of statistical significance was set at a P value of ≤ 0.05.

3. Results

3.1. Resveratrol supplementation at the diauxic shift restricts CLS and increases oxidative stress

During chronological aging, an increase in oxidative stress occurs, which negatively affects CLS [48–50]. Since antioxidant properties, among others, have been reported for potential RSV health benefits, we evaluated the effects of its supplementation at the diauxic shift (Day 0) on both CLS and cellular metabolism. RSV-treated culture showed a decrease of CLS (Fig. 1A) in concert with increased extracellular levels of ethanol and acetate compared with the untreated one (Fig. 1B and C). Ethanol and acetate are two well-known by-products of yeast glucose fermentation that are transiently accumulated in the culture medium. In fact, after the diauxic shift, these C2 compounds are used as substrates of a respiration-based metabolism that, in addition to functional mitochondria, requires the involvement of the glyoxylate/gluconeogenesis pathways. In RSV-treated cells, the enzymatic activities of isocitrate lyase (Icl1), one of the signature enzymes of the glyoxylate shunt, and of the key gluconeogenic enzyme phosphoenol-pyruvate carboxykinase (Pck1), were significantly lower than those in untreated cells (Fig. 1D). In line with a down-regulation of the glyoxylate-requiring gluconeogenesis, a reduction in these cells of
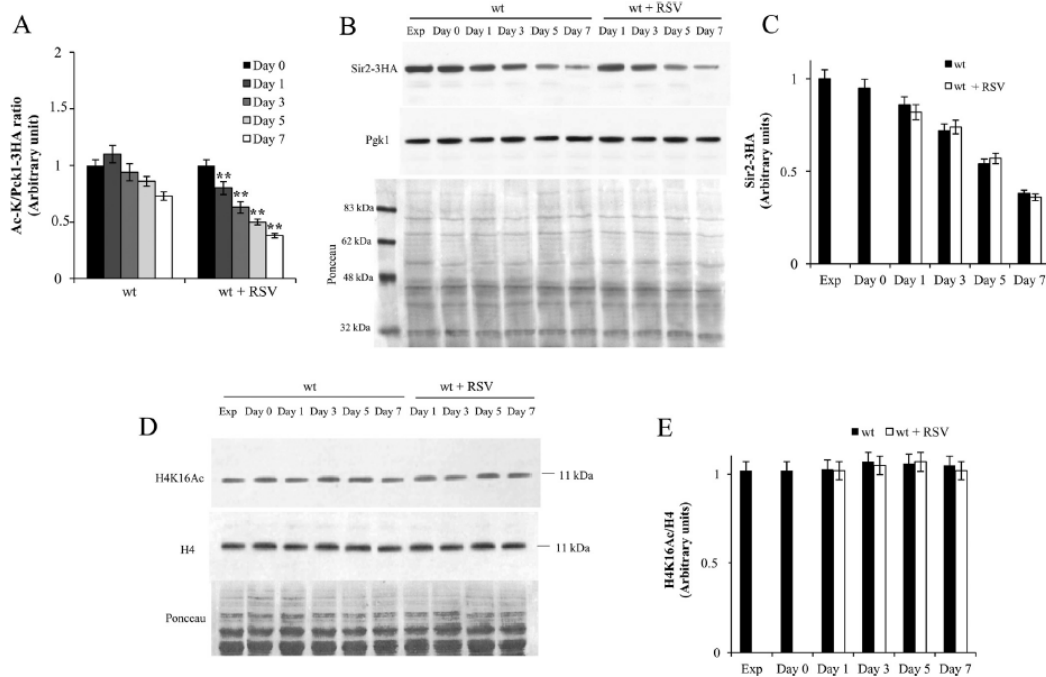
Fig. 3. RSV supplementation at the diauxic shift increases Pck1 deacetylation without affecting Sir2 levels. Wt cells expressing Pck1-3HA were grown and supplied at the diauxic shift (Day 0) with RSV as in Fig. 1. At different time points, total protein extracts from both treated and untreated cultures were prepared and immunoprecipitated with anti-HA antibody. Afterwards, Western analyses were performed with anti-HA and anti-Ac-K antibodies followed by densitometric quantification of signal intensity of the bands relative to the total Pck1 (Pck1-3HA) and the acetylated form (Ac-K). The ratios of Ac-K to correspondent Pck1-3HA values are reported (A). (B) Wt cells expressing Sir2-3HA were grown and supplied at Day 0 with RSV as in Fig. 1. At different time points, total protein extracts from both treated and untreated cultures were prepared and subjected to Western analysis using anti-HA antibody. Protein extracts from exponentially growing cells were also analyzed (Exp). Pgk1 was used as loading control. The filter stained with Ponceau S Red is also shown. One representative filter is shown. (C) Bar chart of the relative levels of Sir2-3HA expressed in arbitrary units. For each time point, band intensities relative to Sir2-HA and Pgk1 detected by Western analysis were quantified and the values of Sir2-3HA signals were normalized against Pgk1 ones. Then, all values obtained were further normalized against the normalized Sir2-3HA level measured in exponential phase, which was arbitrary set to 1. (D) Total protein extracts prepared from cultures in (B) were subjected to Western analysis using antibodies anti-H4K16ac and anti-H4. The filter stained with Ponceau S Red is also shown. (E) Bar chart of the relative levels of H4K16ac expressed in arbitrary units. Densitometric quantification of signal intensity of the bands relative to the total H4 and the acetylated form (K16ac) was performed. The ratios of H4K16ac to correspondent H4 values are reported. All data refer to mean values determined in three independent experiments with three technical replicates each. SD is indicated. Statistical significance as in Fig. 1 (**P ≤ 0.01).

intracellular trehalose stores took place (Fig. 1E). Indeed, the production of trehalose stores relies upon gluconeogenesis, which yields glucose-6-phosphate from the oxaloacetate provided by the glyoxylate shunt. In addition, since this shunt is fed with acetyl-CoA generated from acetate a reduction in the glyoxylate/gluconeogenesis flux also implies a slower depletion of extracellular ethanol and acetate as observed (Fig. 1B and C).

Moreover, RSV supplementation at Day 0 increased cellular respiration rate (J_R) as well as the non-phosphorylating respiration rate (J_{TET}). The latter estimated in the presence of the FoF1-ATPase inhibitor triethyltin bromide (TET, [51]) (Table 1). However, in these cells the net respiration (netR), measured by subtracting J_{TET} from J_R, was extremely low especially 3 days after the diauxic shift (Table 1) indicating that in the presence of RSV the respiration is predominantly uncoupled. No significant differences were detected in the maximal oxygen consumption rate (J_{MAX}, see Materials and Methods) between treated and untreated cultures reflecting a similar maximal respiratory capacity (Table 1).

It is known that a non-phosphorylating respiration state is the source of the superoxide anion ($O_2^{\bullet-}$) [52,53], which is produced by one electron reduction of oxygen due to leakage of electrons from the respiratory chain. $O_2^{\bullet-}$ and the resulting cascade of reactive oxygen

species (ROS) accumulate as a function of age and contribute to the chronological aging phenotype [48,50,54]. In RSV-treated cells an increase in $O_2^{\bullet-}$ content compared to that of the untreated ones was observed (Fig. 2A) in line with an increased non-phosphorylating respiration (Table 1).

An increased $O_2^{\bullet-}$ content reflects a serious imbalance between $O_2^{\bullet-}$ production and the cellular antioxidant capacity. In fact, cells have developed endogenous antioxidant defenses for scavenging $O_2^{\bullet-}$/ROS in order to offset their accumulation and the consequential damaging effects. In particular, starting from the diauxic shift, when cells shift to a respiratory metabolism and the cellular redox environment shifts to a more oxidized state [55,56] these protective mechanisms become increasingly engaged as yeast cells age [49,57]. In this context, antioxidant enzymes such as superoxide dismutases (Sod) and catalases are involved [48,58]. The former catalyze the dismutation of $O_2^{\bullet-}$ into hydrogen peroxide (H_2O_2) and the latter reduce H_2O_2 to water [49]. Consistent with published data [59], in untreated cells both the enzymatic activities of Sod and catalases increased after the diauxic shift (Fig. 2B). Notably, at the same time-points, in RSV-treated cells the same enzymatic activities were always higher (Fig. 2B) indicating that RSV supplementation stimulates the antioxidant defences. Despite this, the $O_2^{\bullet-}$ generated in the RSV presence exceeds the cellular antioxidant
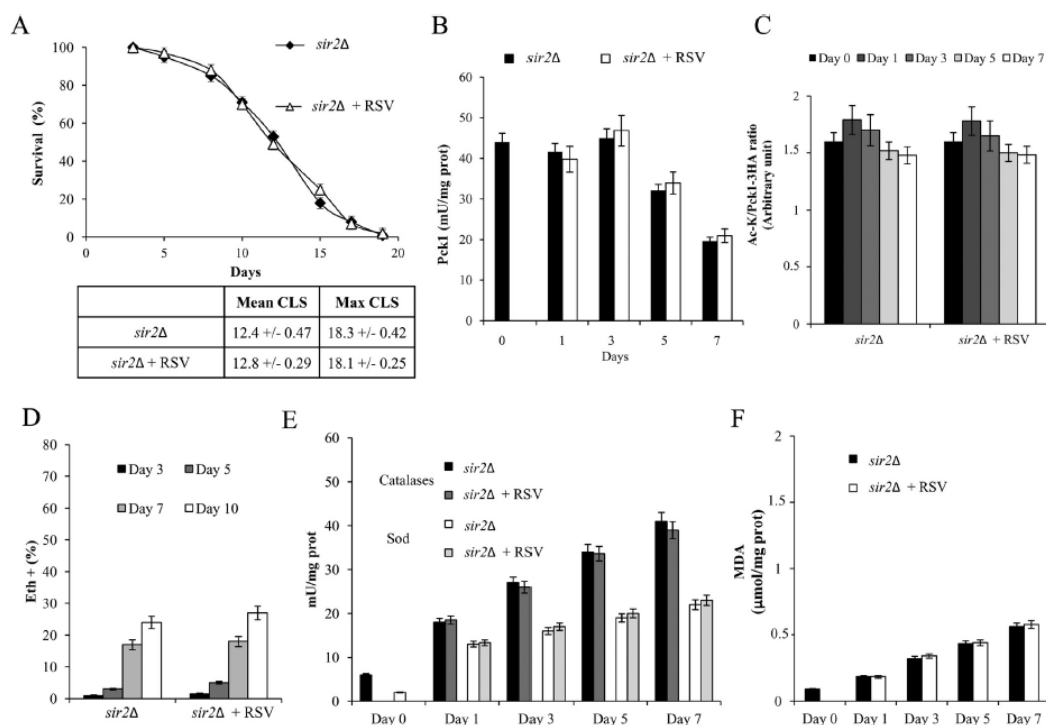
Fig. 4. RSV supplementation at the diauxic shift to *sir2Δ* cells does not determine a short-lived phenotype. *Sir2Δ* cells were grown and supplied at the diauxic shift (Day 0) with RSV as in Fig. 1. (A) Survival over time of treated and untreated cultures was assessed. In the Table are shown Mean CLS and Maximum CLS values. Bar charts report Pck1 enzymatic activity (B), the ratio between Ac-K and Pck1-3HA values (C), the percentage of intracellular superoxide-accumulating cells (D), catalases/Sod enzymatic activities (E) and the levels of intracellular malondialdehyde (MDA) (F) determined for both cultures. All data refer to mean values of three independent experiments with three technical replicates each. SD is indicated.

capacity resulting in an increase of $O_2^{\bullet-}$ levels.

Oxidative stress is associated with the accumulation of macromolecular damages including lipid peroxidation (LPO). This process is initiated by attack of ROS to lipids containing carbon-carbon double bond(s), in particular polyunsaturated fatty acids. Afterwards, a cascade of reactions takes place generating different types of aldehydes, many of which are highly reactive and toxic [60,61]. Malondialdehyde (MDA) is one of these end-products and is used as a convenient and reliable biomarker for LPO analysis [62]. After the diauxic shift in wt cells MDA levels increased (Fig. 2C), in line with the fact that LPO increases as chronological aging progresses [59,63]. At the same time-points, in chronologically aging RSV-treated cells MDA levels were always higher (Fig. 2C) indicating that RSV supplementation exacerbated LPO. All this can contribute to the shortened CLS.

3.2. Lack of Sir2 results in cells unresponsive to RSV supplementation at the diauxic shift

Pck1 is a metabolic enzyme that is highly regulated and, in particular, its gluconeogenic activity strictly depends on its de/acetylation state [35,64]. In agreement with the decrease in Pck1 activity measured following RSV supplementation at the diauxic shift (Fig. 1D), a decrease in the level of the acetylated active form of the enzyme compared with that in the untreated culture was observed (Fig. 3A). No significant difference in the total Pck1 was detected between the two cultures (data not shown). Since RSV has been classified as a naturally occurring STAC [12,14] and Sir2 is the enzyme responsible for Pck1

deacetylation [64], it is plausible to hypothesize that the deacetylase activity of Sir2 can be involved in the metabolic/physiologic changes observed in the presence of RSV. To investigate this, we initially compared total cellular levels of Sir2 in untreated and RSV-treated cells: no significant difference was found (Fig. 3B and C), ruling out any influence of RSV on Sir2 synthesis/stability. In parallel, we also compared the levels of H4 lysine 16 acetylation (H4K16ac). Indeed, the deacetylase activity of Sir2 is required for gene silencing at telomeres, mating-type *loci* (*HML* and *HMR*) and rDNA *locus*, where it maintains a hypoacetylated chromatin state by removing H4K16ac [65]. We did not observe any significant changes in H4K16ac levels between untreated and RSV-treated cells (Fig. 3D and E).

A way to assess if RSV works *via* Sir2 is to analyze its effects in the absence of the enzyme. Thus, RSV was supplied to *sir2Δ* cells at Day 0: all the RSV effects were abolished when *SIR2* was deleted and unlike wt cells, *sir2Δ* ones were unresponsive to RSV (Figs. 4 and S1). Indeed, CLS of *sir2Δ* cells was unaffected (Fig. 4A), as were the metabolic features that characterize a chronologically aging *sir2Δ* culture [35,37] such as fast depletion of extracellular ethanol and low levels of acetate (data not shown), high levels of Icl1 and Pck1 enzymatic activities (Figs. S1A and 4B), high levels of the acetylated Pck1 (Fig. 4C) and enhanced trehalose stores (Fig. S1B). Similarly, also the respiratory activity of chronologically aging *sir2Δ* cells that is particularly characterized by a low J_{TET} [37], was unaffected by RSV presence (Table 1). This was accompanied by low $O_2^{\bullet-}$ levels (Fig. 4D). As far as the enzymatic activities of Sod and catalases were concerned, in *sir2Δ* cells their levels were similar to those measured in the wt ones (Figs. 4E and 2B) in line
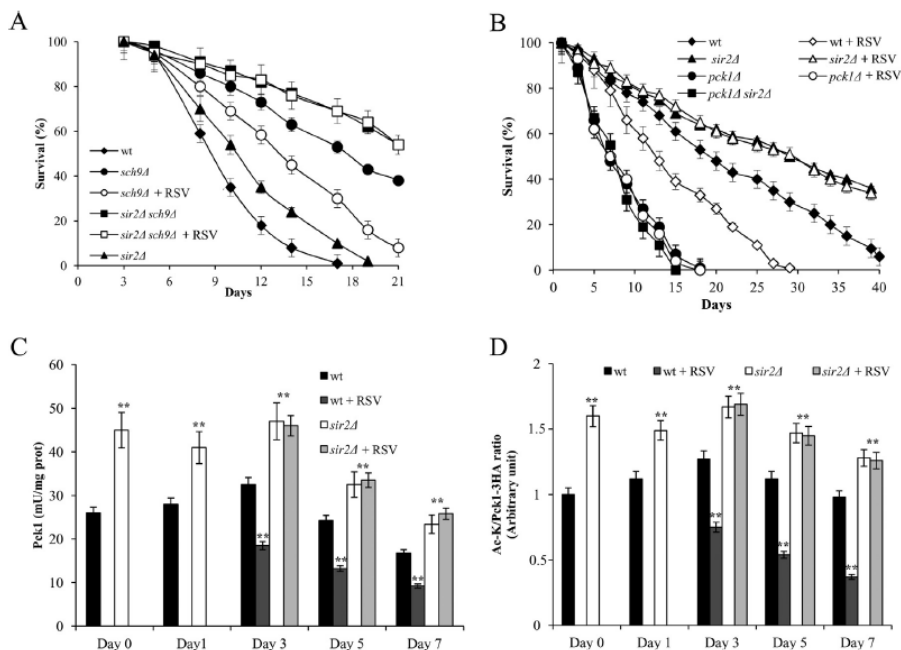
Fig. 5. RSV reduces the beneficial effects induced by *SCH9* deletion and severe CR on CLS. (A) CLS of *sch9Δ* and *sch9Δsir2Δ* cells supplemented with RSV at the diauxic shift (Day 0) as in Fig. 1. Survival of wt and *sir2Δ* strains is also shown for comparison. (B) The indicated strains grown as in Fig. 1, at Day 1 were transferred to water containing 100 μM RSV. Every 48 h, cultures were resuspended in fresh water and each time RSV was added. Survival of both treated and untreated cells was evaluated. In parallel, Pck1 enzymatic activity (C) and the ratio of Ac-K to Pck1-3HA values (D) were determined. All data presented are the mean values ± SD of three biological replicates. Statistical significance as in Fig. 1 (**: P ≤ 0.01).

with published gene expression profiles [36]. RSV supplementation to *sir2Δ* cells had no effect on both the enzymatic activities (Fig. 4E) indicating that in the absence of Sir2 the cellular antioxidant defences are not stimulated by RSV treatment. Finally, lack of Sir2 also determined during chronological aging a strong reduction of LPO as shown by the lower MDA levels compared with those of the wt culture and, in the same way as for the other parameters so far analyzed, they were unaffected by RSV (Figs. 2C and 4F). Thus, overall, following RSV supplementation at the diauxic shift, wt cells acquire metabolic traits that are opposite to those of chronologically aging *sir2Δ* cells. Moreover, taken together these data indicate that Sir2 is required in the acquirement of these traits.

3.3. RSV supplementation at the diauxic shift promotes Sir2-mediated deacetylation of Pck1

The AGC protein kinase Sch9, which is a direct substrate for TORC1 [66], is a negative regulator of CLS and its lack significantly extends CLS ([67] and Fig. 5A). This long-lived phenotype is further exacerbated by RSV treatment. This long-lived phenotype is further exacerbated by *SIR2* deletion ([36] and Fig. 5A). On the contrary, RSV supplementation to *sch9Δ* cells at Day 0 caused a survival reduction, whereas the synergistic effect of the *SIR2* deletion with the *SCH9* one on CLS was unaffected (Fig. 5A). Another condition in which *SIR2* deletion further exacerbates a long-lived phenotype is that of a severe form of CR obtained by transferring post-diauxic cells from their expired medium to water ([35,36] and Fig. 5B). Supplementing RSV to water strongly reduced the beneficial effect on the survival of wt cells produced by the severe CR, whilst had no impact on the extreme CLS extension of the *sir2Δ* culture (Fig. 5B). These data are consistent with the interpretation that the effects of RSV on CLS are mediated by Sir2.

Afterwards, since Pck1 acetylation/enzymatic activity is, on the one

hand, necessary and sufficient for CLS extension in water and, on the other, the key substrate of Sir2 controlling this form of longevity [64], we measured both parameters after RSV supplementation to wt and *sir2Δ* cultures. Once wt cells were switched to water, the presence of RSV determined a decrease in the levels of Pck1 enzymatic activity compared to those detected without RSV (Fig. 5C). This decrease was associated with a reduction in the amount of the acetylated active form of the enzyme (Fig. 5D) in line with a reduced CLS (Fig. 5B). The *sir2Δ* culture in water, characterized by an extreme long-lived phenotype, had higher levels of both the enzymatic activity and acetylated form of Pck1 compared to those of the wt culture (Fig. 5C and D). Moreover, similarly to all the other cellular parameters analyzed, neither did the enzymatic activity and acetylated form of Pck1 change following RSV supplementation to *sir2Δ* cells (Fig. 5C and D). As previously reported, *PCK1* deletion strongly reduced CLS in both water (Fig. 5B and [64]) and in expired medium [64]. The short-lived phenotype of *pck1Δ* cells was unaffected by *SIR2* deletion (Fig. 5B and [35,64]) being *PCK1* epistatic to *SIR2* in this form of longevity [64]. As *SIR2* deletion, RSV supplementation did not affect the CLS of *pck1Δ* cells in both water (Fig. 5B) and in expired medium (data not shown).

Finally, considering that we recently found that nicotinamide (NAM) supplementation at the diauxic shift inhibits Sir2 activity, in particular Sir2-mediated deacetylation of Pck1 resulting in a phenocopy of *SIR2* deletion [37], to further delineate the link between RSV and Sir2, we set out to evaluate whether NAM would cause any effect on RSV-supplemented cells. To this end, post-diauxic wt cells were transferred from their expired medium to RSV-supplemented water. Then, at the time-point where the RSV stationary culture showed 50% (mean CLS) of survival, NAM (5 mM) was added. As shown in Fig. 6A, the negative effect on CLS exerted by RSV presence was almost completely abolished by the longevity-extending activity of NAM as a
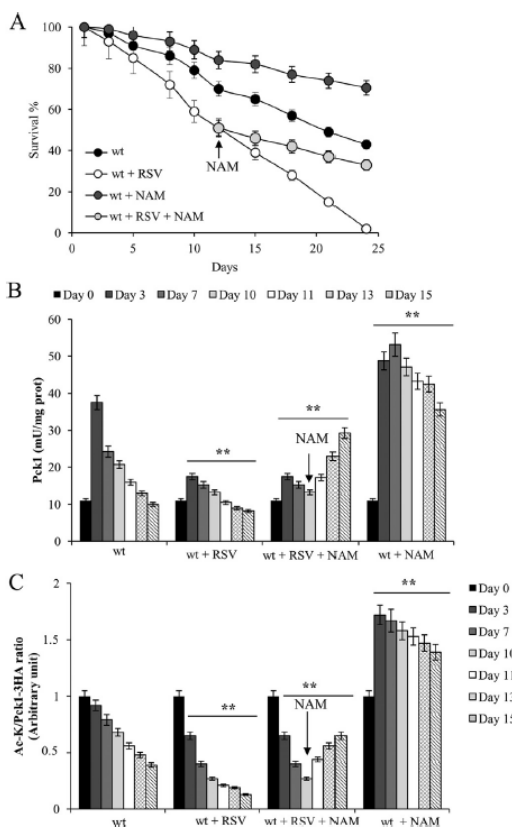
Fig. 6. NAM supplementation during chronological aging rescues the negative effects of RSV on CLS and Pck1 activity. (A) Wt cells were transferred to water as in Fig. 5B supplemented with 100 μM RSV or 5 mM nicotinamide (NAM). Every 48 h, cultures were resuspended in fresh water containing RSV or NAM and survival of the cells over time was monitored. In addition, at the time point corresponding to 50% of survival RSV-treated cells were switched to water supplemented with both NAM and RSV. Survival of wt cells in water is also shown for comparison. During the treatments in (A), at the indicated time points, Pck1 enzymatic activity (B) and the ratio of Ac-K to Pck1-3HA values (C) were determined. All data refer to mean values of three independent experiments with three technical replicates each. SD is indicated. Statistical significance as in Fig. 1 (**: P ≤ 0.01).

function of time in culture. Concomitantly, in the same time-frame, the trend of decrease of the enzymatic activity and the acetylation form of Pck1 was reversed and both increased (Fig. 6B and C). Taken together all these data reinforce the notion that the RSV effects observed herein are mediated by an enhancement of the Sir2 activity and involve its cellular target Pck1.

4. Discussion

In this study we investigated the effects of RSV supplementation at the onset of chronological aging, namely at the diauxic shift, on yeast metabolism and CLS. In effect, at the diauxic shift when cells shift from glucose-driven fermentation to ethanol/acetate-driven respiration, a massive metabolic reconfiguration takes place, leading cells to acquire a set of characteristics that ensure survival in stationary phase. These characteristics are specific to quiescent cells and influence the CLS. The metabolic reconfiguration mainly involves an increase in mitochondrial

respiration and activation of gluconeogenesis that allows cells to utilize the glucose-derived fermentation products, ethanol and acetate, and accumulate sufficient stores for surviving starvation [68]. In particular trehalose, the accumulation of which is beneficial for CLS extension [69], apart from its unequivocal protective activity and contribution as an energy storage carbohydrate in quiescent cells, it plays a key role in fueling cell cycle reentry from quiescence [70]. We found that RSV supplementation affects this metabolic reconfiguration leading to negative outcomes on CLS, such as increased $O_2^{\bullet-}$ levels and a decrease in trehalose stores. Interestingly, all data indicate that the RSV effects on both metabolism and CLS are Sir2-dependent. With regard to the reduction in trehalose stores, it relies on a decrease in gluconeogenesis whose main flux-controlling enzymatic activity, namely Pck1, strongly decreases following RSV supplementation. This decrease is mirrored by the decrease in the acetylated active form of Pck1, which is targeted for deacetylation by Sir2 causing downregulation of gluconeogenesis [35,37,64]. Since Sir2 levels are unaffected by RSV presence, this suggests that the Sir2 enzymatic activity is enhanced. Furthermore, it is well known that the acetylation control of Pck1 gluconeogenic activity is crucial for CLS extension both in expired medium and in extreme CR condition (water) [64]. In both conditions, RSV supplementation determines CLS restriction and reduced levels of both enzymatic activity and acetylated form of Pck1. Notably, the negative effects of RSV on CLS and Pck1 activity/acetylation level are reversed by the supplementation of a non-competitive inhibitor of Sir2 activity, such as NAM, which reacts with an intermediate of the deacetylation reaction reforming NAD^+ and the acetylated substrate [71]. In this context, we recently showed that NAM supplementation at the diauxic shift inhibits Sir2-mediated deacetylation of Pck1 generating a phenocopy of chronologically aging sir2Δ cells [37]. Since these cells display features that are opposite to those of RSV-supplied cells and SIR2 deletion makes cells unresponsive to RSV, taken as a whole, this supports the view that RSV effects stem from an enhancement of Sir2 activity and involve its cellular target Pck1.

In addition, chronologically aging sir2Δ cells and NAM-supplied ones display lower $O_2^{\bullet-}$ levels compared to wt cells (Fig. 4D and [37]). On the contrary, as far as $O_2^{\bullet-}$ levels are concerned, in RSV-treated cells, these levels remain higher compared with untreated ones despite the accompanying stimulation of endogenous cellular antioxidant defenses such as catalases and Sod. It is usually accepted that RSV has antioxidant properties relying in part upon the modulation of enzymes involved in the oxidative stress response [72]; in the chronological context this takes place, but strikingly it seems not to be enough to offset the increased flux of $O_2^{\bullet-}$ generated. It is well known that when cellular antioxidant responses are overwhelmed, oxidative stress occurs leading to the accumulation of macromolecular damages. Indeed, RSV-supplemented cells display enhanced lipid peroxidation. Furthermore, RSV supplementation also reduces trehalose stores and consequently reduces a protection against oxidative damage to proteins and lipids. All this may contribute thereby to restrict CLS.

To sum up, collectively these data are consistent with the notion that RSV supplementation at the diauxic shift requires Sir2 for eliciting its effects. In particular, it negatively influences chronological aging by enhancing Sir2 deacetylase activity. A common mechanism of allosteric activation/stimulation of SIRT1 activity has been proposed for RSV and synthetic STACs in which their binding to the N-terminal domain of SIRT1 leads to lowering the Km for the substrate [14]. Such an N-terminal regulatory domain is also present in Sir2 and provides a means for allosteric regulation of its enzymatic activity. Indeed, interactions between Sir4 and Sir2 involve this domain and enhance Sir2-mediated deacetylation of H4K16 [73,74]. Although we cannot rule out the possibility than RSV might directly target proteins other than Sir2, it is plausible to hypothesize that RSV can interact with Sir2 by a similar mechanism and modify/increase the affinity of Sir2 towards its physiological substrate, the acetylated Pck1, the enzymatic activity of which is essential for gluconeogenesis and CLS extension.

63

Acknowledgement

Appendix A. Supporting information
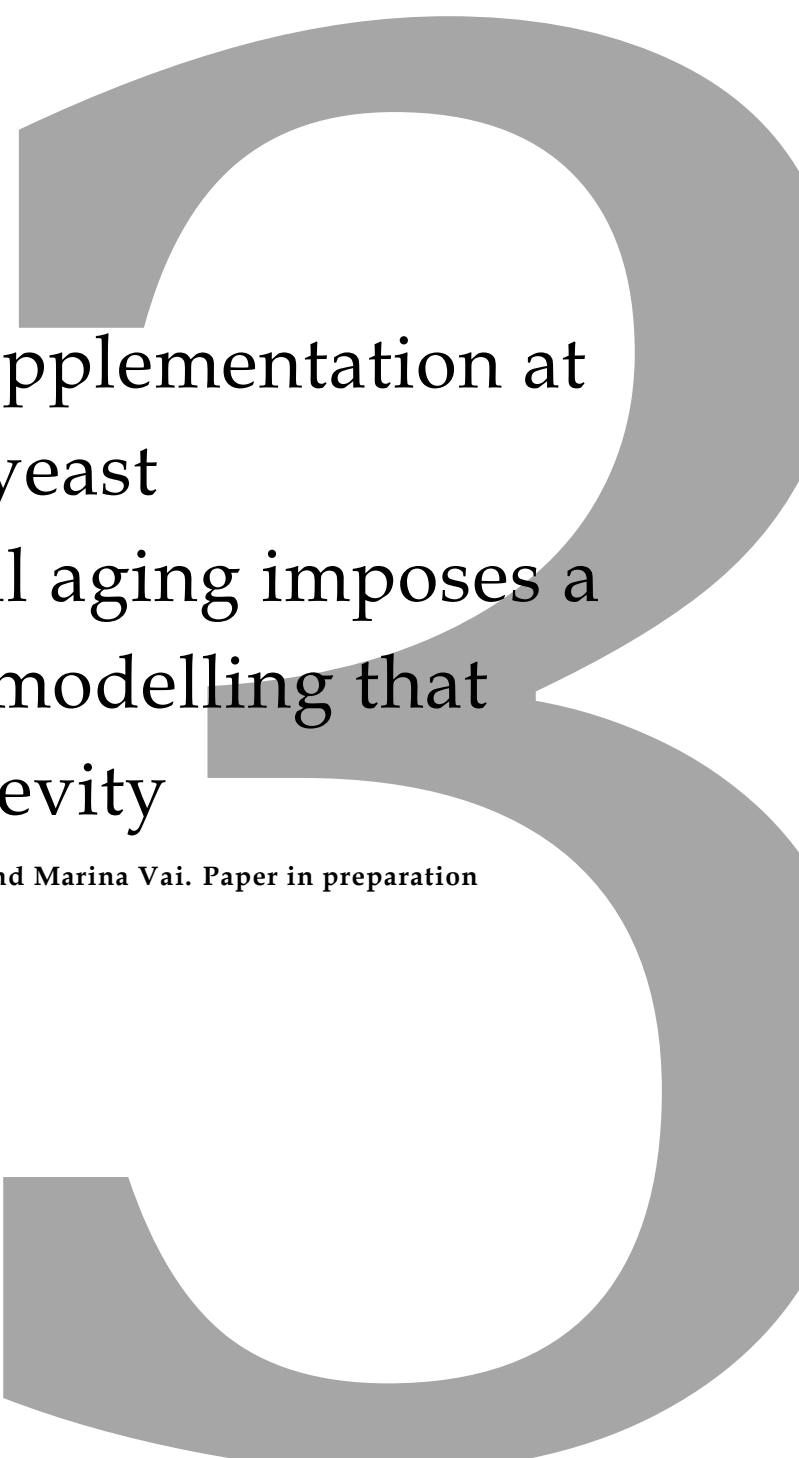
Supplementary data associated with this article can be found in the online version at http://dx.doi.org/10.1016/j.redox.2017.04.015.

References

[1] J. Burns, T. Yokota, H. Ashihara, M.E. Lean, A. Crozier, Plant foods and herbal sources of resveratrol, J. Agric. Food Chem. 50 (11) (2002) 3337–3340.
[2] L. Kursvietiene, I. Staneviciene, A. Mongirdiene, J. Bernatoniene, Multiplicity of effects and health benefits of resveratrol, Medicina 52 (3) (2016) 148–155.
[3] S. Renaud, M. de Lorgeril, Wine, alcohol, platelets, and the French paradox for coronary heart disease, Lancet 339 (8808) (1992) 1523–1526.
[4] B. Catalgol, S. Batirel, Y. Taga, N.K. Ozer, Resveratrol: french paradox revisited, Front. Pharmacol. 3 (2012) (Article ID:141).
[5] C.S. Erdogan, O. Vang, Challenges in analyzing the biological effects of resveratrol, Nutrients 8 (6) (2016) (Article ID: E353).
[6] M.G. Novelle, D. Wahl, C. Dieguez, M. Bernier, R. de Cabo, Resveratrol supplementation: where are we now and where should we go? Ageing Res. Rev. 21 (2015) 1–15.
[7] E.J. Park, J.M. Pezzuto, The pharmacology of resveratrol in animals and humans, Biochim. Biophys. Acta 1852 (6) (2015) 1071–1113.
[8] P.C. Tang, Y.F. Ng, S. Ho, M. Gyda, S.W. Chan, Resveratrol and cardiovascular health - Promising therapeutic or hopeless illusion? Pharmacol. Res. 90 (2014) 88–115.
[9] S.S. Kulkarni, C. Canto, The molecular targets of resveratrol, Biochim. Biophys. Acta 1852 (6) (2015) 1114–1123.
[10] R.I. Tennen, E. Michishita-Kioi, K.F. Chua, Finding a target for resveratrol, Cell 148 (3) (2012) 387–389.
[11] K.T. Howitz, K.J. Bitterman, H.Y. Cohen, D.W. Lamming, S. Lavu, J.G. Wood, R.E. Zipkin, P. Chung, A. Kisielewski, L.L. Zhang, B. Scherer, D.A. Sinclair, Small molecule activators of Sirtuins extend Saccharomyces cerevisiae lifespan, Nature 425 (6954) (2003) 191–196.
[12] B.P. Hubbard, D.A. Sinclair, Small molecule SIRT1 activators for the treatment of aging and age-related diseases, Trends Pharmacol. Sci. 35 (3) (2014) 146–154.
[13] S.J. Park, F. Ahmad, A. Philp, K. Baar, T. Williams, H. Luo, H. Ke, H. Rehmann, R. Taussig, A.L. Brown, M.K. Kim, M.A. Beaven, A.B. Burgin, V. Manganiello, J.H. Chung, Resveratrol ameliorates aging-related metabolic phenotypes by inhibiting cAMP phosphodiesterases, Cell 148 (3) (2012) 421–433.
[14] D.A. Sinclair, L. Guarente, Small-molecule allosteric activators of Sirtuins, Annu. Rev. Pharmacol. Toxicol. 54 (2014) 363–380.
[15] M. Gertz, C. Steegborn, Using mitochondrial sirtuins as drug targets: disease implications and available compounds, Cell. Mol. Life Sci. 73 (15) (2016) 2871–2896.
[16] R.H. Houtkooper, E. Pirinen, J. Auwerx, Sirtuins as regulators of metabolism and healthspan, Nat. Rev. Mol. Cell. Biol. 13 (4) (2012) 225–238.
[17] S. Imai, L. Guarente, NAD⁺ and Sirtuins in aging and disease, Trends Cell. Biol. 24 (8) (2014) 464–471.
[18] B.J. Morris, Seven sirtuins for seven deadly diseases of aging, Free Radic. Biol. Med. 56 (2013) 133–171.
[19] M. Kitada, Y. Ogura, D. Koya, The protective role of Sirt1 in vascular tissue: its relationship to vascular aging and atherosclerosis, Aging (Albany, NY) 8 (10) (2016) 2290–2307.
[20] A. Kumar, S. Chauhan, How much successful are the medicinal chemists in modulation of SIRT1: a critical review, Eur. J. Med. Chem. 119 (2016) 45–69.
[21] N. Poulose, R. Raju, Sirtuin regulation in aging and injury, Biochim. Biophys. Acta 1852 (11) (2015) 2442–2455.
[22] R.A. Frye, Phylogenetic classification of prokaryotic and eukaryotic Sir2-like proteins, Biochem. Biophys. Res. Commun. 273 (2) (2000) 793–798.
[23] V.D. Longo, G.S. Shadel, M. Kaeberlein, B. Kennedy, Replicative and chronological aging in Saccharomyces cerevisiae, Cell Metab. 16 (1) (2012) 18–31.
[24] T. Nystrom, B. Liu, The mystery of aging and rejuvenation - a budding topic, Curr. Opin. Microbiol. 18 (2014) 61–67.
[25] V.D. Longo, B.K. Kennedy, Sirtuins in aging and age-related disease, Cell 126 (2) (2006) 257–268.
[26] S. Imai, C.M. Armstrong, M. Kaeberlein, L. Guarente, Transcriptional silencing and longevity protein Sir2 is an NAD-dependent histone deacetylase, Nature 403 (6771) (2000) 795–800.
[27] M. Kaeberlein, M. McVey, L. Guarente, The SIR2/3/4 complex and SIR2 alone promote longevity in Saccharomyces cerevisiae by two different mechanisms, Genes Dev. 13 (19) (1999) 2570–2580.
[28] S.W. Stumpferl, S.E. Brand, J.C. Jiang, B. Korona, A. Tiwari, J. Dai, J.G. Seo, S.M. Jazwinski, Natural genetic variation in yeast longevity, Genome Res. 22 (10) (2012) 1963–1973.
[29] K.A. Steinkraus, M. Kaeberlein, B.K. Kennedy, Replicative aging in yeast: the means to the end, Annu. Rev. Cell. Dev. Biol. 24 (2008) 29–54.
[30] S. Jarolim, J. Millen, G. Heeren, P. Laun, D.S. Goldfarb, M. Breitenbach, A novel assay for replicative lifespan in Saccharomyces cerevisiae, FEMS Yeast Res. 5 (2) (2004) 169–177.
[31] H. Yang, J.A. Baur, A. Chen, C. Miller, J.K. Adams, A. Kisielewski, K.T. Howitz, R.E. Zipkin, D.A. Sinclair, Design and synthesis of compounds that extend replicative lifespan, Aging Cell 6 (1) (2007) 35–43.
[32] M. Kaeberlein, B.K. Kennedy, Does resveratrol activate yeast Sir2 in vivo? Aging Cell 6 (4) (2007) 415–416.
[33] M. MacLean, N. Harris, P.W. Piper, Chronological lifespan of stationary phase yeast cells; a model for investigating the factors that might influence the ageing of postmitotic tissues in higher organisms, Yeast 18 (6) (2001) 499–509.
[34] P. Fabrizio, V.D. Longo, The chronological life span of Saccharomyces cerevisiae, Methods Mol. Biol. 371 (2007) 89–95.
[35] N. Casatta, A. Porro, I. Orlandi, L. Brambilla, M. Vai, Lack of Sir2 increases acetate consumption and decreases extracellular pro-aging factors, Biochim. Biophys. Acta 1833 (3) (2013) 593–601.
[36] P. Fabrizio, C. Gattazzo, L. Battistella, M. Wei, C. Cheng, K. McGrew, V.D. Longo, Sir2 blocks extreme life-span extension, Cell 123 (4) (2005) 655–667.
[37] I. Orlandi, D. Pellegrino Coppola, M. Strippoli, R. Ronzulli, M. Vai, Nicotinamide supplementation phenocopies SIR2 inactivation by modulating carbon metabolism and respiration during yeast chronological aging, Mech. Ageing Dev. 161 (2017) 277–287.
[38] I. Orlandi, D. Coppola, M. Vai, Rewiring yeast acetate metabolism through MPC1 loss of function leads to mitochondrial damage and decreases chronological lifespan, Microb. Cell 1 (12) (2014) 393–405.
[39] M. Vanoni, M. Vai, L. Popolo, L. Alberghina, Structural heterogeneity in populations of the budding yeast Saccharomyces cerevisiae, J. Bacteriol. 156 (3) (1983) 1282–1291.
[40] I. Orlandi, R. Ronzulli, N. Casatta, M. Vai, Ethanol and acetate acting as carbon/energy sources negatively affect yeast chronological aging, Oxid. Med. Cell. Longev. 2013 (2013) (article ID: 802870).
[41] D.H. Lee, A.L. Goldberg, Proteasome inhibitors cause induction of heat shock proteins and trehalose, which together confer thermotolerance in Saccharomyces cerevisiae, Mol. Cell. Biol. 18 (1) (1998) 30–38.
[42] P. de Jong-Gubbels, P. Vanrolleghem, S. Heijnen, J.P. van Dijken, J.T. Pronk, Regulation of carbon metabolism in chemostat cultures of Saccharomyces cerevisiae grown on mixtures of glucose and ethanol, Yeast 11 (5) (1995) 407–418.
[43] S. Giannattasio, N. Guaragnella, M. Corte-Real, S. Passarella, E. Marra, Acid stress adaptation protects Saccharomyces cerevisiae from acetic acid-induced programmed cell death, Gene 354 (2005) 93–98.
[44] V.Y. Petrova, D. Drescher, A.V. Kujumdzieva, M.J. Schmitt, Dual targeting of yeast catalase A to peroxisomes and mitochondria, Biochem. J. 380 (2) (2004) 393–400.
[45] L. Flohe, F. Otting, Superoxide dismutase assays, Methods Enzymol. 105 (1984) 93–104.
[46] F. Madeo, E. Frohlich, M. Ligr, M. Grey, S.J. Sigrist, D.H. Wolf, K.U. Frohlich, Oxygen stress: a regulator of apoptosis in yeast, J. Cell Biol. 145 (4) (1999) 757–767.
[47] V.V. Kushnirov, Rapid and reliable protein extraction from yeast, Yeast 16 (9) (2000) 857–860.
[48] M. Breitenbach, M. Rinnerthaler, J. Hartl, A. Stincone, J. Vowinckel, H. Breitenbach-Koller, M. Ralser, Mitochondria in ageing: there is metabolism beyond the ROS, FEMS Yeast Res. 14 (1) (2014) 198–212.
[49] E. Herrero, J. Ros, G. Belli, E. Cabiscol, Redox control and oxidative stress in yeast cells, Biochim. Biophys. Acta 1780 (11) (2008) 1217–1235.
[50] Y. Pan, Mitochondria, reactive oxygen species and chronological aging: a message from yeast, Exp. Gerontol. 46 (11) (2011) 847–852.
[51] K. Cain, D.E. Griffiths, Studies of energy-linked reactions. localization of the site of action of trialkyltin in yeast mitochondria, Biochem. J. 162 (3) (1977) 575–580.
[52] S. Guerrero-Castillo, D. Araiza-Olivera, A. Cabrera-Orefice, J. Espinasa-Jaramillo, M. Gutierrez-Aguilar, L.A. Luevano-Martinez, A. Zepeda-Bastida, S. Uribe-Carvajal, Physiological uncoupling of mitochondrial oxidative phosphorylation. studies in different yeast species, J. Bioenerg. Biomembr. 43 (3) (2011) 323–331.
[53] L. Hlavata, H. Aguilaniu, A. Pichova, T. Nystrom, The oncogenic RAS2ᵛᵃˡ¹⁹ mutation locks respiration, independently of PKA, in a mode prone to generate ROS, EMBO J. 22 (13) (2003) 3337–3345.
[54] M.H. Barros, F.M. da Cunha, G.A. Oliveira, E.B. Tahara, A.J. Kowaltowski, Yeast as a model to study mitochondrial mechanisms in ageing, Mech. Ageing Dev. 131 (7–8) (2010) 494–502.
[55] A. Ayer, J. Sanwald, B.A. Pillay, A.J. Meyer, G.G. Perrone, I.W. Dawes, Distinct redox regulation in sub-cellular compartments in response to various stress conditions in Saccharomyces cerevisiae, PLoS One 8 (6) (2013) (Article ID: e65240).
[56] T. Drakulic, M.D. Temple, R. Guido, S. Jarolim, M. Breitenbach, P.V. Attfield, I.W. Dawes, Involvement of oxidative stress response genes in redox homeostasis, the level of reactive oxygen species and ageing in Saccharomyces cerevisiae, FEMS Yeast Res. 5 (12) (2005) 1215–1228.
[57] M.P. Murphy, How mitochondria produce reactive oxygen species, Biochem. J. 417 (1) (2009) 1–13.
[58] V.D. Longo, E.B. Gralla, J.S. Valentine, Superoxide dismutase activity is essential for stationary phase survival in Saccharomyces cerevisiae. Mitochondrial production of toxic oxygen species in vivo, J. Biol. Chem. 271 (21) (1996) 12275–12280.
[59] G. Reverter-Branchat, E. Cabiscol, J. Tamarit, J. Ros, Oxidative damage to specific proteins in replicative and chronological-aged Saccharomyces cerevisiae: common targets and prevention by calorie restriction, J. Biol. Chem. 279 (30) (2004) 31983–31989.

[60] A. Ayala, M.F. Munoz, S. Arguelles, Lipid peroxidation: production, metabolism, and signaling mechanisms of malondialdehyde and 4-hydroxy-2-nonenal, Oxid. Med. Cell. Longev. 2014 (2014) (Article ID: 360438).

[61] A.K. Hauck, D.A. Bernlohr, Oxidative stress and lipotoxicity, J. Lipid Res. 57 (11) (2016) 1976–1986.

[62] H.H. Draper, M. Hadley, Malondialdehyde determination as index of lipid peroxidation, Methods Enzymol. 186 (1990) 421–431.

[63] E. Cabiscol, E. Piulats, P. Echave, E. Herrero, J. Ros, Oxidative stress promotes specific protein damage in *Saccharomyces cerevisiae*, J. Biol. Chem. 275 (35) (2000) 27393–27398.

[64] Y.Y. Lin, J.Y. Lu, J. Zhang, W. Walter, W. Dang, J. Wan, S.C. Tao, J. Qian, Y. Zhao, J.D. Boeke, S.L. Berger, H. Zhu, Protein acetylation microarray reveals that NuA4 controls key metabolic target regulating gluconeogenesis, Cell 136 (6) (2009) 1073–1084.

[65] M.R. Gartenberg, J.S. Smith, The nuts and bolts of transcriptionally silent chromatin in *Saccharomyces cerevisiae*, Genetics 203 (4) (2016) 1563–1599.

[66] R. Loewith, M.N. Hall, Target of rapamycin (TOR) in nutrient signaling and growth control, Genetics 189 (4) (2011) 1177–1201.

[67] P. Fabrizio, F. Pozza, S.D. Pletcher, C.M. Gendron, V.D. Longo, Regulation of longevity and stress resistance by Sch9 in yeast, Science 292 (5515) (2001)

288–290.

[68] C. De Virgilio, The essence of yeast quiescence, FEMS Microbiol. Rev. 36 (2) (2012) 306–339.

[69] A. Ocampo, J. Liu, E.A. Schroeder, G.S. Shadel, A. Barrientos, Mitochondrial respiratory thresholds regulate yeast chronological life span and its extension by caloric restriction, Cell Metab. 16 (1) (2012) 55–67.

[70] L. Shi, B.M. Sutter, X. Ye, B.P. Tu, Trehalose is a key determinant of the quiescent metabolic state that fuels cell cycle progression upon return to growth, Mol. Biol. Cell 21 (12) (2010) 1982–1990.

[71] A.A. Sauve, C. Wolberger, V.L. Schramm, J.D. Boeke, The biochemistry of Sirtuins, Annu. Rev. Biochem. 75 (2006) 435–465.

[72] G.T. Diaz-Gerevini, G. Repossi, A. Dain, M.C. Tarres, U.N. Das, A.R. Eynard, Beneficial action of resveratrol: how and why? Nutrition 32 (2) (2016) 174–178.

[73] H.C. Hsu, C.L. Wang, M. Wang, N. Yang, Z. Chen, R. Sternglanz, R.M. Xu, Structural basis for allosteric stimulation of Sir2 activity by Sir4 binding, Genes Dev. 27 (1) (2013) 64–73.

[74] J.C. Tanny, D.S. Kirkpatrick, S.A. Gerber, S.P. Gygi, D. Moazed, Budding yeast silencing complexes and regulation of Sir2 activity by protein-protein interactions, Mol. Cell. Biol. 24 (16) (2004) 6931–6946.

65

Chapter

3

Quercetin supplementation at the onset of yeast chronological aging imposes a metabolic remodelling that favours longevity

Giulia Stamerra, Ivan Orlandi and Marina Vai. Paper in preparation

3.1 INTRODUCTION

Naturally occurring flavonoids are recognized for their beneficial effects on health and their moderate intake has been proposed to improve the efficacy of pharmacological treatments against the functional decline occurring during aging. Among these, quercetin (3,3',4',5,7-pentahydroxyflavanone) (QUER), is the most commonly consumed one in the human diet, due to its abundance in many foods of plant origin, including capers, onions, broccoli, green tea infusion and nuts (1). QUER is specifically categorized as a flavanol, whose main structure comprises two aromatic rings joined by a γ pyrone ring, which have hydroxyl groups, thanks to which the antioxidant properties of the molecule are ascribed (2). For some time, the therapeutic potential of QUER for preventing such diverse age-related pathologies, such as cancer, cardiovascular and metabolic disorders, has been generally attributed to its direct antioxidant effects (3). Nevertheless, evidence indicate that QUER is also able to improve both glucose and lipid metabolism, all mechanisms by which it may provide its pleiotropic health effects (4, 5).

Among the proposed targets whose activity is modulated by QUER, one of the most relevant is Sirtuin 1 (SIRT1) (6). SIRT1 is an evolutionarily NAD^+-dependent deacetylase, a feature that places its activity in a central role for cellular metabolism, and for the aging process (7). SIRT1 is the mammalian orthologue of Sir2 of *Saccharomyces cerevisiae*. This yeast is widely used as a model organism in the study of the aging process, due to the conservativeness of its pathways with those of complex eukaryotes, contributing to the identification of many mammalian genes that influence aging (8). Indeed, yeast allows us to simulate both the aging process of mitotically active cells and that of post-mitotic mammalian cells (8). In the former, replicative aging, the replicative lifespan (RLS) is measured, which represents the replicative potential of individual yeast cells. Sir2 activity promotes RLS extension (9). In the latter, chronological aging, the chronological lifespan (CLS) is assessed, which measures the capability of quiescent cells in stationary phase to resume growth once returning to rich fresh medium. In this context, Sir2 displays pro-aging effects (10–13). Indeed, when glucose is depleted and the diauxic shift occurs, cells are sustained by a completely respiratory metabolism in which the C2 compounds (ethanol and acetate) resulting from glucose fermentation are used as carbon/energy sources. The mitochondrial respiratory chain can produce anion superoxide ($O_2^{.-}$), which has a negative impact on yeast CLS (13). When also ethanol and acetate are consumed, cells need to use the carbohydrate reserves produced

with gluconeogenesis, namely glycogen and trehalose. This latter, a disaccharide of glucose, is a well- known oxidative stress protector thanks to its chaperon-like activity, which prevents damaged proteins aggregation (14, 15). Sir2 interferes with this metabolic remodelling required during the diauxic shift, leading to a decrease in trehalose reserves and an increase in oxidative damage, ultimately shortening the CLS (13).

No significantly effects have been observed on RLS following QUER addition (16). On the contrary, regarding chronological aging, a QUER pre-treatment during the exponential phase is able to induce an adaptative response from oxidative stress, which results in CLS increase (17).

In this work, we investigated the effects of QUER on chronological aging, by adding the compound at the diauxic shift, crucial moment of the growth characterized by a metabolic asset reorganization, which defines the length of the stationary phase. The results indicate that QUER displays anti-aging properties. Its effects are mediated both by inhibiting the deacetylase activity of Sir2 and promoting lipid catabolism, as well as trehalose storage, which ultimately results in CLS extension.

3.2 MATERIALS AND METHODS

3.2.1 Yeast strains and growth conditions

All yeast strains used in this work are listed in Table 1. All deletion strains were generated by PCR- based methods and accuracy of gene replacement was verified by using internal and flanking primers. Standard methods were used for DNA manipulation and yeast transformation. Cells were grown in batch cultures at 30°C in minimal medium (Difco Yeast Nitrogen Base without amino acids, 6.7 g/l) with 2% w/v glucose and the required supplements added in excess as described (18). Cell growth was measured with a Coulter Counter-Particle Count and Size Analyser by determining cell number (19) and, in parallel, the extracellular concentrations of glucose and ethanol were measured in medium samples collected at different time-points in order to define the growth profile (exponential phase, diauxic shift (Day 0), post-diauxic phase and stationary

phase). Duplication times were obtained by linear regression of the cell number increase over time on a semi-logarithmic plot.

Strain	Relevant genotype	Source
W303-1A	*MATa ade2-1 his3-11,15 leu2-3,112 trp1-1 ura3-1 can1-100*	P.P. Slominski
sir2Δ	W303-1A *sir2Δ::URA3*	(Calzari *et al*, 2006)
PCK1-3HA	W303-1A *PCK1-3HA::KlURA3*	(Casatta *et al*, 2013)
sir2Δ PCK1-3HA	W303-1A *sir2Δ::HIS3* PCK1-3HA::KlURA3	(Casatta *et al*, 2013)
oaf1Δ	W303-1A *oaf1Δ::HIS3*	This study
oaf1Δ sir2Δ	W303-1A *oaf1Δ::HIS3 sir2Δ::URA3*	This study

Table 1. Yeast strains used in this study

3.2.2 CLS determination

CLS assay was performed according to (10) by counting the number of colony forming units (CFUs) starting 72 h (Day 3) after the diauxic shift. The number of CFUs on Day 3 was considered as 100% of survival. The treatment with QUER (dissolved in DMSO, Sigma-Aldrich) was performed by adding the compound at Day 0 at the final concentration of 300 µM.

3.2.3 Metabolite measurements and enzymatic assays

At designated time-points, aliquots of the yeast cultures were centrifuged and both pellets (washed twice) and supernatants were frozen at – 80 °C until used. Glucose, ethanol and acetic acid concentrations in the growth medium were determined using enzymatic assays (K-HKGLU, K-ETOH, K-ACET kits from Megazyme). Intracellular trehalose was extracted and measured as described in (20). The released glucose was measured using the K-HKGLU kit. Immediately after preparation of cell-free extracts, Pck1 and Icl1 activities were determined as reported in (21). Total protein concentration was estimated using the BCA™ Protein Assay Kit (Pierce).

3.2.4 Superoxide levels and lipid peroxidation

Anion superoxide levels were detected with dihydroethidium (DHE, Sigma-Aldrich) according to (22). A Nikon Eclipse E600 fluorescence microscope equipped with a Leica DC 350F ccd camera was used and digital images were acquired with FW4000 software (Leica). Lipid peroxidation was measured by quantifying

malonildialdehyde (MDA) with the BIOXYTECH® LPO-586™ Colorimetric Assay Kit (OxisResearch) as described in (23).

3.2.5 Immunoprecipitation and Western analysis

Total protein extracts preparation, immunoprecipitation and Western analysis were performed as previously described (10). Briefly, proteins were extracted in the presence of protease inhibitors (1 mM phenylmethanesulfonyl fluoride and Complete EDTA-free Protease Inhibitor Cocktail Tablets, Roche) and histone deacetylase inhibitors (100 μM Trichostatin A, 50 mM nicotinamide and 50 mM sodium butyrate). A crude lysate aliquot was stored at − 20 °C as immunoprecipitation input control. For immunoprecipitation, lysates (about 500 μg) were incubated with 2 μg of anti-HA mAb (12CA5, Roche) at 4 °C overnight, followed by the addition of 50 μl Dynabeads Protein A (Dynal Biotech) for 2 h. After five washes with washing buffer (50 mM Tris, pH 7.4, 50 mM NaCl) at 4 °C, bound proteins were eluted by boiling in SDS sample buffer. SDS-PAGE was performed on 12% polyacrylamide slab gels. Gels were blotted onto Hybond-P PVDF membranes (Amersham). Correct loading/transfer was confirmed by staining filters with Ponceau S Red (Sigma-Aldrich). The primary antibodies used were: anti-HA (12CA5, Roche), anti-acetylated-lysine (Ac-K-103, Cell Signaling) and anti-3-phosphoglycerate kinase (Pgk1) (22C5, Invitrogen). Secondary antibodies were purchased from Amersham. Binding was visualized with the ECL Western Blotting Detection Reagent (Amersham). After ECL detection, films were scanned on a Bio-Rad GS-800 calibrated imaging densitometer and quantified with Scion Image software.

3.2.6 Sir2 Inhibition assay

Sir2 inhibition assay was performed as previously describe (24). Briefly, cells in exponential phase or at the diauxic shift (at the same cell concentration of QUER treatment) were dropped (5 μl of a 10^6 cells/ml dilution) onto glucose rich/medium [YEPD, 1% (w/v) yeast extract, 2% (w/v) Bacto Peptone, 2% (w/v) glucose, 2% (w/v) agar] plates supplemented with α-factor at a final concentration of 2.5 μM. A concentration gradient of QUER was formed by loading 5 μl of 300 μM QUER on filter disks placed on the agar. 5 μl of 5 mM splitomicin (dissolved in DMSO, Sigma-Aldrich) was loaded on a filter disk as a control. Plates were incubated at 30°C for 2/3 days.

3.2.7 Lipid analysis

Total lipids were extracted according to (25). Fatty acid concentration was determined using enzymatic assay (Free Fatty Acid Quantitation Kit, Sigma-Aldrich).

3.2.8 Statistical analysis of data

All values are presented as the mean of three independent experiments with the corresponding Standard Deviation (SD). Three technical replicates were analyzed in each independent experiment. Statistical significance was assessed by one-way ANOVA test. P value of ≤ 0.05 was considered statistically significant.

3.3 RESULTS AND DISCUSSION

3.3.1 Quercetin supplementation at the diauxic shift increases CLS, reduces oxidative stress and drives carbon metabolism along the glyoxylate/gluconeogenic axis

During chronological aging, an increase of oxidative stress takes place, which negatively affects CLS (13). Since QUER is recognized for possessing anti-oxidant and anti-aging properties, initially we examined the possible effects on both CLS and oxidative stress following QUER supplementation at the diauxic shift. QUER-treated cells displayed an increase of both medium and maximum CLS (Fig. 1A) in concert with decreased levels of $0_2^{\cdot -}$ and lipid peroxidation (Fig. 1B and C), an oxidative damage affecting cell membranes and lipoproteins (28). During a balanced growth on glucose, cells use it as the main carbon source with the resulting production of ethanol and acetate, C2 compounds whose metabolism influences chronological longevity (12). QUER supplementation resulted in a faster ethanol and acetate depletion compared with non-treated cells (Fig. 1D and E).
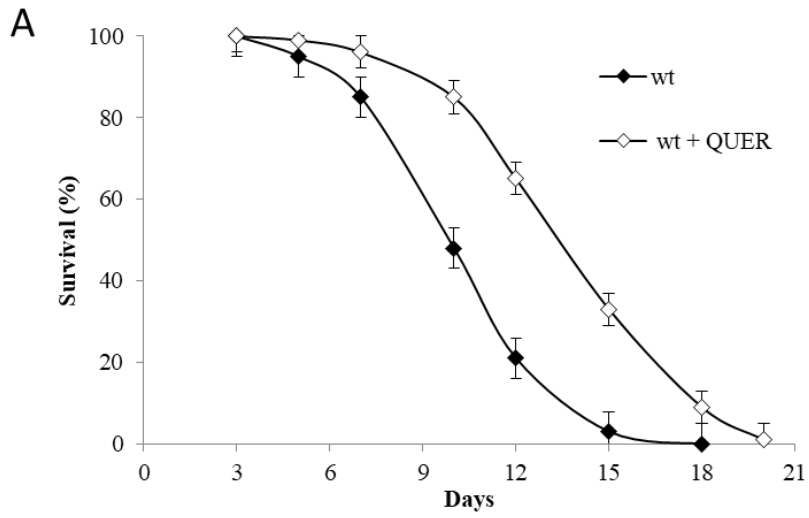
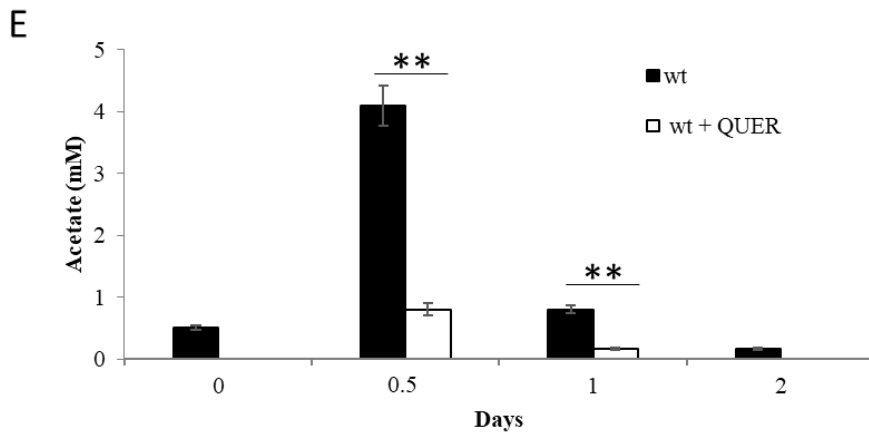| Strain	Mean CLS	Maximum CLS
wt	10.4±0.53	14.61±0.31
wt + QUER	13.78±0.43	17.96±0.37
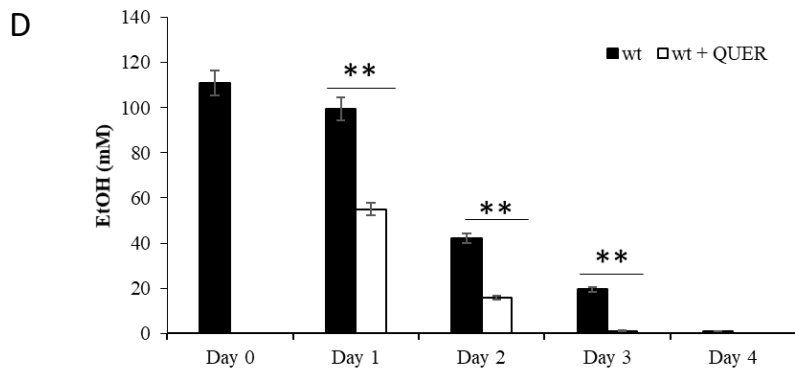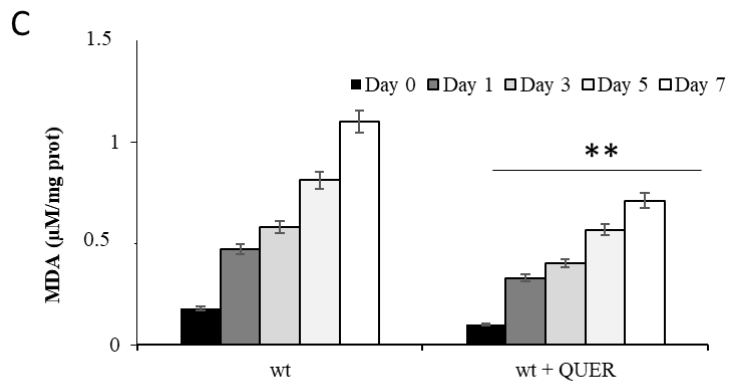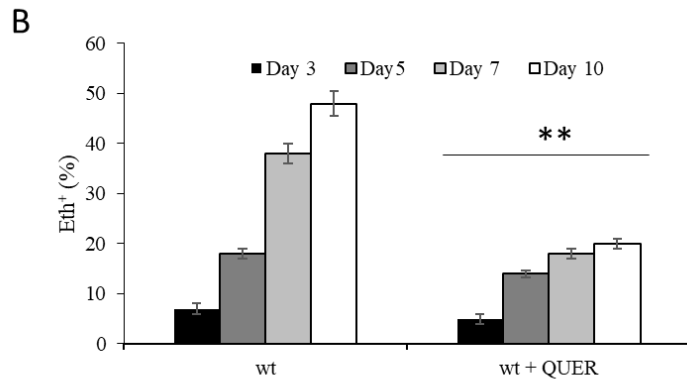
Fig. 1 QUER supplementation at the diauxic shift elicits anti-aging effects. Wild-type (wt) cells were grown in minimal medium/2% glucose and the required supplements in excess. At the diauxic shift (Day 0), QUER (300 μM) was added to the expired media. (A) At each time point, survival was determined by colony-forming capacity on YEPD plates. 72 h after the diauxic shift (Day 3) was considered the first age-point. In parallel, survival of cells in their expired medium without QUER was monitored. Data referring to the time points where chronological aging cultures showed 50% (Mean CLS) and 10% (Maximum CLS) of survival are reported. In parallel, for the same cultures the levels of intracellular superoxide (Eth) (B) and malonyldyaldeide (MDA) (C) were measured. Summary graphs of extracellular ethanol (D) and acetate (E) determined at the time points indicated. Standard deviation (SD) is indicated. Statistical significance as assessed by one-way ANOVA test is indicated (**$p \leq 0.01$).

In the light of this result, the anabolic pathways involved in ethanol and acetate utilization, glyoxylate and gluconeogenesis, were analysed by measuring the enzymatic activity of Icl1, one of the unique enzymes of the glyoxylate cycle, and Pck1, which catalyses the rate-limiting step of gluconeogenesis. In cells treated with QUER the activity of both these enzymes was higher compared with the non-treated ones, indicating an increase of glyoxylate/gluconeogenic pathways, respectively (Fig. 2A and B). These metabolic changes were in line with an enhancement of trehalose reserves (Fig. 2C). It is well known that Pck1 activity is regulated by its (de)acetylation state: the enzyme is active when acetylated, while it is inhibited by Sir2-mediated deacetylation, the Sirtuin whose activity negatively influences CLS (8, 13). The acetylation level of Pck1 increased after the treatment with the compound (Fig. 2D) in agreement with the increase of Pck1 activity. Staying with

these premises we wonder whether the metabolic features acquired by the cells following QUER treatment, could be dependent on the inhibition of Sir2 activity.
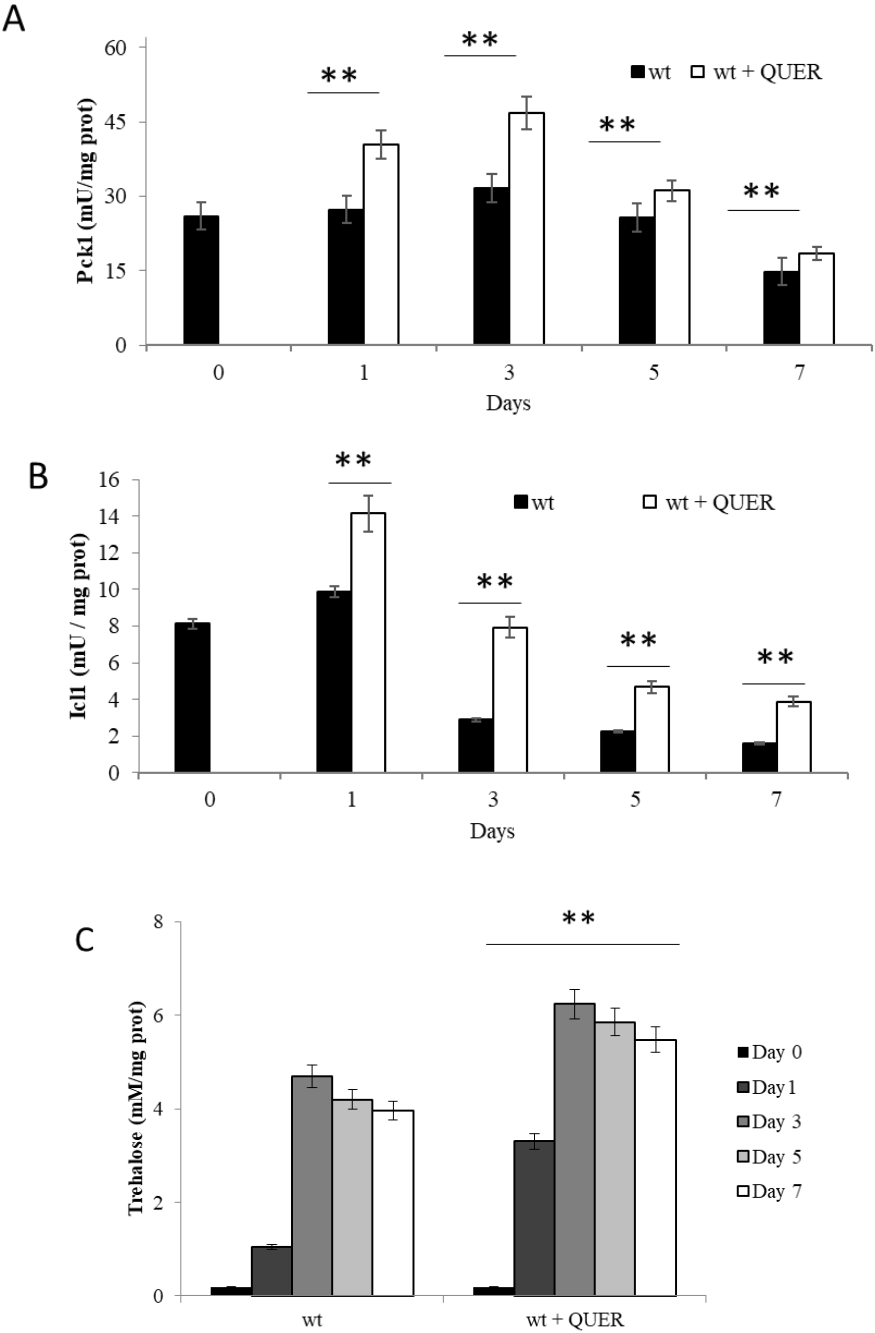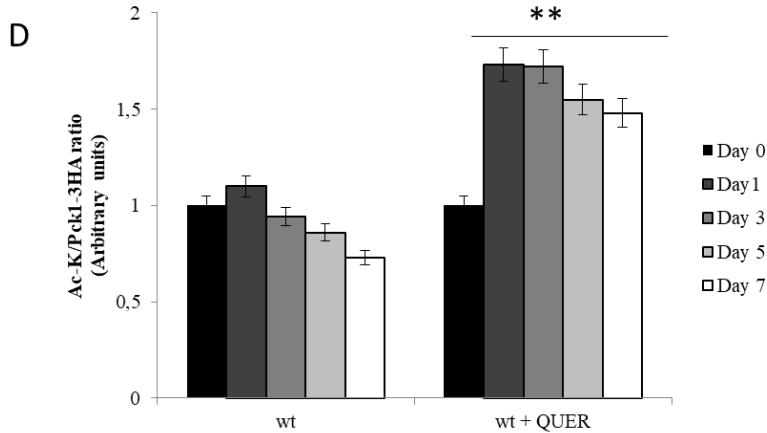
Fig. 2 QUER supplementation at the onset of chronological aging increases the glyoxylate/gluconeogenic flux. Wt cells were grown and supplemented with QUER as in Fig.1. Pck1 (A) and Icl1 (B) enzymatic activities and intracellular trehalose (C) were measured at the indicated time points. (D) Cells expressing Pck1-3HA were grown and supplied at the diauxic shift (Day 0) with QUER. At different time points, total protein extracts from both treated and untreated cultures were prepared and immunoprecipitated with anti-HA antibody. Western analyses were performed with anti-HA and anti Ac-K antibodies followed by densitometric quantification of signal intensity of the bands relative to the total Pck1 (Pck1-3HA) and the acetylated form (Ac-K). The ratios of Ac-K to correspondent Pck1-3HA values are reported. SD is indicated. Statistical significance as in Fig. 1.

In this context, in order to have "*in vivo*" indications, we used an α-factor sensitivity test. Sir2 deacetylase activity is essential for gene silencing at the mating-type *locus*. Its absence in a haploid strain determines a pseudodiploid state linked to the expression of both a and α genes. Consequently, *sir2Δ* being unresponsive to the pheromone in the presence of α-factor continued to grow, while wt cells did not (Fig. 3). On the contrary, in the presence of QUER the wt cells also grew (Fig. 3) indicating that these cells are unresponsive to α-factor. A similar behaviour was observed for wt cells in the presence of splitomicin, used as a control. Splitomicin is a specific and selective inhibitor of Sir2. It creates a conditional phenocopy of a *sir2Δ* mutant. Consequently, cells having silencing defects were unresponsive to the pheromone and grew in its presence (Fig. 3). No effects were observed on the *sir2Δ* mutant (Fig. 3) indicating that in the presence of QUER Sir2 is inhibited.
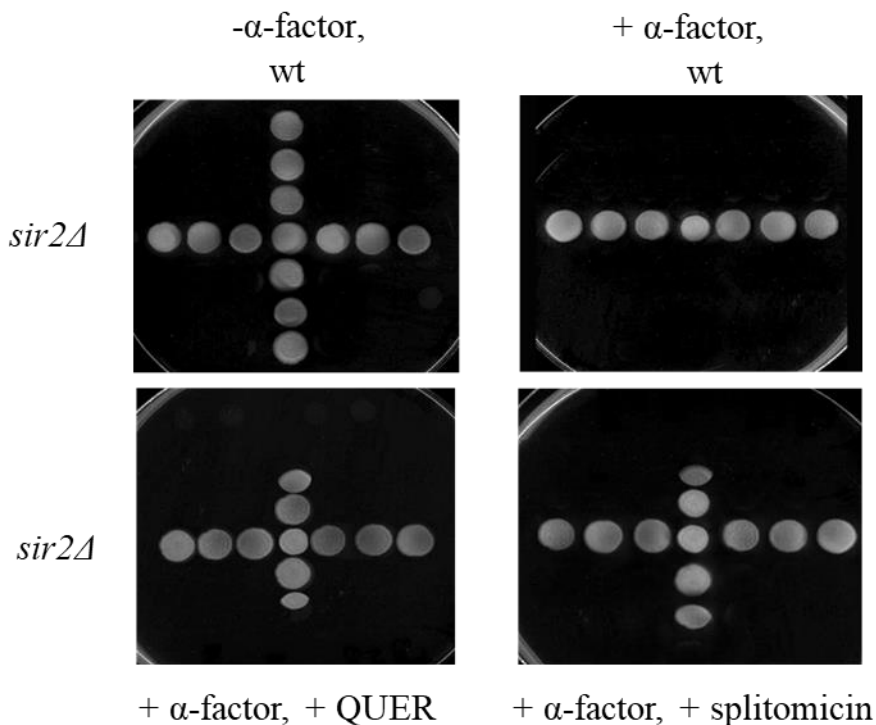
Fig. 3 QUER supplementation inhibits Sir2 activity Wt and *sir2Δ* exponentially growing cells were dropped (5 µl of a 10^6 cells/ml dilution) onto glucose rich/medium plates (top left), supplemented with 2.5 µM α-factor (upper right corner). A concentration gradient of QUER was formed by loading 5 µl of 300 µM QUER on filter disks placed on the agar (lower left corner). 5 µl of 5 mM splitomicin was loaded on a filter disk as a control (lower right corner). Growth was monitored after 3 days at 30°C.

In order to further assess if Sir2 activity is involved in the QUER-mediated effects, the analyses shown in Fig. 1 were performed in a strain in which *SIR2* gene was deleted, inactivation that determines an extension of CLS according to a reduction of oxidative stress and an increased metabolic remodelling towards gluconeogenesis (8, 10, 13). Surprisingly, the beneficial effects of the compound were not only preserved but also exacerbated in *sir2Δ* mutant both regarding CLS and oxidative stress levels as well as carbon metabolism (Fig. 4 and Fig. 5). This suggests that in the absence of Sir2, QUER might exert its activity on other targets. Moreover, despite the increased levels of Pck1 activity in *sir2Δ*-treated cells (Fig.

5A), its acetylation level did not increase further (Fig. 5D). This apparent contradiction can be explained by the fact that Pck1 activity is influenced by another post-translational modification, such as phosphorylation but to date the kinase responsible for this is not known (29).
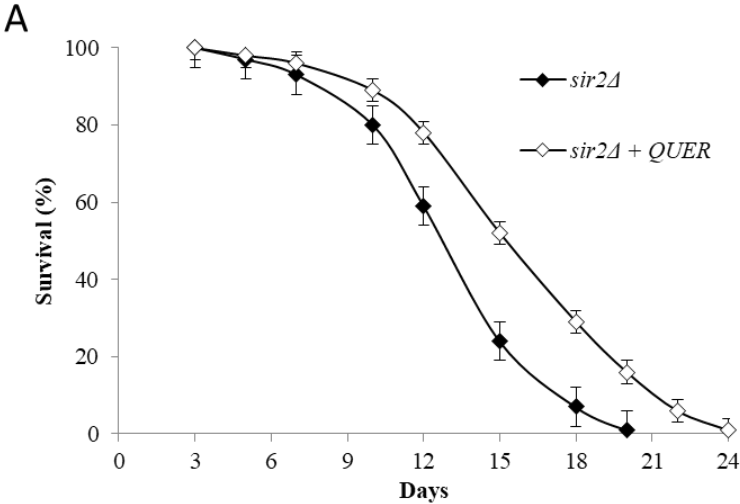
Strain	Mean CLS	Maximum CLS
sir2Δ	13.12±0.33	17.8±0.28
sir2Δ + QUER	15.39±0.43**	21.79±0.37**
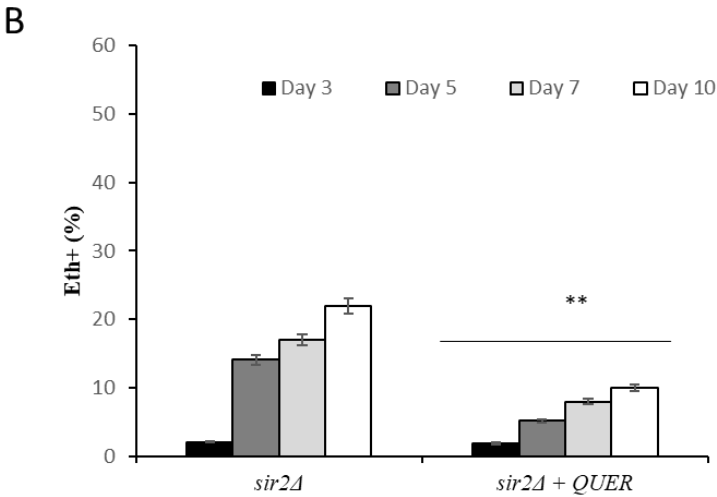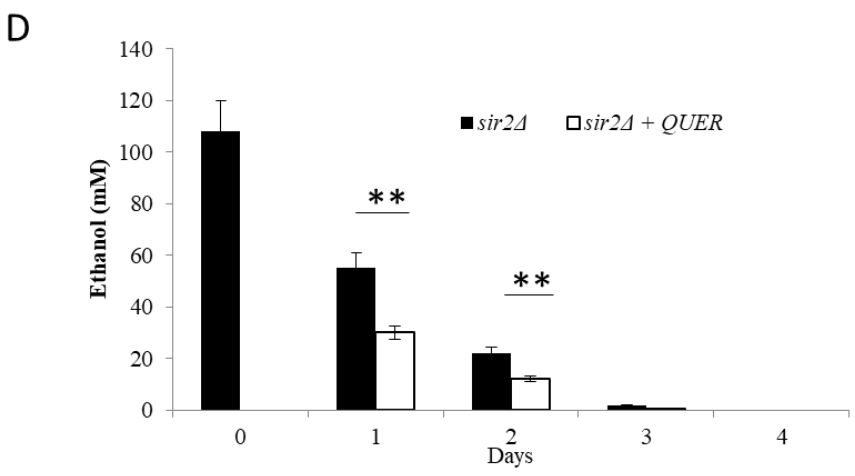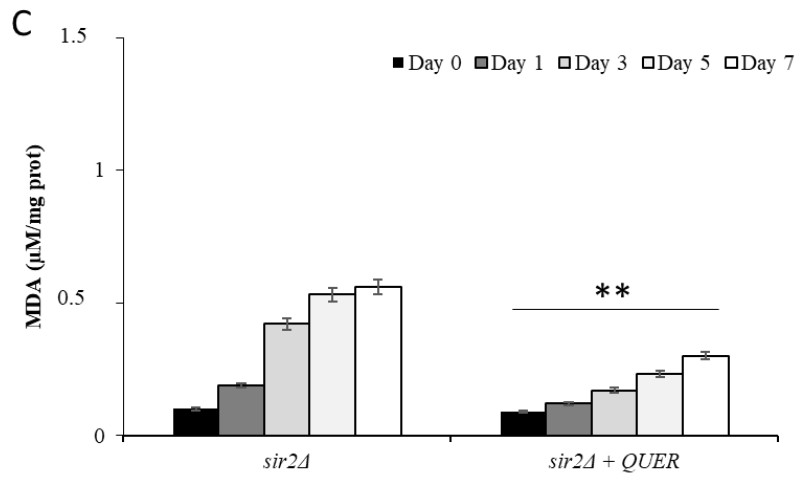
Fig. 4 QUER supplementation at the onset of chronological aging enhances the beneficial effects of the lack of Sir2. (A) *sir2Δ* cells was grown and treated with QUER as in Fig. 1. At each time point, survival was determined as in Fig.1. In parallel, survival of cells in their expired medium without QUER was monitored. Data referring to the time points where chronological aging cultures showed 50% (Mean CLS) and 10% (Maximum CLS) of survival are reported. In parallel, the levels of intracellular superoxide (Eth) (B) and malonyldyaldeide (MDA) (C) were determined. Summary graphs of extracellular ethanol (D) and acetate (E) measured at the indicated time points. SD is indicated. Statistical significance as in Fig. 1.
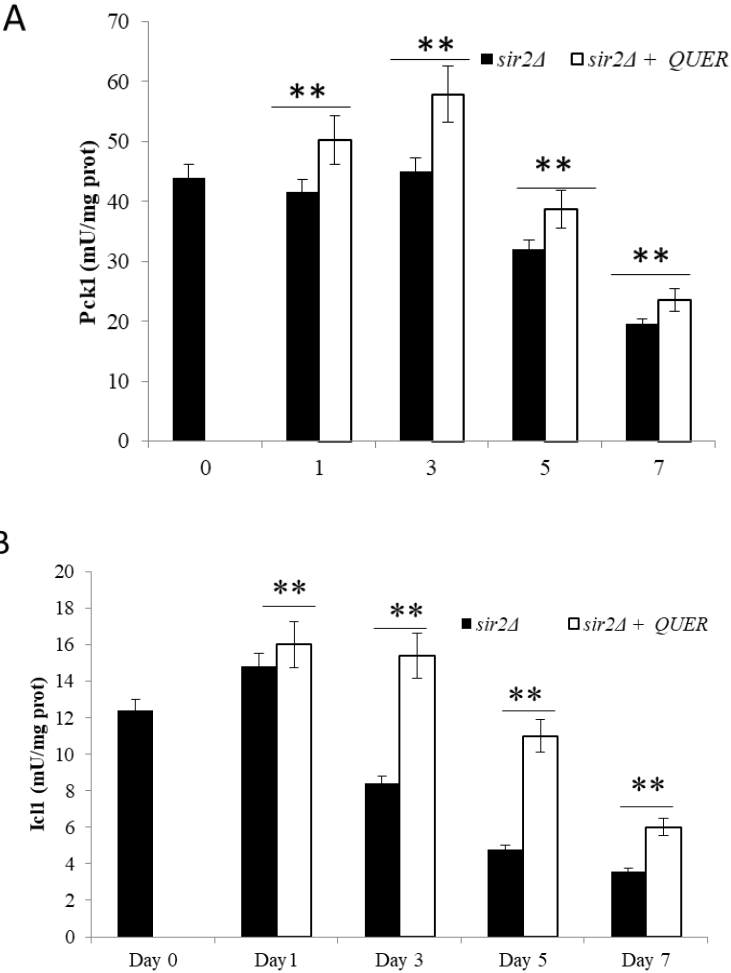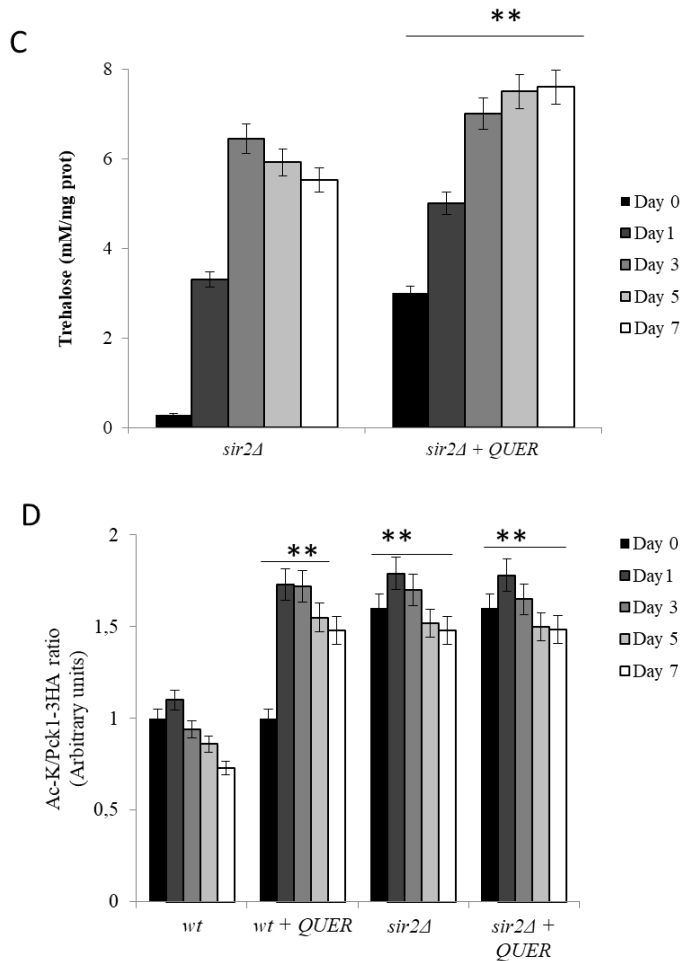
Fig. 5 QUER-treated *sir2Δ* cells display enhanced glyoxylate/gluconeogenic flux. Summary graphs of Pck1 (A) and Icl1 enzymatic activities (B), intracellular trehalose (C), and Pck1 acetylation levels (D) in *sir2Δ* cultures of Fig. 4. Western and densitometric analysis as in Fig. 2. SD are indicated. Statistical significance as in Fig. 1.

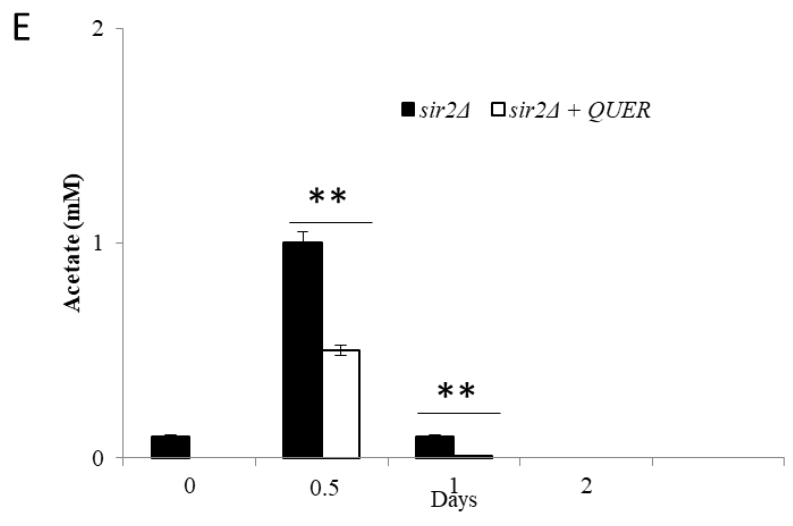3.3.2 Quercetin supplementation at the onset of chronological aging mobilizes lipid reserves

In order to identify other possible targets modulated by QUER treatment, we focused on lipid metabolism given that a critical mechanism underlying the regulation of chronological longevity is the capability to mobilize and utilize lipid reserves (30) and that many polyphenols, including QUER, elicit their effects through a modulation of lipid utilization (31). To this end, we monitored with Nile Red staining the storage, the mobilization and the size of lipid droplets (LD), metabolically active subcellular organelles, which play a key role in lipid

homeostasis (32). Wt cells showed a central and point-shaped distribution of LD at Day 1, distribution that became peripheral at Day 3, indicating lipid reserve utilization/mobilization (33) (Fig. 6A). A similar behaviour was observed in *sir2Δ* cells (Fig. 6A). Following the addition of QUER both wt and *sir2Δ* cells showed a peripheral distribution of LD already at Day 1, supporting that QUER can improve lipid utilization/mobilization (Fig. 6A).

The *OAF1* gene encodes the oleate-activated transcription factor involved in beta-oxidation of fatty acids and peroxisome biogenesis (34). The lack of *OAF1* results in cell inability to use lipid reserves, which is manifested with the emergence of large LD that were not metabolized over time (Fig. 6B and Vai. unpublished data). The addition of QUER was sufficient to restore a wt-like phenotype (Fig. 6B), further supporting the notion that this compound can improve lipid utilization/mobilization. Similar results were also observed for the double mutant *oaf1Δsir2Δ* (data not shown). Since in LD are stored fatty acids (FA), next we measured FA content in the presence and absence of QUER. As shown in Fig. 6C QUER supplementation at the diauxic shift reduced the FA levels in both wt and *sir2Δ* cells as well as in *oaf1Δ* ones, confirming that QUER affects lipid utilization/mobilization. Since a stronger mobilization of lipid reserves was also observed in *oaf1Δ* mutant, we excluded an involvement of beta-oxidation in this process.
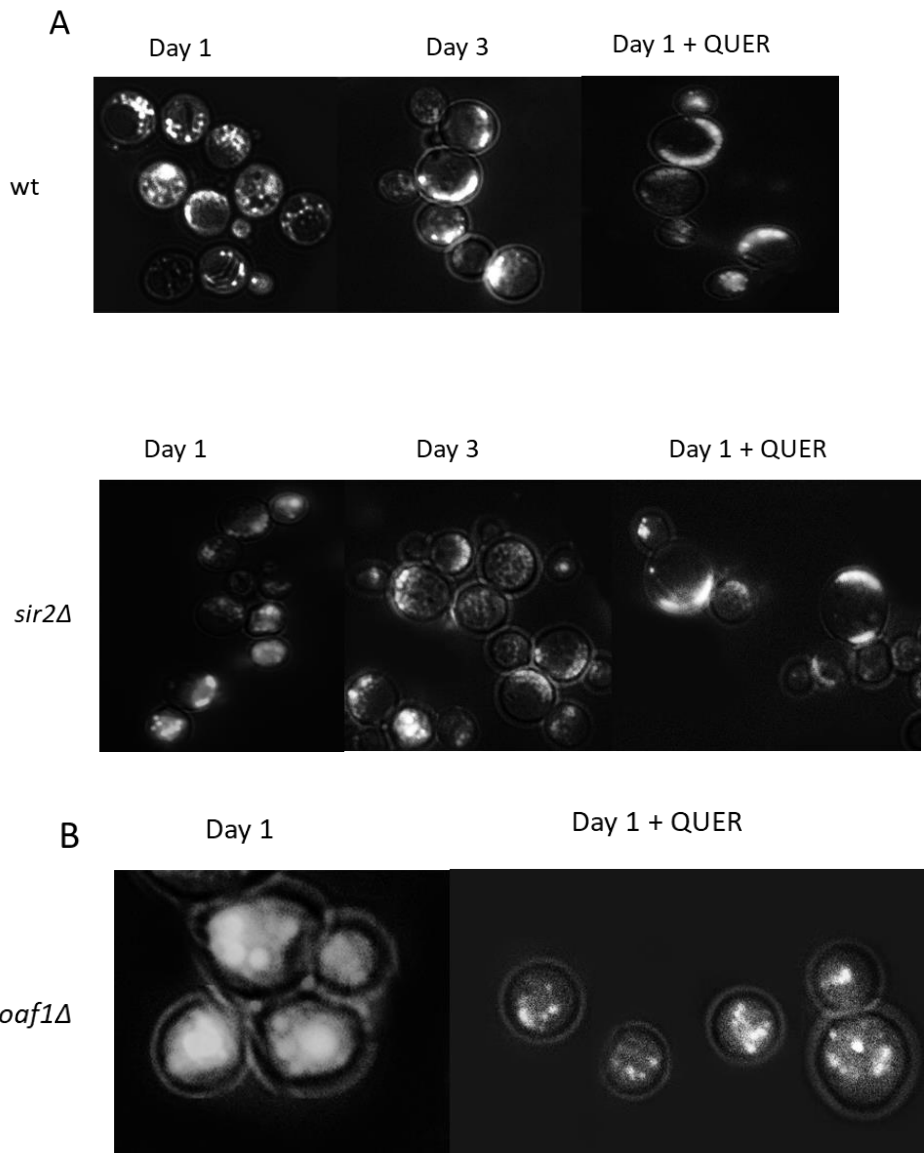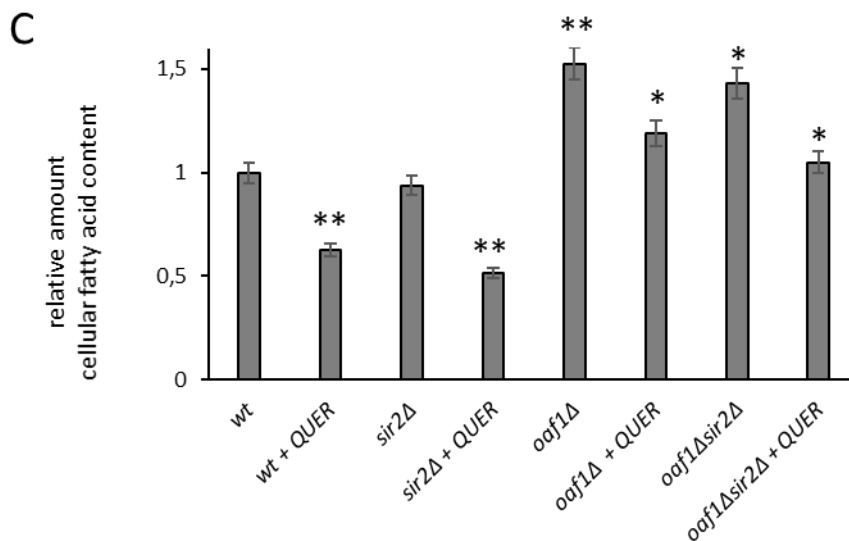
Fig. 6 QUER supplementation at the diauxic shift triggers lipid catabolism. (A, B) The indicated strains were grown as in Fig. 1 and lipid droplets stained with Nile Red (2.5 µg/ml). (C) Summary graph of the fatty acid content of the same cultures determined at Day 1. SD is indicated. Statistical significance as in Fig. 1.

3.3.4 CONCLUSIONS

QUER is one of the most prominent anti-oxidant polyphenols present in the human diet. Given its biological effects against radical species, QUER has aroused much interest in improving the aging process, which is strongly and negatively affected by oxidative stress. In this context, evidence of its anti-aging potential emerged from studies performed in *S. cerevisiae*. For example, a QUER pre-treatment during the exponential phase protects cells from both oxidative stress and apoptosis, with a significant increase in CLS (35). Similar results have been obtained in *tel1Δ,* mutant that displays early aging marker due to its high sensitivity to oxidative and pro-apoptotic agents. QUER pre-treatment in exponential phase is sufficient to protect these cells from stressors and to extend CLS (36). The beneficial effects of QUER are also mediated by the activation of Msn2/4 transcription factors, which play a pivotal role in the yeast adaptive response against oxidative stress, as well as the entry in stationary phase (37). In this work we have shown that the addition of QUER at the diauxic shift not only significantly reduces oxidative stress but also imposes a metabolic remodelling in favour of the glyoxylate/gluconeogenic flux, which allows the trehalose storage and CLS lengthening.

The data are in line with previous findings showing that QUER treatment up-regulated the transcription of several genes related with carbohydrate metabolism, the expression of which increases after the diauxic shift, when the gluconeogenesis pathway is activated. Indeed, QUER enhanced, on the one hand, the transcription of genes for glycogen synthesis and breakdown, namely Glycogen Synthase 2 (*GSY2*) and Glycogen Phosphorylase 1 (*GPH1*) and, on the other, the transcription of genes for trehalose synthesis and utilization, such as Trehalose-6-Phosphate Synthase 1 (*TPS1*) and Neutral TreHalase (*NTH1*) (38).

Moreover, our results highlight that the increase of trehalose amount following QUER addition, is also dependent on Pck1, crucial enzyme in controlling the gluconeogenesis flux, whose activity strongly enhanced after the treatment with the compound. The increased activity of Pck1 depended on the inhibition of Sir2 deacetylase activity following QUER treatment, consistent with previous work that suggested a modulation of SIRT1 by QUER in complex eukaryotes (6). QUER supplementation also improved both survival and metabolism in the absence of Sir2, leading us to find other targets modulated by this compound. Among its biological activities, QUER is recognized for possessing properties against dyslipidaemia. Considering that long-term survival in the stationary phase relies also on the ability to use lipid reserves, we investigated lipid utilization/mobilization following QUER supplementation. A significantly reduction of total fatty acids occurred in QUER-treated cells. Accordingly with our results, QUER supplementation in diabetic rats induced lipolysis but actually the specific pathway and the enzymes implicated are still unknown (39). Our work not only adds new knowledge to the action mechanism of this polyphenol widely present in the human diet, but also highlights the feasibility of using yeast as a model system to understand the molecular functioning of nutraceutical compounds in order to develop/improve therapies against the major age-related diseases.

3.3.5 REFERENCES

1.   Li, Y., Yao, J., Han, C., Yang, J., Chaudhry, M. T., Wang, S., Liu, H., and Yin, Y. (2016) Quercetin, inflammation and immunity. *Nutrients*. **8**, 1–14

2.   Bhuiya, S., Haque, L., Pradhan, A. B., and Das, S. (2017) Inhibitory effects of the dietary flavonoid quercetin on the enzyme activity of zinc(II)-dependent yeast alcohol dehydrogenase: Spectroscopic and molecular docking studies. *Int. J. Biol. Macromol.* **95**, 177–184

3.   Russo, M., Spagnuolo, C., Tedesco, I., Bilotto, S., and Russo, G. L. (2012) The flavonoid quercetin in disease prevention and therapy: Facts and fancies. *Biochem. Pharmacol.* **83**, 6–15

4.   Peng, J., Li, Q., Li, K., Zhu, L., Lin, X., Lin, X., Shen, Q., Li, G., and Xie, X. (2017) Quercetin Improves Glucose and Lipid Metabolism of Diabetic Rats : Involvement of Akt Signaling and SIRT1. *J. Diabetes Research* **2017**, 1–10

5.   Costa, L. G., Garrick, J. M., Roquè, P. J., and Pellacani, C. (2016) Mechanisms of Neuroprotection by Quercetin : Counteracting Oxidative Stress and More. *Oxid. Med. Cell. Longev*. **2016**, 1–10

6.   Kemelo, M. K., Canová, N. K., Horinek, A., and Farghali, H. (2017) Sirtuin-Activating Compounds (STACs) Alleviate D-Galactosamine/Lipopolysaccharide-Induced Hepatotoxicity in Rats : Involvement of Sirtuin 1 and Heme Oxygenase 1. *Physiol. Res.* **66**, 497–505

7.   Ghosh, H. S. (2008) The anti-aging, metabolism potential of SIRT1. *Curr. Opin. Investig. Drugs*. **9**, 1095–102

8.   Longo, V. D., Shadel, G. S., Kaeberlein, M., and Kennedy, B. (2012) Replicative and Chronological Aging in *Saccharomyces cerevisiae*. *Cell Metab.* **16**, 18–31

9.   Steinkraus, K. A., Kaeberlein, M., and Kennedy, B. K. (2008) Replicative Aging in Yeast: The Means to the End. *Annu. Rev. Cell Dev. Biol.* **24**, 29–54

10.   Casatta, N., Porro, A., Orlandi, I., Brambilla, L., and Vai, M. (2013) Lack of Sir2 increases acetate consumption and decreases extracellular pro-aging factors. *Biochim. Biophys. Acta - Mol. Cell Res*. **1833**, 593-601

11.   Fabrizio, P., Gattazzo, C., Battistella, L., Wei, M., Cheng, C., McGrew, K., and Longo, V. D. (2005) Sir2 blocks extreme life-span extension. *Cell*. **123**, 655–667

12.   Orlandi, I., Ronzulli, R., Casatta, N., and Vai, M. (2013) Ethanol and acetate acting as carbon/energy sources negatively affect yeast chronological aging. *Oxid. Med. Cell.*

Longev. **2013**, 1-10

13. Orlandi, I., Pellegrino Coppola, D., Strippoli, M., Ronzulli, R., and Vai, M. (2017) Nicotinamide supplementation phenocopies *SIR2* inactivation by modulating carbon metabolism and respiration during yeast chronological aging. *Mech. Ageing Dev.* **161**, 277–287

14. Tapia, H., and Koshland, D. E. (2014) Trehalose is a versatile and long-lived chaperone for desiccation tolerance. *Curr. Biol.* **24**, 2758–2766

15. Kaushik, J. K., and Bhat, R. (2003) Why is trehalose an exceptional protein stabilizer? An analysis of the thermal stability of proteins in the presence of the compatible osmolyte trehalose. *J. Biol. Chem.* **278**, 26458–26465

16. Howitz, K., Bitterman, K., Cohen, H., Lamming, D., Lavu, S., Wood, J., Zipkin, R., Chung, P., Kisielewski, A., Zhang, L., Scherer, B., Sinclair, D. (2003) Small molecule activators of sirtuins extend *Saccharomyces cerevisiae* lifespan. *Nature*. **425**, 191-196

17. Belinha, I., Amorim, M. A., Rodrigues, P., De Freitas, V., Moradas-Ferreira, P., Mateus, N., and Costa, V. (2007) Quercetin increases oxidative stress resistance and longevity in *Saccharomyces cerevisiae*. *J. Agric. Food Chem.* **55**, 2446–2451

18. Orlandi, I., Coppola, D., and Vai, M. (2014) Rewiring yeast acetate metabolism through MPC1 loss of function leads to mitochondrial damage and decreases chronological lifespan. *Microb. Cell*. **1**, 393–405

19. Vanoni, M., Vai, M., Popolo, L., Alberghina, L., Comparata, B., Generali, B., and Milano, U. (1983) Structural Heterogeneity in Populations of the Budding Yeast *Saccharomyces cerevisiae*. *J. Bacteriol.* **156**, 1282–1291

20. Lee, D., Goldberg, A. (1998) Proteasome inhibitors cause induction of heat shock proteins and trehalose, which together confer thermotolerance in *Saccharomyces cerevisiae. Mol. Cell. Biol.* **18**, 30-38

21. De Jong-Gubbels, P., Vanrolleghem, P., Heijnen, S., Van Dijken, P., Pronk, J. (1995) Regulation of carbon metabolism in chemostat cultures of *Saccharomyces cerevisiae* grown on mixtures of glucose and ethanol. *Yeast.* **11**, 407-418

22. Madeo, F., Fröhlich, E., Ligr, M., Grey, M., Sigrist, S. J., Wolf, D. H., Fröhlich, K., Institut, P., Tübingen, U., Institut, A., Biochemie, I., Stuttgart, U., Goethe-universität, W., and Main, F. (1999) Oxygen Stress : A Regulator of Apoptosis in Yeast. *J. Cell Biol.* **145**, 757–767

23. Orlandi, I., Stamerra, G., Strippoli, M., and Vai, M. (2017) During yeast chronological aging resveratrol supplementation results in a short-lived phenotype Sir2-dependent. *Redox Biol.* **12**, 745–754

24. Calzari, L., Orlandi, I., Alberghina, L., and Vai, M. (2006) The histone deubiquitinating enzyme Ubp10 is involved in rDNA locus control in *Saccharomyces cerevisiae* by affecting Sir2p association. *Genetics.* **174**, 2249–2254

25. Bourque, S. D., and Titorenko, V. I. (2009) A Quantitative Assessment of The Yeast Lipidome using Electrospray Ionization Mass Spectrometry. *J. Vis. Exp.* 1-3

28. Ayala, A., Muñoz, M. F., and Argüelles, S. (2014) Lipid Peroxidation : Production, Metabolism, and Signaling Mechanisms of Malondialdehyde and 4-Hydroxy-2-Nonenal. *Oxid. Med. Cell. Longev.* **2014,** 1-31

29. Oliveira, A. P., and Sauer, U. (2012) The importance of post-translational modifications in regulating *Saccharomyces cerevisiae* metabolism. *FEMS Yeast Res.* **12**, 104–117

30. Eisenberg, T., and Buttner, S. (2014) Lipids and cell death in yeast. *FEMS Yeast Res.* **14**, 179–197

31. Sahebkar, A. (2017) Effects of quercetin supplementation on lipid profile: A systematic review and meta-analysis of randomized controlled trials. *Crit. Rev. Food Sci. Nutr.* **57**, 666–676

32. Wang, C. W. (2015) Lipid droplet dynamics in budding yeast. *Cell. Mol. Life Sci.* **72**, 2677–2695

33. Welte, M. A. (2009) Fat on the move: intracellular motion of lipid droplets. *Biochem. Soc. Trans.* **37**, 991–996

34. Baumgartner, U., Hamilton, B., Piskacek, M., Ruis, H., and Rottensteiner, H. (1999) Functional Analysis of the Zn 2 Cys 6 Transcription Factors Oaf1p and Pip2p. *J. Biol. Chem.* **274**, 22208–22216

35. Alugoju, P., Janardhanshetty, S., Subaramanian, S., Periyasamy L., Dyavaiah, M. (2018) Quercetin Protects Yeast *Saccharomyces cerevisiae* pep4 Mutant from Oxidative and Apoptotic Stress and Extends Chronological Lifespan. *Curr. Microbiol.* **75**, 519-530

36. Alugoju, P., Periyasamy, L., Dyavaiah, M., Quercetin enhances stress resistance in *Saccharomyces cerevisiae tel1* mutant cells to different stressors. *J. Food Sci. Technol*. **55**, 1455-1466

37.   Bayliak, M., Burdylyuk, N., Lushchak, V. (2016) Quercetin increases stress resistance in the yeast *Saccharomyces cerevisiae* not only as an antioxidant. **66**, 569-576

38.   Vilaca, R., Mendes, V., Vaz Mendes, M., Carreto, L., Amorim, M., de Freitas, V., Ferreira, P., Mateus, Costa, V. (2012) Quercetin protects *Saccharomyces cerevisiae* against oxidative stress by inducing trehalose biosynthesis and the cell wall   integrity pathway. *PLOS ONE*. **7**, 1-11

39.   Zhao, Y., Chen, B., Shen, J., Wan, L., Zhu, Y., Yi, T., Xiao, Z. (2017) The Beneficial Effects of Quercetin, Curcumin, and Resveratrol in Obesity.

Chapter

Mitochondrial Metabolism and Aging in Yeast

Giacomo Baccolo, Giulia Stamerra, Damiano Pellegrino Coppola, Ivan Orlandi and Marina Vai.

Mitochondrial Metabolism and Aging in Yeast

Giacomo Baccolo*,§, Giulia Stamerra*,§,
Coppola Damiano Pellegrino§, Ivan Orlandi*,§ and Marina Vai*,§,1

*SYSBIO Centre for Systems Biology, Milano, Italy
§Dipartimento di Biotecnologie e Bioscienze, Università di Milano-Bicocca, Milano, Italy
1Correspondence: E-mail: marina.vai@unimib.it

Contents

Abstract

Mitochondrial functionality is one of the main factors involved in cell survival, and mitochondrial dysfunctions have been identified as an aging hallmark. In particular, the insurgence of mitochondrial dysfunctions is tightly connected to mitochondrial metabolism. During aging, both mitochondrial oxidative and biosynthetic metabolisms are progressively altered, with the development of malfunctions, in turn affecting

1

mitochondrial functionality. In this context, the relation between mitochondrial pathways and aging is evolutionarily conserved from single-celled organisms, such as yeasts, to complex multicellular organisms, such as humans. Useful information has been provided by the yeast *Saccharomyces cerevisiae*, which is being increasingly acknowledged as a valuable model system to uncover mechanisms underlying cellular longevity in humans. On this basis, we review the impact of specific aspects of mitochondrial metabolism on aging supported by the contributions brought by numerous studies performed employing yeast. Initially, we will focus on the tricarboxylic acid cycle and oxidative phosphorylation, describing how their modulation has consequences on cellular longevity. Afterward, we will report information regarding the importance of nicotinamide adenine dinucleotide (NAD) metabolism during aging, highlighting its relation with mitochondrial functionality. The comprehension of these key points regarding mitochondrial metabolism and their physiological importance is an essential first step for the development of therapeutic interventions that point to increase life quality during aging, therefore promoting "healthy aging," as well as lifespan itself.

1. INTRODUCTION

Mitochondria are unquestionably essential organelles for eukaryotic aerobic metabolism since they provide a unique metabolic pathway that generates the energy required for all cellular functions in a utilizable form. In addition, mitochondria exhibit many other functions, including biosynthesis of intermediary metabolites, such as amino acids and nucleotides, formation of iron—sulfur clusters, and regulation of Ca^{2+} homeostasis.

By providing essential cellular functions, mitochondria support the metabolism of the whole cell and contribute to cellular and organismal homeostasis. Consequently, their impairment is associated not only with several diseases, but dysfunctional mitochondria are considered a hallmark of aging (López-Otín et al., 2013), and an altered mitochondrial metabolism characterizes many aging-related pathologies, including degenerative disorders (Lane et al., 2015). As far as aging is concerned, mitochondria have been/are intensively studied regarding, in particular, mitochondrial adenosine triphosphate (ATP) production and reactive oxygen species (ROS) leakage from the respiratory chain. Here, we also discuss other central functions of mitochondrial metabolism that are equally important, such as mitochondrial carbon metabolism and NAD homeostasis as parts of a complex mechanism, providing reducing equivalents and biosynthetic intermediates for the cell.

Since the single-celled yeast *Saccharomyces cerevisiae* is a valuable model system in the field of aging-related research, here we mainly refer to this organism to highlight the critical importance of this organelle. Two complementary models of aging are well established in *S. cerevisiae*: replicative and chronological aging that allow us to simulate the aging process of mitotically active and postmitotic quiescent mammalian cells, respectively (Longo and Kennedy, 2006; MacLean et al., 2001). In the former, replicative lifespan (RLS) defines the reproductive potential of individual yeast cells. In the latter, chronological lifespan (CLS) is measured as the time a culture of quiescent cells remains viable in a metabolically active nondividing state. Both models have contributed to the discovery of evolutionarily conserved factors associated with mitochondrial dysfunctions that proved to be involved in the aging process.

2. THE TRICARBOXYLIC ACID CYCLE

In terms of energetic metabolism, the mitochondrion is primarily a device for coupling the synthesis of ATP to the oxidative reactions of the tricarboxylic acid (TCA) cycle. This universal attribute of all mitochondria is referred to as oxidative phosphorylation (OXPHOS). Indeed, mitochondria catalyze aerobic oxidation of acetyl–CoA to CO_2 and water by means of the TCA cycle and produce energy, which is stored in the form of high-energy bonds of ATP.

Basically the TCA cycle consists of a series of both oxidative and hydrolytic reactions (Fig. 1). Upon condensation of acetyl–CoA with oxaloacetate generating citrate, the cycle starts with the reversible dehydration of citrate to cis–aconitate and the hydration of cis–aconitate to isocitrate, catalyzed by aconitase. The following steps are sequential redox reactions: oxidation of isocitrate to α-ketoglutarate; oxidation of α-ketoglutarate to succinyl–CoA and CO_2; and oxidation of succinate to fumarate. Then, fumarase catalyzes the reversible hydration of fumarate to malate, whose final oxidation to oxaloacetate completes the cycle. All the oxidative steps require cofactors in the oxidized forms of NAD or flavin adenine dinucleotide (FAD) as acceptors of reducing equivalents.

Besides this basic view of the cycle starting with acetyl–CoA as input to form citrate, TCA can be also fueled at the level of some of its intermediates. Indeed, the availability of glutamic acid leads to a "modified" cycle: glutamate is converted to α-ketoglutarate, which being a TCA intermediate is oxidized via the cycle to oxaloacetate. Afterward, most of the oxaloacetate
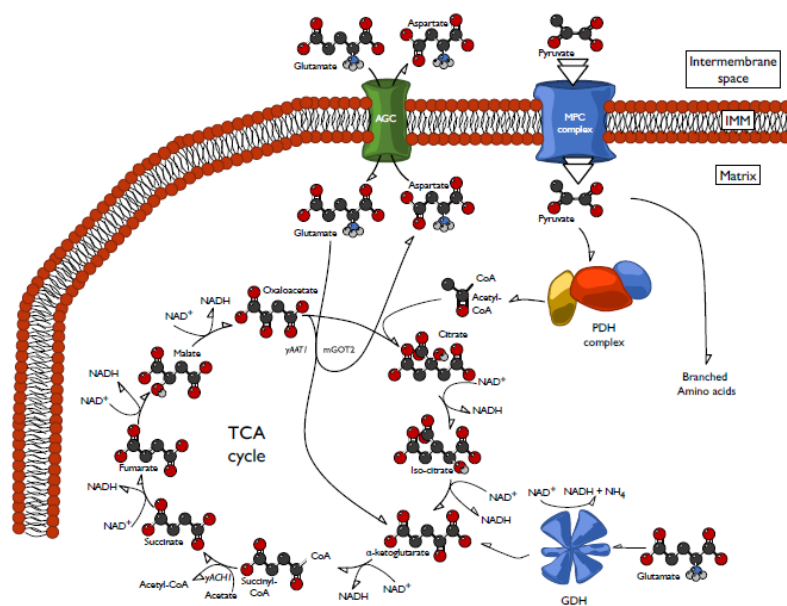
Figure 1 Scheme of the TCA cycle and its connections with the uptake of pyruvate and glutamate. *AGC*, aspartate/glutamate carrier; *GDH*, glutamate dehydrogenase complex; *IMM*, inner mitochondrial membrane; *mGOT2*, mammal glutamic-oxaloacetic transaminase 2; *MPC*, mitochondrial pyruvate carrier; *PDH*, pyruvate dehydrogenase complex; *yAat1*, yeast aspartate aminotransferase 1; *yAch1*, yeast acetyl-CoA hydrolase 1.

reacts by transamination with a second molecule of glutamate, generating aspartate and α–ketoglutarate. In such a way, the TCA cycle is connected with the anabolic biosynthesis of amino acids and vice versa (Fig. 1).

3. TRICARBOXYLIC ACID CYCLE DYSFUNCTIONS AND AGING

During chronological aging in yeast, TCA enzymatic activities have been shown to change (Samokhvalov et al., 2004). In particular, citrate synthase, α–ketoglutarate dehydrogenase, and malate dehydrogenase display a reduced activity, whilst that of succinate dehydrogenase (also known as Complex II) increases. Such an increase has been proposed to be part of a compensation mechanism induced by aged cells to maintain their respiratory competency (see Section 7.2). In this compensation mechanism is also involved the glyoxylate cycle, which leads to an increase in succinate

formation (Samokhvalov et al., 2004). The glyoxylate cycle is present in yeast and operates as a shunt of the TCA cycle. During chronological aging, this cycle is operative and replenishes the TCA cycle of intermediates to keep it functioning. Briefly, both cycles share the first steps in which citrate synthase catalyzes the condensation of oxaloacetate and acetyl-CoA to form citrate and aconitase converts citrate to isocitrate. In addition, the glyoxylate cycle is completed by two unique enzymes that are isocitrate lyase (Icl1) and malate synthase. The former cleaves isocitrate to glyoxylate and succinate, and the latter converts glyoxylate and acetyl-CoA to malate. Finally, malate dehydrogenase catalyzes the oxidation of malate to oxaloacetate. This end product of the shunt can be also utilized for gluconeogenesis, a pathway that is essential for the extension of CLS (Lin et al., 2009).

In mammalian cells, TCA enzymatic activity also changes during aging, displaying a decrease that mainly concerns the NAD-dependent dehydrogenases and damage-redox sensitive enzymes such as aconitase (Ingram and Chakrabarti, 2016; Kumaran et al., 2005; Stauch et al., 2015; Yarian et al., 2006). In this context, it is well known that oxidative modifications of proteins can lead to an impairment or a complete loss of protein function. In particular, protein carbonylation is one of the most studied irreversible modifications occurring during aging (Cabiscol et al., 2014; Nyström, 2005). Both in yeast and mammalian cells, TCA enzymes, as well as the mitochondrial ATPase synthase, have been shown to be target of carbonylation (Ahmed et al., 2010; Cabiscol et al., 2014; Reverter-Branchat et al., 2004; Tamarit et al., 2012).

4. IMPAIRED MITOCHONDRIAL PYRUVATE/ACETYL-COA METABOLISM AND AGING

Glucose-derived pyruvate is one of the most important metabolic input for mitochondria where it is converted to acetyl-CoA by the pyruvate dehydrogenase (PDH) complex (Fig. 1). Pyruvate is produced at the end of glycolysis in the cytoplasm and enters the mitochondrial matrix through the mitochondrial pyruvate carrier (MPC; Bricker et al., 2012; Herzig et al., 2012). The MPC is a heteromeric complex of which Mpc1/MPC1 in yeast or mammalian cells is the major structural subunit (Bricker et al., 2012). During chronological aging, loss of Mpc1 significantly reduces CLS (Eisenberg et al., 2014; Orlandi et al., 2014). Furthermore, the *mpc1Δ* mutant accumulates pyruvate, while TCA cycle intermediates, such as citrate, succinate, and malate, are decreased (Orlandi et al., 2014).

Similarly, depletion of human MPC1 impairs pyruvate oxidation (Bricker et al., 2012), and in these cells, intracellular level of pyruvate is strongly increased, whereas citrate level is decreased (Vacanti et al., 2014).

In both yeast and human cells, a metabolic reprogramming takes place to compensate for the decrease of mitochondrial pyruvate, allowing cells to use other substrates for both respiration and anabolic purposes. In yeast, the lack of a functional MPC is associated with an increased activity of the mitochondrial malic enzyme, that by decarboxylating malate to pyruvate, it provides a mitochondrial pyruvate pool (Orlandi et al., 2014). In such a way, the TCA cycle operates in a "branched" fashion and is depleted of intermediates. In order to fulfill the needs of the TCA cycle, mutant cells increase the activities of the glyoxylate cycle, which can feed of C4 compounds the TCA cycle. In the case of human cells, which do not possess the glyoxylate cycle, in order to cope with the lack of mitochondrial pyruvate uptake, they strongly increase glutamine utilization (Vacanti et al., 2014; Yang et al., 2014). This necessarily occurs since glutamine can be deaminated to glutamate, which in turn is converted to α-ketoglutarate to replenish the TCA cycle. Then, mitochondrial isoforms of malic enzyme, ME2 and ME3, as in yeast, transform malate into pyruvate.

These mechanisms, which allow the cells to compensate for the mitochondrial pyruvate deficiency, on the other hand, render them more vulnerable. In yeast, the defect of the TCA cycle functioning, ultimately, results in an inefficient mitochondrial acetyl-CoA metabolism (Eisenberg et al., 2014; Orlandi et al., 2014). This latter consequence is associated with an increased nucleocytosolic acetyl-CoA metabolism, which in turn also affects histone acetylation, leading to a repression of genes encoding proteins required for autophagy, a process that plays a critical role for cell survival during chronological aging (Eisenberg et al., 2014). Thus, the perturbation of mitochondrial metabolism is connected to the chromatin structure.

Similarly, blocking the mitochondrial route to acetyl-CoA by deletion of ACH1 increases nucleocytosolic acetyl-CoA metabolism that ultimately triggers histone acetylation and repression of autophagy genes (Eisenberg et al., 2014). This results in a short CLS (Eisenberg et al., 2014; Orlandi et al., 2014). The mitochondrial Ach1 displays a CoA-transferase activity: it catalyzes the CoASH transfer from succinyl-CoA (produced by the TCA cycle) to acetate producing acetyl-CoA (Fleck and Brock, 2009; Fig. 1). In the mitochondria, the reaction catalyzed by Ach1 allows, on the one hand, to save one ATP compared with the acetate activation to

acetyl-CoA by the acetyl-CoA synthetase 1 and, on the other, to protect mitochondrial function from the toxic effects of acetate accumulation. In line with this the reduced CLS of the *ach1Δ* mutant is associated with an impaired mitochondrial functionality (Orlandi et al., 2012). Moreover, consistent with a role of the mitochondrial detoxifying enzyme, Ach1 has been identified to be resistant to oxidative damage (Tamarit et al., 2012).

Furthermore, *LSC1* encodes the alpha subunit of succinyl-CoA ligase, the enzyme that catalyzes the nucleotide-dependent conversion of succinyl-CoA to succinate. Interestingly, *LSC1* deletion decreases the CLS (Fabrizio et al., 2010; Powers et al., 2006). These convergent short-lived phenotypes evidence a critical role of the succinate node for the functionality of the TCA cycle.

5. MITOCHONDRIAL METABOLISM OF BRANCHED-CHAIN AMINO ACIDS AND AGING

The TCA cycle and the biosynthesis of amino acids are strongly interconnected. In addition to the α-ketoglutarate/glutamate connection, another link is found with malate, which is a precursor in the anabolic pathway of the branched-chain amino acids (BCAAs). In the reaction catalyzed by the mitochondrial malic enzyme, as mentioned previously, malate is converted in pyruvate, which is consequently used to synthesize leucine, isoleucine, and valine, collectively known as BCAAs (Fig. 1). These amino acids are synthesized in yeast by a unique pathway localized in the mitochondria, in which common enzymes catalyze similar reactions. Thus, this mitochondrial pathway contributes to the amino acids homeostasis, which is a key process involved in the long-term viability during both replicative and chronological aging (Aris et al., 2012; Kamei et al., 2014). Indeed, the levels of transcripts encoding enzymes involved in the biosynthesis of BCAAs, as well as the BCAA metabolic profile, decrease during replicative aging (Kamei et al., 2014). Furthermore, during chronological aging, not all the amino acids are equally effective. This is mirrored by the fact that the availability of specific amino acids, compared with the availability of all amino acids, has a greater importance in amino acid homeostasis. In particular, among the amino acids, leucine makes the greatest contribution to the CLS extension (Alvers et al., 2009). The importance of leucine is supported by the fact that the CLS of the *leu2* auxotroph mutant, which has a short-lived phenotype, is extended by restoring *LEU2* (Alvers et al., 2009). Intriguingly, BCAAs enhance CLS

in both autophagy-deficient and autophagy-competent strains (Alvers et al., 2009). Thus, a strictly nutritional function cannot completely account for their prolongevity effect under conditions in which autophagy provides an efficient recycling of amino acids and other metabolic building blocks. In agreement, it has been proposed that isoleucine, valine, and threonine also act via a regulatory mechanism that involves the well-known general amino acid control (GAAC) pathway. This pathway regulates amino acid homeostasis in yeast (Hinnebusch, 2005) and is induced by limiting amounts of specific amino acids, such as BCAAs, with critical repercussions on longevity, while an increased level of BCAAs curtails the activity of the GAAC pathway, enhancing CLS (Alvers et al., 2009). BCAAs, by this way, prevent the activation of an anabolic process that has deep impact on the energy and metabolite resources during chronological aging.

Notably, as far as valine and threonine are concerned, it has also been reported to determine stress sensitization and reduce CLS by activating the TORC1/Sch9 pathway (Mirisola et al., 2014). This is a nutrient-sensing pathway, the activation of which promotes chronological aging (Fontana et al., 2010; Kaeberlein, 2010). The conflicting results about valine and threonine supplementations require further investigations but probably rely on different experimental conditions/yeast genetic background used (Alvers et al., 2009; Mirisola et al., 2014) and the many unresolved questions concerning the regulatory linkages between the GAAC and TOR pathways.

Amino acid homeostasis is important not only for yeast but also for humans in the maintenance of cellular integrity during aging. Since in human cells amino acid synthesis is limited to few amino acids and the availability of most of them, including BCAAs, depends on diet, a proper management of amino acids and related metabolites is essential for cellular homeostasis. However, the effects of the diet and, in particular of amino acid assumption, can vary among the different tissues, which are characterized by specific/different metabolic features. In this context, BCAAs have been shown to play an important role in the metabolic regulation of peripheral tissues, such as white adipose tissue, liver, and muscle with different outcomes according to catabolic or anabolic conditions. For example, BCAA supplementation, in particular leucine, stimulates protein synthesis in muscle and improve sarcopenia, the age-associated loss of muscle mass and function (Dillon et al., 2009; Fujita and Volpi, 2006; Pansarasa et al., 2008; Shimomura et al., 2006). On the contrary, in patients with

metabolic disorders, such as obesity and insulin resistance, BCAAs exert negative effects depending on the prevalence in these conditions of catabolic signals. BCAA supplementation seems to cause an impaired amino acid oxidation, leading to the accumulation of toxic intermediates, such as branched-chain keto acids (Berg et al., 2016; Mihalik et al., 2010).

Thus given the discrepancy found in the effects of BCAA administration, the understanding of the mechanisms that regulate amino acid metabolism assumes extreme importance for the development of effective dietary approaches to contrast aging effects (see Longo et al., 2015).

6. THE OXIDATIVE PHOSPHORYLATION

The OXPHOS results from the coupling between the electron transport chain (ETC) and the F_1F_0-ATP synthase (Complex V). Under normal conditions of mitochondrial respiration, the reducing equivalents provided by the TCA cycle through redox reactions fuel the ETC (Fig. 2). The ETC consists of four enzymatic complexes (Complex I—IV) located in the inner mitochondrial membrane and two mobile electron carriers, namely coenzyme Q (ubiquinone) and cytochrome c. They allow the transfer of high-energy electrons from NADH and $FADH_2$ through redox reactions. In the ETC, electrons enter at the level of Complex I (NADH dehydrogenases in yeast) in the form of NADH and at Complex II as $FADH_2$. The last one is generated following succinate oxidation to fumarate catalyzed by succinate dehydrogenase (Complex II), which is part of both the ETC and TCA cycle. The flux of electrons along the chain terminates at the level of Complex IV (cytochrome c oxidase) in a four-electron reduction of molecular oxygen, producing two molecules of water (Fig. 2). In addition, the electron transfer is coupled to the translocation of protons into the intermembrane space. This proton pumping determines the formation of an electrochemical gradient that is dissipated by the F_1F_0-ATP synthase to drive phosphorylation of ADP to ATP (Wallace, 2009).

Respiration, and consequently the ETC, is the main source of cellular energy, making this system central and fundamental throughout the whole life of the cell and, therefore, also during the aging process.

Respiration and its dysfunctions are central in the attempt to explain the aging phenomenon. In this context, one of the most widely accepted and popular theories is the Free Radical Theory of Aging. It was proposed by Harman in 1956 (Harman, 1956) and, substantially, attributed the cause of
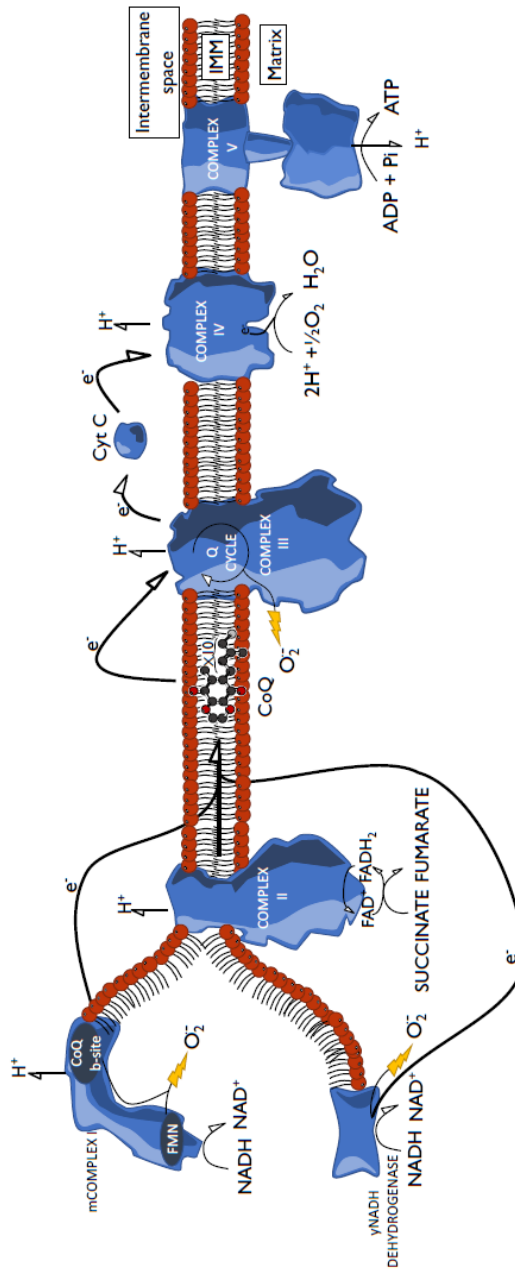
Figure 2 *Scheme of the OXPHOS.* Electron transfer along the electron transport chain, ATP production, and the main sites involved in ROS generation are shown. *CoQ B-site,* CoQ binding site; *CoQ,* coenzyme Q; *Cyt C,* cytochrome C; *FMN,* flavin mononucleotide; *IMM,* inner mitochondrial membrane; *mCOMPLEX I,* mammal COMPLEX I; *yNADH DEHYDROGENASE,* yeast NADH DEHYDROGENASE.

aging to damages generated by free radicals produced in redox reactions. The theory was proposed when direct evidence of ROS production by the cell was not yet available. However, Harman supposed that: "*The most likely source of •OH and HO₂ radicals, at least in the animal cell, would be the interaction of the respiratory enzymes involved in the direct utilization of molecular oxygen*". To date, this hypothesis has been confirmed, and mitochondria are recognized as the main source of ROS within the cell. ROS are part of the free radical family, that is, atoms, molecules, and ions that have an unpaired valence electron, making these substances extremely reactive. Therefore, the term ROS does not refer to a specific molecule but to superoxide $O_2^{\cdot-}$, radical hydroxyl •OH, hydrogen peroxide H_2O_2, and singlet oxygen $^1O_2$. Leakage of electrons from the ETC leads to the formation of the $O_2^{\cdot-}$, as oxygen can readily accept single electrons in a nonenzymatic transfer. The resulting cascade of ROS can damage not only many macromolecules but can target mitochondria with detrimental effects. ROS levels increase as a function of age, and a decline in mitochondrial functionality throughout the aging process takes place (Barros et al., 2010; Breitenbach et al., 2014).

7. RESPIRATION, ROS PRODUCTION AND AGING: A COMPLEX INTERPLAY

The specific mechanism by which each single complex in the respiratory chain is involved in the production of radical species and, thus, contributes to cell damage, and aging still remains to be completely elucidated. Here, the features of each complex will be reported in order to clarify their contribution to the aging process.

7.1 Complex I

Complex I, also known as NADH:ubiquinone oxidoreductase, transfers two electrons from NADH to ubiquinone, reducing it to ubiquinol. Complex I is the principal entry point for electrons in the ETC and plays a crucial role in ROS production (Stefanatos and Sanz, 2011) (Fig. 2). Indeed, from Complex I, electrons can leak and react with oxygen, with the resulting production of superoxide anion. Oxygen can access the electrons leaked from this complex from at least two sites: the flavin moiety and the ubiquinone-binding site (Hirst et al., 2008). Complex I dysfunctions and mutations in the genes encoding its subunits have frequently been correlated with altered ROS levels and diseases (Fato et al., 2008).

In mammals, Complex I comprises 38 subunits encoded by nuclear genes and seven encoded by the mitochondrial genome. It contains many thiol groups, which may be susceptible to oxidative damage during aging, leading to the loss of its activity. Indeed, some authors showed a strong age-dependent reduction of Complex I enzymatic activity in rat cortex mitochondria (Tatarková et al., 2011). These detrimental effects on the respiratory metabolism are dependent on an increase of oxidative stress that causes damage to protein and lipid peroxidation. Similar results were also observed in aged rats heart mitochondria (Petrosillo et al., 2009). The authors, by measuring different parameters related to mitochondrial metabolism, including basal respiration, membrane potential, ROS accumulation, and Complex I activity, found an age-dependent decline of mitochondrial performance in concert with increased levels of oxidized cardiolipin. This latter is a phospholipid required to ensure a proper Complex I activity.

In *S. cerevisiae*, Complex I is replaced by Ndi1, an NADH dehydrogenase, which does not pump protons in the inner membrane. As observed for mammals, also yeast Ndi1 has been reported to be related to the aging process. Indeed, *NDI1* overexpression in yeast determines an increase of ROS levels and $\Delta\Psi$ loss in concert with a caspase-independent apoptotic phenotype (Cui et al., 2012; Li et al., 2006). Furthermore, *NDI1*-overexpressing cells exhibit typical features of aged cells. In line with this, *NDI1* deletion determines CLS extension (Li et al., 2006). On the other hand, *NDI1* deletion in the context of replicative aging decreases RLS accompanied by elevated levels of superoxide radicals (Hacioglu et al., 2012).

7.2 Complex II

Complex II, or succinate dehydrogenase, is a tetrameric iron—sulfur flavoprotein highly conserved in mammals and yeast. It is a physical link between the ETC and the TCA cycle since it oxidizes succinate to fumarate in the TCA cycle and reduces ubiquinone to ubiquinol in the ETC.

Several studies highlight that this complex does not significantly contribute to ROS production and aging (Raha and Robinson, 2001; Robinson, 1998). However, some authors showed that by providing succinate (millimolar) to isolated mitochondria (Hansford et al., 1997), a high ROS generation occurs depending on a reverse electron transport (Scialò et al., 2017). However, in in vivo conditions, succinate concentration is not so high (micromolar) to promote this reverse electron transport,

explaining why the contribution of this complex to ROS production is not significant in vivo (Hansford et al., 1997). In addition, when Complex I and III are compromised and succinate levels are low, Complex II generates high levels of H_2O_2 in rat skeletal muscle mitochondria. On the contrary, when succinate concentration is high, the levels of the aforementioned radical species reverse to physiological ones (Quinlan et al., 2012). Authors propose that at least three mechanisms may be involved:

1. High succinate levels reduce flavin semiquinone concentration, namely the species that in reaction with oxygen can generate ROS.
2. Succinate binds the complex and reduces its reactive potential.
3. Succinate occupies the access site for oxygen.
   A synergistic effect of these mechanisms is not excluded.

Concerning the relationship between Complex II and the aging process, it has been demonstrated an age-dependent decline of its activity in human skin fibroblasts caused by a lower expression of genes encoding its subunits (Bowman and Birch-Machin, 2016).

Although the role of Complex II in the aging process of mammalian cells still merits a more exhaustive analysis, in yeast, there is clear evidence of its involvement in such a process. Cells deleted in *SDH1*, *SDH2*, or *SDH4* genes, encoding subunits of succinate dehydrogenase, have the shortest CLS among 33 single ETC component-deleted strains (Kwon et al., 2015). In addition, mutants for Complex II display higher levels of mitochondrial ROS than those of the other mutants (Kwon et al., 2015). The short-lived phenotype of *sdh1*, *sdh2*, and *sdh4* mutants is in line with the results of (Samokhvalov et al., 2004) showing that in chronological aging cells, an intensification of succinate formation and oxidation takes place to counteract a decrease in the activities of all NAD-dependent dehydrogenases in the TCA cycle. The oxidative metabolism of succinate necessarily involves the ETC Complex II and, probably, its enhancement is an adaptation mechanism supporting cell survival. Furthermore, the succinate formation requires the cytosolic glyoxylate shunt. During chronological aging, this shunt is triggered, providing C4 dicarboxylic acids that are required to replenish the TCA cycle with intermediates, among which is succinate. This compound is produced after cleavage of isocitrate by Icl1 and then transported into the mitochondria where is oxidized by Complex II. Notably, a high enzymatic activity of Icl1 is a property of surviving cells (Samokhvalov et al., 2004), while *ICL1* deletion significantly reduces CLS (Casatta et al., 2013). The importance of this complex is demonstrated

also during replicative aging. The absence of *TCM62*, which encodes a chaperonin required for the assembly of the complex, determines a reduction in the RLS (Hacioglu et al., 2012).

7.3 Complex III

Complex III, also called cytochrome bc_1 complex, is recognized as one of the main sources of $O_2^{\cdot-}$ in the ETC. The electrons are transferred from Complex I and II to Complex III by ubiquinol. The electron transfer from ubiquinol to Complex III, known as Q-cycle, is the main cause of $O_2^{\cdot-}$ production at this ETC point (Korshunov et al., 1997; Fig. 2). The two electrons transferred to Complex III follow different fates: one is carried by cytochrome c passing through the Rieske iron–sulfur protein and cytochrome c_1. The other is carried by ubiquinone passing through the b_L and b_H heme of cytochrome b. Considering that the ubiquinone is located on the matrix side (N side), which has high levels of negative charges, the electron transfer through the b_L to b_H heme is against electric gradient. Moreover, ubiquinone requires two electrons to be completely reduced, implying that another electron will have to follow the same counter-gradient route. Therefore, the ubiquinone reduction occurs in two sequential phases and involves the formation of a highly reactive semi-reduced form $Q^{-\cdot}$. Under normal conditions, $Q^{-\cdot}$ is rapidly reduced to QH_2, preventing $O_2^{\cdot-}$ formation. On the contrary, when $\Delta\Psi$ is high, the electron transfer is slower, making $Q^{-\cdot}$ more stable, thus promoting reactivity with O_2 and leading to $O_2^{\cdot-}$ formation (Sugrue and Tatton, 2001).

It has been shown that reducing the electron flow toward Complex III strongly limits ROS production in isolated rats mitochondria, confirming the central role of this complex in radical species generation (Chen et al., 2003). Moreover, the lowering of Complex III activity in *Caenorhabditis elegans* correlates with an increase of lifespan (Dillin et al., 2002). Together, these results confirm the importance of this complex in ROS production and its impact on the aging process.

In yeast, inhibition of Complex III by treating cells with antimycin A results in a significative reduction of respiration that correlates with a strong decrease of CLS (Ocampo et al., 2012). This effect depends on the Q-cycle. Indeed, since the binding site of antimycin A is the high potential b_H heme (Fang and Beattie, 2003), this could inhibit electron transfer from b_H heme to semiquinone, favoring the accumulation of ROS. Instead, the treatment of yeast cells with sodium cyanide, a molecule that blocks the Complex IV, reduces ROS levels from Complex III, maintaining cytochrome c and

ubiquinone reduced. This effect determines an increase of CLS, demonstrating that Complex III is central in ROS production and that interventions counteracting their formation promote longevity (Longo et al., 1999). In the context of replicative aging, it has been shown that the lack of *RIP1*, *CYT1*, and *QCR8* genes encoding Complex III subunits determines a strong reduction of RLS (Hacioglu et al., 2012).

7.4 Complex IV

Complex IV, or cytochrome c oxidase, is the last enzyme in the ETC. It transfers electrons from cytochrome c to molecular oxygen, reducing it to water. Differently from the other complexes, Complex IV to the best of our knowledge does not seem to be significantly involved in ROS production. However, an interesting link between the reduction of Complex IV activity and lifespan has been found (Tatarková et al., 2011). Indeed, its activity in cardiac mitochondria of 26-month-old rats significantly decreases compared with young animals, and its reduction is the highest compared with other complexes. These results outline the need for future investigations in order to clarify the connection of this complex with aging.

In *S. cerevisiae*, the deletion of some genes encoding subunits of Complex IV impairs the proton flow along the respiratory system, determining a strong reduction of CLS. This correlates with a reduction in ATP concentration (Kwon et al., 2015). Regarding replicative aging, similar results were observed, with a decrease of RLS and respiratory deficiency (Hacioglu et al., 2012).

7.5 F_1F_O ATPase

Mitochondrial ATPase, also defined as F_1F_O-ATP synthase or Complex V, is located in the inner mitochondrial membrane together with the ETC Complexes I–IV. It is a rotary enzyme that exploits the proton gradient across the inner membrane generated by the ETC to synthesize ATP. During the aging process, a decline on ETC and ATPase activities has been widely observed (Camacho-Pereira et al., 2016; Chistiakov et al., 2014; Porter et al., 2015). For example, it has been shown that ATP content and production decrease by about 50% in gastrocnemius muscle of aged rats, and this could be one of the factors promoting sarcopenia (Drew et al., 2003). Similar results were obtained in the heart of aged rats, showing a strong reduction in the RNA levels of the genes encoding the ATPase subunits. This correlates with a marked decrease in the enzymatic activity of

ATPase, with reduced ATP production and oxygen consumption (Preston et al., 2008). The role of this complex and the maintenance of adequate production of ATP are therefore crucial in the aging process. This is also supported by evidence of premature senescence in fibroblasts treated with oligomycin, an inhibitor of Complex V (Stöckl et al., 2006).

In *S. cerevisiae*, mutations in *ATP2*, encoding the β-subunit of the F_1 complex of ATPase, determine a decrease of mitochondrial membrane potential (Lai et al., 2002). In addition, daughter cells have the same RLS of old mother cells due to the inability of mother cells to retain damaged mitochondria. Furthermore, also the deletion of *ATP11*, required for the proper assembly of F_1 complex, results in a reduced RLS associated with significative levels of ROS (Hacioglu et al., 2012).

Other studies highlight that a transposon mutant (HsTnII), in which the expression of genes encoding subunits of the ETC and of Complex V is strongly downregulated, displays decreased CLS (Aerts et al., 2009). Moreover, also in this case, accelerated aging is associated with a loss of $\Delta\Psi$. In agreement with these results, it has been shown that the deletion of many genes encoding subunits of the ATPase correlated with a strong reduction in ATP levels and CLS (Kwon et al., 2015).

8. ROLE OF NAD^+ METABOLISM IN MITOCHONDRIAL FUNCTIONALITY

As described previously, the electrons transfer along the ETC starts from the universal cofactor NAD. Its molecular structure encompasses two covalently joined mononucleotides, namely nicotinamide mononucleotide (NMN) and adenosine monophosphate. In bioenergetic pathways, the molecule is subject to reversible reduction and oxidation cycles, from its oxidized form, NAD^+, to the reduced one, NADH.

Since the TCA cycle and ETC require the oxidized and the reduced form of NAD, respectively, a correct NAD^+/NADH balance is essential for an efficient mitochondrial metabolism and to preserve the whole-cell redox state (Stein and Imai, 2012). The correct maintenance of the NAD^+ pool by regulating its biosynthesis, cellular localization, and transport of its precursors plays a key role in regulating different cellular processes (Houtkooper et al., 2010).

From yeast to mammalian cells, there are different pathways for NAD^+ biosynthesis: the two major ones are de novo synthesis (de novo pathway) and the synthesis from its precursors (the NAD^+ salvage pathway;

Stein and Imai, 2012). The d*e novo* pathway starts from tryptophan in the cytosol and proceeds by the kynurenine pathway, involving a total of five steps (Bogan and Brenner, 2008). The importance of this essential aromatic amino acid in NAD^+ biosynthesis emerged from studies on the positive effect given by tryptophan administration in treatment of pellagra, a disease caused by NAD^+ deficiency (Sauve, 2008). The NAD^+ salvage pathway starts from two main forms of vitamin B_3, nicotinic acid (NA) and its amidic form nicotinamide (NAM), both defined as niacin, or from the conversion of nicotinamide riboside (NR) (Houtkooper et al., 2010). In yeast, Ntd1/2 have been identified as transporters able to import NAD^+ in mitochondria (Todisco et al., 2006). For mammals, the most current model for NAD^+ synthesis in mitochondria provides that NAD^+ precursors, such as NAM and NR, are converted to NMN in cytosol from nicotinamide phosphoribosyltransferase (NAMPT) and nicotinamide riboside kinase 1/2 (NRK1/2), respectively. Then, NMN is transported into the mitochondria and converted in NAD^+ by the nicotinamide nucleotide adenyltransferase 3 (NMNAT3; Nikiforov et al., 2011). This is because the mitochondrial compartment lacks both transferase and kinase activity of NAMPT and NRK1/2 (Kitani et al., 2003; Ratajczak et al., 2016). Fig. 3 shows the most accepted model, both in mammalian and yeast cells.

9. NAD$^+$ METABOLISM AND AGING

Diet, exercise, and the aging process influence the NAD^+/NADH ratio, by modulating the expression of genes encoding enzymes involved in NAD^+ biosynthesis (Verdin, 2015; White and Schenk, 2012; Yang et al., 2007; Fig. 4). Calorie restriction (CR), a dietary regimen known to extend the lifespan in a wide spectrum of species (Ruetenik and Barrientos, 2015), which in most cases is obtained by reducing calorie intake of about 20%–40% compared to normal intake (Lee and Longo, 2016), increases NAD^+ levels (Yang et al., 2007). In this context, NAMPT has been identified as a nutrient-responsive gene, able to promote cell survival by boosting mitochondrial NAD^+ level in liver of rats fasted for 48 h (Yang et al., 2007). Similarly, the levels of NAMPT and NAD^+ increase in 24-h fasted mice liver (Hayashida et al., 2010), suggesting that NAD^+ levels are strongly upregulated by nutrient restriction, and this is crucial for cell survival (Yang et al., 2007).
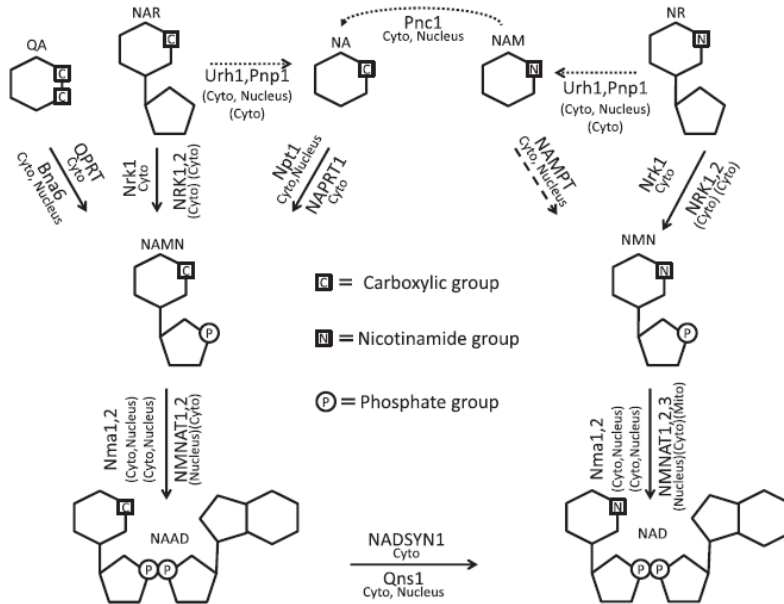
Figure 3 *Comparative scheme of NAD$^+$ biosynthesis in mammals and yeast.* Mammalian and yeast cells share the same precursors required for NAD$^+$ biosynthesis. Quinolinic acid (QA) derives from the kynurenine pathway. QA is converted to nicotinic acid mononucleotide (NAMN) by quinolinate phosphoribosyltransferase (QPRT) in mammals and by Bna6 in yeast. Nicotinic acid riboside (NAR) is converted by mammalian nicotinamide riboside kinase 1,2 (NRK1,2) and Nrk1 of yeast to NAMN. NAMN is also obtained from nicotinic acid (NA) by nicotinic acid phophoribosyltransferase 1 (NAPRT1) in mammal and by Npt1 in yeast. Nicotinamide mononucleotide adenylyltransferase 1,2 (NMNAT1,2) in mammals and Nma1,2 in yeast converts NAMN to nicotinic acid adenine dinucleotide (NAAD). NAD$^+$ is obtained from NAAD by nicotinamide adenine dinucleotide synthetase 1 (NADSYN1) in mammals and by Qns1 in yeast. Starting from QA, NA, and NAR, mammals and yeast share the same reactions for NAD$^+$ biosynthesis. However, yeast can also convert NAR to NA by Urh1 and Pnp1. Nicotinamide (NAM) has different metabolic routes in mammals and yeast. In mammals, NAM is converted into nicotinamide mononucleotide (NMN) by the enzyme Nicotinamide mononucleotidephophoribosyl transferase (NAMPT), which has no ortholog in yeast. Nicotinamide riboside is converted to NMN both in mammals and yeast by NRK1,2 and Nrk1, respectively. NMN is converted to NAD$^+$ by NMNAT1,2,3 in mammals and by Nma1,2 in yeast. In yeast, NR is converted to NAM by Urh1 and Pnp1. NAM can be used for NAD$^+$ biosynthesis only upon its conversion to NA by Pnc1. $\vec{x}$ indicates common reactions among mammals and yeast, $--$> indicates mammalian-specific reactions, and ■■■> indicates yeast-specific reactions.

108
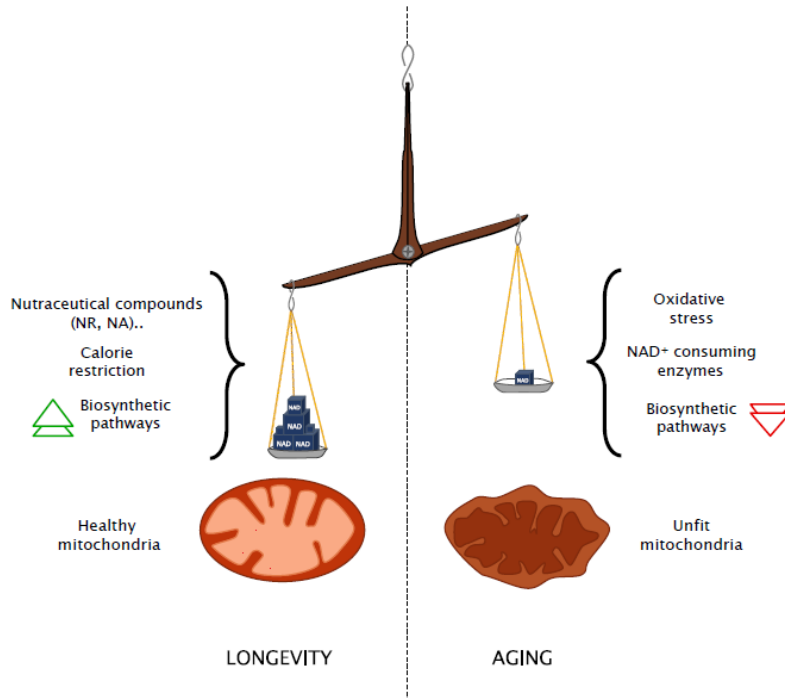
Figure 4 NAD^+ *is involved in the maintenance of mitochondria functionality.* Calorie restriction, NAD^+ precursors, and enzymes that synthesize NAD^+, all contribute to preserve NAD^+ levels, favoring the maintenance of mitochondria functionality (mammalian PGC1-α axis) and longevity. Oxidative stress and reduction in the activity of NAD^+ biosynthetic pathways unfit mitochondria and promote aging.

CR of yeast cells can be accomplished by a reduction in the glucose content in the growth media from 2% to 0.5% (Lin et al., 2002). NADH levels in these conditions decrease by about 50%, and the RLS increases significantly (Lin et al., 2002). It has been proposed that this is probably due to a metabolic shift from a predominantly fermentation-based metabolism to a respiration-based one determined by CR. This triggers a significant decrease in NADH, which is used by the ETC. Indeed, during respiratory growth, mitochondrial NADH is reoxidized by NADH dehydrogenase in the respiratory chain (Bakker et al., 2001).

However, this hypothesis is in contrast with the RLS increase observed in calorie-restricted respiratory deficient rho[0] mutants (Kaeberlein et al., 2005). Due to the absence of mitochondrial DNA, rho[0] lacks functional ETC and has an impaired TCA cycle (Jazwinski, 2005). The loss of mitochondrial membrane potential, which has a fundamental role in supporting the transport of biosynthetic intermediates outside the mitochondrion (Miceli et al., 2012; Passarella et al., 2003), results in the activation in rho[0] mutants of the retrograde response pathway, that in turn can extend RLS (Kirchman et al., 1999). The retrograde signaling is one of the most well-studied and conserved pathways involved in the cross-talk between nucleus and mitochondrion (da Cunha et al., 2015). Its main function is the upregulation of a wide range of metabolic and stress response genes in order to cope with the impairment of the TCA cycle activity. This transcriptional response resembles the one that is induced during CR (Jiang et al., 2002; Wang et al., 2010). In rho[0] cells the first three reactions of the TCA cycle are functional (Jazwinski, 2013), allowing the synthesis of α-ketoglutarate, precursor of glutamate that supplies nitrogen in biosyntheses, starting from citrate. The latter comes from the activation of the glyoxylate cycle, which synthetizes citrate from oxaloacetate and acetyl-CoA, but without any release of CO_2, preserving the two carbons of acetate, thus allowing the first three reactions of the TCA to proceed. This metabolic adaptation to the deficiency of biosynthetic intermediates is decisive for the increase of RLS in rho[0] cells (Jazwinski, 2013). Studies performed by Jiang et al. led to the identification of the target responsible for RLS extension after retrograde signaling activation (Jiang et al., 2016). Indeed, among the different candidates causing RLS lengthening, only the deletion of *PHO84*, which encodes a transporter of inorganic phosphate, suppressed the long-lived phenotype of rho[0] strains. Regarding chronological aging, the lack of mtDNA that causes respiratory-deficiency results in CLS shortening (Ocampo et al., 2012).

The aging process also influences NAD^+ levels in an opposite way compared with CR; indeed, aging is associated with different pathophysiological impacts, including the reduction of NAMPT-mediated NAD^+ biosynthesis (Imai and Yoshino, 2013). It is known that tumor necrosis factor-α and oxidative stress, which are decisive for the inflammatory process, reduce NAMPT and NAD^+ levels in primary hepatocytes (Yoshino et al., 2011). Considering that both the inflammatory cytokine production and the increase in oxidative stress significantly contribute to chronic age-associated inflammation (Singh and Newman, 2011), the development of chronic inflammation during aging may be the reason for the reduction of

NAMPT levels. However, other studies have shown that NAMPT levels and its enzymatic activity are reduced in human vascular smooth muscle cells during aging without inflammation (Van Der Veer et al., 2007), suggesting that chronic inflammation is certainly not the only cause of NAMPT reduction. Similarly, a reduction of both protein and messenger RNA (mRNA) levels of NAMPT has been found in mesenchymal stem cells (MSCs) obtained from aged rats (Ma et al., 2017). In both cases, the over-expression of NAMPT gene is sufficient to attenuate cellular senescence (Fig. 4). As mentioned previously, in mammals, NAMPT converts NAM to NMN in the cytosol; then NMN is transported in mitochondria where it is used for NAD^+ biosynthesis by NMNAT3. The activity of this enzyme is crucial to preserve the NAD^+ pool in mitochondria. NMNAT3 expression, as well as that of NAMPT, are susceptible to aging. A reduction of both NMNAT3 and mitochondrial NAD^+ levels has been also observed in aged human MSCs (Son et al., 2016); NMNAT3 overexpression in these cells is sufficient to delay replicative senescence. A proposed mechanism by which NAMPT activity might reverse the aged phenotype and increase lifespan relies on the activation of SIRT1, a member of the Sirtuin family endowed with an NAD^+-dependent deacetylase activity (Prolla and Denu, 2014).

Some studies suggest that NAMPT is the equivalent in terms of function of yeast Pnc1 (Yang et al., 2006), given that both these enzymes catalyze the first and rate-limiting step of NAD^+ biosynthesis from NAM (Revollo et al., 2004; Rongvaux et al., 2002) and that their expression increases in nutrient-restricted condition (Mei and Brenner, 2014; Yang et al., 2007). Similarly to NAMPT, RLS extension by CR requires PNC1 (Anderson et al., 2003). The authors provide evidence that this is linked to an increase of NAD^+ levels that promotes Silent Information Regulator 2 (Sir2) activity. Sir2 is the ortholog of mammalian SIRT1 and founding member of the Sirtuin family. In the context of yeast replicative aging, SIR2 is a prolongevity gene (Longo et al., 2012). Since PNC1 functions in the NAD^+ salvage pathway, converting NAM in NA, it could promote Sir2 activation by increasing the availability of its co-substrate, NAD^+, and lowering that of its physiological inhibitor, NAM.

In addition to the biosynthetic pathway, the malate—aspartate shuttle also contributes to maintaining the mitochondrial physiological NAD^+ pool. It has been shown that the mitochondrial components of the malate—aspartate NADH shuttle are longevity factors required for lifespan extension in calorie-restricted yeast cells (Easlon et al., 2008). Some studies highlight that the lifespan increase observed in yeast in nutrient-restricted

condition also depends on Npt1, an enzyme that catalyzes the conversion of NA to NAMN, contributing to the maintenance of NAD^+ levels (Lin et al., 2004). However, how nutritional conditions and aging affect the complex dynamics of NAMPT/*PNC1*/NAD^+ network, defined by some authors as the "NAD World" (Imai, 2010), still remains unclear. Understanding this mechanism is a fundamental investigation to develop approaches able to mitigate the detrimental effects of the aging process. Indeed, if NAMPT-mediated NAD^+ biosynthesis is compromised during aging, a way to preserve NAD^+ levels could be to provide other key intermediates such as NMN and NR. For example, Belenky et al. showed that NR supplementation to yeast cells increases RLS, through an increase of NAD^+ levels mediated by Nrk1, enzyme that converts NR to NMN (Belenky et al., 2007). For this reason, nutraceutical interventions could represent a valid alternative to pharmacological treatments to improve the aging process (Fig. 4).

10. NAD^+ IS A KEY MODULATOR OF PATHWAYS INVOLVED IN THE AGING PROCESS

NAD^+ is not only used in redox reactions but also as a co-substrate for some NAD^+-consuming enzymes in different cellular pathways (Imai and Guarente, 2014). Among these, we include Sirtuins, poly-ADP-ribose polymerase 1 (PARP-1), and CD38/CD157 ectoenzymes, which cleave the glycosidic bond between NAM moiety and ADP-ribose moiety of NAD^+.

Sirtuins are a family of NAD^+-dependent protein deacetylases. Sir2 of *S. cerevisiae* is the founding member of this family and regulates silencing at the mating-type loci, telomeres, and ribosomal DNA loci (Kaeberlein et al., 1999). In mammals, there are seven Sirtuin isoforms (SIRT1-7), which share a conserved NAD^+-binding and catalytic core domain with Sir2 (Li and Kazgan, 2011). The link between Sirtuins and aging was first observed in yeast. Indeed, Sir2 is required for RLS extension (Kaeberlein et al., 1999). In mice, at least two Sirtuins are involved in lifespan extension, SIRT6 and SIRT1. Ubiquitous SIRT6 overexpression determines an increase of lifespan, while the lack of SIRT6 results in accelerated aging, referred also as progeroid phenotype (Kanfi et al., 2012; Mostoslavsky et al., 2006). SIRT1 is the most well-studied of the mammalian Sirtuins. It is involved in epigenetic regulation, mitochondrial functionality, and aging (Yuan et al., 2016). Particularly, it has been proposed that SIRT1 may delay aging by the deacetylation of different substrates, including peroxisome

proliferator-activated receptor-gamma coactivator 1 alpha (PGC-1α), which is the principal regulator of mitochondrial biogenesis (NAD^+/SIRT1/PGC-1α axis). Furthermore, SIRT1 decreases during aging, leading to a decrease of mitochondrial biogenesis in concert with an impaired mitochondrial turnover (Yuan et al., 2016). In the field of aging research, the modulation of SIRT1 activity represents a promising strategy to promote beneficial health effects and delay aging (Blum et al., 2011).

In *S. cerevisiae*, whereas Sir2 promotes RLS extension, most evidence so far supports a proaging role in CLS (Casatta et al., 2013; Fabrizio et al., 2005; Longo et al., 2012). Furthermore, when postdiauxic cells are transferred from expired medium to water (a severe CR condition), CLS significantly increases, and lack of Sir2 further exacerbates this effect (Casatta et al., 2013; Fabrizio et al., 2005). A further extension of CLS is also observed when *sir2Δ* mutant is combined with long-lived mutants that reduce the activity of two major nutrient-sensing pathways, such as TORC1-Sch9 and Ras-PKA ones. Since nutrient signaling attenuation determines an increase of CLS by ultimately activating endogenous defense mechanisms (Wei et al., 2008), it is plausible to assume that Sir2 also interferes with the same targets. Consistent with this, lack of Sir2 confers resistance to oxidative and heat stresses (Fabrizio et al., 2005).

Phosphoenolpyruvate carboxykinase (Pck1), enzyme catalyzing the rate-limiting step of gluconeogenesis, represents the cytosolic target of Sir2. Briefly, Sir2 is the enzyme responsible for the deacetylation and subsequent inactivation of Pck1 (Lin et al., 2009). During chronological aging, the lack of Sir2 deacetylase activity results in a major metabolic rearrangement toward gluconeogenesis, allowing an increase of trehalose stores essential for CLS (Casatta et al., 2013; Ocampo et al., 2012). Notably, chronological aging *sir2Δ* cells display other features that are useful for long-term survival of nondividing cells. Indeed, mutant cells have a high respiratory capacity and reduced levels of nonphosphorylating respiration in concert with a low $O_2^{\cdot-}$ content. Finally, they preserve functional mitochondria (Orlandi et al., 2017a, 2017b). NAM is an endogenous noncompetitive inhibitor of Sir2 activity; cells grown in the presence of NAM have a reduced RLS (Bitterman et al., 2002). Consistent with this, the overexpression of *PNC1*, which depletes NAM levels, increases RLS (Anderson et al., 2003). During chronological aging, NAM supplementation phenocopies the lack of Sir2. It determines the same anabolic and respiratory changes that lead to an increase of protective factors and low harmful $O_2^{\cdot-}$ levels, which ensure a longer CLS (Orlandi et al., 2017a).

PARP-1 is a multifunctional enzyme found in most Eukaryotes except for yeast (Hassa et al., 2006). It catalyzes the polymerization of ADP-ribose units of NAD^+, binding linear and branched poly ADP-ribose (PAR) polymers to itself, as well as to target proteins, following genotoxic stress (Luo and Lee Kraus, 2012). Indeed, PARP-1 is involved in the DNA damage response: it stabilizes the DNA replication fork by modifying its chromatin structure. Deficiency in PARP-1 accelerates aging in mice (Piskunova et al., 2008). In $PARP1^{-/-}$ mice, a reduction of both mean and maximum lifespan of 13.3% and 16.4%, respectively, was observed. These results are consistent with the idea that a proper DNA repair and longevity are positively correlated during aging. Other studies highlight that PARP-1 inhibition brings about an increase of oxidative metabolism, specifically an increase of O_2 consumption, via activation of SIRT1 (Bai et al., 2011). Since PARP-1 is a major cellular NAD^+ consumer, its activation depletes NAD^+ levels, which are important for Sirtuin activity. This aspect emphasizes that PARP-1 and SIRT1 compete for NAD^+ and entails that a proper balance of their enzymatic activity is crucial to regulate mitochondria maintenance and aging.

CD38 was identified in 1980 by studies focused on the identification of surface molecules involved in the immune system recognition (Reinherz et al., 1980). It is considered the homologous of CD157 because both belong to a gene family encoding enzymes that mediate cell—cell interaction (Quarona et al., 2013). Since they are located on the cellular surface, are classified as ectoenzymes able to modulate different cellular signals (from extracellular to intracellular environment and vice versa). To the best of our knowledge, CD38/CD157 are not directly involved in the aging process but are among the master regulators of intracellular NAD^+ levels in mammalian cells, influencing Sirtuin activity (Chini, 2009). As mentioned in the previous paragraphs, NAD^+ levels decrease during aging, promoting different age-related diseases. Several theories have been proposed to explain why NAD^+ levels are negatively affected during aging. However, to date, the specific contribution of metabolic pathways that modulate NAD^+ levels during the aging process still remains to be completely defined. Camacho-Pereira et al. suggest that CD38 dictates an age-dependent NAD^+ decline and mitochondria dysfunction through a SIRT3-mediated mechanism (Camacho-Pereira et al., 2016). The protein and mRNA levels of CD38 increase in several aged murine tissues,

including liver, white adipose tissue, spleen, and skeletal muscle, leading to a strong reduction of NAD^+ levels. Concomitantly, a decrease of mitochondrial performance, in terms of respiration coupled to ATP synthesis, and a reduction of NAD^+/NADH ratio in mitochondria take place. These effects on oxidative mitochondrial metabolism depend on the deacetylase activity of SIRT3, which is localized in mitochondria. This age-dependent CD38 increase is also present in humans. Indeed, as observed for aged mice, also in aged human adipose tissue, CD38 mRNA levels increase of about 2.5 times compared with younger subjects (Camacho-Pereira et al., 2016).

11. CONCLUSIONS

All the aspects discussed previously indicate that mitochondrial metabolism plays a critical role in the maintenance of mitochondria functionality during aging, and its alterations lead to mitochondrial dysfunctions. These intensify progressively during aging and have detrimental consequences on cellular lifespan. On the one hand, the TCA cycle appears to function as a hub for mitochondrial metabolism. Indeed, many pathways converge at the level of this cycle, where signals are integrated in a dynamic and plastic, yet robust network that supports respiration and biosynthesis of BCAAs. As a consequence, an alteration in the TCA cycle can affect mitochondrial metabolism from different sides, with always a common negative effect on longevity. On the other hand, the complexes of ETC are the largest producers of ROS in the cell. Damage caused by ROS is frequently cited as one of the main causes of aging. In addition, the theory of the vicious circle proposes that ROS produced by respiration affect mitochondrial performance leading to more ROS and mitochondrial damage. Therefore, it is essential that the ETC remains efficient and respiration coupled in order to avoid the emergence of this vicious circle and ensure healthy aging. In addition, NAD metabolism is highlighted as a relevant connection between nutrients and respiration, capable of modulating the activity of Sirtuins.

Taking all together, mitochondrial metabolism progressively changes in time, with repercussions that extend to the whole cell causing a gradual decline of cellular functions, which define the onset of organismal weakening and the advancement of aging. The data reported in this review offer the rational basis to develop new promising strategies to prevent and control age-related disorders in humans.

ACKNOWLEDGMENTS

REFERENCES

Aerts, A.M., Zabrocki, P., Govaert, G., Mathys, J., Carmona-Gutierrez, D., Madeo, F., et al., 2009. Mitochondrial dysfunction leads to reduced chronological lifespan and increased apoptosis in yeast. FEBS Lett. 583, 113−117.

Ahmed, E.K., Rogowska-Wrzesinska, A., Roepstorff, P., Bulteau, A.L., Friguet, B., 2010. Protein modification and replicative senescence of WI-38 human embryonic fibroblasts. Aging Cell 9, 252−272.

Alvers, A.L., Fishwick, L.K., Wood, M.S., Hu, D., Chung, H.S., Dunn Jr., W.A., Aris, J.P., 2009. Autophagy and amino acid homeostasis are required for chronological longevity in *Saccharomyces cerevisiae*. Aging Cell 8, 353−369.

Anderson, R.M., Bitterman, K.J., Wood, J.G., Medvedik, O., Sinclair, D.A., 2003. Nicotin-amide and *PNC1* govern lifespan extension by calorie restriction in *Saccharomyces cerevisiae*. Nature 423, 181−185.

Aris, J.P., Fishwick, L.K., Marraffini, M.L., Seo, A.Y., Leeuwenburgh, C., Dunn Jr., W.A., 2012. Amino acid homeostasis and chronological longevity in *Saccharomyces cerevisiae*. Subcell. Biochem. 57, 161−186.

Bai, P., Cantó, C., Oudart, H., Brunyánszki, A., Cen, Y., Thomas, C., et al., 2011. PARP-1 inhibition increases mitochondrial metabolism through SIRT1 activation. Cell Metab. 13, 461−468.

Bakker, B.M., Overkamp, K.M., Van Maris, A.J.A., Kötter, P., Luttik, M.A.H., Van Dijken, J.P., Pronk, J.T., 2001. Stoichiometry and compartmentation of NADH meta-bolism in *Saccharomyces cerevisiae*. FEMS Microbiol. Rev. 25, 15−37.

Barros, M.H., da Cunha, F.M., Oliveira, G.A., Tahara, E.B., Kowaltowski, A.J., 2010. Yeast as a model to study mitochondrial mechanisms in ageing. Mech. Ageing Dev. 131, 494−502.

Belenky, P., Racette, F.G., Bogan, K.L., McClure, J.M., Smith, J.S., Brenner, C., 2007. Nicotinamide riboside promotes Sir2 silencing and extends lifespan via Nrk and Urh1/Pnp1/Meu1 pathways to NAD$^+$. Cell 129, 473−484.

Berg, S.M., Beck-Nielsen, H., Færgeman, N.J., Gaster, M., 2016. Carnitine acetyltransfer-ase: a new player in skeletal muscle insulin resistance? Biochem. Biophys. Rep. 9, 47−50.

Bitterman, K.J., Anderson, R.M., Cohen, H.Y., Latorre-Esteves, M., Sinclair, D.A., 2002. Inhibition of silencing and accelerated aging by nicotinamide, a putative negative regu-lator of yeast Sir2 and human SIRT1. J. Biol. Chem. 277, 45099−45107.

Blum, C.A., Ellis, J.L., Loh, C., Ng, P.Y., Perni, R.B., Stein, R.L., 2011. SIRT1 modu-lation as a novel approach to the treatment of diseases of aging. J. Med. Chem. 54, 417−432.

Bogan, K.L., Brenner, C., 2008. Nicotinic acid, nicotinamide, and nicotinamide riboside: a molecular evaluation of NAD$^+$ precursor vitamins in human nutrition. Annu. Rev. Nutr. 28, 115−130.

Bowman, A., Birch-Machin, M.A., 2016. Age-dependent decrease of mitochondrial com-plex II activity in human skin fibroblasts. J. Invest. Dermatol. 136, 912−919.

Breitenbach, M., Rinnerthaler, M., Hartl, J., Stincone, A., Vowinckel, J., Breitenbach-Koller, H., Ralser, M., 2014. Mitochondria in ageing: there is metabolism beyond the ROS. FEMS Yeast Res. 14, 198−212.

Bricker, D.K., Taylor, E.B., Schell, J.C., Orsak, T., Boutron, A., Chen, Y.C., et al., 2012. A mitochondrial pyruvate carrier required for pyruvate uptake in yeast, *Drosophila*, and humans. Science 337, 96–100.

Cabiscol, E., Tamarit, J., Ros, J., 2014. Protein carbonylation: proteomics, specificity and relevance to aging. Mass Spectrom. Rev. 33, 21–48.

Camacho-Pereira, J., Tarragó, M.G., Chini, C.C.S., Nin, V., Escande, C., Warner, G.M., et al., 2016. CD38 dictates age-related NAD decline and mitochondrial dysfunction through an SIRT3-dependent mechanism. Cell Metab. 23, 1127–1139.

Casatta, N., Porro, A., Orlandi, I., Brambilla, L., Vai, M., 2013. Lack of Sir2 increases acetate consumption and decreases extracellular pro-aging factors. Biochim. Biophys. Acta Mol. Cell Res. 1833, 593–601.

Chen, Q., Vazquez, E.J., Moghaddas, S., Hoppel, C.L., Lesnefsky, E.J., 2003. Production of reactive oxygen species by mitochondria: central role of complex III. J. Biol. Chem. 278, 36027–36031.

Chini, E.N., 2009. CD38 as a regulator of cellular NAD: a novel potential pharmacological target for metabolic conditions. Curr. Pharm. Des. 15, 57–63.

Chistiakov, D.A., Sobenin, I.A., Revin, V.V., Orekhov, A.N., Bobryshev, Y.V., 2014. Mitochondrial aging and age-related dysfunction of mitochondria. BioMed Res. Int. 2014, 238463.

Cui, Y., Zhao, S., Wu, Z., Dai, P., Zhou, B., 2012. Mitochondrial release of the NADH dehydrogenase Ndi1 induces apoptosis in yeast. Mol. Biol. Cell 23, 4373–4382.

Da Cunha, F.M., Torelli, N.Q., Kowaltowski, A.J., 2015. Mitochondrial retrograde signaling: triggers, pathways, and outcomes. Oxid. Med. Cell. Longev. 2015, 482582.

Dillin, A., Hsu, A.L., Arantes-Oliveira, N., Lehrer-Graiwer, J., Hsin, H., Fraser, A.G., et al., 2002. Rates of behaviour and aging specified by mitochondrial function during development. Science 298, 2398–2401.

Dillon, E.L., Sheffield-Moore, M., Paddon-Jones, D., Gilkison, C., Sanford, A.P., Casperson, S.L., et al., 2009. Amino acid supplementation increases lean body mass, basal muscle protein synthesis, and insulin-like growth factor-I expression in older women. J. Clin. Endocr. Metab. 94, 1630–1637.

Drew, B., Phaneuf, S., Dirks, A., Selman, C., Gredilla, R., Lezza, A., et al., 2003. Effects of aging and caloric restriction on mitochondrial energy production in gastrocnemius muscle and heart. Am. J. Physiol. Regul. Integr. Comp. Physiol. 284, R474–R480.

Easlon, E., Tsang, F., Skinner, C., Wang, C., Lin, S., 2008. The malate-aspartate NADH shuttle components are novel metabolic longevity regulators required for calorie restriction-mediated life span extension in yeast. Genes Dev. 22, 931–944.

Eisenberg, T., Schroeder, S., Andryushkova, A., Pendl, T., Küttner, V., Bhukel, A., et al., 2014. Nucleocytosolic depletion of the energy metabolite acetyl-coenzyme a stimulates autophagy and prolongs lifespan. Cell Metab. 19, 431–444.

Fabrizio, P., Gattazzo, C., Battistella, L., Wei, M., Cheng, C., McGrew, K., Longo, V.D., 2005. Sir2 blocks extreme life-span extension. Cell 123, 655–667.

Fabrizio, P., Hoon, S., Shamalnasab, M., Galbani, A., Wei, M., Giaever, G., et al., 2010. Genome-wide screen in *Saccharomyces cerevisiae* identifies vacuolar protein sorting, autophagy, biosynthetic, and tRNA methylation genes involved in life span regulation. PLoS Genet. 6, e1001024.

Fang, J., Beattie, D.S., 2003. External alternative NADH dehydrogenase of *Saccharomyces cerevisiae*: a potential source of superoxide. Free Radic. Biol. Med. 34, 478–488.

Fato, R., Bergamini, C., Leoni, S., Lenaz, G., 2008. Mitochondrial production of reactive oxygen species: role of complex I and quinone analogues. Biofactors 32, 31–39.

Fleck, C.B., Brock, M., 2009. Re-characterisation of *Saccharomyces cerevisiae* Ach1p: fungal CoA-transferases are involved in acetic acid detoxification. Fungal. Genet. Biol. 46, 473–485.

Fontana, L., Partridge, L., Longo, V.D., 2010. Extending healthy life span—from yeast to humans. Science 328, 321—326.

Fujita, S., Volpi, E., 2006. Amino acids and muscle loss with aging. J. Nutr. 136, 277S—280S.

Hacioglu, E., Demir, A.B., Koc, A., 2012. Identification of respiratory chain gene mutations that shorten replicative life span in yeast. Exp. Gerontol. 47, 149—153.

Hansford, R.G., Hogue, B.A., Mildaziene, V., 1997. Dependence of H_2O_2 formation by rat heart mitochondria on substrate availability and donor age. J. Bioenerg. Biomembr. 29, 89—95.

Harman, D., 1956. Aging: a theory based on free radical and radiation chemistry. J. Gerontol. 11, 298—300.

Hassa, P.O., Haenni, S.S., Elser, M., Hottiger, M.O., 2006. Nuclear ADP-ribosylation reactions in mammalian cells: where are we today and where are we going? Microbiol. Mol. Biol. Rev. 70, 789—829.

Hayashida, S., Arimoto, A., Kuramoto, Y., Kozako, T., Honda, S.I., Shimeno, H., Soeda, S., 2010. Fasting promotes the expression of SIRT1, an NAD^+-dependent protein deacetylase, via activation of PPARα in mice. Mol. Cell. Biochem. 339, 285—292.

Herzig, S., Raemy, E., Montessuit, S., Veuthey, J.L., Zamboni, N., Westermann, B., et al., 2012. Identification and functional expression of the mitochondrial pyruvate carrier. Science 337, 93—96.

Hinnebusch, A.G., 2005. Translational regulation of GCN4 and the general amino acid control of yeast. Annu. Rev. Microbiol. 59, 407—450.

Hirst, J., King, M.S., Pryde, K.R., 2008. The production of reactive oxygen species by complex I. Biochem. Soc. Trans. 36, 976—980.

Houtkooper, R.H., Cantó, C., Wanders, R.J., Auwerx, J., 2010. The secret life of NAD^+: an old metabolite controlling new metabolic signaling pathways. Endocr. Rev. 31, 194—223.

Imai, S., 2010. "Clocks" in the NAD World: NAD as a metabolic oscillator for the regulation of metabolism and aging. Biochim. Biophys. Acta Proteins Proteomics 1804, 1584—1590.

Imai, S., Guarente, L., 2014. NAD^+ and sirtuins in aging and disease. Trends Cell Biol. 24, 464—471.

Imai, S., Yoshino, J., 2013. The importance of NAMPT/NAD/SIRT1 in the systemic regulation of metabolism and ageing. Diabetes Obes. Metab. 15, 26—33.

Ingram, T., Chakrabarti, L., 2016. Proteomic profiling of mitochondria: what does it tell us about the ageing brain? Aging (Albany NY) 8. Article ID: 3161.

Jazwinski, S.M., 2005. Rtg2 protein: at the nexus of yeast longevity and aging. FEMS Yeast Res. 5, 1253—1259.

Jazwinski, S.M., 2013. The retrograde response: when mitochondrial quality control is not enough. Biochim. Biophys. Acta Mol. Cell Res. 1833, 400—409.

Jiang, J.C., Stumpferl, S.W., Tiwari, A., Qin, Q., Rodriguez-Quiñones, J.F., Jazwinski, S.M., 2016. Identification of the target of the retrograde response that mediates replicative lifespan extension in Saccharomyces cerevisiae. Genetics 204, 659—673.

Jiang, J.C., Wawryn, J., Kumara, H.S., Jazwinski, S.M., 2002. Distinct roles of processes modulated by histone deacetylases Rpd3p, Hda1p, and Sir2p in life extension by caloric restriction in yeast. Exp. Gerontol. 37, 1023—1030.

Kaeberlein, M., 2010. Lessons on longevity from budding yeast. Nature 464, 513—519.

Kaeberlein, M., Hu, D., Kerr, E.O., Tsuchiya, M., Westman, E.A., Dang, N., Fields, S., Kennedy, B.K., 2005. Increased life span due to calorie restriction in respiratory-deficient yeast. PLoS Genet. 1, e69.

Kaeberlein, M., McVey, M., Guarente, L., 1999. The SIR2/3/4 complex and SIR2 alone promote longevity in Saccharomyces cerevisiae by two different mechanisms. Genes Dev. 13, 2570—2580.

118

Kamei, Y., Tamada, Y., Nakayama, Y., Fukusaki, E., Mukai, Y., 2014. Changes in transcription and metabolism during the early stage of replicative cellular senescence in budding yeast. J. Biol. Chem. 289, 32081–32093.

Kanfi, Y., Naiman, S., Amir, G., Peshti, V., Zinman, G., Nahum, L., et al., 2012. The sirtuin SIRT6 regulates lifespan in male mice. Nature 483, 218–221.

Kirchman, P.A., Kim, S., Lai, C.Y., Jazwinski, S.M., 1999. Interorganelle signaling is a determinant of longevity in *Saccharomyces cerevisiae*. Genetics 152, 179–190.

Kitani, T., Okuno, S., Fujisawa, H., 2003. Growth phase-dependent changes in the subcellular localization of pre-B-cell colony-enhancing factor. FEBS Lett. 544, 74–78.

Korshunov, S.S., Skulachev, V.P., Starkov, A.A., 1997. High protonic potential actuates a mechanism of production of reactive oxygen species in mitochondria. FEBS Lett. 416, 15–18.

Kumaran, S., Subathra, M., Balu, M., Panneerselvam, C., 2005. Supplementation of L-carnitine improves mitochondrial enzymes in heart and skeletal muscle of aged rats. Exp. Aging Res. 31, 55–67.

Kwon, Y., Choi, K., Cho, C., Lee, C., 2015. Mitochondrial efficiency-dependent viability of *Saccharomyces cerevisiae* mutants carrying individual electron transport chain component deletions. Mol. Cells 38, 1054–1063.

Lai, C.Y., Jaruga, E., Borghouts, C., Jazwinski, S.M., 2002. A mutation in the *ATP2* gene abrogates the age asymmetry between mother and daughter cells of the yeast *Saccharomyces cerevisiae*. Genetics 162, 73–87.

Lane, R.K., Hilsabeck, T., Rea, S.L., 2015. The role of mitochondrial dysfunction in age-related diseases. Biochim. Biophys. Acta Bioenerg. 1847, 1387–1400.

Lee, C., Longo, V., 2016. Dietary restriction with and without caloric restriction for healthy aging. F1000Res. 5, 1–7.

Li, W., Sun, L., Liang, Q., Wang, J., Mo, W., Zhou, B., 2006. Yeast AMID homologue Ndi1p displays respiration-restricted apoptotic activity and is involved in chronological aging. Mol. Biol. Cell 17, 1802–1811.

Li, X., Kazgan, N., 2011. Mammalian sirtuins and energy metabolism. Int. J. Biol. Sci. 7, 575–587.

Lin, S.J., Ford, E., Haigis, M., Liszt, G., Guarente, L., 2004. Calorie restriction extends yeast life span by lowering the level of NADH. Genes Dev. 18, 12–16.

Lin, S.J., Kaeberlein, M., Andalis, A.A., Sturtz, L.A., Defossez, P.A., Culotta, V.C., et al., 2002. Calorie restriction extends *Saccharomyces cerevisiae* lifespan by increasing respiration. Nature 418, 344–348.

Lin, Y.Y., Lu, J.Y., Zhang, J., Walter, W., Dang, W., Wan, J., et al., 2009. Protein acetylation microarray reveals that Nua4 controls key metabolic target regulating gluconeogenesis. Cell 136, 1073–1084.

Longo, V.D., Kennedy, B.K., 2006. Sirtuins in aging and age-related disease. Cell 126, 257–268.

Longo, V.D., Antebi, A., Bartke, A., Barzilai, N., Brown-Borg, H.M., Caruso, C., Ingram, D., 2015. Interventions to slow aging in humans: are we ready? Aging Cell 14, 497–510.

Longo, V.D., Liou, L.L., Valentine, J.S., Gralla, E.B., 1999. Mitochondrial superoxide decreases yeast survival in stationary phase. Arch. Biochem. Biophys. 365, 131–142.

Longo, V.D., Shadel, G.S., Kaeberlein, M., Kennedy, B., 2012. Replicative and chronological aging in *Saccharomyces cerevisiae*. Cell Metab. 16, 18–31.

López-Otín, C., Blasco, M.A., Partridge, L., Serrano, M., Kroemer, G., 2013. The hallmarks of aging. Cell 153, 1194–1217.

Luo, X., Lee Kraus, W., 2012. On par with PARP: cellular stress signaling through poly(-ADP-ribose) and PARP-1. Genes Dev. 26, 417–432.

Ma, C., Pi, C., Yang, Y., Lin, L., Shi, Y., Li, Y., et al., 2017. Nampt expression decreases age-related senescence in rat bone marrow mesenchymal stem cells by targeting Sirt1. PLoS One 12, 1—18.

MacLean, M., Harris, N., Piper, P.W., 2001. Chronological lifespan of stationary phase yeast cells; a model for investigating the factors that might influence the ageing of postmitotic tissues in higher organisms. Yeast 18, 499—509.

Mei, S.C., Brenner, C., 2014. Quantification of protein copy number in yeast: the NAD^+ metabolome. PLoS One 9, 1—10.

Miceli, M.V., Jiang, J.C., Tiwari, A., Rodriguez-Quiñones, J.F., Jazwinski, S.M., 2012. Loss of mitochondrial membrane potential triggers the retrograde response extending yeast replicative lifespan. Front. Genet. 2, e102.

Mihalik, S.J., Goodpaster, B.H., Kelley, D.E., et al., 2010. Increased levels of plasma acylcar-nitines in obesity and type 2 diabetes and identification of a marker of glucolipotoxicity. Obesity 18, 1695—1700.

Mirisola, M.G., Taormina, G., Fabrizio, P., Wei, M., Hu, J., Longo, V.D., 2014. Serine-and threonine/valine-dependent activation of PDK and Tor orthologs converge on Sch9 to promote aging. PLoS Genet. 10, e1004113.

Mostoslavsky, R., Chua, K.F., Lombard, D.B., Pang, W.W., Fischer, M.R., Gellon, L., et al., 2006. Genomic instability and aging-like phenotype in the absence of mammalian SIRT6. Cell 124, 315—329.

Nikiforov, A., Dölle, C., Niere, M., Ziegler, M., 2011. Pathways and subcellular compart-mentation of NAD biosynthesis in human cells: from entry of extracellular precursors to mitochondrial NAD generation. J. Biol. Chem. 286, 21767—21778.

Nyström, T., 2005. Role of oxidative carbonylation in protein quality control and senescence. EMBO J. 24, 1311—1317.

Ocampo, A., Liu, J., Schroeder, E.A., Shadel, G.S., Barrientos, A., 2012. Mitochondrial res-piratory thresholds regulate yeast chronological life span and its extension by caloric restriction. Cell Metab. 16, 55—67.

Orlandi, I., Casatta, N., Vai, M., 2012. Lack of Ach1 CoA-transferase triggers apoptosis and decreases chronological lifespan in yeast. Front. Oncol. 2. Article ID: 67.

Orlandi, I., Pellegrino Coppola, D., Vai, M., 2014. Rewiring yeast acetate metabolism through MPC1 loss of function leads to mitochondrial damage and decreases chronolog-ical lifespan. Microbial. Cell 1, 393—405.

Orlandi, I., Pellegrino Coppola, D., Strippoli, M., Ronzulli, R., Vai, M., 2017a. Nicotin-amide supplementation phenocopies SIR2 inactivation by modulating carbon meta-bolism and respiration during yeast chronological aging. Mech. Ageing Dev. 161, 277—287.

Orlandi, I., Stamerra, G., Strippoli, M., Vai, M., 2017b. During yeast chronological aging resveratrol supplementation results in a short-lived phenotype Sir2-dependent. Redox Biol. 12, 745—754.

Pansarasa, O., Flati, V., Corsetti, G., Brocca, L., Pasini, E., D'Antona, G., 2008. Oral amino acid supplementation counteracts age-induced sarcopenia in elderly rats. Am. J. Cardiol. 101, 35E—41E.

Passarella, S., Atlante, A., Valenti, D., de Bari, L., 2003. The role of mitochondrial transport in energy metabolism. Mitochondrion 2, 319—343.

Petrosillo, G., Matera, M., Moro, N., Ruggiero, F.M., Paradies, G., 2009. Mitochondrial complex I dysfunction in rat heart with aging: critical role of reactive oxygen species and cardiolipin. Free Radic. Biol. Med. 46, 88—94.

Piskunova, T.S., Yurova, M.N., Ovsyannikov, A.I., Semenchenko, A.V., Zabezhinski, M.A., Popovich, I.G., et al., 2008. Deficiency in poly(ADP-ribose) poly-merase-1 (PARP-1) accelerates aging and spontaneous carcinogenesis in mice. Curr. Gerontol. Geriatr. Res. 2008. Article ID: 754190.

Porter, C., Hurren, N.M., Cotter, M.V., Bhattarai, N., Reidy, P.T., Dillon, E.L., et al., 2015. Mitochondrial respiratory capacity and coupling control decline with age in human skeletal muscle. Am. J. Physiol. Endocrinol. Metab. 309, E224–E232.

Powers 3rd, R.W., Kaeberlein, M., Caldwell, S.D., Kennedy, B.K., Fields, S., 2006. Extension of chronological life span in yeast by decreased TOR pathway signaling. Genes Dev. 20, 174–184.

Preston, C.C., Oberlin, A.S., Holmuhamedov, E.L., Gupta, A., Sagar, S., Syed, R.H.K., et al., 2008. Aging-induced alterations in gene transcripts and functional activity of mitochondrial oxidative phosphorylation complexes in the heart. Mech. Ageing Dev. 129, 304–312.

Prolla, T.A., Denu, J.M., 2014. NAD^+ deficiency in age-related mitochondrial dysfunction. Cell Metab. 19, 178–180.

Quarona, V., Zaccarello, G., Chillemi, A., Brunetti, E., Singh, V.K., Ferrero, E., et al., 2013. CD38 and CD157: a long journey from activation markers to multifunctional molecules. Cytom. Part B Clin. Cytom. 84, 207–217.

Quinlan, C.L., Orr, A.L., Perevoshchikova, I.V., Treberg, J.R., Ackrell, B.A., Brand, M.D., 2012. Mitochondrial complex II can generate reactive oxygen species at high rates in both the forward and reverse reactions. J. Biol. Chem. 287, 27255–27264.

Raha, S., Robinson, B.H., 2001. Mitochondria, oxygen free radicals, and apoptosis. Am. J. Med. Genet. Semin. Med. Genet. 106, 62–70.

Ratajczak, J., Joffraud, M., Trammell, S.A.J., Ras, R., Canela, N., Boutant, M., et al., 2016. NRK1 controls nicotinamide mononucleotide and nicotinamide riboside metabolism in mammalian cells. Nat. Commun. 7. Article ID: 13103.

Reinherz, E.L., Kung, P.C., Goldstein, G., Levey, R.H., Schlossman, S.F., 1980. Discrete stages of human intrathymic differentiation: analysis of normal thymocytes and leukemic lymphoblasts of T-cell lineage. Proc. Natl. Acad. Sci. U. S. A. 77, 1588–1592.

Reverter-Branchat, G., Cabiscol, E., Tamarit, J., Ros, J., 2004. Oxidative damage to specific proteins in replicative and chronological-aged Saccharomyces cerevisiae common targets and prevention by calorie restriction. J. Biol. Chem. 279, 31983–31989.

Revollo, J.R., Grimm, A.A., Imai, S.I., 2004. The NAD biosynthesis pathway mediated by nicotinamide phosphoribosyltransferase regulates Sir2 activity in mammalian cells. J. Biol. Chem. 279, 50754–50763.

Robinson, B.H., 1998. Human complex I deficiency: clinical spectrum and involvement of oxygen free radicals in the pathogenicity of the defect. Biochim. Biophys. Acta Bioenerg. 1364, 271–286.

Rongvaux, A., She, R.J., Mulks, M.H., Gigot, D., Urbain, J., Leo, O., Andris, F., 2002. Pre-B-cell colony-enhancing factor, whose expression is up-regulated in activated lymphocytes, is a nicotinamide phosphoribosyltransferase, a cytosolic enzyme involved in NAF biosynthesis. Eur. J. Immunol. 32, 3225–3234.

Ruetenik, A., Barrientos, A., 2015. Dietary restriction, mitochondrial function and aging: from yeast to humans. Biochim. Biophys. Acta Bioenerg. 1847, 1434–1447.

Samokhvalov, V., Ignatov, V., Kondrashova, M., 2004. Inhibition of Krebs cycle and activation of glyoxylate cycle in the course of chronological aging of Saccharomyces cerevisiae. Compensatory role of succinate oxidation. Biochimie 86, 39–46.

Sauve, A.A., 2008. NAD^+ and vitamin B_3: from metabolism to therapies. J. Pharmacol. Exp. Ther. 324, 883–893.

Scialò, F., Fernández-Ayala, D.J., Sanz, A., 2017. Role of mitochondrial reverse electron transport in ROS signaling: potential roles in health and disease. Front. Physiol. 8. Article ID: 428.

Shimomura, Y., Yamamoto, Y., Bajotto, G., Sato, J., Murakami, T., Shimomura, N., et al., 2006. Nutraceutical effects of branched-chainamino acids on skeletal muscle. J. Nutr. 136, 529S–532S.

Singh, T., Newman, A., 2011. Inflammatory markers in population studies of ageing. Ageing Res. Rev. 10, 2−22.

Son, M.J., Kwon, Y., Son, T., Cho, Y.S., 2016. Restoration of mitochondrial NAD$^+$ levels delays stem cell senescence and facilitates reprogramming of aged somatic cells. Stem Cell. 34, 2840−2851.

Stauch, K.L., Purnell, P.R., Villeneuve, L.M., Fox, H.S., 2015. Proteomic analysis and functional characterization of mouse brain mitochondria during aging reveal alterations in energy metabolism. Proteomics 15, 1574−1586.

Stefanatos, R., Sanz, A., 2011. Mitochondrial complex I: a central regulator of the aging process. Cell Cycle 10, 1528−1532.

Stein, L.R., Imai, S.I., 2012. The dynamic regulation of NAD metabolism in mitochondria. Trends Endocrinol. Metab. 23, 420−428.

Stöckl, P., Hütter, E., Zwerschke, W., Jansen-Dürr, P., 2006. Sustained inhibition of oxidative phosphorylation impairs cell proliferation and induces premature senescence in human fibroblasts. Exp. Gerontol. 41, 674−682.

Sugrue, M.M., Tatton, W.G., 2001. Mitochondrial membrane potential in aging cells. Biol. Signals Recept. 10, 176−188.

Tamarit, J., de Hoogh, A., Obis, E., Alsina, D., Cabiscol, E., Ros, J., 2012. Analysis of oxidative stress-induced protein carbonylation using fluorescent hydrazides. J. Proteomics 75, 3778−3788.

Tatarková, Z., Kuka, S., Račay, P., Lehotský, J., Dobrota, D., Mištuna, D., Kaplán, P., 2011. Effects of aging on activities of mitochondrial electron transport chain complexes and oxidative damage in rat heart. Physiol. Res. 60, 281−289.

Todisco, S., Agrimi, G., Castegna, A., Palmieri, F., 2006. Identification of the mitochondrial NAD$^+$ transporter in *Saccharomyces cerevisiae*. J. Biol. Chem. 281, 1524−1531.

Vacanti, N.M., Divakaruni, A.S., Green, C.R., Parker, S.J., Henry, R.R., Ciaraldi, T.P., et al., 2014. Regulation of substrate utilization by the mitochondrial pyruvate Carrier. Mol. Cell 56, 425−435.

Van Der Veer, E., Ho, C., O'Neil, C., Barbosa, N., Scott, R., Cregan, S.P., Pickering, J.G., 2007. Extension of human cell lifespan by nicotinamide phosphoribosyltransferase. J. Biol. Chem. 282, 10841−10845.

Verdin, E., 2015. NAD$^+$ in aging, metabolism, and neurodegeneration. Science 350, 1208−1213.

Wallace, D.C., 2009. Mitochondria, bioenergetics, and the epigenome in eukaryotic and human evolution. Cold Spring Harb. Symp. Quant. Biol. 74, 383−393.

Wang, J., Jiang, J.C., Jazwinski, S.M., 2010. Gene regulatory changes in yeast during life extension by nutrient limitation. Exp. Gerontol. 45, 621−631.

Wei, M., Fabrizio, P., Hu, J., Ge, H., Cheng, C., Li, L., Longo, V.D., 2008. Life span extension by calorie restriction depends on Rim15 and transcription factors downstream of Ras/PKA, Tor, and Sch9. PLoS Genet. 4, 0139−0149.

White, A.T., Schenk, S., 2012. NAD$^+$/NADH and skeletal muscle mitochondrial adaptations to exercise. Am. J. Physiol. Endocrinol. Metab. 303, E308−E321.

Yang, C., Ko, B., Hensley, C.T., Jiang, L., Wasti, A.T., Kim, J., et al., 2014. Glutamine oxidation maintains the TCA cycle and cell survival during impaired mitochondrial pyruvate transport. Mol. Cell 56, 414−424.

Yang, H., Lavu, S., Sinclair, D.A., 2006. Nampt/PBEF/Visfatin: a regulator of mammalian health and longevity? Exp. Gerontol. 41, 718−726.

Yang, H., Yang, T., Baur, J.A., Perez, E., Matsui, T., Carmona, J.J., Lamming, D.W.W., et al., 2007. Nutrient-sensitive mitochondrial NAD$^+$ levels dictate cell survival. Cell 130, 1095−1107.

Yarian, C.S., Toroser, D., Sohal, R.S., 2006. Aconitase is the main functional target of aging in the citric acid cycle of kidney mitochondria from mice. Mech. Ageing Dev. 127, 79−84.

Yoshino, J., Mills, K.F., Yoon, M.J., Imai, S.I., 2011. Nicotinamide mononucleotide, a key NAD$^+$ intermediate, treats the pathophysiology of diet- and age-induced diabetes in mice. Cell Metab. 14, 528−536.

Yuan, Y., Cruzat, V.F., Newshome, P., Cheng, J., Chen, Y., Lu, Y., 2016. Regulation of SIRT1 in aging: roles in mitochondrial function and biogenesis. Mech. Ageing Dev. 155, 10−21.

Chapter 5

Altered Expression of Mitochondrial NAD+ Carriers Influences Yeast Chronological Lifespan by Modulating Cytosolic and Mitochondrial Metabolism

Ivan Orlandi, Giulia Stamerra and Marina Vai.

Altered Expression of Mitochondrial NAD⁺ Carriers Influences Yeast Chronological Lifespan by Modulating Cytosolic and Mitochondrial Metabolism

Ivan Orlandi[1,2], Giulia Stamerra[2] and Marina Vai[2]*

[1] SYSBIO Centre for Systems Biology, Milan, Italy, [2] Dipartimento di Biotecnologie e Bioscienze, Università di Milano-Bicocca, Milan, Italy

Nicotinamide adenine dinucleotide (NAD⁺) represents an essential cofactor in sustaining cellular bioenergetics and maintaining cellular fitness, and has emerged as a therapeutic target to counteract aging and age-related diseases. Besides NAD⁺ involvement in multiple redox reactions, it is also required as co-substrate for the activity of Sirtuins, a family of evolutionary conserved NAD⁺-dependent deacetylases that regulate both metabolism and aging. The founding member of this family is Sir2 of *Saccharomyces cerevisiae*, a well-established model system for studying aging of post-mitotic mammalian cells. In this context, it refers to chronological aging, in which the chronological lifespan (CLS) is measured. In this paper, we investigated the effects of changes in the cellular content of NAD⁺ on CLS by altering the expression of mitochondrial NAD⁺ carriers, namely Ndt1 and Ndt2. We found that the deletion or overexpression of these carriers alters the intracellular levels of NAD⁺ with opposite outcomes on CLS. In particular, lack of both carriers decreases NAD⁺ content and extends CLS, whereas *NDT1* overexpression increases NAD⁺ content and reduces CLS. This correlates with opposite cytosolic and mitochondrial metabolic assets shown by the two types of mutants. In the former, an increase in the efficiency of oxidative phosphorylation is observed together with an enhancement of a pro-longevity anabolic metabolism toward gluconeogenesis and trehalose storage. On the contrary, *NDT1* overexpression brings about on the one hand, a decrease in the respiratory efficiency generating harmful superoxide anions, and on the other, a decrease in gluconeogenesis and trehalose stores: all this is reflected into a time-dependent loss of mitochondrial functionality during chronological aging.

Keywords: NAD⁺, chronological lifespan, Ndt1, Ndt2, *Saccharomyces cerevisiae*

INTRODUCTION

Significant progress has been made in elucidating fundamental processes such as human aging/longevity as a result of studies performed in the budding yeast *Saccharomyces cerevisiae*. In this single-celled yeast, replicative aging and chronological aging are two complementary models that are used to simulate cellular aging of mitotically active and post-mitotic mammalian cells,

125

respectively (MacLean et al., 2001; Longo and Kennedy, 2006; Longo et al., 2012). The former cell type is exemplified by fibroblasts and the latter by myocytes.

In the presence of nutrients, *S.cerevisiae* divides asymmetrically (budding) resulting in a large mother cell and a smaller daughter (bud). In this context, the replicative lifespan (RLS), namely the number of buds generated by a mother cell before senescence, indicates the reproductive potential of individual yeast cells (Steinkraus et al., 2008). The chronological lifespan (CLS), instead, refers to the rate of post-mitotic survival of a non-dividing quiescent yeast culture; viability is assessed by measuring the percentage of cells able to resume growth and form a colony after transfer from the depleted medium to the rich fresh one (Fabrizio and Longo, 2007). In a standard CLS experiment, yeast cells are grown in synthetic media with 2% glucose. When glucose becomes limiting, the diauxic shift occurs and cells shift from glucose-driven fermentation to ethanol-driven respiration. This shift determines a metabolic reprogramming, the outcomes of which influence the CLS. Afterwards cell proliferation stops and the yeast culture enters a quiescent stationary phase (Gray et al., 2004; Wanichthanarak et al., 2015). CLS is determined starting 72 h after the diauxic shift (Fabrizio and Longo, 2007).

The signaling pathways and regulators controlling RLS and CLS are evolutionary conserved (Fontana et al., 2010; Swinnen et al., 2014; Bitto et al., 2015; Baccolo et al., 2018). In particular, nicotinamide adenine dinucleotide (NAD$^+$) homeostasis has emerged as a critical element in the regulation of aging/longevity (Imai, 2010, 2016) and accumulating evidence suggests that a reduction of NAD$^+$ levels in diverse organisms contributes to the development of age-associated metabolic decline (Imai and Guarente, 2014, 2016; Verdin, 2015). Indeed, in addition to its central role in cellular metabolism participating as essential coenzyme in many redox reactions, NAD$^+$ is absolutely required as a co-substrate by Sirtuins, a family of NAD$^+$-dependent deacetylases, the founding member of which is Sir2 of *S.cerevisiae* (Houtkooper et al., 2012; Imai and Guarente, 2014). In mammals, there are seven Sirtuin isoforms (SIRT1-7) and among them SIRT1 is a key component of the systemic regulatory network called "the NAD world," a comprehensive concept that connects NAD$^+$ metabolism and aging/longevity control in mammals (Imai, 2009, 2010, 2016). The nutrient-sensing SIRT1 is the closest mammalian ortholog of Sir2 (Frye, 2000). Sir2 activity is involved in both replicative and chronological aging: in the former Sir2 extends RLS (Kaeberlein et al., 1999; Imai et al., 2000), whilst in the latter it has a pro-aging role (Fabrizio et al., 2005; Smith et al., 2007; Casatta et al., 2013; Orlandi et al., 2017a).

The other key component of the NAD world is represented by NAD$^+$ biosynthesis (Imai, 2009, 2010). From yeast to mammalian cells, NAD$^+$ synthesis occurs either *de novo* from L-tryptophan or through *salvage* pathway(s) from its precursors, namely nicotinamide riboside, nicotinic acid, and its amide form, nicotinamide (Bogan and Brenner, 2008; Canto et al., 2015). Cells mainly rely on the *salvage* pathway(s) for the correct maintenance of NAD$^+$ levels and it has been observed that the supplementation of NAD$^+$ precursors is sufficient

to attenuate several metabolic defects common to the aging process (Johnson and Imai, 2018; Mitchell et al., 2018; Rajman et al., 2018). However, NAD$^+$ levels, as well as those of its precursors, are different depending on the type of tissue and cellular compartment (Dolle et al., 2010; Houtkooper et al., 2010; Cambronne et al., 2016) and it remains unclear in which cellular compartment(s) NAD$^+$ decrease can be relevant to aging. This has increased the interest on the role, on the one hand, of inter-tissue communications (Imai, 2016) and, on the other hand, of the relative subcellular localization of NAD$^+$ and its precursors during the aging process (Koch-Nolte et al., 2011; Rajman et al., 2018).

In yeast, NAD$^+$ is synthesized in the cytosol and can be imported across the inner mitochondrial membrane by two specific mitochondrial NAD$^+$ carriers, namely Ndt1 and Ndt2, which share 70% homology (Todisco et al., 2006). The physiological effects linked to an *NDT1* and *NDT2* double deletion and to the overexpression of *NDT1*, which encodes the main isoform of the NAD$^+$ transporter (Todisco et al., 2006), have been examined on cells growing with an oxidative or respiro-fermentative metabolism in batch and glucose-limited chemostat cultures (Agrimi et al., 2011).

Here, we show that during chronological aging an altered expression of the specific mitochondrial NAD$^+$ carriers deeply influences the metabolic reprogramming that enables cells to acquire features required to maintain viability during chronological aging. In particular, lack of *NDT1* and *NDT2* extends CLS, whereas *NDT1* overexpression determines a CLS reduction. This opposite effect on CLS correlates with opposite metabolic features displayed by the two mutants.

MATERIALS AND METHODS

Yeast Strains, Growth Conditions and CLS Determination

The *ndt1Δntd2Δ* strain and the strain overexpressing *NDT1* (*NDT1*-over strain) were constructed in a previous work (Agrimi et al., 2011) and were derivatives of CEN.PK113-7D (*MAT*a, *MAL*2-8c, *SUC*2). A null mutant *ndt1Δntd2Δ* (*ndt1Δ::URA3 ntd2Δ::KlLEU2*) was generated by PCR-based methods in a W303-1A background (*MAT*a *ade2-1 his3-11,15 leu2-3,112 trp1-1 ura3-1 can1-100*). The accurancy of gene replacements was verified by PCR with flanking and internal primers. Cells were grown in batches at 30°C in minimal medium (Difco Yeast Nitrogen Base without amino acids, 6.7 g/L) with 2% w/v glucose. Auxotrophies were compensated for with supplements added in excess (Orlandi et al., 2014). Cell number and cellular volumes were determined using a Coulter Counter-Particle Count and Size Analyser (Vanoni et al., 1983). Duplication time (Td) was obtained by linear regression of the cell number increase over time on a semi-logarithmic plot. For CLS experiments, cells were grown in 2% glucose and the extracellular concentration of glucose and ethanol were measured in medium samples collected at different time-points in order to define the growth profile [exponential phase, diauxic shift (Day 0), post-diauxic phase and stationary phase of the cultures] (Orlandi et al., 2013). CLS was

126

measured according to (Fabrizio et al., 2005) by counting colony-forming units (CFU) starting with 72 h (Day 3, first age-point) after Day 0. The number of CFU on Day 3 was considered the initial survival (100%).

Isolation of Mitochondria

Mitochondria were prepared from chronologically aging cells essentially as described by Meisinger et al. (2006) with minor modifications. At each time-point, 10^9 cells were collected by centrifugation and spheroplasts were obtained by digestion with Zymolyase 20T. Then, spheroplasts were homogenized by 20 strokes using a Dounce homogenizer and mitochondria collected after differential centrifugation (Meisinger et al., 2006). Fresh crude mitochondrial pellets were used for measurements of NAD$^+$, NADH, and protein contents.

Metabolite Measurements and Enzymatic Assays

At designated time-points, aliquots of the yeast cultures were centrifuged, and both pellets (washed twice) and supernatants were collected and frozen at $-80°C$ until used. Rapid sampling for intracellular metabolite measurements was performed as previously described (Orlandi et al., 2014). The concentrations of glucose, ethanol, citrate, succinate, and malate were determined using enzymatic assays (K-HKGLU, K-ETOH, K-SUCC, K-CITR, and K-LMALR kits from Megazyme).

To measure NADH and NAD$^+$ contents, alkali, and acid extractions were performed essentially as described (Lin et al., 2001), except that before incubation of both the alkali extract and the acid one at for 30 min, an additional step was performed in order to improve cells lysis. Alkali or acid-washed glass beads were added to the two types of extracts and cells broken by vortexing (3 cycles of 1 min, interspersed with cooling on ice). NAD$^+$ and NADH concentrations were determined using the EnzyChrom^{TM} NAD$^+$/NADH assay kit (BioAssay Systems). The rate of dye formation (formazan) at 565 nm correlates with the level of pyridine nucleotides. Duplicate reactions were performed in multi-well plates or in cuvettes. Different amounts of each sample were used in cycling reactions to obtain values within the linear portion of a standard curve that was prepared every time.

Immediately after preparation of cell-free extracts (Orlandi et al., 2014), the activities of cytosolic and mitochondrial aldehyde dehydrogenase (Ald) were assayed according to Aranda and del Olmo (2003), of phosphoenolpyruvate carboxykinase (Pck1) and isocitrate lyase (Icl1) as described in de Jong-Gubbels et al. (1995). Total protein concentration was estimated using the BCA^{TM} Protein Assay Kit (Pierce).

Fluorescence Microscopy

Dihydroethidium (DHE, Sigma-Aldrich) staining was performed as reported in Madeo et al. (1999) to detect superoxide anion (O_2^-). A Nikon Eclipse E600 fluorescence microscope equipped with a Nikon Digital Sight DS Qi1 camera was used. Digital images were acquired and processed using Nikon software NIS-Elements.

Estimation of Oxygen Consumption Rates and Index of Respiratory Competence

The basal oxygen consumption of intact cells was measured at 30°C using a "Clark-type" oxygen electrode (Oxygraph System, Hansatech Instruments, Nortfolk, UK) as reported (Orlandi et al., 2013). The non-phosphorylating respiration and the maximal/uncoupled respiratory capacity were measured in the presence of 37.5 mM triethyltin bromide (TET, Sigma-Aldrich) and 10 μM of the uncoupler carbonyl cyanide 3-chlorophenylhydrazone (CCCP, Sigma-Aldrich), respectively (Orlandi et al., 2017a). The addition of 2 M antimycin A (Sigma-Aldrich) accounted for non-mitochondrial oxygen consumption. Respiratory rates for the basal oxygen consumption (J_R), the maximal/uncoupled oxygen consumption (J_{MAX}) and the non-phosphorylating oxygen consumption (J_{TET}) were determined from the slope of a plot of O_2 concentration against time, divided by the cellular concentration.

Index of respiratory competence (IRC) was measured according to Parrella and Longo (2008) by plating identical cell samples on YEP (1% w/v yeast extract, 2% w/v bacto peptone)/2% glucose (YEPD) plates and on rich medium/3% glycerol (YEPG) plates. IRC was calculated as colonies on YEPG divided by colonies on YEPD times 100%.

Statistical Analysis of Data

All values are presented as the mean of three independent experiments ± Standard Deviation (SD). Three technical replicates were analyzed in each independent experiment. Statistical significance was assessed by one-way ANOVA test. The level of statistical significance was set at a P value of ≤ 0.05.

RESULTS AND DISCUSSION

Altered Expression of the Specific Mitochondrial NAD$^+$ Carriers Affects CLS

Due to the importance of NAD$^+$ homeostasis in the aging process from yeast to humans (Baccolo et al., 2018; Rajman et al., 2018; Yaku et al., 2018), we wished to test whether changes in the cellular content of this dinucleotide would cause any effects on CLS. To this end we chose to use the $ndt1\Delta ndt2\Delta$ and $NDT1$-over mutant strains: the former lacking the two mitochondrial NAD$^+$ carriers, Ndt1 and Ndt2, identified so far and the latter overexpressing Ndt1, which is the main isoform of the carrier (Todisco et al., 2006; Agrimi et al., 2011). These strains have been previously characterized as far as NAD content is concerned (Agrimi et al., 2011). In particular, under a fully respiratory metabolism such as growth on ethanol, Ndt1 overexpression determined an increase in cellular and mitochondrial NAD$^+$ levels without affecting growth. On the contrary, on ethanol the $ndt1\Delta ndt2\Delta$ mutant displayed a lower cellular and mitochondrial NAD$^+$ content and a decrease in the growth rate (Agrimi et al., 2011). Here, an $ndt1\Delta ndt2\Delta$ double mutant generated in the W303-1A background was also included. Indeed, the W303-1A strain is commonly used in chronological aging research due to its robust respiratory capacity (Ocampo et al., 2012).

127

FIGURE 1 | The *NDT1*-over mutant and the *ndt1Δndt2Δ* one have a short-lived and a long-lived phenotype, respectively. The indicated strains were grown in minimal medium/2% glucose and the required supplements in excess (see section Materials and Methods) and followed up to stationary phase. **(A,B)** CLS was determined by assessing clonogenicity on YEPD plates. 72 h after the diauxic shift (Day 3) was considered the first age-point (100% survival). Day 0, diauxic shift. In parallel, intracellular NAD$^+$ **(C)**, NADH **(D)** and extracellular ethanol **(E,F)** concentrations were determined at the indicated time-points. Exp, exponential growth phase. All data refer to mean values of three independent experiments with three technical replicates each. Standard deviation (SD) is indicated. Statistical significance as assessed by one-way ANOVA test is indicated (*$P \leq 0.05$ and **$P \leq 0.01$).

Initially, in the context of a standard CLS experiment (Fabrizio and Longo, 2007), we measured CLS and NAD content. As shown in **Figure 1A**, Ndt1 overexpression significantly reduced CLS, whilst the strain devoid of the two mitochondrial NAD$^+$ carriers lived longer than the prototrophic wild type (wt) CEN.PK 113-7D. The same long-lived phenotype was observed in the auxotrophic background W303-1A (**Figure 1B**) indicating that the different composition of amino acids in the medium does not influence the results. Measurements of intracellular

NAD$^+$ and NADH contents indicated that in the wt, they decreased progressively after the diauxic shift (**Figures 1C,D**). We calculated values of NAD$^+$ and NADH estimating cell size with a Coulter Counter-Particle Count and Size Analyser: cell size that changes according to the yeast strain and the growth phase of the cell cycle. If we assume a yeast cell size of 70 μm^3 (Sherman, 2002) our measurements of 595 μM NAD$^+$ (**Figure 1C**) and 215 μM NADH for CEN.PK 113-7D in exponential phase (**Figure 1D**) correspond to 1.42 mM NAD$^+$

128

FIGURE 2 | Altered expression of mitochondrial NAD⁺ carriers influences Ald enzymatic activities. In the context of CLS experiments of **Figure 1**, total Ald **(A)**, Ald4/5 **(B)**, and Ald6 **(C)** enzymatic activities were measured at the indicated time-points. Day 0, diauxic shift. All data are the mean ± SD obtained from three independent experiments with three technical replicates each. Statistical significance as in **Figure 1** (**$P \leq 0.01$).

and 0.82 mM NADH, in reasonable agreement with values of previous reports (Lin et al., 2004). In the context of the CLS experimental set-up, as the diauxic shift occurs and cells utilize the excreted fermentation by-product, ethanol, in the $ndt1\Delta ndt2\Delta$ mutant, and in the $NDT1$-over one NAD⁺ and NADH levels decreased, but both remained constantly lower in the $ndt1\Delta ndt2\Delta$ mutant and higher in the $NDT1$-over mutant than those measured in the wt (**Figures 1C,D**). This opposite trend of the dinucleotide contents observed in the two different types of mutants is in line with that detected during exponential growth on ethanol (Agrimi et al., 2011).

It is well known that NAD⁺ is an essential coenzyme for oxidoreductases of both cytosolic and mitochondrial redox reactions, many of which are involved in the metabolic remodeling that takes place at the diauxic shift. Indeed, at the diauxic shift carbon metabolism shifts from fermentation to mitochondrial respiration and gluconeogenesis allowing cells to be better primed for survival during chronological aging. Thus, we analyzed the metabolic features of the short-lived $NDT1$-over strain and those of the long-lived $ndt1\Delta ndt2\Delta$ one. Since the respiration-based metabolism is due to the utilization of ethanol, we initially measured the consumption of this C2
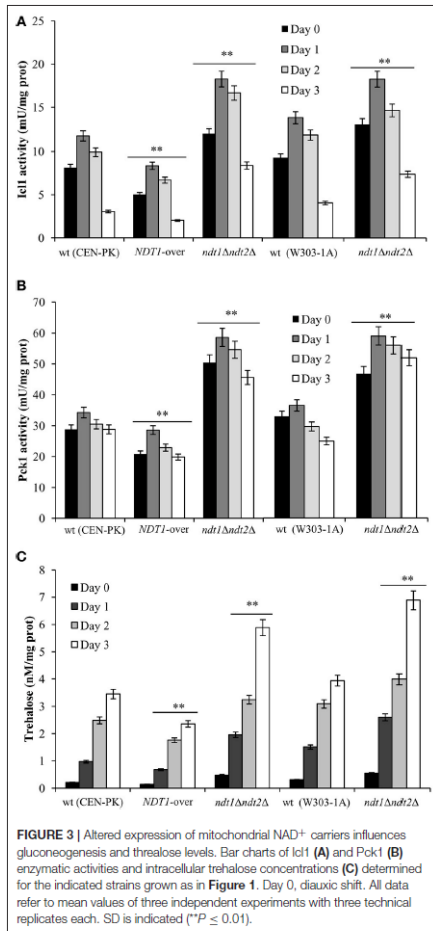
129

TABLE 1 | Effects of altered expression of mitochondrial NAD$^+$ carriers on the enzymatic activity of Ald isoforms.

|	Day 0	Day 1	Day 2	Day 3
wt (CEN-PK 113-7D)				
Total Ald	227.8 ± 8.7	202.2 ± 3.9	188.3 ± 4.1	170.8 ± 6.9
% Ald6	57	59	58	59
% Ald4/5	43	41	42	41
***NDT1*-OVER**				
Total Ald	231.3 ± 4.2	203.6 ± 6.5	182.1 ± 2.7	176.2 ± 1.4
% Ald6	32**	33**	30**	29**
% Ald4/5	68**	67**	70**	71**
ndt1Δndt2Δ				
Total Ald	190.4** ± 5.6	171.6** ± 7.2	159.5** ± 4.3	155.6** ± 8.1
% Ald6	78**	79**	81**	77**
% Ald4/5	22**	21**	19**	23**
wt (W303-1A)				
Total Ald	202.9 ± 6.4	185.6 ± 3.8	172.4 ± 7.6	156.2 ± 4.7
% Ald6	59	61	55	63
% Ald4/5	41	39	45	37
ndt1Δndt2Δ				
Total Ald	174.3** ± 2.9	157.8** ± 8.3	146.1** ± 6.1	128.9** ± 7.7
% Ald6	83**	78**	84**	79**
% Ald4/5	17**	22**	16**	21**

For each time-point total Ald, Ald6, and Ald4/5 enzymatic activities were determined as in **Figure 2** and the percentage of the different Ald isoforms was calculated. Day 0, diauxic shift. Data refer to mean values determined in three independent experiments with three technical replicates each. SD is indicated. Values obtained for wt strains were used as reference for comparisons with NDT1-over and ndt1Δ ndt2Δ cells. (**P ≤ 0.01, one-way ANOVA test).

compound. At the diauxic shift (Day 0), the maximal amount of the extracellular ethanol was not affected either by the lack of Ndt1 and Ndt2 or by the Ndt1 overexpression (**Figures 1E,F**). Differently, during the post-diauxic phase in the *ndt1Δndt2Δ* mutant ethanol decreased more slowly (**Figures 1C,D**). This is indicative of an impairment in ethanol utilization in line with the slow growth rate on medium containing ethanol as carbon source (Agrimi et al., 2011). Consequently, starting from Day 0, we determined the enzymatic activities of the acetaldehyde dehydrogenases (Alds). These enzymes are implicated in the ethanol utilization: they oxidize the acetaldehyde generated from ethanol oxidation producing acetate, which is subsequently converted to acetyl-CoA. In addition, Alds require NAD$^+$ or NADP$^+$. No difference was detected between the wt and the *NDT1*-over strain in the total Ald activity levels (**Figure 2A**). On the contrary, in the *ndt1Δndt2Δ* strain a significant decrease was observed (**Figure 2A**) consistent with the reduced ethanol utilization. Notably, interesting results were obtained by measuring the different isoforms of Alds, namely the mitochondrial Ald4/5, and the primary cytosolic counterpart Ald6 (Saint-Prix et al., 2004). Indeed, the activity levels of Ald4/5 were higher and those of Ald6 lower in the *NDT1*-over strain compared with the wt ones, whilst in the *ndt1Δndt2Δ* strain the Ald6 activity prevailed (**Figures 2B,C**). Since, alterations of mitochondrial NAD$^+$ transport are accompanied by a different prevalent subcellular localization of Ald enzymatic activities (**Table 1**), it is reasonable to speculate that in the two different

mutants the metabolic pathways that are fed by mitochondrial or cytosolic acetate/acetyl-CoA could be affected. In this context, we initially measured the enzymatic activity of one of the unique enzymes of the glyoxylate shunt, such as isocitrate lyase (Icl1), and that of phosphoenolpyruvate carboxykinase (Pck1), which catalyzes the rate-limiting step in gluconeogenesis. Indeed, starting from the diauxic shift, the glyoxylate shunt becomes operative. It is an anaplerotic device of the TCA cycle, is fed by the cytosolic acetyl-CoA and is the sole possible provider for the Pck1 substrate, namely oxaloacetate (Lee et al., 2011). In the *NDT1*-over strain a decrease in the enzymatic activities of Icl1 and Pck1 was observed, whilst in the *ndt1Δndt2Δ* mutant both activities strongly increased (**Figures 3A,B**). Since glucose-6-phosphate produced by gluconeogenesis is used for the synthesis of threalose during the post-diauxic phase, we also examined the accumulation of this disaccharide, the intracellular stores of which are advantageous for survival during chronological aging (Shi et al., 2010). In the *NDT1*-over strain a reduction in trehalose levels took place (**Figure 3C**), consistent with the decrease of the Pck1 activity. On the contrary, the *ndt1Δndt2Δ* cells accumulated more trehalose (**Figure 3C**), consistent with the increase of the Pck1 activity. Taken together, these results indicate that the lack of the two mitochondrial NAD$^+$ carriers elicits an enhancement along the cytosolic Ald6/glyoxylate/gluconeogenesis axis, whereas Ndt1 overexpression elicits a down-regulation.

130

FIGURE 3 | Altered expression of mitochondrial NAD⁺ carriers influences gluconeogenesis and threalose levels. Bar charts of Icl1 (A) and Pck1 (B) enzymatic activities and intracellular trehalose concentrations (C) determined for the indicated strains grown as in **Figure 1**. Day 0, diauxic shift. All data refer to mean values of three independent experiments with three technical replicates each. SD is indicated (**$P \leq 0.01$).

FIGURE 4 | The ndt1Δndt2Δ mutant displays decreased levels of TCA intermediates. The indicated strains were grown as in **Figure 1** and intracellular concentrations of citrate (A), succinate (B) and malate (C) were measured. Day 0, diauxic shift. Bar charts show the mean values determined in three independent experiments with three technical replicates each. SD is indicated (**$P \leq 0.01$).

Following on, since the TCA cycle is fed by the mitochondrial acetyl-CoA, we assessed the levels of some of its intermediates, such as citrate, malate, and succinate. Starting from the diauxic shift, the levels of these C4 dicarboxylic acids in the *NDT1*-over strain mirrored those measured in the wt (**Figure 4**). On the contrary, in the *ndt1Δndt2Δ* mutant all these metabolites significantly decreased (**Figure 4**) suggesting an impairment in the TCA cycle.

131
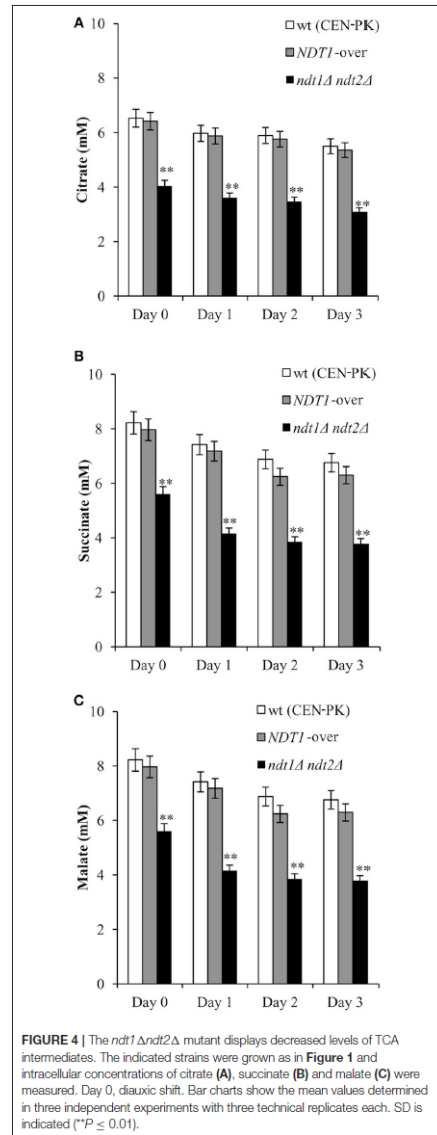
The *ndt1Δndt2Δ* Mutant Preserves Functional Mitochondria During Chronological Aging
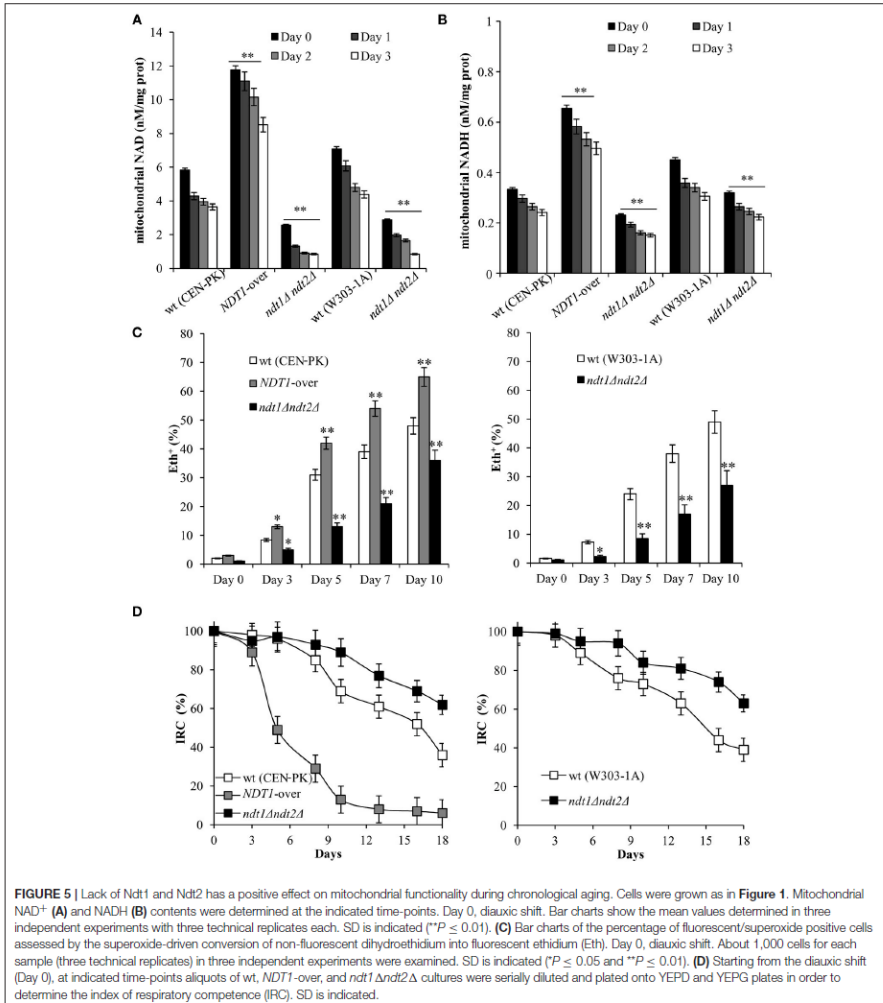
Considering that during respiration the TCA cycle provides the electron transport chain (ETC) with reducing equivalents through redox reactions and that respiration affects the CLS (Bonawitz et al., 2006; Ocampo et al., 2012; Baccolo et al., 2018), we measured next the respiratory activity in the *NDT1*-over and *ndt1Δndt2Δ* strains. During the exponential phase, the respiratory parameters for the *NDT1*-over and *ndt1Δndt2Δ* strains were very similar to those of the wt (**Table 2**) in good agreement with (Agrimi et al., 2011). Differences were observed starting from the diauxic shift (respiratory metabolism). Indeed, in the double deleted mutant, basal oxygen consumption (J_R) was lower than the wt one (**Table 2**). This can be ascribed to a depletion/limitation of reducing equivalents since in the presence of the uncoupler CCCP, which dissipates the proton gradient across the mitochondrial membrane, the maximal oxygen consumption rate (J_{MAX}) of the *ndt1Δndt2Δ* cells was always lower than that of the wt (**Table 2**). Interestingly, the *ndt1Δndt2Δ* cells displayed a non-phosphorylating respiration (J_{TET}) strongly reduced compared with that of the wt, the levels of which increased as a function of time in culture (**Table 2**) as expected (Orlandi et al., 2017a,b). As a consequence, in the double deleted mutant the net respiration, which estimates the coupled respiration, was close to the wt one (**Table 2**) indicating that, despite a reduced J_R, during the post-diauxic phase the *ndt1Δndt2Δ* strain has a better coupling between electron transport and ATP synthesis. On the contrary, the *NDT1*-over strain had a J_R similar to the wt one and a J_{MAX} higher (**Table 2**). Nevertheless, in this strain the net respiration was lower due to a J_{TET} significantly higher than that of the wt (**Table 2**) indicative of an increase of uncoupled respiration. These differences in both the level and in the state of the respiration of the two mutants were accompanied by differences in mitochondrial NAD+ and NADH contents: in the *ndt1Δndt2Δ* mutant and in the *NDT1*-over one a decrease and an increase of NAD+ and NADH contents, respectively, were observed compared with those of the wt (**Figures 5A,B**). This opposite trend in the mitochondrial dinucleotide contents, as well as the different respiratory efficiency, of the two types of mutants are in line with those detected during exponential growth on ethanol (Agrimi et al., 2011).

To the best of our knowledge, Ndt1 and Ndt2 are the only mitochondrial NAD+ carriers described so far in *S.cerevisiae* (Todisco et al., 2006) and their transport activity for NAD+ is also consistent with the cellular localization of the enzymes involved in NAD+ biosynthesis, which are outside the mitochondria, and with the lack of NAD+ -synthesizing enzymes in the yeast mitochondria (Kato and Lin, 2014). However, since in the mitochondria of the *ndt1Δndt2Δ* mutant, NAD+ is present, albeit at low levels, it cannot be excluded that this dinucleotide can be imported in the mitochondria with lower efficiency by other carrier systems. Indeed, many mitochondrial transporters often exhibit some overlapping of the transported substrates

TABLE 2 | Respiratory parameters determined for *NDT1*-over and *ndt1Δ ndt2Δ* strains.

Genetic Background	Strain	J_R					J_{MAX}				
		Exp	Day 0	Day 1	Day 2	Day 3	Exp	Day 0	Day 1	Day 2	Day 3
CEN-PK 113-7D	wt	7.12 ± 0.29	11.23 ± 0.29	14.24 ± 0.32	10.63 ± 0.16	7.59 ± 0.12	17.32 ± 0.29	21.76 ± 0.59	27.65 ± 0.13	25.11 ± 0.26	21.31 ± 0.31
	NDT1-over	7.28 ± 0.31	11.98 ± 0.17	13.88 ± 0.32	10.25 ± 0.24	7.38 ± 0.17	17.48 ± 0.21	26.29** ± 0.19	30.15** ± 0.37	28.26** ± 0.25	23.67** ± 0.31
	ndt1Δndt2Δ	7.09 ± 0.22	9.66** ± 0.41	10.77** ± 0.27	8.52** ± 0.17	6.53** ± 0.26	16.76 ± 0.16	18.12** ± 013	21.35** ± 013	19.57** ± 0.14	17.73** ± 0.09
W303-1A	wt	7.76 ± 0.07	9.47 ± 0.13	14.41 ± 0.25	11.69 ± 0.15	7.52 ± 0.21	16.23 ± 0.37	19.97 ± 0.27	26.33 ± 0.26	25.41 ± 0.17	24.28 ± 0.24
	ndt1Δndt2Δ	7.55 ± 0.35	8.42** ± 0.17	11.83** ± 0.28	9.64** ± 0.36	6.38** ± 0.24	15.97 ± 0.25	17.34* ± 0.27	20.13** ± 0.19	18.99** ± 0.31	16.54** ± 0.26

Genetic Background	Strain	J_{TET}					net_R				
		Exp	Day 0	Day 1	Day 2	Day 3	Exp	Day 0	Day 1	Day 2	Day 3
CEN-PK 113-7D	wt	1.43 ± 0.41	2.13 ± 0.19	2.80 ± 0.45	3.30 ± 0.29	3.89 ± 0.19	5.32 ± 0.27	9.12 ± 0.16	11.44 ± 0.26	7.26 ± 0.16	3.69 ± 0.23
	NDT1-over	1.72 ± 0.09	3.47** ± 0.26	3.97** ± 0.27	4.22** ± 0.37	5.58** ± 0.33	5.55 ± 0.09	8.51 ± 0.17	9.91 ± 0.32	5.93** ± 0.24	1.82** ± 0.17
	ndt1Δndt2Δ	1.24 ± 0.38	1.31** ± 0.12	1.43** ± 0.38	1.51** ± 0.18	1.84** ± 0.26	5.61 ± 0.13	8.35 ± 026	9.37 ± 0.16	7.12 ± 0.17	4.73** ± 0.26
W303-1A	wt	1.24 ± 0.38	1.58 ± 0.38	3.23 ± 0.44	3.55 ± 0.22	3.98 ± 0.19	6.52 ± 0.23	7.87 ± 0.26	11.18 ± 0.11	8.14 ± 0.31	3.54 ± 0.13
	ndt1Δndt2Δ	1.04 ± 0.26	1.18** ± 0.09	1.27** ± 0.32	1.46** ± 0.29	1.59** ± 0.27	6.14 ± 0.19	7.23 ± 0.08	10.59* ± 0.14	8.06 ± 0.23	4.53* ± 0.21

Oxygen consumption rates (J) are expressed as pmol/10^6 cells/s. Basal respiration rate (J_R), uncoupled respiration rate (J_{MAX}), non-phosphorylating respiration (J_{TET}), and net respiration ($net_R = J_R - J_{TET}$). Substrates and inhibitors used in the measurements of the respiratory parameters are detailed in the text. Exp, exponential growth phase; Day 0, diauxic shift. Data refer to mean values determined in three independent experiments with three technical replicates each. SD is indicated. Values obtained for wt were used as reference for comparisons with NDT1-over and ndt1Δndt2Δ cells. *P ≤ 0.05 and **P ≤ 0.01, one-way ANOVA test). Mean values are provided in bold.

132

FIGURE 5 | Lack of Ndt1 and Ndt2 has a positive effect on mitochondrial functionality during chronological aging. Cells were grown as in Figure 1. Mitochondrial NAD$^+$ (A) and NADH (B) contents were determined at the indicated time-points. Day 0, diauxic shift. Bar charts show the mean values determined in three independent experiments with three technical replicates each. SD is indicated (**$P \leq 0.01$). (C) Bar charts of the percentage of fluorescent/superoxide positive cells assessed by the superoxide-driven conversion of non-fluorescent dihydroethidium into fluorescent ethidium (Eth). Day 0, diauxic shift. About 1,000 cells for each sample (three technical replicates) in three independent experiments were examined. SD is indicated (*$P \leq 0.05$ and **$P \leq 0.01$). (D) Starting from the diauxic shift (Day 0), at indicated time-points aliquots of wt, NDT1-over, and ndt1Δndt2Δ cultures were serially diluted and plated onto YEPD and YEPG plates in order to determine the index of respiratory competence (IRC). SD is indicated.

(Palmieri et al., 2006). In addition, other systems contribute to the homeostasis of the intramitochondrial NAD pool, as well as to balance dinucleotide pools between mitochondria and cytosol/nucleus. They include, among others, two NADH dehydrogenases (Nde1 and Nde2) distributed on the external surface of the inner mitochondrial membrane and the glycerol-3-phosphate shuttle (Bakker et al., 2001). Nde1 and Nde2 directly catalyze the transfer of electrons from cytosolic NADH
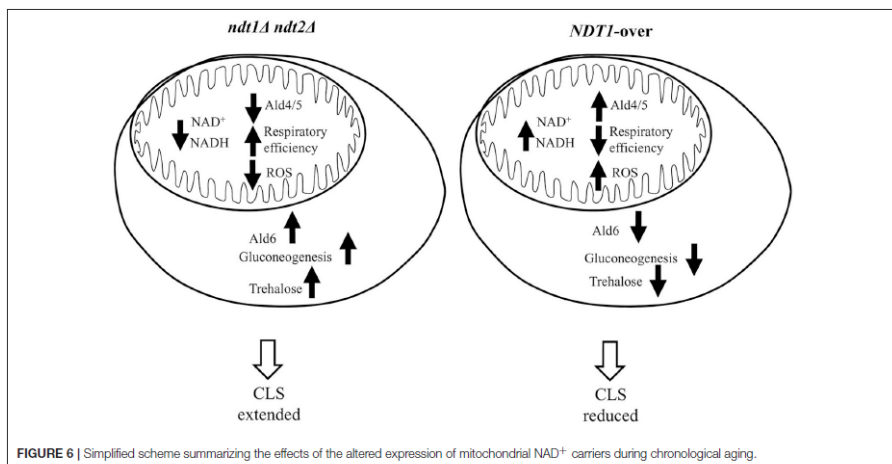
133

to ubiquinone without the translocation of protons across the membrane. In such a way, the ETC is supplied with electrons (Baccolo et al., 2018). The expression of NDE1 and NDE2 is induced after the diauxic shift (Bakker et al., 2001). With regard to the glycerol-3-phosphate shuttle, it is a system of crucial importance under conditions where the availability of energy is limited (Rigoulet et al., 2004). In the glycerol-3-phosphate shuttle, cytosolic glycerol-3-phosphate dehydrogenase oxidizes cytosolic NADH catalyzing the reduction of dihydroxyacetone phosphate to glycerol-3-phosphate. Subsequently, into the mitochondrial matrix, glycerol-3-phosphate delivers its electrons to ubiquinone via the FAD-dependent glycerol-3-phosphate dehydrogenase, Gut2 (Bakker et al., 2001). The result is a stepwise transfer of electrons from the cytosol to the respiratory chain. Consequently, despite the low mitochondrial dinucleotide contents, the ndt1Δndt2Δ mutant might feed the oxidative phosphorylation with the NADH produced in the cytosol.

Afterward, given the differences in the state of respiration, we decided to analyze the content of superoxide anion (O_2^-), which is the primary mitochondrial reactive oxygen species (ROS) produced by electron leakage from the respiratory chain. It is known that O_2^-/ROS accumulation limits the long-term survival of yeast cells during CLS (Pan, 2011; Breitenbach et al., 2014; Baccolo et al., 2018). In the ndt1Δndt2Δ chronologically cells and in the NDT1-over ones, a strong decrease and increase in O_2^- content was observed, respectively, compared to that of the wt (**Figure 5C**) consistent with non-phosphorylating respiration data (**Table 2**). Indeed, it is a state of non-phosphorylating respiration prone to generate O_2^- (Hlavata et al., 2003; Guerrero-Castillo et al., 2011). In addition, we analyzed the mitochondrial functionality by measuring the IRC, which defines the percentage of viable cells competent to respire (Parrella and Longo, 2008). Starting from the diauxic shift where all the strains were respiration-competent, a different trend of the IRC was observed for the ndt1Δndt2Δ strain and in the NDT1-over one. In the former, a lower decrease in the mitochondrial functionality was detected and at Day 18 the IRC was still about 60% against about 40% in the wt (**Figure 5D**). In the NDT1-over chronologically aging cells, a dramatic time-dependent loss of mitochondrial functionality was observed reaching at Day 18 values close to zero (**Figure 5D**). This is in line with the increased O_2^- formation because it is known that ROS levels influence mitochondrial fitness and mitochondrial dysfunctions, in turn, lead to a higher propensity to produce ROS (Breitenbach et al., 2014).

Thus, taken together all the results clearly indicate that, in the context of a standard CLS experiment, alterations in the expression of the specific mitochondrial NAD$^+$ carriers determined by NDT1 and NDT2 double deletion and NDT1 overexpression deeply influence the metabolism with opposite outcomes on chronological longevity (**Figure 6**). We found that the former extends CLS, whereas the latter shortens it. This is a direct consequence, on the one hand, of the participation of NAD$^+$ together with its reduced counterpart, NADH, in a wide range of metabolic reactions modulating the activity of compartment-specific pathways among which

the TCA cycle and the ETC in the mitochondria and the glycolysis/gluconeogenesis in the cytosol. On the other hand, the CLS is regulated by signaling pathways that coordinate the metabolic reprogramming required to ensure longevity (Breitenbach et al., 2014; Zhang and Cao, 2017). On the whole, in the ndt1Δndt2Δ chronologically aging cells and in the NDT1-over ones an opposite metabolic remodeling is observed, involving both cytosolic (gluconeogenesis), and mitochondrial (TCA and respiration) metabolic pathways (**Figure 6**), which are operative during chronological aging. Lack of the mitochondrial NAD$^+$ carriers results in a reduced oxygen consumption that does not depend upon dysfunctional mitochondria but most likely upon a decreased amount of reducing equivalents provided by a TCA cycle, the activity of which is reduced. Nevertheless, this mutant maintains a net respiration close to that of the wt indicating that in the mutant the respiration, albeit reduced, is more efficient. This confirms previous data on ndt1Δndt2Δ cells exponentially growing on ethanol that show a better coupling of respiration and phosphorylation (Agrimi et al., 2011). Such a state of more coupled respiration is less prone to generate hazardous O_2^- decreasing the risk of inducing oxidative stress and its detrimental effects on cell survival of non-dividing cells during chronological aging: in agreement with this, ndt1Δndt2Δ cells are long-lived. In agreement with a short-lived phenotype accompanied by O_2^- accumulation and severe mitochondrial damage, NDT1-over chronologically aging cells display an enhanced uncoupled respiration and a lower respiratory efficiency. As in the case of the ndt1Δndt2Δ cells, changes in the state of respiration have been already observed in NDT1-over cells exponentially growing on ethanol (Agrimi et al., 2011). In this context of fully respiratory metabolism, the NDT1 overexpression determines a decrease in the respiratory efficiency similar to that described here when cells have exhausted glucose and shift to ethanol-driven respiration. These results further underline how the mitochondrial NAD$^+$ carriers and, consequently, the availability of mitochondrial NAD$^+$, and/or NADH is important to achieve an efficient respiration and how this aspect can influence the CLS.

Concerning gluconeogenesis, the enzymatic activity of Pck1 is generally considered the main flux-controlling step in the pathway. The gluconeogenic activity of this enzyme depends on its de/acetylation state (Lin et al., 2009; Casatta et al., 2013). Indeed, an increase in the enzymatic activity of Pck1 correlates with an increase in its acetylated active form promoting gluconeogenesis and CLS (Lin et al., 2009; Casatta et al., 2013; Orlandi et al., 2017a,b). The enzyme responsible for Pck1 deacetylation (inactive form) is the NAD$^+$-dependent deacetylase Sir2 (Lin et al., 2009). During chronological aging, lack of Sir2 correlates with an increase of the acetylated Pck1 and with a carbohydrate metabolism shift toward glyoxylate-requiring gluconeogenesis increasing CLS (Casatta et al., 2013; Orlandi et al., 2017a,b). It is conceivable that, as the deacetylase activity of Sir2 relies on NAD$^+$, the low level of this dinucleotide in the ndt1Δndt2Δ mutant might decrease Sir2-mediated deacetylation of Pck1 and consequently increase gluconeogenesis and CLS. Differently, in the NDT1-over mutant, a different

134

FIGURE 6 | Simplified scheme summarizing the effects of the altered expression of mitochondrial NAD$^+$ carriers during chronological aging.

availability of NAD$^+$ might favor Sir2 enzymatic activity leading to an increase of the deacetylated inactive form of Pck1 and to the observed decrease of gluconeogenesis and CLS.

Furthermore, in the *ndt1Δndt2Δ* mutant and the *NDT1*-over one, other metabolic traits that result from an enhancement and a down-regulation, respectively, of the cytosolic Ald6/glyoxylate/gluconeogenesis axis fit-well with their CLS. Indeed, Ald6 activity requires NADP$^+$ providing NADPH, which is also provided by the pentose phosphate pathway fueled by the gluconeogenesis with glucose-6 phosphate. NADPH is a source of reducing energy and an essential cofactor for glutathione/thioredoxin-dependent enzymes that are essential for protecting cells from oxidative stress (Pollak et al., 2007). Thus, NADPH availability can contribute to influence the physiological state of the cells and consequently their survival. In this context, the *ndt1Δndt2Δ* mutant might be further favored by an enhanced gluconeogenic activity that leading also to increased intracellular trehalose stores, ensures viability during chronological aging. On the contrary the down-regulation of the Ald6/glyoxylate/gluconeogenesis axis observed in the *NDT1*-over mutant decreasing cellular protection systems, might contribute to affect negatively the CLS.

To date, substantial number of evidence points out that lowering NAD$^+$ levels can decrease Sirtuin activities and affect the aging process both in *S.cerevisiae* and mammalian cells (Imai and Guarente, 2016). In particular, in yeast lack of the nicotinic acid phosphoribosyltransferase, Npt1, which in the salvage pathway generates NAD$^+$ from nicotinic acid (NA), reduces NAD$^+$ content. This is accompanied by loss of silencing and decrease in RLS (Smith et al., 2000), as NAD$^+$ levels are not sufficient for Sir2 to function (Ondracek et al., 2017). Addition of nicotinamide riboside (an NAD$^+$ precursor) corrects the deficit in NAD$^+$ content of the *npt1Δ* mutant, promotes Sir2-dependent silencing and extends RLS (Belenky et al., 2007). Furthermore, yeast cells grown in media lacking NA has a short RLS and low NAD$^+$ levels; supplementation of isonicotinamide extends RLS in a Sir2-dependent manner by restoring NAD$^+$ content and alleviating the nicotinamide (NAM) inhibition on Sir2 (McClure et al., 2012). Indeed, NAM is an NAD$^+$ precursor that is also an endogenous non-competitive inhibitor of Sir2 (Sauve et al., 2005). Yeast cells grown in the presence of NAM have the same phenotype of *sir2Δ* ones such as silencing defects and a short RLS (Sauve et al., 2005). In the context of chronological aging, NAM supplementation at the diauxic shift results in a phenocopy of chronologically aging *sir2Δ* cells: due to the inhibition of Sir2, Pck1 enzymatic activity, and gluconeogenesis are promoted and CLS is extended (Orlandi et al., 2017a). On the opposite, resveratrol, a Sirtuin activating compound, restricts CLS by enhancing Sir2 activity, in particular Sir2-mediated deacetylation of Pck1, and consequently gluconeogenesis is decreased (Orlandi et al., 2017b).

In conclusion, taken together all our results show that affecting the cellular distribution and the content of NAD$^+$ has a deep impact on both metabolism and chronological aging and that a critical functional role is played by the Sir2 activity. In addition, our data indicate that in order to elucidate the intimate interplay between NAD$^+$, Sirtuins and aging, it will be important to determine how NAD$^+$ levels change in different compartments during aging and the tissue-specific regulation of NAD metabolism and Sirtuin activity.

135

AUTHOR CONTRIBUTIONS

MV conceived the project. MV and IO designed the experiments. IO and GS performed the experiments. MV wrote the manuscript. All authors have read and approved the final version of the manuscript.

ACKNOWLEDGMENTS

REFERENCES

Agrimi, G., Brambilla, L., Frascotti, G., Pisano, I., Porro, D., Vai, M., et al. (2011). Deletion or overexpression of mitochondrial NAD$^+$ carriers in *Saccharomyces cerevisiae* alters cellular NAD and ATP contents and affects mitochondrial metabolism and the rate of glycolysis. *Appl. Environ. Microbiol.* 77, 2239–2246. doi: 10.1128/AEM.01703-10

Aranda, A., and del Olmo, M. (2003). Response to acetaldehyde stress in the yeast *Saccharomyces cerevisiae* involves a strain-dependent regulation of several *ALD* genes and is mediated by the general stress response pathway. *Yeast* 20, 747–759. doi: 10.1002/yea.991

Baccolo, G., Stamerra, G., Pellegrino Coppola, D., Orlandi, I., and Vai, M. (2018). Mitochondrial metabolism and aging in yeast. *Int. Rev. Cell Mol. Biol.* 340, 1–33. doi: 10.1016/bs.ircmb.2018.05.001

Bakker, B. M., Overkamp, K. M., van Maris, A. J., Kotter, P., Luttik, M. A., van Dijken, J. P., et al. (2001). Stoichiometry and compartmentation of NADH metabolism in *Saccharomyces cerevisiae*. *FEMS Microbiol. Rev.* 25, 15–37. doi: 10.1111/j.1574-6976.2001.tb00570.x

Belenky, P., Racette, F. G., Bogan, K. L., McClure, J. M., Smith, J. S., and Brenner, C. (2007). Nicotinamide riboside promotes Sir2 silencing and extends lifespan via Nrk and Urh1/Pnp1/Meu1 pathways to NAD$^+$. *Cell* 129, 473–484. doi: 10.1016/j.cell.2007.03.024

Bitto, A., Wang, A., Bennett, C., and Kaeberlein, M. (2015). Biochemical genetic pathways that modulate aging in multiple species. *Cold Spring Harb. Perspect. Med.* 5:a025114. doi: 10.1101/cshperspect.a025114

Bogan, K. L., and Brenner, C. (2008). Nicotinic acid, nicotinamide, and nicotinamide riboside: a molecular evaluation of NAD$^+$ precursor vitamins in human nutrition. *Annu. Rev. Nutr.* 28, 115–130. doi: 10.1146/annurev.nutr.28.061807.155443

Bonawitz, N. D., Rodeheffer, M. S., and Shadel, G. S. (2006). Defective mitochondrial gene expression results in reactive oxygen species-mediated inhibition of respiration and reduction of yeast life span. *Mol. Cell. Biol.* 26, 4818–4829. doi: 10.1128/MCB.02360-05

Breitenbach, M., Rinnerthaler, M., Hartl, J., Stincone, A., Vowinckel, J., Breitenbach-Koller, H., et al. (2014). Mitochondria in ageing: there is metabolism beyond the ROS. *FEMS Yeast Res.* 14, 198–212. doi: 10.1111/1567-1364.12134

Cambronne, X. A., Stewart, M. L., Kim, D., Jones-Brunette, A. M., Morgan, R. K., Farrens, D. L., et al. (2016). Biosensor reveals multiple sources for mitochondrial NAD$^+$. *Science* 352, 1474–1477. doi: 10.1126/science.aad5168

Canto, C., Menzies, K. J., and Auwerx, J. (2015). NAD$^+$ metabolism and the control of energy homeostasis: a balancing act between mitochondria and the nucleus. *Cell Metab.* 22, 31–53. doi: 10.1016/j.cmet.2015.05.023

Casatta, N., Porro, A., Orlandi, I., Brambilla, L., and Vai, M. (2013). Lack of Sir2 increases acetate consumption and decreases extracellular pro-aging factors. *Biochim. Biophys. Acta* 1833, 593–601. doi: 10.1016/j.bbamcr.2012.11.008

de Jong-Gubbels, P., Vanrolleghem, P., Heijnen, S., van Dijken, J. P., and Pronk, J. T. (1995). Regulation of carbon metabolism in chemostat cultures of *Saccharomyces cerevisiae* grown on mixtures of glucose and ethanol. *Yeast* 11, 407–418. doi: 10.1002/yea.320110503

Dolle, C., Niere, M., Lohndal, E., and Ziegler, M. (2010). Visualization of subcellular NAD pools and intra-organellar protein localization by poly-ADP-ribose formation. *Cell. Mol. Life Sci.* 67, 433–443. doi: 10.1007/s00018-009-0190-4

Fabrizio, P., Gattazzo, C., Battistella, L., Wei, M., Cheng, C., McGrew, K., et al. (2005). Sir2 blocks extreme life-span extension. *Cell* 123, 655–667. doi: 10.1016/j.cell.2005.08.042

Fabrizio, P., and Longo, V. D. (2007). The chronological life span of *Saccharomyces cerevisiae*. *Methods Mol. Biol.* 371, 89–95. doi: 10.1007/978-1-59745-361-5_8

Fontana, L., Partridge, L., and Longo, V. D. (2010). Extending healthy life span - from yeast to humans. *Science* 328, 321–326. doi: 10.1126/science.1172539

Frye, R. A. (2000). Phylogenetic classification of prokaryotic and eukaryotic Sir2-like proteins. *Biochem. Biophys. Res. Commun.* 273, 793–798. doi: 10.1006/bbrc.2000.3000

Gray, J. V., Petsko, G. A., Johnston, G. C., Ringe, D., Singer, R. A., and Werner-Washburne, M. (2004). "Sleeping beauty": quiescence in *Saccharomyces cerevisiae*. *Microbiol. Mol. Biol. Rev.* 68, 187–206. doi: 10.1128/MMBR.68.2.187-206.2004

Guerrero-Castillo, S., Araiza-Olivera, D., Cabrera-Orefice, A., Espinasa-Jaramillo, J., Gutierrez-Aguilar, M., Luevano-Martinez, L. A., et al. (2011). Physiological uncoupling of mitochondrial oxidative phosphorylation. Studies in different yeast species. *J. Bioenerg. Biomembr.* 43, 323–331. doi: 10.1007/s10863-011-9356-5

Hlavata, L., Aguilaniu, H., Pichova, A., and Nystrom, T. (2003). The oncogenic RAS2^{val19} mutation locks respiration, independently of PKA, in a mode prone to generate ROS. *EMBO J.* 22, 3337–3345. doi: 10.1093/emboj/cdg314

Houtkooper, R. H., Canto, C., Wanders, R. J., and Auwerx, J. (2010). The secret life of NAD$^+$: an old metabolite controlling new metabolic signaling pathways. *Endocr. Rev.* 31, 194–223. doi: 10.1210/er.2009-0026

Houtkooper, R. H., Pirinen, E., and Auwerx, J. (2012). Sirtuins as regulators of metabolism and healthspan. *Nat. Rev. Mol. Cell Biol.* 13, 225–238. doi: 10.1038/nrm3293

Imai, S. (2009). From heterochromatin islands to the NAD World: a hierarchical view of aging through the functions of mammalian Sirt1 and systemic NAD biosynthesis. *Biochim. Biophys.* 1790, 997–1004. doi: 10.1016/j.bbagen.2009.03.005

Imai, S. (2010). "Clocks" in the NAD World: NAD as a metabolic oscillator for the regulation of metabolism and aging. *Biochim. Biophys. Acta* 1804, 1584–1590. doi: 10.1016/j.bbapap.2009.10.024

Imai, S., Armstrong, C. M., Kaeberlein, M., and Guarente, L. (2000). Transcriptional silencing and longevity protein Sir2 is an NAD-dependent histone deacetylase. *Nature* 403, 795–800. doi: 10.1038/35001622

Imai, S., and Guarente, L. (2014). NAD$^+$ and sirtuins in aging and disease. *Trends Cell Biol.* 24, 464–471. doi: 10.1016/j.tcb.2014.04.002

Imai, S. I. (2016). The NAD World 2.0: the importance of the inter-tissue communication mediated by NAMPT/NAD($^+$)/SIRT1 in mammalian aging and longevity control. *NPJ Syst. Biol. Appl.* 2:16018. doi: 10.1038/npjsba.2016.18

Imai, S. I., and Guarente, L. (2016). It takes two to tango: NAD($^+$) and sirtuins in aging/longevity control. *NPJ Aging Mech. Dis.* 2:16017. doi: 10.1038/npjamd.2016.17

Johnson, S., and Imai, S. I. (2018). NAD ($^+$) biosynthesis, aging, and disease. *F1000 Res.* 7:132. doi: 10.12688/f1000research.12120.1

Kaeberlein, M., McVey, M., and Guarente, L. (1999). The SIR2/3/4 complex and SIR2 alone promote longevity in *Saccharomyces cerevisiae* by two different mechanisms. *Genes Dev.* 13, 2570–2580. doi: 10.1101/gad.13.19.2570

Kato, M., and Lin, S. J. (2014). Regulation of NAD$^+$ metabolism, signaling and compartmentalization in the yeast *Saccharomyces cerevisiae*. *DNA Repair* 23, 49–58. doi: 10.1016/j.dnarep.2014.07.009

Koch-Nolte, F., Fischer, S., Haag, F., and Ziegler, M. (2011). Compartmentation of NAD$^+$-dependent signalling. *FEBS Lett.* 585, 1651–1656. doi: 10.1016/j.febslet.2011.03.045

Lee, Y. J., Jang, J. W., Kim, K. J., and Maeng, P. J. (2011). TCA cycle-independent acetate metabolism via the glyoxylate cycle in *Saccharomyces cerevisiae*. *Yeast* 28, 153–166. doi: 10.1002/yea.1828

136

Lin, S. J., Ford, E., Haigis, M., Liszt, G., and Guarente, L. (2004). Calorie restriction extends yeast life span by lowering the level of NADH. *Genes Dev.* 18, 12–16. doi: 10.1101/gad.1164804

Lin, S. S., Manchester, J. K., and Gordon, J. I. (2001). Enhanced gluconeogenesis and increased energy storage as hallmarks of aging in *Saccharomyces cerevisiae*. *J. Biol. Chem.* 276, 36000–36007. doi: 10.1074/jbc.M103509200

Lin, Y. Y., Lu, J. Y., Zhang, J., Walter, W., Dang, W., Wan, J., et al. (2009). Protein acetylation microarray reveals that NuA4 controls key metabolic target regulating gluconeogenesis. *Cell* 136, 1073–1084. doi: 10.1016/j.cell.2009.01.033

Longo, V. D., and Kennedy, B. K. (2006). Sirtuins in aging and age-related disease. *Cell* 126, 257–268. doi: 10.1016/j.cell.2006.07.002

Longo, V. D., Shadel, G. S., Kaeberlein, M., and Kennedy, B. (2012). Replicative and chronological aging in *Saccharomyces cerevisiae*. *Cell Metab.* 16, 18–31. doi: 10.1016/j.cmet.2012.06.002

MacLean, M., Harris, N., and Piper, P. W. (2001). Chronological lifespan of stationary phase yeast cells; a model for investigating the factors that might influence the ageing of postmitotic tissues in higher organisms. *Yeast* 18, 499–509. doi: 10.1002/yea.701

Madeo, F., Frohlich, E., Ligr, M., Grey, M., Sigrist, S. J., Wolf, D. H., et al. (1999). Oxygen stress: a regulator of apoptosis in yeast. *J. Cell Biol.* 145, 757–767. doi: 10.1083/jcb.145.4.757

McClure, J. M., Wierman, M. B., Maqani, N., and Smith, J. S. (2012). Isonicotinamide enhances Sir2 protein-mediated silencing and longevity in yeast by raising intracellular NAD$^+$ concentration. *J. Biol. Chem.* 287, 20957–20966. doi: 10.1074/jbc.M112.367524

Meisinger, C., Pfanner, N., and Truscott, K. N. (2006). Isolation of yeast mitochondria. *Methods Mol. Biol.* 313, 33–39. doi: 10.1385/1-59259-958-3:033

Mitchell, S. J., Bernier, M., Aon, M. A., Cortassa, S., Kim, E. Y., Fang, E. F., et al. (2018). Nicotinamide improves aspects of healthspan, but not lifespan, in mice. *Cell Metab.* 27, 667–676. doi: 10.1016/j.cmet.2018.02.001

Ocampo, A., Liu, J., Schroeder, E. A., Shadel, G. S., and Barrientos, A. (2012). Mitochondrial respiratory thresholds regulate yeast chronological life span and its extension by caloric restriction. *Cell Metab.* 16, 55–67. doi: 10.1016/j.cmet.2012.05.013

Ondracek, C. R., Frappier, V., Ringel, A. E., Wolberger, C., and Guarente, L. (2017). Mutations that allow *SIR2* orthologs to function in a NAD($^+$)-depleted environment. *Cell Rep.* 18, 2310–2319. doi: 10.1016/j.celrep.2017.02.031

Orlandi, I., Pellegrino Coppola, D., Strippoli, M., Ronzulli, R., and Vai, M. (2017a). Nicotinamide supplementation phenocopies *SIR2* inactivation by modulating carbon metabolism and respiration during yeast chronological aging. *Mech. Ageing Dev.* 161, 277–287. doi: 10.1016/j.mad.2016.06.006

Orlandi, I., Pellegrino Coppola, D., and Vai, M. (2014). Rewiring yeast acetate metabolism through MPC1 loss of function leads to mitochondrial damage and decreases chronological lifespan. *Microb. Cell* 1, 393–405. doi: 10.15698/mic2014.12.178

Orlandi, I., Ronzulli, R., Casatta, N., and Vai, M. (2013). Ethanol and acetate acting as carbon/energy sources negatively affect yeast chronological aging. *Oxid. Med. Cell. Longev.* 2013:802870. doi: 10.1155/2013/802870

Orlandi, I., Stamerra, G., Strippoli, M., and Vai, M. (2017b). During yeast chronological aging resveratrol supplementation results in a short-lived phenotype Sir2-dependent. *Redox Biol.* 12, 745–754. doi: 10.1016/j.redox.2017.04.015

Palmieri, F., Agrimi, G., Blanco, E., Castegna, A., Di Noia, M. A., Iacobazzi, V., et al. (2006). Identification of mitochondrial carriers in *Saccharomyces cerevisiae* by transport assay of reconstituted recombinant proteins. *Biochim. Biophys. Acta* 1757, 1249–1262. doi: 10.1016/j.bbabio.2006.05.023

Pan, Y. (2011). Mitochondria, reactive oxygen species, and chronological aging: a message from yeast. *Exp. Gerontol.* 46, 847–852. doi: 10.1016/j.exger.2011.08.007

Parrella, E., and Longo, V. D. (2008). The chronological life span of *Saccharomyces cerevisiae* to study mitochondrial dysfunction and disease. *Methods* 46, 256–262. doi: 10.1016/j.ymeth.2008.10.004

Pollak, N., Dolle, C., and Ziegler, M. (2007). The power to reduce: pyridine nucleotides - small molecules with a multitude of functions. *Biochem. J.* 402, 205–218. doi: 10.1042/BJ20061638

Rajman, L., Chwalek, K., and Sinclair, D. A. (2018). Therapeutic potential of NAD-boosting molecules: the *in vivo* evidence. *Cell Metab.* 27, 529–547. doi: 10.1016/j.cmet.2018.02.011

Rigoulet, M., Aguilaniu, H., Averet, N., Bunoust, O., Camougrand, N., Grandier-Vazeille, X., et al. (2004). Organization and regulation of the cytosolic NADH metabolism in the yeast *Saccharomyces cerevisiae*. *Mol. Cell. Biochem.* 256–257, 73–81. doi: 10.1023/B:MCBI.0000009888.79484.fd

Saint-Prix, F., Bonquist, L., and Dequin, S. (2004). Functional analysis of the *ALD* gene family of *Saccharomyces cerevisiae* during anaerobic growth on glucose: the NADP$^+$-dependent Ald6p and Ald5p isoforms play a major role in acetate formation. *Microbiology* 150, 2209–2220. doi: 10.1099/mic.0.26999-0

Sauve, A. A., Moir, R. D., Schramm, V. L., and Willis, I. M. (2005). Chemical activation of Sir2-dependent silencing by relief of nicotinamide inhibition. *Mol. Cell* 17, 595–601. doi: 10.1016/j.molcel.2004.12.032

Sherman, F. (2002). Getting started with yeast. *Meth. Enzymol.* 350, 3–41. doi: 10.1016/S0076-6879(02)50954-X

Shi, L., Sutter, B. M., Ye, X., and Tu, B. P. (2010). Trehalose is a key determinant of the quiescent metabolic state that fuels cell cycle progression upon return to growth. *Mol. Biol. Cell* 21, 1982–1990. doi: 10.1091/mbc.e10-01-0056

Smith, D. L. Jr., McClure, J. M., Matecic, M., and Smith, J. S. (2007). Calorie restriction extends the chronological lifespan of *Saccharomyces cerevisiae* independently of the Sirtuins. *Aging Cell* 6, 649–662. doi: 10.1111/j.1474-9726.2007.00326.x

Smith, J. S., Brachmann, C. B., Celic, I., Kenna, M. A., Muhammad, S., Starai, V. J., et al. (2000). A phylogenetically conserved NAD$^+$-dependent protein deacetylase activity in the Sir2 protein family. *Proc. Natl. Acad. Sci. U.S.A.* 97, 6658–6663. doi: 10.1073/pnas.97.12.6658

Steinkraus, K. A., Kaeberlein, M., and Kennedy, B. K. (2008). Replicative aging in yeast: the means to the end. *Annu. Rev. Cell Dev. Biol.* 24, 29–54. doi: 10.1146/annurev.cellbio.23.090506.123509

Swinnen, E., Ghillebert, R., Wilms, T., and Winderickx, J. (2014). Molecular mechanisms linking the evolutionary conserved TORC1-Sch9 nutrient signalling branch to lifespan regulation in *Saccharomyces cerevisiae*. *FEMS Yeast Res.* 14, 17–32. doi: 10.1111/1567-1364.12097

Todisco, S., Agrimi, G., Castegna, A., and Palmieri, F. (2006). Identification of the mitochondrial NAD$^+$ transporter in *Saccharomyces cerevisiae*. *J. Biol. Chem.* 281, 1524–1531. doi: 10.1074/jbc.M510425200

Vanoni, M., Vai, M., Popolo, L., and Alberghina, L. (1983). Structural heterogeneity in populations of the budding yeast *Saccharomyces cerevisiae*. *J. Bacteriol.* 156, 1282–1291.

Verdin, E. (2015). NAD($^+$) in aging, metabolism, and neurodegeneration. *Science* 350, 1208–1213. doi: 10.1126/science.aac4854

Wanichthanarak, K., Wongtosrad, N., and Petranovic, D. (2015). Genome-wide expression analyses of the stationary phase model of ageing in yeast. *Mech. Ageing Dev.* 149, 65–74. doi: 10.1016/j.mad.2015.05.008

Yaku, K., Okabe, K., and Nakagawa, T. (2018). NAD metabolism: implications in aging and longevity. *Ageing Res. Rev.* 47, 1–17. doi: 10.1016/j.arr.2018.05.006

Zhang, N., and Cao, L. (2017). Starvation signals in yeast are integrated to coordinate metabolic reprogramming and stress response to ensure longevity. *Curr. Genet.* 63, 839–843. doi: 10.1007/s00294-017-0697-4

137

Chapter 6

Skin infections are eliminated by cooperation of the fibrinolytic and innate immune systems

William Santus, Simona Barresi, Francesca Mingozzi, Achille Broggi, Ivan Orlandi, Giulia Stamerra, Marina Vai, Alessandra M. Martorana, Alessandra Polissi, Julia R. Köhler, Ningning Liu, Ivan Zanoni, Francesca Granucci.

Participation in the demonstrative video for the paper "Deep dermal injection as a model of *Candida albicans* skin infection for histological analyses"

https://www.jove.com/video/57574/deep-dermal-injection-as-model-candida-albicans-skin-infection-for

Skin infections are eliminated by cooperation of the fibrinolytic and innate immune systems

William Santus,[1]* Simona Barresi,[1]* Francesca Mingozzi,[1]* Achille Broggi,[2]* Ivan Orlandi,[1] Giulia Stamerra,[1] Marina Vai,[1] Alessandra M. Martorana,[1] Alessandra Polissi,[3] Julia R. Köhler,[4] Ningning Liu,[4] Ivan Zanoni,[1,2]†‡ Francesca Granucci[1]†‡

Nuclear factor of activated T cells (NFAT) is activated in innate immune cells downstream of pattern recognition receptors, but little is known about NFAT's functions in innate immunity compared with adaptive immunity. We show that early activation of NFAT balances the two major phases of the innate response to *Candida albicans* skin infections: the protective containment (abscess) and the elimination (expulsion) phases. During the early containment phase, transforming growth factor–β (TGF-β) induces the deposit of collagen around newly recruited polymorphonuclear cells to prevent microbial spreading. During the elimination phase, interferon-γ (IFN-γ) blocks differentiation of fibroblasts into myofibroblasts by antagonizing TGF-β signaling. IFN-γ also induces the formation of plasmin that, in turn, promotes abscess capsule digestion and skin ulceration for microbial discharge. NFAT controls innate IFN-γ production and microbial expulsion. This cross-talk between the innate immune and the fibrinolytic systems also occurs during infection with *Staphylococcus aureus* and is a protective response to minimize tissue damage and optimize pathogen elimination.

INTRODUCTION

Nuclear factor of activated T cells (NFAT) proteins form a family of transcription factors that are estimated to have evolved about 500 million years ago, around the same time as the appearance of vertebrates (1). Given the relatively late appearance of NFAT proteins in evolution, their major roles were believed to center on regulation of the adaptive immunity, the more recent form of immunity that appeared with vertebrates. In contrast, innate immunity (the ancient form of immunity) was thought to be controlled primarily by signaling pathways that are conserved during evolution (2), and the prevailing consensus was that NFATs were not involved in this form of immunity (3). However, we and others have shown that the NFAT family can be activated during innate immune responses to bacterial or fungal infections downstream of pattern recognition receptors (4–6).

The NFAT pathway in phagocytes is most effectively activated in response to β-glucan–bearing fungi (7–9). Fungal infections can develop at a variety of anatomical sites. Although these infections are readily controlled by healthy individuals, they may become systemic in immunocompromised individuals, hospitalized patients, or individuals with inherited mutations in immune genes. Calcineurin is a phosphatase involved in the activation of NFAT transcription factors, and calcineurin inhibitors, such as cyclosporine A (CsA) and tacrolimus, are commonly used as immunosuppressors for treating acute transplant rejection (10), autoimmune diseases (such as psoriasis) (11), and other immunological conditions (such as atopic dermatitis) (12). Although such inhibitors are highly efficient, they

have potent side effects that include susceptibility to opportunistic infections from pathogens, such as *Candida albicans*, *Aspergillus fumigatus*, and many bacterial species, which are normally well controlled by innate and adaptive immunity (13, 14). In principle, CsA and tacrolimus block interleukin-2 (IL-2) and other NFAT-dependent cytokine production by T cells; but increasing evidence supports the notion that susceptibility to microbial infections could mainly arise via inhibition of the NFAT pathway in innate immune cells (6), although the mechanisms that underlie this vulnerability remain elusive.

Here, we have investigated how NFAT activation during innate responses regulates the development and the progress of the inflammatory process induced in the skin by microorganisms and leads to the protection against microbial spreading and, eventually, to microbe elimination.

RESULTS

NFATc2 is required for the elimination of *C. albicans* skin infections by innate immune cells

We first investigated the role of NFATc2 in the innate control of *C. albicans* infections in the skin. We focused on the study of NFATc2, which is primarily activated in dendritic cells (DCs) and is not expressed in neutrophils, one of the major populations known to fight fungal infections [fig. S1A; (6)]. Thus, in this model, the neutrophil response is not altered [their phagocytic capacity remains unaltered compared to wild-type (WT) neutrophils; fig. S1B], whereas other phagocyte responses may be affected by the absence of NFATc2.

To investigate whether NFATc2 participates in the innate immune responses to fungal infections, we used NFATc2-deficient and WT mice in a model of *C. albicans* skin infection. Mice were infected in the deep dermis with *C. albicans* hyphae, and the temporal course of the lesions was evaluated. WT animals displayed skin ulceration at about 2 days after infection (Fig. 1, A and B, and figs. S2 and S3), whereas NFATc2-deficient mice exhibited a capsulated abscess containing *C. albicans* with no ulceration (Fig. 1, A to C, and

[1]Department of Biotechnology and Biosciences, University of Milano-Bicocca, Piazza della Scienza 2, 20126 Milan, Italy. [2]Harvard Medical School and Division of Gastroenterology, Hepatology and Nutrition, Boston Children's Hospital, Boston, MA 02115, USA. [3]Dipartimento di Scienze Farmacologiche e Biomolecolari, Università degli Studi di Milano, Milan, Italy. [4]Harvard Medical School and Division of Infectious Diseases, Boston Children's Hospital, Boston, MA 02115, USA.
*These authors contributed equally to this work.
†These authors contributed equally to this work.
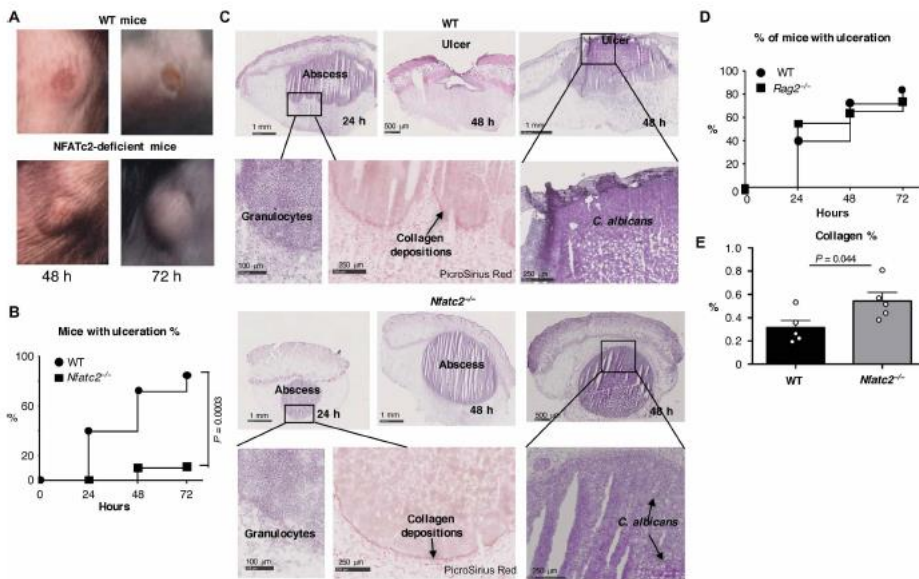‡Corresponding author. Email: francesca.granucci@unimib.it (F.G.); ivan.zanoni@childrens.harvard.edu (I.Z.)

Fig. 1. NFATc2-deficient mice do not eliminate skin *C. albicans* infections. (**A**) Lesions in WT and NFATc2-deficient mice at the indicated time points after *C. albicans* hyphae injection in the deep derma. WT animals (top) undergo ulceration and *C. albicans* elimination, whereas NFATc2-deficient mice (bottom) develop a persistent abscess. (**B**) Kaplan-Meier curve showing the percentage of WT and NFATc2-deficient mice undergoing ulceration after *C. albicans* administration at the indicated time points; $n = 10$; log-rank test. Results are representative of at least six independent experiments. (**C**) Hematoxylin and eosin staining of WT (top) and NFATc2-deficient (bottom) mouse skin lesions at the indicated time points after *C. albicans* infections. Larger magnification of selected areas of the same section are shown to evidence granulocyte recruitment (left). PicroSirius Red staining is also shown to evidence collagen depositions (right, red deposits) and periodic acid–Schiff (PAS) staining to evidence *Candida*. See also fig. S2 for higher magnifications. Representative histological sections of four independent experiments are shown; see also fig. S3 (A and B). (**D**) WT and RAG-2–deficient mice respond similarly to primary skin infections with *C. albicans*. The Kaplan-Meier curve shows the percentage of WT and RAG-2–deficient mice undergoing ulceration after *C. albicans* administration at the indicated time points; $n = 18$ per group. (**E**) Digital image analysis quantification of collagen staining. Five fields from two sections (24 hours after infection) of two independent experiments were analyzed. The analyzed fields covered the entire sections excluding the skin. Means and SEM are depicted. $n = 5$; statistical significance, two-tailed t test.

figs. S2 and S3). Although *C. albicans* could not be eliminated in NFATc2-deficient mice, the infection remained confined in the abscess with no further spreading (fig. S4). The phenotype of the NFATc2-deficient mice was not primarily due to the absence of NFATc2 expression in adaptive immune cells because $Rag2^{-/-}$ mice, which lack an adaptive immune system, had a response like that of WT mice (Fig. 1D).

Histological analyses revealed that the abscess was formed by granulocytes recruited to the site of the *C. albicans* infection, suggesting that recruitment was unchanged between WT and NFATc2-deficient mice (Fig. 1C and figs. S2 and S3). Use of quantitative reverse transcription polymerase chain reaction (qRT-PCR) to characterize other cell types recruited to the infection site showed that neutrophils, eosinophils, and basophils were present in both animal types (fig. S5). Monocytes were also recruited in both groups (fig. S5). Although a few differences in the composition of the infiltrate were measurable at specific time points (more eosinophils

were recruited in WT mice, and more basophils were recruited in NFATc2-deficient mice), the capacity of WT and NFATc2-deficient animals to recruit immune cells was very similar.

Histological analyses of WT mice also showed that the abscess was surrounded by collagen deposits (Fig. 1, C and E, and figs. S2B and S3). Starting at 48 hours after infection, abscess formation was followed by skin ulceration and the discharge of dead cells and *C. albicans* from the skin (Fig. 1C and fig. S3). Complete elimination of *C. albicans* in WT mice occurred in about 6 to 7 days after infection (fig. S6), whereas *C. albicans* persisted inside the abscess in NFATc2-deficient mice (fig. S6). However, infected skin in NFATc2-deficient mice showed the formation of an abscess surrounded by a well-organized thick collagen capsule (Fig. 1C and figs. S2B and S3), with *C. albicans* contained inside the abscess (Fig. 1C and figs. S3 and S6). A quantification of collagen deposits around the abscess 24 hours after infection showed significantly less collagen deposit in WT compared with NFATc2 mice (Fig. 1E).

140

Fibroblasts surrounded the newly recruited granulocytes in both WT and NFATc2-deficient mice (Fig. 2A). Nevertheless, over time, in NFATc2-deficient but not WT mice, fibroblasts differentiated into myofibroblasts, as indicated by the expression of the α–smooth muscle actin (α-SMA) marker (Fig. 2B and fig. S7). These data indicate that WT animals contain and eliminate *C. albicans* skin infections, whereas NFATc2-deficient mice restrain the infection by forming a thick capsule around the abscess but are not able to eliminate the microorganism.

Transforming growth factor–β is required for the initial phase of infection containment by promoting fibrosis and is overactive in NFATc2-deficient mice

The response that we observed in NFATc2-deficient mice had a prominent fibrotic component. Because the transforming growth factor–β (TGF-β) is a well-known profibrotic factor (*15*), we hypothesized that an overactivation of the TGF-β pathway was responsible for the behavior of mutant mice. To test this possibility, we examined the activation of the TGF-β transduction pathway in WT and NFATc2-deficient mice, evaluating the presence of phosphorylated SMAD2,3 proteins both histologically and by Western blot analysis. As shown in Fig. 3A, the TGF-β pathway was activated in both strains; however, the activation was three to four times more pronounced in NFATc2-deficient mice relative to WT mice. In addition, in the histologic evaluation, phosphorylated SMAD2,3 staining was more pronounced in sections from NFATc2-deficient mice (Fig. 3B and fig. S8).

Mice were next treated with an inhibitor of the TGF-β transduction pathway (SB-431542) to investigate whether TGF-β inhibition could restore the WT phenotype. Therefore, the effect of the inhibitor on the formation of the encapsulated abscess was analyzed after *C. albicans* infection. We observed that, in response to the reduced activation of the TGF-β pathway, both WT and NFATc2-deficient mouse responses were affected. *C. albicans* was not contained and instead diffused into the subcutaneous space; this led to multiple granulocyte accumulations in both WT and NFATc2-deficient mice (Fig. 3C). Accordingly, the formation of nonorganized collagen deposits around the abscesses was observed in both mouse groups (Fig. 3D and figs. S9 and S10). Overall, these data suggest that the incapability to form adequate collagen capsules when the TGF-β pathway was down-modulated was responsible for the reduced containment of the infection.

These data demonstrate that the TGF-β pathway activation is required during the initial phase of the inflammatory process for the proper containment of the infection. However, the pathway is overactive in *Nfatc2*^{−/−} animals and contributes to the formation of excessive collagen deposits around the abscess. The overactivation of the TGF-β pathway only partially explains the phenotype of NFATc2-deficient mice because ulceration was not restored in this group of mice even after TGF-β inhibition.
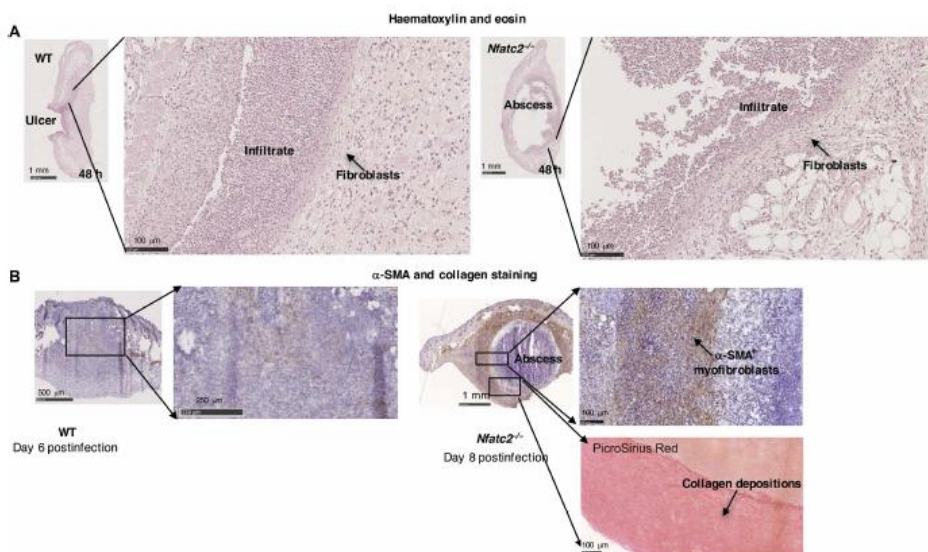

Fig. 2. Fibroblast activation in WT and NFATc2-deficient mice. (**A**) Histology of lesions induced by *C. albicans* hyphae in WT and NFATc2-deficient mice 48 hours after infections. Fibroblasts surrounding granulocytes are highlighted with black arrows. (**B**) Representative images of α-SMA immunohistochemical staining in skin sections of WT and NFATc2-deficient mice 6 and 8 days after *C. albicans* infection. PicroSirius Red staining is also shown to evidence collagen capsule. Representative histological sections of three independent experiments are shown; see also fig. S7.
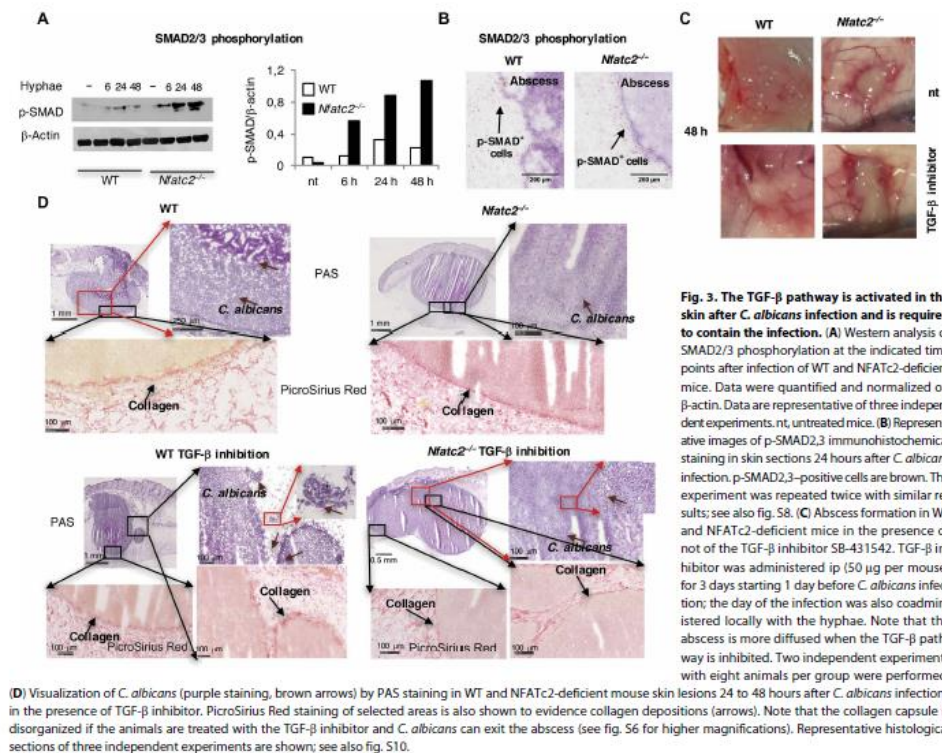
141

Fig. 3. The TGF-β pathway is activated in the skin after *C. albicans* infection and is required to contain the infection. (**A**) Western analysis of SMAD2/3 phosphorylation at the indicated time points after infection of WT and NFATc2-deficient mice. Data were quantified and normalized on β-actin. Data are representative of three independent experiments. nt, untreated mice. (**B**) Representative images of p-SMAD2,3 immunohistochemical staining in skin sections 24 hours after *C. albicans* infection. p-SMAD2,3–positive cells are brown. The experiment was repeated twice with similar results; see also fig. S8. (**C**) Abscess formation in WT and NFATc2-deficient mice in the presence or not of the TGF-β inhibitor SB-431542. TGF-β inhibitor was administered ip (50 μg per mouse) for 3 days starting 1 day before *C. albicans* infection; the day of the infection was also coadministered locally with the hyphae. Note that the abscess is more diffused when the TGF-β pathway is inhibited. Two independent experiments with eight animals per group were performed. (**D**) Visualization of *C. albicans* (purple staining, brown arrows) by PAS staining in WT and NFATc2-deficient mouse skin lesions 24 to 48 hours after *C. albicans* infections in the presence of TGF-β inhibitor. PicroSirius Red staining of selected areas is also shown to evidence collagen depositions (arrows). Note that the collagen capsule is disorganized if the animals are treated with the TGF-β inhibitor and *C. albicans* can exit the abscess (see fig. S6 for higher magnifications). Representative histological sections of three independent experiments are shown; see also fig. S10.

Interferon-γ antagonizes TGF-β signaling in WT animals

We next focused on the molecular mechanism that drives the overactivation of the TGF-β pathway in NFATc2-deficient mice. In the tissue, TGF-β is present in an inactive form and is associated with the extracellular matrix. Various factors, including reactive oxygen species, pH, integrins, and proteases, can induce the release of the active cytokine (*16–19*). Because the TGF-β pathway was activated and required for infection containment in both animal groups (Fig. 3A) but was more active in NFATc2-deficient mice, we hypothesized that active TGF-β is released in WT and NFATc2-deficient mice but is then antagonized in WT animals by factors that are produced in an NFATc2-dependent manner. Interferon-γ (IFN-γ) is a very potent antagonist of TGF-β (*20, 21*), and NFATc2-deficient mice were previously described to be prone to develop type 2 responses rather than type 1, IFN-γ–dependent responses (*22*). Therefore, we hypothesized that NFATc2-deficient mice showed a deficit in IFN-γ production that could explain the differences between the two animal groups. We compared the levels of IFN-γ in infected skins from WT and NFATc2-deficient mice. A significant up-regulation of

IFN-γ mRNA was observed in WT controls but not in NFATc2-deficient mice (Fig. 4A), and more IFN-γ⁺ cells were found in WT compared with NFATc2-deficient skins by immunohistochemical staining (Fig. 4B and fig. S11). Administration of recombinant IFN-γ in NFATc2-deficient mice at the time of *C. albicans* infection was sufficient to induce ulceration (Fig. 4, C and D), and this correlated with a reduction of the TGF-β pathway activation (Fig. 4E). In contrast, when IFN-γ was blocked in WT animals, they exhibited the same phenotype of NFATc2-deficient mice, namely, no ulceration (Fig. 4, C and D) and strong activation of the TGF-β pathway (Fig. 4F). In accordance with these observations, blocking IFN-γ in WT animals favored the formation of a well-organized collagen capsule (Fig. 4D). On the other hand, the exogenous administration of IFN-γ to NFATc2-deficient mice hampered the formation of a thick collagen capsule (Fig. 4D). Accordingly, in vitro TGF-β promoted skin fibroblast proliferation that was antagonized by IFN-γ (Fig. 4G).

IFN-γ–deficient mice were also analyzed to investigate whether they could recapitulate the phenotype of NFATc2-deficient mice. As expected, IFN-γ–deficient mice did not undergo ulceration
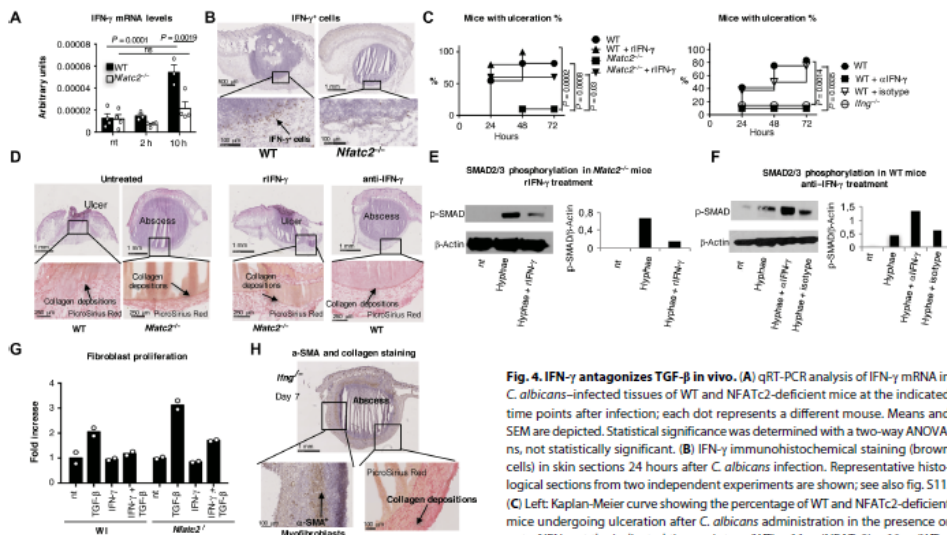
142

Fig. 4. IFN-γ antagonizes TGF-β in vivo. (A) qRT-PCR analysis of IFN-γ mRNA in *C. albicans*–infected tissues of WT and NFATc2-deficient mice at the indicated time points after infection; each dot represents a different mouse. Means and SEM are depicted. Statistical significance was determined with a two-way ANOVA. ns, not statistically significant. **(B)** IFN-γ immunohistochemical staining (brown cells) in skin sections 24 hours after *C. albicans* infection. Representative histological sections from two independent experiments are shown; see also fig. S11. **(C)** Left: Kaplan-Meier curve showing the percentage of WT and NFATc2-deficient mice undergoing ulceration after *C. albicans* administration in the presence or not of IFN-γ at the indicated time points; *n* (WT) = 11, *n* (NFATc2) = 10, *n* (WT + rIFN-γ) = 5, *n* (NFATc2 + rIFN-γ) = 5. rIFN-γ, recombinant IFN-γ. Right: Kaplan-Meier curve showing the percentage of WT and IFN-γ–deficient mice undergoing ulceration after *C. albicans* administration in the presence or not of the indicated antibodies at the indicated time points; *n* (WT + isotype control) = 8, *n* (WT) = 12, *n* (WT + α–IFN-γ) = 10, *n* (IFN-γ–deficient) = 14; log-rank test. **(D)** Hematoxylin and eosin staining of WT and NFATc2-deficient mouse skin lesions 48 hours after *C. albicans* infections in the presence or not of the indicated stimuli. Larger magnification of PicroSirius Red staining of selected areas is also shown to evidence collagen depositions. The collagen capsule is loose in NFATc2-deficient mice if they are treated with rIFN-γ (1 μg per mouse). In contrast, the collagen capsule becomes thick in WT animals if IFN-γ is neutralized by an anti–IFN-γ antibody (50 μg per mouse). **(E)** Western blot analysis of SMAD2/3 phosphorylation in WT animals treated with *C. albicans* hyphae or *C. albicans* hyphae and rIFN-γ. Western blot analysis was performed 6 hours after *C. albicans* infection. Data were quantified and normalized on β-actin. Data are representative of two independent experiments. **(F)** Western blot analysis of SMAD2/3 phosphorylation from the infected skin of WT animals treated with *C. albicans* hyphae, *C. albicans* hyphae and the IFN-γ neutralizing antibody, or *C. albicans* hyphae and the isotype control antibody. Western blot analysis was performed 24 hours after *C. albicans* infection. Data were quantified and normalized on β-actin. Data are representative of three independent experiments. **(G)** In vitro WT and NFATc2-deficient skin fibroblast proliferation in the presence or not of the indicated stimuli (TGF-β, 3 ng/ml; IFN-γ, 150 U/ml). Each dot represents a different sample. **(H)** α-SMA immunohistochemical staining in skin sections of IFN-γ–deficient mice 7 days after *C. albicans* infection. PicroSirius Red staining is also shown to evidence collagen capsule.

(Fig. 4C) and formed a thick fibroblast and collagen capsule, and fibroblasts differentiated into myofibroblasts (Fig. 4H). Overall, our data support a model in which IFN-γ controls abscess capsule formation at least in part by antagonizing TGF-β signaling.

IFN-γ controls collagen capsule degradation by controlling the activation of the fibrinolytic system

As evidenced above, the pharmacological treatment with IFN-γ, but not the inhibition of the TGF-β pathway, can fully restore the response to *C. albicans* skin infection in NFATc2-deficient mice. These observations imply that the effect of IFN-γ cannot be explained with only the antagonistic effect on TGF-β. Therefore, we predicted that, in addition to TGF-β inhibition, IFN-γ also contributed to the induction of factors required for capsule degradation and ulceration. This hypothesis was also supported by the observation that the process of capsule disruption in WT animals was further potentiated upon recombinant IFN-γ administration (fig. S12). We first focused on factors required for capsule degradation. Under several pathophysiological conditions, a collagen capsule is digested

by metalloproteinases that are released by innate immune and stromal cells. Nevertheless, metalloproteinases are released in an inactive form and need to be activated by other proteases, such as plasmin (23–25). To investigate the potential role of plasmin in capsule digestion, we evaluated the levels of active plasmin in the tissue. These were significantly higher in WT compared with NFATc2-deficient mice (Fig. 5A).

To confirm plasmin involvement in capsule digestion, we administered plasminogen activator inhibitor–1 (PAI-1) (26), an endogenous inhibitor of plasminogen-to-plasmin conversion, to WT animals to verify whether ulceration could be inhibited. PAI-1 administration initially led to the formation of an encapsulated abscess and no ulceration (Fig. 5, B and C, and fig. S13), confirming that plasmin is required for capsule digestion and ulceration. Nevertheless, at later time points, the abscess did not show the organization exhibited in NFATc2-deficient mice, and no differentiation of fibroblasts in myofibroblasts was observed (Fig. 5D). This was predictable given the presence of IFN-γ (which inhibits TGF-β) in the skin of WT animals.

143

Plasminogen-to-plasmin conversion is induced by activators of plasminogen, such as tissue plasminogen activator (tPA). We therefore evaluated the presence of tPA in the tissue of infected mice. In line with our prediction, tPA levels were much higher in WT compared with NFATc2-deficient mice (Fig. 5E). We also analyzed the levels of endogenous PAI-1 that inhibits plasmin formation. PAI-1 was also more expressed in WT compared with NFATc2-deficient mice (Fig. 5E). In WT animals, tPA production was induced early, when PAI-1 was not present in the tissue (Fig. 5E). The counterregulation of tPA and PAI-1 observed in WT animals is presumably required to first allow plasmin generation and then avoid excessive plasmin accumulation.

Given that plasmin is required for capsule digestion, we investigated whether IFN-γ influenced the activation of the fibrinolytic system. We tested our hypothesis both by administering IFN-γ to NFATc2-deficient mice and by blocking IFN-γ in WT animals. As expected, adding IFN-γ restored tPA and PAI-1 production in NFATc2-deficient mice (Fig. 5E). On the contrary, blocking IFN-γ in WT animals inhibited the release of tPA and PAI-1 (Fig. 5E). This indicates that the entire pathway that leads to plasmin formation is altered by the absence of IFN-γ in NFATc2-deficient mice. To further support our conclusions, we also measured active plasmin in the tissue of NFATc2-deficient mice treated or not with IFN-γ and of WT animals treated or not with a blocking IFN-γ antibody at the time
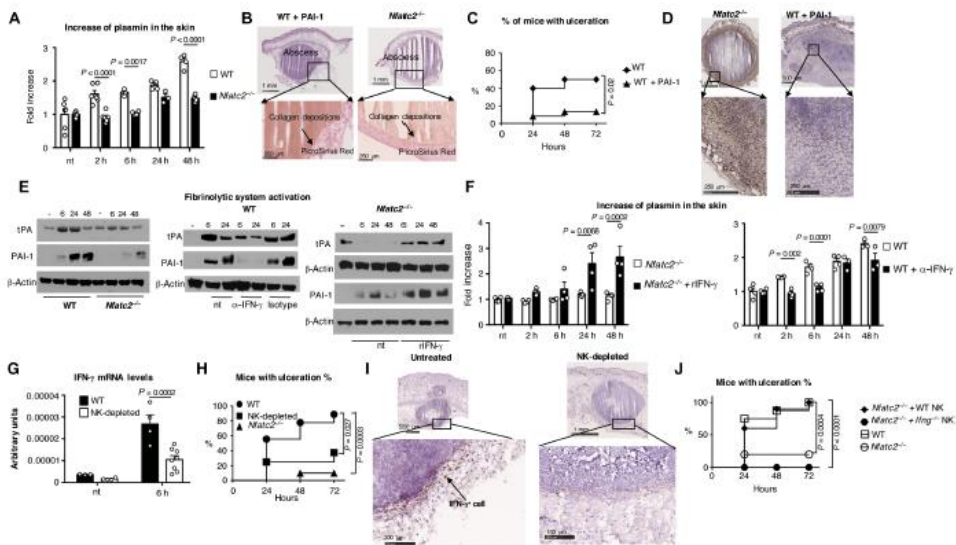

Fig. 5. IFN-γ activates the fibrinolytic system. (A) Increase of active plasmin levels in WT and NFATc2-deficient mice at the indicated time points after *C. albicans* infection. Each dot represents a single mouse. Means and SEM are depicted; a two-way ANOVA was used for statistics. The experiment was repeated twice with similar results. (B) Hematoxylin and eosin staining of WT mouse skin lesions 48 hours after *C. albicans* infections in the presence of PAI-1 (0.65 μg per mouse) and NFATc2-deficient mice skin lesions. Larger magnification of PicroSirius Red staining of selected areas is also shown to evidence collagen depositions. Representative histological sections from two independent experiments are shown; see also fig. S13. (C) Kaplan-Meier curves showing the percentage of mice undergoing ulceration after *C. albicans* administration. Where indicated, mice were treated with PAI-1 (0.65 μg per mouse, coadministered with *C. albicans*). n (WT) = 10, n (WT + PAI-1) = 24; log-rank test. (D) Representative images of α-SMA immunohistochemical staining in skin sections of NFATc2-deficient and PAI-1–treated WT animals 8 and 7 days after *C. albicans* infection. (E) Left: Western blot analysis of tPA and PAI-1 levels measured in WT and NFATc2-deficient animals at the indicated hours after *C. albicans* infection. Data are representative of three independent experiments. Middle and right: Western blot analysis of tPA and PAI-1 levels measured in WT and NFATc2-deficient animals treated with an anti–IFN-γ blocking antibody and with rIFN-γ, respectively, at the time of *C. albicans* infection. The analysis was performed at the indicated time points. Data are representative of two independent experiments. (F) Left: Increase of active plasmin levels in NFATc2-deficient mice at the indicated time points after *C. albicans* infection in the presence or not of rIFN-γ. Right: Increase of active plasmin levels in WT mice at the indicated time points after *C. albicans* infection in the presence or not of anti–IFN-γ blocking antibody. Each dot represents a single mouse. Means and SEM are depicted; a two-way ANOVA was used for statistics. (G) qRT-PCR analysis of IFN-γ mRNA in *C. albicans*–infected tissues before and 6 hours after the infection in WT animals depleted or not of NK cells. Each dot represents a single mouse. Means and SEM are depicted; a two-way ANOVA was used for statistics. (H) Kaplan-Meier curve showing the percentage of WT (n = 9), NK cell–depleted WT (n = 8), and NFATc2-deficient mice (n = 10) undergoing ulceration after *C. albicans* administration at the indicated time points. Log-rank test was used. (I) IFN-γ immunohistochemical staining in skin sections (brown cells) of WT mice treated or not with anti-asialo GM to eliminate NK cells (NK-depleted) and infected with *C. albicans*. Note that IFN-γ⁺ cells are strongly reduced in NK-depleted mice. (J) Kaplan-Meier curve showing the percentage of NFATc2-deficient mice (n = 10), NFATc2-deficient mice reconstituted with activated IFN-γ–sufficient NK cells (n = 10) or IFN-γ–deficient NK cells (n = 10), and WT animals (n = 8) undergoing ulceration at the indicated time points after *C. albicans* administration. Log-rank test was used.
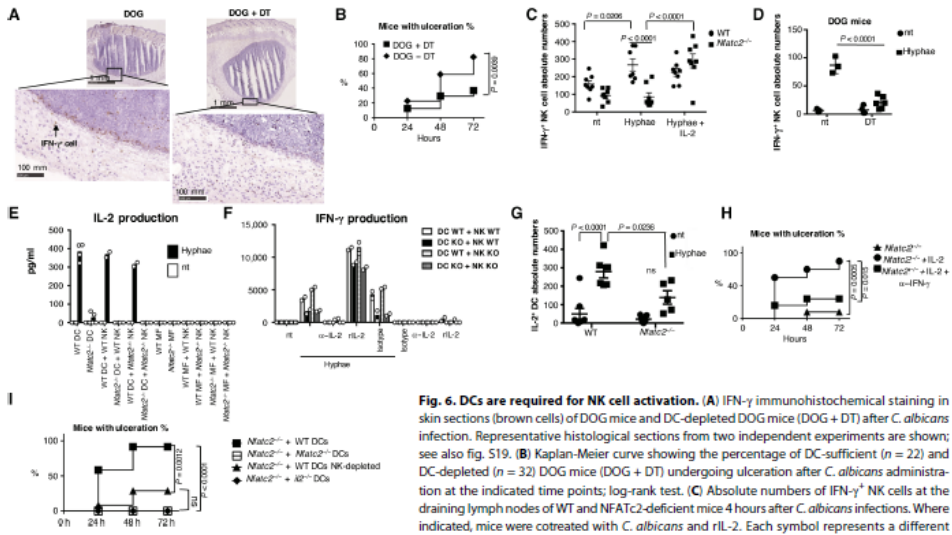
144

Fig. 6. DCs are required for NK cell activation. (**A**) IFN-γ immunohistochemical staining in skin sections (brown cells) of DOG mice and DC-depleted DOG mice (DOG + DT) after *C. albicans* infection. Representative histological sections from two independent experiments are shown; see also fig. S19. (**B**) Kaplan-Meier curve showing the percentage of DC-sufficient (*n* = 22) and DC-depleted (*n* = 32) DOG mice (DOG + DT) undergoing ulceration after *C. albicans* administration at the indicated time points; log-rank test. (**C**) Absolute numbers of IFN-γ⁺ NK cells at the draining lymph nodes of WT and NFATc2-deficient mice 4 hours after *C. albicans* infections. Where indicated, mice were cotreated with *C. albicans* and rIL-2. Each symbol represents a different mouse. Means and SDM are depicted; a two-way ANOVA test was used for statistics. (**D**) Absolute numbers of IFN-γ⁺ NK cells at the draining lymph nodes of DOG mice treated or not with DT 4 hours after *C. albicans* infections. Each symbol represents a different mouse. Means and SDM are depicted; a two-way ANOVA test was used for statistics. (**E**) IL-2 released in the supernatants by WT or NFATc2-deficient BMDCs and BM macrophages (MF) before and after *C. albicans* exposure (MOI, 0.05). IL-2 released by DCs–NK cell and macrophages–NK cell cocultures is also shown. Each dot represents a different sample. (**F**) Immature or *C. albicans*–activated WT and NFATc2-deficient BMDCs were cultured with NK cells for 18 hours. Where indicated, IL-2 was blocked using the S4B6 anti–IL-2 antibody (α–IL-2), or rIL-2 was added to the cultures. Levels of IFN-γ in the supernatant were then quantified by ELISA. Each dot represents a different sample. Representative data of two independent experiments are shown. KO, knockout. (**G**) Absolute numbers of IL-2⁺ DCs at the draining lymph nodes of WT and NFATc2-deficient mice 4 hours after *C. albicans* infections. Each symbol represents a different mouse. Means and SDM are depicted; a two-way ANOVA test was used for statistics. (**H**) Kaplan-Meier curves showing the percentage of NFATc2-deficient mice undergoing ulceration after *C. albicans* administration in the presence or not of the indicated stimuli and at the indicated time points; *n* (*Nfatc2⁻/⁻*) = 10, *n* (*Nfatc2⁻/⁻* + IL-2) = 8, *n* (*Nfatc2⁻/⁻* + IL-2 + α–IFN-γ) = 10; log-rank test. (**I**) Kaplan-Meier curves showing the percentage of NFATc2-deficient mice reconstituted with DCs of the indicated genotype undergoing ulceration after *C. albicans* administration. Where indicated, NK cells were depleted. *n* = 12 per group; log-rank test.

of *C. albicans* administration. As shown in Fig. 5F, IFN-γ restored plasmin generation in NFATc2-deficient mice, whereas the inhibition of IFN-γ down-modulated plasmin formation in WT animals.

Last, we evaluated the levels and function of activated matrix metalloproteinase–3 (MMP-3) during the infection. We focused on MMP-3 because it is efficiently activated by plasmin and is a master metalloproteinase that activates downstream metalloproteinases, such as MMP-9, and digests extracellular matrix components (*23*, *27*). As shown in fig. S14A, the increase of activated MMP-3 during the infection paralleled the increase of plasmin with the same relevant differences during abscess formation. In addition, treatment with an MMP-3 peptide inhibitor (MMP-3 inhibitor I) upon *C. albicans* administration inhibited ulceration (fig. S14B).

Natural killer cells are the major source of IFN-γ in WT animals, and DCs are essential accessory cells for natural killer cell activation during fungal infections

The next step was to determine the source of IFN-γ. Because *Rag2⁻/⁻* mice behaved like WT animals and showed a potent up-regulation of IFN-γ mRNA in the skin after infection (Fig. 1D and fig. S15), we

excluded a T cell origin for the IFN-γ and focused on innate immune cells. Elimination of natural killer (NK) cells by anti-asialo GM treatment strongly affected the levels of IFN-γ mRNA, as measured by qRT-PCR (Fig. 5G). Similarly, in the absence of NK cells, ulceration was strongly diminished after *C. albicans* infection of WT animals (Fig. 5H). Upon NK cell depletion, no IFN-γ⁺ cells were observed in the infected skins (Fig. 5I). These data confirm that NK cells are the major source of IFN-γ in our experimental system.

To formally demonstrate that NK cells are necessary and sufficient to provide IFN-γ under our experimental conditions, we first activated in vivo WT and IFN-γ–deficient NK cells and then adoptively transferred the activated NK cells into NFATc2-deficient mice infected with *C. albicans*. The course of the infection was then followed over time. After the adoptive transfer of activated WT but not IFN-γ–deficient NK cells, NFATc2-deficient mice showed ulceration (Fig. 5J). These data confirmed that IFN-γ provided by NK cells is necessary and sufficient to induce capsule degradation and ulceration.

Next, we unveiled the connection between NFATc2 and IFN-γ production by NK cells. In vitro, we observed that NFATc2 expression in accessory cells (e.g., DCs), but not in NK cells themselves,
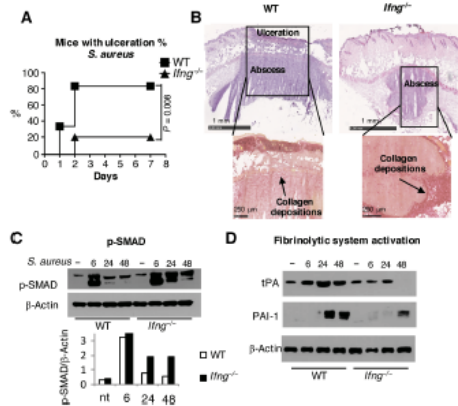
Fig. 7. Innate immune and fibrinolytic systems cooperate also during bacterial infections. (**A**) Kaplan-Meier curve showing the percentage of WT ($n = 6$) and IFN-γ–deficient mice ($n = 10$) undergoing ulceration after S. aureus administration at the indicated time points; log-rank test. Representative data of two independent experiments. (**B**) Hematoxylin and eosin staining of WT and IFN-γ–deficient mice skin lesions 48 hours after S. aureus infection. PicroSirius Red staining is also shown to evidence collagen depositions. (**C**) Western blot analysis of SMAD2/3 phosphorylation at the indicated time points after S. aureus infection of WT and IFN-γ–deficient mice. Data were quantified and normalized on β-actin. Data are representative of three independent experiments. (**D**) Western blot analysis of tPA and PAI-1 levels measured in WT and IFN-γ–deficient animals at the indicated hours after S. aureus infection.

was necessary for the production of IFN-γ by NK cells upon *C. albicans* encounter (fig. S16, A and B). We therefore predicted that eliminating DCs in vivo would influence IFN-γ production by NK cells after infection by *C. albicans*. We thus used B6.Cg-Tg(Itgax-DTR/OVA/EGFP)1Gjh/Crl (DOG) mice [which express a diphtheria toxin (DT) receptor under the CD11c promoter to eliminate DCs (28)] and studied the course of the infection in the absence of DCs. As we previously showed, DT treatment eliminated DCs from the skin, lymph node, and spleen (fig. S17) (29–31). The recruitment of inflammatory cells was not altered by DC depletion (fig. S18). IFN-γ+ cells were strongly diminished in DC-deficient skins compared with DC-sufficient mice, as revealed by immunohistochemistry (Fig. 6A and fig. S19). Accordingly, as depicted in Fig. 6B, the number of animals undergoing ulceration was significantly reduced. This finding suggests that DCs are required to elicit IFN-γ production by NK cells after *C. albicans* infection. In keeping with this observation, IFN-γ+ NK cells were strongly diminished in the lymph nodes of NFATc2-deficient and DC-deficient mice after infection, compared with control animals (Fig. 6, C and D).

We then determined why NFATc2-deficient DCs are not able to activate NK cells. Two cytokines involved in NK cell activation, namely, IL-12 and IL-2, were described to be produced in an NFAT-dependent manner by DCs in response to zymosan (5). We first measured IL-12p70 production by DCs after *C. albicans* hyphae infection, but, although it was previously shown to be induced in DCs upon zymosan administration, we found no IL-12 production

in response to the *C. albicans* hyphae challenge (fig. S20). We therefore focused on IL-2, described to be strongly induced in DCs during *C. albicans* hyphae infections as well (32–34) and also described to be necessary for eliciting IFN-γ production by NK cells during bacterial infections (30, 35). Figure 6 (E and F) shows that DC-derived IL-2 is required for NK cell activation in the presence of *C. albicans* in vitro and that NFATc2-deficient DCs were unable to activate NK cells because they do not produce IL-2. We thus evaluated the presence of IL-2+ DCs in the lymph nodes of WT and NFATc2-deficient mice after *C. albicans* administration. Whereas the numbers of DCs that produce IL-2 were strongly increased in WT animals after infection, no induction of IL-2 production by DCs was detected in NFATc2-deficient mice (Fig. 6G). Accordingly, in vivo IL-2 administration to NFATc2-deficient mice at the time of *C. albicans* infection restored NK cell activation (Fig. 6C). Moreover, after IL-2 administration, NFATc2-deficient mice presented ulceration (Fig. 6H). The restoration of ulcer formation in NFATc2-deficient mice upon IL-2 administration was inhibited when a blocking anti–IFN-γ antibody was also administered (Fig. 6H). These data demonstrate that after *C. albicans* infection, NFATc2-deficient DCs do not produce IL-2 and, consequently, do not induce IFN-γ release by NK cells.

To test whether DC-derived IL-2, produced in an NFATc2-depedent manner in response to *C. albicans* administration, was necessary and sufficient to induce ulceration, we performed the following experiment. NFATc2-deficient mice were adoptively transferred with WT, NFATc2-deficient, and IL-2–deficient DCs at the time of *C. albicans* administration, and the course of the infection was analyzed. As depicted in Fig. 6I, only mice that received WT DCs showed ulceration. Moreover, if NK cells were eliminated after the administration of WT DCs, ulceration was prevented (Fig. 6I).

Collectively, these data indicate that activation of NFATc2 in DCs during fungal infection regulates IL-2 production, which then elicits IFN-γ production by NK cells. In turn, IFN-γ is necessary for counteracting the TGF-β pathway and for allowing plasmin formation, collagen capsule digestion, and *C. albicans* expulsion.

IFN-γ antagonizes TGF-β signaling and allows abscess elimination through the activation of the fibrinolytic systems also during Staphylococcus aureus infections

Last, we investigated whether the cross-talk between the fibrinolytic and the innate immune systems, which regulates the persistence of the encapsulated abscess and the elimination of the microbes, applies not only to fungal but also to bacterial infections. Mice were infected with the Gram-positive bacterium S. aureus, which can infect the skin and form abscess. As shown in Fig. 7 (A and B), the infection induced skin ulceration in WT animals, whereas an encapsulated abscess formed in IFN-γ–deficient mice. As with *C. albicans* infections, excessive activation of the TGF-β pathway and overproduction of tPA and PAI-1 in WT with respect to IFN-γ–deficient mice were observed (Fig. 7, C and D). This indicates that also during bacterial infections, IFN-γ can induce the activation of the fibrinolytic system to favor microbial elimination.

DISCUSSION

In this study, we report two phases of the inflammatory response elicited by microbial infections of the skin. The first is the phase of infection containment. In this phase, granulocytes and fibroblasts
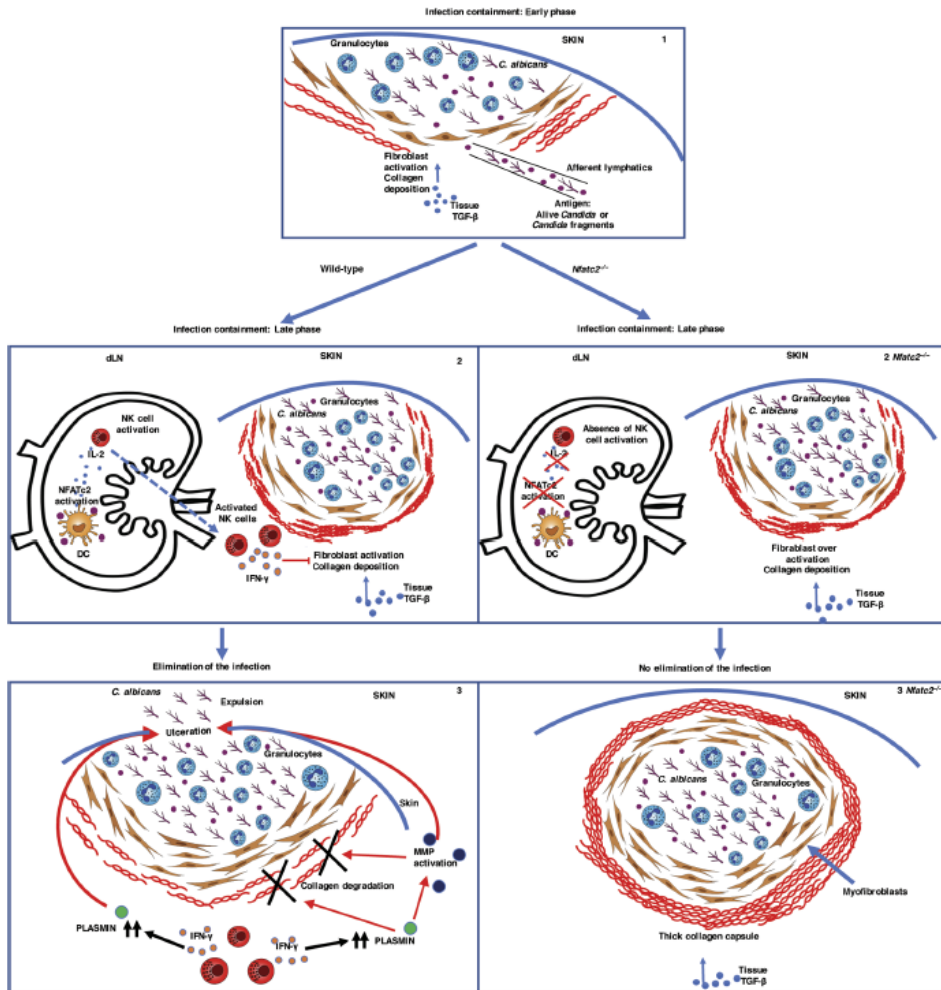
146

Fig. 8. NFAT activation in innate immune cells dictates the sterilization of *C. albicans* skin infection. Schematic of *C. albicans* skin infection containment and elimination. Distinct phases can be identified in the inflammatory process that takes place after *C. albicans* skin infections. During the very early phases (1), granulocytes are recruited and form an abscess around the invading microorganisms to avoid infection spreading. The containment of the infection is ensured by fibroblasts that, once activated by TGF-β, proliferate and deposit collagen around the abscess to form a capsule. Later, IFN-γ, produced by NK cells activated in the draining lymph nodes (dLN), antagonizes TGF-β and thus avoids excessive fibroblast activation and excessive collagen deposition and also avoids the differentiation of fibroblasts into myofibroblasts (2). Last, IFN-γ ensures the activation of the fibrinolytic system and the consequent activation of metalloproteinases by plasmin (3). During the elimination phase, proteinases digest the collagen capsule and induce skin ulceration for the microbial expulsion out of the skin (3). NFATc2 activation in DCs after *C. albicans* exposure leads to IL-2 production. In turn, IL-2 is required to elicit IFN-γ release by NK cells (2). In the absence of NFATc2, IFN-γ is not produced in sufficient amount to counteract the TGF-β pathway (2 *Nfatc2*−/−) and to induce the activation of the fibrinolytic system (3 *Nfatc2*−/−); therefore, fibroblasts are hyperactive, deposit excessive collagen, and differentiate in myofibroblasts (3 *Nfatc2*−/−). This leads to the formation of a thick capsule that prevents skin ulceration and microbial expulsion out of the skin.

147

form an organized abscess to control tissue damage and microbial spreading. The second phase leads to microbial elimination. This phase requires the activation of the fibrinolytic system that allows the discharge of microbes out of the skin. Upon infection, granulocytes are recruited to surround microbes, and active TGF-β promotes a profibrotic response that favors the deposit of collagen around the abscess to improve microbial containment. The release of IFN-γ in the skin by NK cells (previously activated in the lymph node by DCs) avoids excessive collagen deposition and the differentiation of fibroblasts into myofibroblasts, owing to the antagonistic effect of IFN-γ on the TGF-β pathway. IFN-γ also favors plasmin generation by inducing the production of tPA. Plasmin activates the process of collagen capsule digestion, skin ulceration, and microbe discharge (Fig. 8). NFATc2 regulates IL-2 production by DCs after fungal encounter, and DC-derived IL-2 is required for eliciting IFN-γ secretion by NK cells. In the absence of NFATc2, IFN-γ is not produced; therefore, the continuous signaling of TGF-β and the consequent differentiation of fibroblasts into myofibroblasts, together with the limited activation of the fibrinolytic system, lead to the generation of a very thick capsule around the abscess. The thick capsule hampers skin ulceration and microbial elimination; thus, only the containment phase takes place.

The containment phase of the inflammatory process, although efficient, is an evolutionary primitive way to control the infections because a mechanical insult could be sufficient to break the containment and spread the infection. This type of infection control is probably reminiscent of ancient innate responses with microbial confinement via encapsulation and melanization (2). The appearance of the NFAT signaling pathway in evolution has eventually enabled the elimination phase favoring the interaction between the innate immune system and the fibrinolytic system.

From the pathogen side, the generation of plasmin has been described to favor microbial invasiveness by favoring extracellular matrix degradation (36). We show here that the fibrinolytic system can also help microbial elimination if activated in the correct time frame. The early activation of the TGF-β pathway is likely to take place to also counteract the effects of premature plasmin generation.

The requirement of IL-2 for IFN-γ production and the requirement of IFN-γ for plasmin activation and *Candida* eradication provide a molecular explanation for why some patients with chronic mucocutaneous candidiasis show *C. albicans*–specific defects in IL-2 and/or IFN-γ production (37–40).

It is known that NFATc2 promotes T helper 1 (T_H1) and suppresses T_H2 responses (22). This has been attributed to the capacity of NFATc2 to regulate IFN-γ production by T cells (41). We show here that NK cells as well show a deficit of IFN-γ production in NFATc2-deficient mice. Diversely from T cells, the defect is not NK cell–intrinsic but affects DCs.

A previous work demonstrates that human NK cells can be directly activated by *C. albicans* (42), whereas we show here that mouse NK cells do not respond directly to *Candida* but need the presence of DCs to acquire the effector functions necessary to fight the infection. Our data may seem to conflict with these findings or may suggest that human and mouse NK cells behave differently. Nevertheless, the discrepancy between the two works could only be ostensible. In the work by Hellwig *et al*. (42), NK cells are maintained in culture in the presence of IL-2, and we show that IL-2 is indeed fundamental to induce NK cell activation. Therefore, accessory cells

could be required, also in humans, to provide an endogenous source of IL-2.

We showed that the absence of NFATc2 alters the levels of IFN-γ, and IFN-γ is required for capsule digestion and microbial expulsion from skin. Nevertheless, we cannot exclude the fact that other molecular events regulated by NFATc2 contribute to the formation of encapsulated abscesses during skin fungal infections. For instance, it is known that cardiac expression of α-SMA, which regulates the contractile activity of myofibroblasts, is induced by TGF-β via the activation of the NFAT signaling pathway in both fibroblasts and mesangial cells (43, 44). Therefore, it is also possible that the absence of NFATc2 could (directly or indirectly via deregulation of other NFAT member activation) generate a spontaneous tendency of fibroblasts to proliferate and differentiate into myofibroblasts. Although we found here that NK cells are activated at the draining lymph node, we cannot exclude the fact that NK cell activation can occur in the skin as well.

In conclusion, our study evidences the importance of the fibrinolytic system for the eradication of skin infections. Moreover, this work shows previously unknown roles for TGF-β and IFN-γ during the inflammatory process induced by microorganisms in the skin. TGF-β is mainly considered an anti-inflammatory cytokine that intervenes during the late phases of the inflammatory process to down-regulate inflammation and to start the resolution phase. In this study, it also emerges as a fundamental cytokine during the initial phases of the inflammatory response. By exerting its profibrotic functions, TGF-β increases the effectiveness of the inflammatory process to avoid excessive microbial spreading in the tissue. Moreover, IFN-γ contributes to microbial elimination not only by the induction of type 1 macrophages and neutrophils but also via the regulation of fibroblast functions (by antagonizing TGF-β) and the activation of the fibrinolytic system. IFN-γ–induced plasmin generation avoids excessive confinement of the infection (which obstructs microbial discharge) and allows microbial elimination that occurs not only via the phagocytic and antimicrobial activities of macrophages and neutrophils but also through direct microorganism elimination out of the ulcerated skin.

MATERIALS AND METHODS
Study design
The overall objective of the study was to analyze the role of NFATc2 in the innate immune response to *C. albicans* and *S. aureus* infections of the skin. There was not a predefined study component. Mice were injected in the deep derma with *C. albicans* or *S. aureus*, and the inflammatory response in the skin was investigated by histology, Western blot and cytofluorimetric analyses, and qRT-PCR. The study was not blind. For each experiment, the number of biological replicates is indicated in the figure legend.

Mouse strains
All mice, housed under specific pathogen–free conditions, had been on a B6 background for at least 12 generations and were used at 7 to 12 weeks of age. WT C57BL/6 mice were supplied by Envigo, Italy. IFN-γ–deficient mice were from the Jackson Laboratory. $Rag2^{-/-}$ mice were from CNRS Centre de Distribution, Typage et Archivage animal in Orleans, France. CD11c.DOG mice were provided by N. Garbi (Institute of Molecular Medicine and Experimental Immunology, Bonn, Germany). In these mice, a specific DC ablation

148

can be induced by DT injection. IL-2–deficient mice were provided by A. Schimpl (University of Würzburg, Würzburg, Germany) NFATc2-deficient mice were provided by E. Serfling (University of Würzburg, Germany).

C. albicans growth conditions and hyphal induction

The *C. albicans* strain CAF3-1 (*ura3Δ::imm434/ura3Δ::imm434*), provided by W. A. Fonzi (Georgetown University), was routinely grown at 25°C in rich medium [YEPD (yeast extract, peptone, dextrose), 1% (w/v) yeast extract, 2% (w/v) Bacto Peptone, and 2% (w/v) glucose] supplemented with uridine (50 mg/liter) as described. In this growth condition, cells showed a typical yeast morphology, and growth was monitored by counting the cell number using a Coulter Counter-Particle Count and Size Analyser. Once cells reached a concentration of about 8×10^6 cells/ml, the total culture was harvested by centrifugation and resuspended in an equivalent volume of YEPD-uridine medium buffered with Hepes (50 mM, pH 7.5). Cells were incubated at 37°C for hyphal induction. Formation of hyphae was evaluated under a microscope at different time points following induction until its amount was assessed at 95%.

S. aureus

S. aureus ATCC6538P cells were grown in LB medium (Difco) at 37°C. For subcutaneous infections, stationary phase cultures were diluted to an optical density at 600 nm (OD_{600}) of 0.05 and then grown until they reached an OD_{600} of 0.25 that corresponded approximately to 10^8 colony-forming units (CFU)/ml. Cells were washed in phosphate-buffered saline, and appropriate dilutions were injected in mice.

In vivo infections

Mice were prepared by shaving the dorsal region at least 24 hours before injection. Mice were then injected in the deep derma with *C. albicans* hyphae (5×10^6 in a total volume of 50 µl) or 10^6 CFU of *S. aureus* in a final volume of 50 µl in the shaved dorsal regions and macroscopically analyzed 1, 2, 3, and 7 days later for skin ulceration. In addition, infected skin was collected at different time points for histological and biochemical analyses.

In some experiments, recombinant IFN-γ [1 µg per mouse subcutaneously (sc); catalog no. 315-05, PeproTech] or LEAF purified anti-mouse IFN-γ (50 µg per mouse sc; clone R4-6A2, catalog no. 505706; BioLegend) were co-injected together with *C. albicans* hyphae. LEAF purified rat immunoglobulin G1 κ (IgG1 κ) (clone RTK2071, BioLegend) was used as isotype control (35 µg per mouse sc); SB-431542 (catalog no. 13031, Cayman Chemical) was used as TGF-β inhibitor. It was injected daily intraperitoneally (ip) for 3 days, starting from day −1 (50 µg per mouse). For MMP-3 inhibition, MMP-3 inhibitor I was purchased from Calbiochem (catalog no. 444218) and injected sc together with *C. albicans* hyphae at a dosage of 125 µg per mouse. The inhibitor was then reinjected 6 hours after infection (250 µg per mouse) intravenously (iv). Plasmin activation was blocked by injecting human PAI-1 (0.65 µg per mouse) (25 µg; catalog no. A8111, Sigma-Aldrich) sc 6 hours before infection. Last, recombinant IL-2 (1 µg per mouse, 402-ML carrier-free, R&D Systems) was co-injected sc with *C. albicans*.

For NK cell depletion, mice received anti-asialo GM1 polyclonal antibodies (eBioscience, 30µg per mouse iv) at days −3, −1, and +1. For DC depletion, DOG mice were treated with DT (Sigma-Aldrich, 16 ng/g) sc and iv 4 hours before *C. albicans* infection. DT was readministered iv 48 hours later.

Histopathology

Immunohistochemistry

Explanted skins were embedded in optimal cutting temperature freezing media (Bio-Optica). Sections (5 µm) were cut on a cryostat, adhered to a Superfrost Plus slide (Thermo Scientific), fixed with acetone, and blocked with Normal Goat Serum (1:10) for 30 min at room temperature. Sections were then stained with primary antibody specific for α-SMA (ab5694, Abcam), p-SMAD2/3 (clone D27F4, Cell Signaling), or IFN-γ (XMG1.2, Thermo Scientific), 1 hour at room temperature. LEAF purified rat IgG1 κ (clone RTK2071, BioLegend) was used as isotype control for IFN-γ staining, whereas purified rabbit polyclonal IgG (BD Pharmingen) was used as isotype control for α-SMA and p-SMAD2/3 (see fig. S26). Sections were washed with tris-buffered saline buffer, then labeled 30 min at room temperature with the Dako EnVision Anti-Rabbit System-HRP according to the manufacturer's recommendations, and counterstained with Meyer's hematoxylin solution (Bio-Optica). After dehydration, stained slides were mounted with Eukitt, and images were acquired with the NanoZoomer (Hamamatsu).

Hematoxylin and eosin staining

Skin sections (5 µm) were stained with Meyer's hematoxylin solution for 8 min and then washed in warm running tap water for 5 min. Sections were stained with Eosin Y solution for 1 min, washed in warm running tap water for 5 min, rinsed in distilled water, and then dehydrated through passages in 95% and absolute alcohol. After dehydration, stained slides were cleared in xylene and mounted with Eukitt. Images were acquired with the NanoZoomer (Hamamatsu).

PicroSirius Red staining

Sections were stained with Meyer's hematoxylin solution for 8 min and then washed for 10 min in running tap water. Sections were stained in PicroSirius Red for 1 hour and then washed in two changes of acidified water. After dehydration in three changes of 100% ethanol, slides were cleared in xylene and mounted in Eukitt. Images were acquired with the NanoZoomer (Hamamatsu).

For collagen quantification, five fields (20×) from two sections per group were analyzed by separation into a red, green, and blue (RGB) filter, and the red area was mathematically divided by the RGB area and multiplied by 100%. This calculation represents the percentage area staining positively for collagen fibers.

Periodic acid–Schiff staining

Sections were fixed with acetone for 1 min at room temperature and then washed for 1 min in slowly running tap water. Slides were rinsed in periodic acid solution for 5 min at room temperature. Slides were rinsed with several changes of distilled water and then with Schiff's reagent for 15 min at room temperature. After washing in running tap water, slides were counterstained in hematoxylin solution for 5 min. Last, slides were dehydrated in three changes of 100% ethanol, cleared in xylene, and mounted in Eukitt. Images were acquired with the NanoZoomer (Hamamatsu).

Flow cytometry

Intracellular staining was performed on lymph node single-cell suspension using Cytofix/Cytoperm reagents (BD Biosciences) according to the manufacturer's instructions. Single-cell suspensions were kept for 3 hours in the presence of brefeldin A (10 µg/ml; Sigma-Aldrich) before staining.

The antibodies used were as follows: phycoerythrin (PE)–anti-mouse CD49b (clone DX5, catalog no. 108908; BioLegend); allophycocyanin (APC)–anti-mouse IFN-γ (clone XMG1.2, catalog no. 505810; BioLegend); fluorescein isothiocyanate (FITC)–anti-mouse

149

CD3 (clone 17A2, (catalog no. 100204; BioLegend); APC–anti-mouse CD11b (clone M1/70, catalog no. 101212; BioLegend); PE–anti-mouse CD11c (clone N418, catalog no. 117308; BioLegend); APC–anti-mouse CD11c (clone N418, catalog no. 117310; BioLegend); APC/Cy7–anti-mouse CD3 (clone 17A2, catalog no.100222; BioLegend); and peridinin chlorophyll protein–anti-mouse NK1.1 (clone PK136); Alexa 488–anti-mouse I-Ab antibody (clone AF&-120.1); and PE–anti-mouse IL-2 (clone JES6-5H4) (all from BioLegend).

The antibodies used as isotype controls were as follows: PE mouse IgG2a, κ (catalog no. 400211, BioLegend); FITC rat IgG2b, κ (catalog no. 400605, BioLegend); APC rat IgG1, κ (catalog number 400411); PE rat IgG2b, κ (catalog no. 400607, BioLegend); PE/Cy7 mouse IgG2a, κ (catalog no. 400253, BioLegend); and APC/Cy7 Armenian hamster IgG (catalog no. 400927, BioLegend). NK cells were identified as NK1.1$^+$CD3$^-$ lymphocytes. DCs were identified as CD11c$^+$MHCII$^+$ cells. Samples were acquired with a Gallios flow cytometer (Beckman Coulter).

Cells

Bone marrow–derived dendritic cells (BMDCs) were generated by culturing bone marrow (BM) precursors, flushed from femurs, in Iscove's modified Dulbecco's medium (IMDM) (Euroclone) containing 10% heat-inactivated fetal bovine serum (Euroclone), 100 IU of penicillin, streptomycin (100 μg/ml), 2 mM L-glutamine (Euroclone), and granulocyte-macrophage colony-stimulating factor (CSF) (10 to 20 ng/ml) for 8 days. BM-derived macrophages were cultured in IMDM containing 100 IU of penicillin, streptomycin (100 μg/ml), 2 mM L-glutamine (all from Euroclone), and macrophage CSF (10 to 20 ng/ml) for 10 days.

DCs for adoptive transfer experiments were expanded in vivo by transplanting mice with B16 tumor cells transduced with Flt3 ligand (FLT3L). Ten days after in vivo expansion, CD11c$^+$ cells were purified from spleen by magnetic-activated cell sorting (MACS) by positive selection using CD11c microbeads (Miltenyi Biotec).

NK cells for in vitro experiments and for adoptive transfer experiments were purified from splenocytes (after red blood cell lysis) by MACS positive selection using CD49b (DX5) microbeads (Miltenyi Biotec). Purity was assessed by fluorescence-activated cell sorting (FACS) analysis and was routinely between 93 and 96%.

Skin fibroblasts were isolated and differentiated from the ears of adult C57BL/6 WT and NFATc2-deficient mice. Mice were euthanized and ears were removed. The ears were then divided into two layers and cut into small pieces that were placed in a six-well tissue culture plate with 3 ml of Dulbecco's modified Eagle's medium (catalog no. ECB7501L, Euroclone) containing 10% heat-inactivated fetal bovine serum (catalog no. 10270, Gibco), 100 IU of penicillin, streptomycin (100 μg/ml), 2 mM L-glutamine (all from Euroclone), epidermal growth factor (1 μg/ml) (SRP3196, Sigma-Aldrich), and fibroblast growth factor 2 (1 ng/ml) (SRP4038, Sigma-Aldrich) for 1 week. After 1 week, adherent fibroblasts were detached with trypsin/EDTA (catalog no. ECB3001D, Euroclone) and grown in tissue culture plates. At 80% of confluence, cells were detached and divided by a ratio of 1:2 until passages 4 and 5 when they were used for experimental procedures.

NK-DC cocultures

BMDCs (1×10^5 per well) and NK cells (5×10^4 per well for IFN-γ release assays) were cocultured in flat-bottom 96-well plates in the presence or absence of *C. albicans* hyphae [multiplicity of infection (MOI), 0.005], and, where indicated, recombinant IL-2 (rIL-2) (7.5 ng/ml)

(402-ML carrier-free, R&D Systems), or purified rat anti-mouse IL-2 (5 μg/ml) (BD Biosciences) or purified rat IgG2a (5 μg/ml) (BD Biosciences) as isotype control. Two hours after stimulation, amphotericin B (2.5 μg/ml) (Sigma-Aldrich) was added to the cultures.

TNF-α, IL-2, IFN-γ, and IL-12 measurement

Concentrations of IL-2, TNF-α, IFN-γ, and IL-12 in supernatants were assessed by enzyme-linked immunosorbent assay (ELISA) kits purchased from BD OptEIA, eBioscience, and R&D Systems, respectively.

Quantitative reverse transcription polymerase chain reaction

Pieces of lateral skin were homogenized in TRIzol reagent, and then RNA was extracted using Qiagen RNeasy Mini Kit (catalog no. 74104). Single-strand complementary DNA (cDNA) was synthesized using High-Capacity cDNA Reverse Transcription Kits (catalog no. 4368814, Applied Biosystems). The NanoDrop (Thermo Scientific) was used to titer mRNA, and amplification was performed using either the TaqMan Gene Expression Master Mix (catalog no. 4369016, Applied Biosystems) and TaqMan probes (Ifng, Mm01168134_m1; Fcer1a, Mm00438867_m1; SiglecF, Mm00523987_m1; Ly6c, Mm03009946_m1; Cd11c Mm00498698_m1; Nfatc1, Mm00479445_m1; Nfatc2, Mm01240677_m1; Nfatc3, Mm01249200_m1; 18S, Mm03928990_g1;Gapdh, Mm99999915_g1) or the Power SYBR Green PCR Master Mix (Applied Biosystems) (Ly-6G: forward, 5′-TGGACTCTCA-CAGAAGCAAAG-3′ and reverse, 5′-GCAGAGGTCTTCCTTC-CAACA-3′; Gapdh: forward, 5′-CTGGCCAAGGTCATCCATG-3′ and reverse, 5′-GCCATGCCAGTGAGCTTCC-3′). Relative mRNA expression was calculated using the ΔC_t method, using either *Gapdh* or *18S* as a reference gene.

Western blot

Pieces of lateral skin were cut, put in Eppendorf tubes, and immersed in liquid nitrogen for snap freezing. Tissues were smashed and homogenized in 1 ml of lysis buffer [50 mM tris-HCl (pH 7.4), 150 mM NaCl, 10% glycerol, and 1% NP-40 supplemented with protease and phosphatase inhibitor cocktails; Roche] using a TissueLyser (full speed for 20 min, Qiagen). Samples were then maintained in constant agitation for 2 hours at 4°C and centrifuged for 20 min at 13,000g at 4°C. The supernatants were collected into a new Falcon tube. Proteins were quantified using a bicinchoninic acid assay (Euroclone). Cell lysates (150 μg) were run on a 10% polyacrylamide gel, and SDS–polyacrylamide gel electrophoresis was performed following standard procedures. After protein transfer, nitrocellulose membranes (Thermo Scientific) were incubated with the antibodies specific for phosphorylated SMAD2/3 (clone D27F4, Cell Signaling), mSerpin E1 (goat polyclonal IgG, R&D Systems), tPA (rabbit polyclonal, NOVUS Biologicals), and β-actin (rabbit polyclonal, Cell Signaling) and developed using an enhanced chemiluminesence substrate reagent (Thermo Scientific).

Plasmin and MMP-3 activity assays

Pieces of lateral skin were cut, put in Eppendorf tubes, and immersed in liquid nitrogen for snap freezing. Tissues were smashed and homogenized in 1 ml of an optimized buffer [150 nM NaCl, 1% NP-40, and 50 mM tris-HCl (pH 8.0)] with a TissueLyser (Qiagen) (full speed for 20 min at 4°C). Samples were then maintained in

150

constant agitation for 2 hours at 4°C and centrifuged for 20 min at 13,000g at 4°C. Samples (50 μl) were then used for plasmin measurement using the Plasmin Activity Assay Kit (Abcam) and for active MMP-3 measurement using the Activity Assay Kit (Abcam).

Adoptive transfer experiments

For the adoptive transfer of NK cells, WT or IFN-γ–deficient mice were injected iv with lipopolysaccharide (LPS) (2 mg LPS/gbw) to activate NK cells. Two hours and 30 min after activation, NK cells were purified from spleen and administered iv to NFATc2-deficient mice (2×10^6 per mouse) 4 hours after *C. albicans* infection.

For the experiments of DC adoptive transfer, DCs were purified form the spleen of WT, NFATc2-deficient, and IL-2–deficient mice. Purified DCs were then co-injected with *C. albicans* (2×10^6 per mouse). The same mice also received purified DCs by intravenous administration (10^6 per mouse) after *C. albicans* infection.

Statistical analysis

Means were compared by either unpaired parametric *t* tests or two-way analysis of variance (ANOVA). Data are expressed and plotted as means ± squared deviations from the mean (SDM) or ± SEM values. Sample sizes for each experimental condition are provided in the figure legends. *P* values for Kaplan-Meier curves were calculated with log-rank test. All *P* values were calculated using Prism (GraphPad). Differences were considered significant if $P \leq 0.05$.

SUPPLEMENTARY MATERIALS

Immunology.sciencemag.org/cgi/content/full/2/15/eaan2725/DC1
Fig. S1. Expression of NFATc1, NFATc2, and NFATc3 in immune cells.
Fig. S2. Magnifications of the selected areas shown in Fig. 1C.
Fig. S3. Additional histological images of the abscess after *C. albicans* infection.
Fig. S4. Histology of the abscess 1 month after infection of NFATc2-deficient mice.
Fig. S5. Granulocyte and monocyte recruitment at the infection site of WT and NFATc2-deficient mice.
Fig. S6. Visualization of *C. albicans* at the infection site 6 to 8 days after infection.
Fig. S7. Additional histological images of α-SMA staining in skin sections of WT and NFATc2-deficient mice.
Fig. S8. Additional histological images of p-SMAD2,3 staining.
Fig. S9. Magnifications of the selected areas shown in Fig. 3D.
Fig. S10. Additional histological images of the abscesses after *C. albicans* infection in the presence of a TGF-β inhibitor.
Fig. S11. Additional histological images of IFN-γ staining.
Fig. S12. IFN-γ induces capsule digestion.
Fig. S13. Additional histological images of the abscesses after *C. albicans* infection in the presence of PAI-1.
Fig. S14. Inhibition of plasmin or MMP-3 interferes with *C. albicans* elimination.
Fig. S15. IFN-γ mRNA is up-regulated in the infected skin of RAG-2-deficient mice.
Fig. S16. DCs are necessary for the activation of NK cells in the presence of *C. albicans* in vitro.
Fig. S17. DC depletion after DT injection in DOG mice.
Fig. S18. Granulocyte and monocyte recruitment at the infection site of DOG mice treated or not with DT to deplete DCs.
Fig. S19. Additional histological images of IFN-γ staining in the infected skin of DOG mice.
Fig. S20. IL-12 production by BMDCs after *C. albicans* stimulation.
Fig. S21. Original Western blots shown in Fig. 3A.
Fig. S22. Original Western blots shown in Fig. 4 (E and F).
Fig. S23. Original Western blots shown in Fig. 5E.
Fig. S24. Original Western blots shown in Fig. 7C.
Fig. S25. Original Western blots shown in Fig. 7D.
Fig. S26. Representative isotype control stainings for immunohistochemical analyses.
Fig. S27. Gating strategies used in cytofluorimetric analyses.
Fig. S28. Representative isotype control stainings for cytofluorimetric analyses.
Raw data for Figs. 1 (B, D, and E), 4 (A, C, and G), 5 (A, C, F, G, H, and J), 6 (B to I), and 7A; and figs. S1 (A and B), S5, S14, S15, S16, S17A, S18, and S20 (Microsoft Excel format).

Santus et al., Sci. Immunol. 2, eaan2725 (2017)   22 September 2017

REFERENCES AND NOTES

1. M. R. Müller, A. Rao, NFAT, immunity and cancer: A transcription factor comes of age. *Nat. Rev. Immunol.* **10**, 645–656 (2010).
2. L.-M. Vanha-Aho, S. Valanne, M. Rämet, Cytokines in *Drosophila* immunity. *Immunol. Lett.* **170**, 42–51 (2016).
3. H. Wu, A. Peisley, I. A. Graef, G. R. Crabtree, NFAT signaling and the invention of vertebrates. *Trends Cell Biol.* **17**, 251–260 (2007).
4. I. Zanoni R. Ostuni, G. Capuano, M. Collini, M. Caccia, A. E. Ronchi, M. Rocchetti, F. Mingozzi, M. Foti, G. Chirico, B. Costa, A. Zaza, P. Ricciardi-Castagnoli, F. Granucci, CD14 regulates the dendritic cell life cycle after LPS exposure through NFAT activation. *Nature* **460**, 264 (2009).
5. H. S. Goodridge, R. M. Simmons, D. M. Underhill, Dectin-1 stimulation by *Candida albicans* yeast or zymosan triggers NFAT activation in macrophages and dendritic cells. *J. Immunol.* **178**, 3107–3115 (2007).
6. M. B. Greenblatt, A. Aliprantis, B. Hu, L. H. Glimcher, Calcineurin regulates innate antifungal immunity in neutrophils. *J. Exp. Med.* **207**, 923–931 (2010).
7. S. Xu, J. Huo, K. G. Lee, T. Kurosaki, K. P. Lam, Phospholipase Cγ2 is critical for Dectin-1-mediated Ca2+ flux and cytokine production in dendritic cells. *J. Biol. Chem.* **284**, 7038 (2009).
8. D. Mourão-Sá, M. J. Robinson, S. Zelenay, D. Sancho, P. Chakravarty, R. Larsen, M. Plantinga, N. Van Rooijen, M. P. Soares, B. Lambrecht, C. Reis e Sousa, CLEC-2 signaling via Syk in myeloid cells can regulate inflammatory responses. *Eur. J. Immunol.* **41**, 3040–3053 (2011).
9. T. Yamasaki, W. Ariyoshi, T. Okinaga, Y. Adachi, R. Hosokawa, S. Mochizuki, K. Sakurai, T. Nishihara, The dectin 1 agonist curdlan regulates osteoclastogenesis by inhibiting nuclear factor of activated T cells cytoplasmic 1 (NFATc1) through Syk kinase. *J. Biol. Chem.* **289**, 19191–19203 (2014).
10. N. Perico, G. Remuzzi, Prevention of transplant rejection: Current treatment guidelines and future developments. *Drugs* **54**, 533–570 (1997).
11. M. S. Deleuran, C. Vestergaard, Therapy of severe atopic dermatitis in adults. *J. Dtsch. Dermatol. Ges.* **10**, 399–406 (2012).
12. E. Roekevisch, P. I. Spuls, D. Kuester, J. Limpens, J. Schmitt, Efficacy and safety of systemic treatments for moderate-to-severe atopic dermatitis: A systematic review. *J. Allergy Clin. Immunol.* **133**, 429–438 (2014).
13. S. W. Kashem, B. Z. Igyarto, M. Gerami-Nejad, Y. Kumamoto, J. A. Mohammed, E. Jarrett, R. A. Drummond, S. M. Zurawski, G. Zurawski, J. Berman, A. Iwasaki, G. D. Brown, D. H. Kaplan, *Candida albicans* morphology and dendritic cell subsets determine T helper cell differentiation. *Immunity* **42**, 356–366 (2015).
14. J. A. Fishman, Infections in immunocompromised hosts and organ transplant recipients: Essentials. *Liver Transpl.* **17** (suppl. 3), S34–S37 (2011).
15. X.-m. Meng, D. J. Nikolic-Paterson, H. Y. Lan, TGF-β: The master regulator of fibrosis. *Nat. Rev. Nephrol.* **12**, 325–338 (2016).
16. N. Khalil, TGF-β: From latent to active. *Microbes Infect.* **1**, 1255–1263 (1999).
17. M. A. Travis, D. Sheppard, TGF-β activation and function in immunity. *Annu. Rev. Immunol.* **32**, 51–82 (2014).
18. A. W. Taylor, Review of the activation of TGF-β in immunity. *J. Leukoc. Biol.* **85**, 29–33 (2009).
19. X. Dong, B. Zhao, R. E. Iacob, J. Zhu, A. C. Koksal, C. Lu, J. R. Engen, T. A. Springer, Force interacts with macromolecular structure in activation of TGF-β. *Nature* **542**, 55–59 (2017).
20. L. Ulloa, J. Doody, J. Massagué, Inhibition of transforming growth factor-β/SMAD signalling by the interferon-γ/STAT pathway. *Nature* **397**, 710–713 (1999).
21. O. Eickelberg, A. Pansky, E. Koehler, M. Bihl, M. Tamm, P. Hildebrand, A. P. Perruchoud, M. Kashgarian, M. Roth, Molecular mechanisms of TGF-β antagonism by interferon γ and cyclosporine A in lung fibroblasts. *FASEB J.* **15**, 797–806 (2001).
22. K. J. Erb, T. Twardzik, A. Palmetshofer, G. Wohlleben, U. Tatsch, E. Serfling, Mice deficient in nuclear factor of activated T-cell transcription factor c2 mount increased Th2 responses after infection with *Nippostrongylus brasiliensis* and decreased Th1 responses after mycobacterial infection. *Infect. Immun.* **71**, 6641–6647 (2003).
23. N. Ramos-DeSimone, E. Hahn-Dantona, J. Sipley, H. Nagase, D. L. French, J. P. Quigley, Activation of matrix metalloproteinase-9 (MMP-9) via a converging plasmin/stromelysin-1 cascade enhances tumor cell invasion. *J. Biol. Chem.* **274**, 13066–13076 (1999).
24. G. E. Davis, K. A. Pintar Allen, R. Salazar, S. A. Maxwell, Matrix metalloproteinase-1 and -9 activation by plasmin regulates a novel endothelial cell-mediated mechanism of collagen gel contraction and capillary tube regression in three-dimensional collagen matrices. *J. Cell Sci.* **114**, 917–930 (2001).
25. S. Monea, K. Lehti, J. Keski-Oja, P. Mignatti, Plasmin activates pro-matrix metalloproteinase-2 with a membrane-type 1 matrix metalloproteinase-dependent mechanism. *J. Cell. Physiol.* **192**, 160–170 (2002).
26. D. M. Dupont, J. B. Madsen, T. Kristensen, J. S. Bodker, G. E. Blouse, T. Wind, P. A. Andreasen, Biochemical properties of plasminogen activator inhibitor-1. *Front. Biosci. (Landmark Ed.)* **14**, 1337–1361 (2009).

13 of 14

151

27. H. R. Lijnen, Plasmin and matrix metalloproteinases in vascular remodeling. *Thromb. Haemost.* **86**, 324–333 (2001).

28. K. Hochweller, J. Striegler, G. J. Hämmerling, N. Garbi, A novel CD11c.DTR transgenic mouse for depletion of dendritic cells reveals their requirement for homeostatic proliferation of natural killer cells. *Eur. J. Immunol.* **38**, 2776–2783 (2008).

29. I. Zanoni, R. Ostuni, S. Barresi, M. Di Gioia, A. Broggi, B. Costa, R. Marzi, F. Granucci, CD14 and NFAT mediate lipopolysaccharide-induced skin edema formation in mice. *J. Clin. Invest.* **122**, 1747–1757 (2012).

30. I. Zanoni, R. Spreafico, C. Bodio, M. Di Gioia, C. Cigni, A. Broggi, T. Gorletta, M. Caccia, G. Chirico, L. Sironi, M. Collini, M. P. Colombo, N. Garbi, F. Granucci, IL-15 *cis* presentation is required for optimal NK cell activation in lipopolysaccharide-mediated inflammatory conditions. *Cell Rep.* **4**, 1235–1249 (2013).

31. F. Mingozzi, R. Spreafico, T. Gorletta, C. Cigni, M. Di Gioia, M. Caccia, L. Sironi, M. Collini, M. Soncini, M. Rusconi, U. H. von Andrian, G. Chirico, I. Zanoni, F. Granucci, Prolonged contact with dendritic cells turns lymph node-resident NK cells into anti-tumor effectors. *EMBO Mol. Med.* **8**, 1039–1051 (2016).

32. N. C. Rogers, E. C. Slack, A. D. Edwards, M. A. Nolte, O. Schulz, E. Schweighoffer, D. L. Williams, S. Gordon, V. L. Tybulewicz, G. D. Brown, C. Reis e Sousa, Syk-dependent cytokine induction by Dectin-1 reveals a novel pattern recognition pathway for C type lectins. *Immunity* **22**, 507–517 (2005).

33. T. Zelante, A. Y. W. Wong, T. J. Ping, J. Chen, H. R. Sumatoh, E. Vigano, Y. Hong Bing, B. Lee, F. Zolezzi, J. Fric, E. W. Newell, A. Mortellaro, M. Poidinger, P. Puccetti, P. Ricciardi-Castagnoli, CD103+ dendritic cells control Th17 cell function in the lung. *Cell Rep.* **12**, 1789–1801 (2015).

34. O. Boyman, J. Sprent, The role of interleukin-2 during homeostasis and activation of the immune system. *Nat. Rev. Immunol.* **12**, 180–190 (2012).

35. F. Granucci, I. Zanoni, N. Pavelka, S. L. H. van Dommelen, C. E. Andoniou, F. Belardelli, M. A. Degli Esposti, P. Ricciardi-Castagnoli, A contribution of mouse dendritic cell-derived IL-2 for NK cell activation. *J. Exp. Med.* **200**, 287–295 (2004).

36. S. Bergmann, S. Hammerschmidt, Fibrinolysis and host response in bacterial infections. *Thromb. Haemost.* **98**, 512–520 (2007).

37. F. L. van de Veerdonk, T. S. Plantinga, A. Hoischen, S. P. Smeekens, L. A. B. Joosten, C. Gilissen, P. Arts, D. C. Rosentul, A. J. Carmichael, C. A. A. Smits-van der Graaf, B. J. Kullberg, J. W. M. van der Meer, D. Lilic, J. A. Veltman, M. G. Netea, STAT1 mutations in autosomal dominant chronic mucocutaneous candidiasis. *N. Engl. J. Med.* **365**, 54–61 (2011).

38. K. Eyerich, S. Rombold, S. Foerster, H. Behrendt, H. Hofmann, J. Ring, C. Traidl-Hoffmann, Altered, but not diminished specific T cell response in chronic mucocutaneous candidiasis patients. *Arch. Dermatol. Res.* **299**, 475–481 (2007).

39. D. de Moraes-Vasconcelos, N. M. Orii, C. C. Romano, R. Y. Iqueoka, A. J. D. S. Duarte, Characterization of the cellular immune function of patients with chronic mucocutaneous candidiasis. *Clin. Exp. Immunol.* **123**, 247–253 (2001).

40. D. Lilic, I. Gravenor, N. Robson, D. A. Lammas, P. Drysdale, J. E. Calvert, A. J. Cant, M. Abinun, Deregulated production of protective cytokines in response to *Candida albicans* infection in patients with chronic mucocutaneous candidiasis. *Infect. Immun.* **71**, 5690–5699 (2003).

41. A. Kiani, F. J. Garcia-Cózar, I. Habermann, S. Laforsch, T. Aebischer, G. Ehninger, A. Rao, Regulation of interferon-γ gene expression by nuclear factor of activated T cells. *Blood* **98**, 1480–1488 (2001).

42. D. Hellwig, J. Voigt, M. Bouzani, J. Löffler, D. Albrecht-Eckardt, M. Weber, S. Brunke, R. Martin, O. Kurzai, K. Hünniger, *Candida albicans* induces metabolic reprogramming in human NK cells and responds to perforin with a zinc depletion response. *Front. Microbiol.* **7**, 750 (2016).

43. S. L. Cobbs, J. L. Gooch, NFATc is required for TGFβ-mediated transcriptional regulation of fibronectin. *Biochem. Biophys. Res. Commun.* **362**, 288–294 (2007).

44. K. M. Herum, I. G. Lunde, B. Skrbic, G. Florholmen, D. Behmen, I. Sjaastad, C. R. Carlson, M. F. Gomez, G. Christensen, Syndecan-4 signaling via NFAT regulates extracellular matrix production and cardiac myofibroblast differentiation in response to mechanical stress. *J. Mol. Cell. Cardiol.* **54**, 73–81 (2013).

Citation: W. Santus, S. Barresi, F. Mingozzi, A. Broggi, I. Orlandi, G. Stamerra, M. Val, A. M. Martorana, A. Polissi, J. R. Köhler, N. Liu, I. Zanoni, F. Granucci, Skin infections are eliminated by cooperation of the fibrinolytic and innate immune systems. *Sci. Immunol.* **2**, eaan2725 (2017).

152

RIASSUNTO

A partire dalla seconda metà del secolo scorso in molti Paesi sviluppati, l'aspettativa di vita è progressivamente aumentata, raggiungendo e in molti casi superando la soglia degli 85 anni.

Comunque, questo aumento dell'aspettativa di vita non è associato con un altrettanto aumento delle condizioni di salute nella popolazione anziana.

Oggigiorno, un'ampia parte di popolazione al di sopra dei 65 anni soffre di molteplici malattie, molte delle quali debilitanti, come le malattie cardiovascolari, i tumori o i disordini neurodegenerativi. Questo aspetto ha aumentato l'interesse per le tematiche legate all'invecchiamento, enfatizzando l'importanza di ridurre il gap tra longevità salute durante l'invecchiamento.

A questo proposito, gli sforzi di molte linee di ricerca sono focalizzati nel tentativo di comprendere quali sono i principali fattori che influenzano l'invecchiamento, allo scopo di sviluppare approcci capaci di mitigare gli effetti dannosi dell'invecchiamento sulla salute. Molti pathway associati all'invecchiamento sono evolutivamente conservati dagli organismi unicellulari a quelli più complessi. Questo ci ha permesso di semplici organismi modello per studiare questo complesso fenomeno biologico. In questo lavoro abbiamo utilizzato l'eucariote unicellulare *Saccharomyces cerevisiae*, che va incontro sia all'invecchiamento replicativo che a quello cronologico, due modelli complementari di invecchiamento, che rispettivamente simulano il processo di invecchiamento delle cellule mitoticamente attive e quello delle cellule post-mitotiche. In questo contesto la replicative lifespan (RLS) è definita come il numero di cellule figlie generate da una cellula madre in presenza di nutrienti prima della morte. Al contrario, la chronological lifespan (CLS) è il periodo di sopravvivenza medio e massimo di una popolazione di cellule di lievito in fase stazionaria. Essa è determinata, partendo tre giorni dallo shift diauxico, dalla capacità di cellule quiescenti di riprendere la crescita una volta tornate su terreno fresco ricco.

Considerata l'esistenza di una forte connessione tra invecchiamento cellulare, nutrienti e metabolismo, abbiamo studiato i possibili effetti di alcuni composti nutraceutici, allo scopo di identificare molecole per sviluppare interventi anti-aging, oltre che aggiungere informazioni utili per comprendere meglio il processo di invecchiamento. A questo scopo, durante il primo e il secondo anno del mio

progetto di dottorato, ho studiato gli effetti del resveratrolo (RSV) sulla CLS. RSV è un composto polifenolico annoverato tra i composti attivatori delle Sirtuine (STAC) ed è riconosciuto per conferire benefici su molte patologie legate all'invecchiamento. Le Sirtuine sono una famiglia di deacetilasi NAD^+-dipendenti, il cui capostipite è Sir2 di *S. cerevisiae*, la cui attività è coinvolta sia nell'RLS che nella CLS. Inaspettatamente, abbiamo osservato che il trattamento con RSV incrementava lo stress ossidativo, in concomitanza con una notevole riduzione del pathway anti-aging della gluconeogenesi. L'attività deacetilasica di Sir2 sul suo target gluconeogenico Pck1 era incrementata, determinandone la sua inattivazione e indicando che RSV effettivamente agisce come STAC. Come conseguenza, questo causava effetti negativi sul metabolismo, determinando un fenotipo short-lived. Successivamente, ci siamo focalizzati sulla quercitina (QUER), un composto nutraceutico con proprietà benefiche su diverse patologie, incluse le malattie cardiovascolari, il cancro e la dislipidemia. Ciononostante, i target cellulari della QUER devono essere ancora esplorati. Abbiamo visto che la QUER possiede proprietà anti-aging che favoriscono un'estensione della CLS. Tutti i dati indicano un'inibizione dell'attività deacetilasica di Sir2 a seguito del trattamento con la QUER, determinando un incremento dei livelli di acetilazione e di attività di Pck1. Questo determina un rimodellamento metabolico a favore del pathway della gluconeogenesi, incrementando le riserve di trealosio e garantendo un miglioramento del processo di invecchiamento. Un altro aspetto analizzato in questa tesi riguarda l'omeostasi del cofattore nicotinammide adenin dinucleotide (NAD^+) durante l'invecchiamento cronologico, poiché, insieme ai suoi precursori biosintetici, sta emergendo come potenziale composto nutraceutico e i suoi livelli influenzano criticamente l'attività di Sir2. A questo proposito l'espressione dei carriers specifici mitocondriali, Ndt1 e Ndt2, è stata alterata, con effetti opposti sia sul metabolismo che sulla CLS. La mancanza di entrambi i carriers diminuisce i livelli di NAD^+ e incrementa la CLS, mentre l'overespressione di *NDT*1 aumenta il contenuto di NAD^+ e influisce negativamente sulla CLS. Tutti i risultati hanno dimostrato che l'attività deacetilasica di Sir2 influisce significativamente sulla longevità cronologica, identificandolo come un target cruciale nel processo di invecchiamento. Nei mammiferi, SIRT1, ortologo funzionale di Sir2 di lievito, svolge un ruolo importante nell'orchestrare il metabolismo e la sopravvivenza cellulare, sottolineando la reale possibilità di trasporre le conoscenze acquisite dal lievito a organismi complessi, compreso l'uomo. Inoltre, i risultati ottenuti per RSV

e QUER evidenziano che la somministrazione di un composto nutraceutico ad un organismo più complesso con organi/tessuti con profili metabolici diversi potrebbe determinare una risposta fisiologica inaspettata a causa della sua interazione con specifici target. La capacità di sviluppare cibi personalizzati e di veicolarli verso il target di interesse rappresenta il prossimo obiettivo nello sviluppo di interventi nutraceutici.